Master of Science thesis “Bypass - Itajaí-Açu”

Impact study on the implementation of a bypass in the Itajaí-Açu River, Brazil

Delft University of Technology
Civil Engineering – Coastal Engineering

Graduation Committee
Prof. dr. ir. J.C. Winterwerp (DUT)
Prof. dr. ir. Z.B. Wang (DUT)
ir. J. van Overeem (ARCADIS/DUT)
ir. L. Perk (ARCADIS)

Author
J.W.L. Wijs

Preface

With this Master of Science Thesis I have completed my study Civil Engineering at the Delft University of Technology at the department of Hydraulic Engineering. After several internship projects at different engineering companies ARCADIS offered me the opportunity to investigate the impact of the implementation of a bypass in the Itajaí-Açu River system.

This study has led me along several interesting processes that are going on in a tidal area such as the Itajaí-Açu River. With the resources provided to me by ARCADIS I was able to investigate the most relevant processes to come to a first conclusion about the feasibility of a bypass as a solution to the problems at hand in Itajaí.

After eight months of modelling and evaluating data I came to a positive conclusion. A bypass is indeed a solution provided that it is implemented in the right way considering the insight gained in this thesis.

I would like to thank my entire committee prof. dr. ir. J.C. Winterwerp (Delft University of Technology), prof. dr. ir. Z.B. Wang (Delft University of Technology), ir. J. van Overeem (Delft University of Technology and ARCADIS) and especially ir. L. Perk (ARCADIS) who has helped me on a daily basis during my thesis. They all have enabled me to achieve this result. Besides my committee I would like to thank Bart Grasmeijer, Jeroen Adema and Ivo Pasmans as they helped me at difficult moments during the build-up of the model. And I also want to thank my friends in Delft, who helped me during my thesis with discussions and support. And of course my girlfriend for always being there to support me every day.

Jurian Wijs
Delft, September 2013

Abstract

The city of Itajaí is located in the province of Santa Catharina in Brazil. The people of Itajaí have been coping with flood risk for the past decades. During historic discharges, Itajaí has been flooded several times. During normal conditions the Itajaí-Açu River is a rather calm river that is used for navigation and the harbour area. The populated area is therefore located near the water in a flat coastal area. This means that during rare events of an extreme high discharge large areas get flooded. Recovering from the past two floods in 2008 and 2011 have cost more than over several hundreds of millions of dollars.

Together with flood risk the river is subject to several sediment transporting mechanisms: sedimentation during calm periods and erosion during extreme events. Sedimentation that occurs on a daily basis is eroded away during extreme events. This keeps the system in balance. However, the erosion is not a gentle process that erodes the bottom in a uniform way. In some place extreme scour holes are formed during those extreme discharges. During these extreme discharges large volumes of sediment are deposited elsewhere in the system. Rendering parts of the harbour unnavigable.

These three issues could be mitigated with a bypass. The bypass will be a channel that diverts a portion of water away from the current branch to decrease flood risk by lowering the water level. A diversion of water means that less water flows through the current branch. Less discharge there means a lower water level at that bifurcation. Further upstream the water level is less and less affected by the bypass and will approach the initial water levels again. But the Itajaí area can be covered well with a bypass if it is connected just upstream of the city.

The solution to erosion is parallel to the solution to the flood risk issue. The cause of erosion is a high flow velocity. This is reduced the same way as the high water levels by diverting water through a bypass.

The sedimentation problem is likely to increase with the implementation of a bypass. If the bypass is permanently open it also diverts water during normal conditions. If this happens the flow velocities decrease also during day to day conditions. Since it is known that sedimentation occurs due to low flow velocities during day to day conditions, one can assume that sedimentation will arise. However, this cannot be stated in advance since it is a more complex process than just river flow.

The result of this thesis is an understanding of the impact of such a bypass. By analysing the consequences on different processes that contribute to the aforementioned flood risk and sediment transport mechanism, good insight can be attained on how to design a bypass. What are disadvantages of such a bypass and how can these disadvantages be dealt with.

First of all a good understanding of the flow distribution in estuarine branches is required. The process that influences the sediment transport is flow. Main driving forces behind the flow are the river discharge, tide and density currents due to salinity. These three contributors have a different behaviour in a single channel compared to a 2-channel system as designed here. In this thesis it is investigated how the discharge will be divided over the bypass. Influence by flow resistance and gravitational flow have shown that a rigorous change such as a bypass has equal rigorous implications for the systems behaviour.

An important part of the investigation is done with numerical modelling in Delft3D. Delft3D is a numerical modelling program, it simulates the behaviour of a system by calculating change during small time steps. Every time step continues with the results of the previous time step. Step by step the model develops itself. An advantage of this programme is that one can implement one or several processes instead of simulating the complete model at once. This makes it possible to relate different processes to each other.

The first aspect to investigate, is the river discharge distribution. It was found that during low discharges the system behaves different than during high discharges. At high discharges the distribution is fixed due to dominating resistance that changes equally in both channels.

During research on the tide and water levels it was found that the tidal flow is divided over the current existing branch and the bypass. Due to this, the tidal flow amplitude will decrease in the current channel and the bypass downstream of the bifurcation. This is obvious when considering the scenario where the tidal flow in the current branch would remain the same and additionally the tidal flow in the bypass would be much larger as resistance is smaller. This would result in a tidal prism which is much larger than in the current scenario. This would result in a tidal elevation range which is a few times larger than it is today. For this it would require a tidal flow which is a multiple of what it is in the current scenario. This is impossible to happen as friction would resist this. Hence the increased capacity of the bypass and the current branch combined will not be used completely. This results in tidal diminishing in the current branch.

The salinity dynamics show a remarkable result in the 2-channel system. During low discharge the force of the heavy sea water on the current branch's mouth is so much larger than on the bypass mouth that an average flow in an upstream direction is possible through the current branch. This is only during low to average discharges. However, the net influx through the current branch is a very negative result since salt intrusion increases drastically.

When looking at the resulting magnitude of these changes it can be said that the tidal change due to the bypass has the largest impact. The decreased tidal velocities due to the increased cross-sectional area diminishes the tidal action in the current branch. The tidal flow has appeared to be the largest mobilizing force for sediment as it causes the largest flow velocities. The bed shear stresses have indeed been severely decreased. Without further investigation on sedimentation it can be said that maintenance cost due to this tidal diminishment can be tremendous. This issue disappears as soon as the tidal flow is not the dominant sediment mobilizing force anymore. This is during high discharges when the effect of the tidal wave decreases compared to the river discharge and when the discharge causes enough bed shear stress to mobilize and transport sediment. In the full fluvial mode this is inherently true when there is no tidal reversal anymore. However in this bypass situation the full fluvial mode will require a much higher upstream river discharge than in the today's situation. This is due to the diversion of water through the bypass.

The salinity has shown to be of influence at low flow velocities. The bypass results in two implications:

- First of all it has been shown that in the scenario without salinity the flow velocities have decreased in the current branch. This results in a higher intrusion length of the salt water body in the current branch stretching beyond the confluence of the Itajaí-Mirim and the

Itajaí-Açu. This means that the water quality in the Itajaí-Mirim might become too low for the water purification plant in the Itajaí-Mirim.

- The second consequence is a combination of the bypass and the salinity. Since the mouth of the current branch is much deeper than the mouth of the bypass there is a much larger force directed from the sea into the current branch than from the sea into the bypass as a result from the density difference between fresh water and salt water. At low discharges this means that the force difference can cause a net flow through the current branch that has an upstream direction. During flood the flood flow through the current branch is boosted by the density difference. And during ebb flow a strong resistance from the sea slows down this ebb flow. With a two channel system this increased resistance means that the flow will seek the way of least resistance and exit through the bypass. A result is that the combination of the bypass and salinity increases the intrusion further than just would be expected from the flow velocity reduction.

For the reduction of flood risk and high water levels the bypass works very effective. The lower the resistance of the bypass the better it works. This means that for that matter the bypass can be tuned to the desired reduction of flood risk. On the other hand, the combination of the bypass with low discharges has shown to have rather negative effects. For both the tide and the salt intrusion the combination with the bypass results in an undesirable scenario. This means that during low to average discharges the bypass has a negative effect. The lower the resistance of the bypass the higher the river discharge needs to be for the current branch to cope with the negative results from the combination of the bypass with the tide and the salt intrusion.

The general conclusion of this research is that for a functional bypass it is inevitable to close this bypass during low discharges. A better performance of the bypass during high water results in worse results during normal to low discharges. However, it has shown to have great potential. The most important question now is the cost consideration. The bypass with a mechanical closure is rather expensive, especially at this scale. It also causes the bypass to silt up at the sea mouth when the closure prevents flow to flush out the bypass. This is also an important research question for future research. Therefore it might take several decades to get a return on investment in the form of reduced risk. Nevertheless, since the past two extreme events happened in a bit over five years and cost several hundreds of millions of dollars it is most likely to be profitable.

Index

List of tables

List of figures

1 Introduction

High discharges of the Itajaí-Açu River caused serious problems for the city of Itajaí and the surrounding area in 2008 and 2011. After the 2008 floods, USD 850 million was sent as government aid to the affected area. Well over 100 people perished (CNN.com 2008). The impact can be seen in Fig. 1-1.

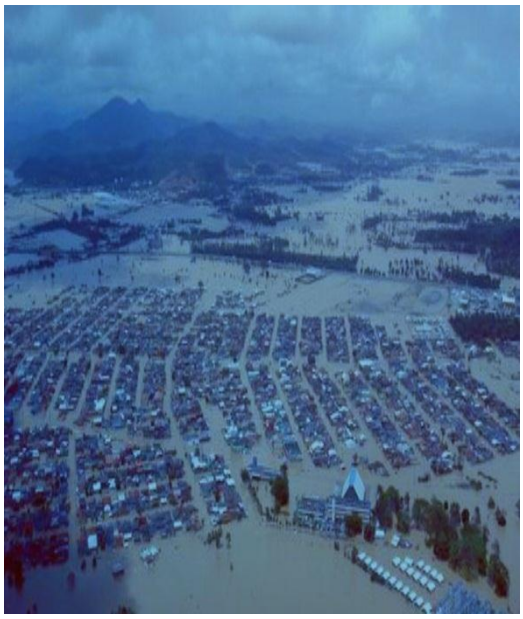

Fig. 1-1: Itajaí 2008 flood (2008)

Previous to this thesis a solution has been proposed to implement a bypass to prevent floods like this in the future. The idea behind a bypass is to divert a part of the total river discharge through an additional channel. Besides the effect of reducing flow velocities in the current branch there is also another result. When two channels discharge the total river discharge together, they will lower the water level at the point where they meet, this is the bifurcation point. The lowering of water level is due to their combined capacity that is larger than the capacity of the current branch that needs to cope with the total discharge alone. This two channel system will reduce flood risk by lowering water levels. The influence of lowering water levels will be both upstream and downstream of the bifurcation point as this influence stretches over a certain length.

This report will describe the impact of a 'river bypass channel' that reduces the flood risk for the city of Itajaí. Additional to the flood risk reduction, it is also investigated if this channel can contribute to a reduction of the sedimentation/erosion issues in the harbours of Itajaí. Flood risk reduction and sedimentation/erosion reduction serve two different parties. The flood risk reduction will mainly be an issue for the local public. On the other hand, there is the sedimentation/erosion problem for the harbours in the area. Another aspect that will be looked at is the salinity in the system. As the system will partly change into a 2-channel parallel system the behaviour can change significantly. With a purification plant near the sea in the Itajaí-Mirim river, changes can have negative consequences.

1.1 Problem definition

As mentioned before there are three problems that will be addressed here. The flood risk, sedimentation and the erosion problem. Since the erosion and sedimentation behaviour are different, they will be treated separately. The erosion problem occurs during high discharges and causes scour. Sedimentation happens on a daily basis during low to average discharges. A different aspect that has been investigated already in previous studies, is salt intrusion and the salt dynamics in general. The harbour expansions have increased the intrusion, which can become a problem for water quality. In anticipation of the expected consequences of the bypass on salt intrusion this is investigated as well.

1.1.1 Flood risk

During events with high discharges, it has become clear that Itajaí is faced with a high flood risk. This is a result of a river that has been constricted by urbanisation. Urbanisation has been going on

along the Itajaí-Açu since European settlers arrived a long time ago in this area. When a highly concentrated population is located near a river in a low lying area with extreme discharges, the consequences of a flood can be devastating as has been seen in the past. Therefore diminishing the flood risk is very important to the area. In this thesis it is investigated if by diverting a part of the discharge of the Itajaí-Açu River, it is possible to reduce extreme water levels downstream and upstream of this diversion.

1.1.2 Sedimentation

Sedimentation occurs almost all year round. It has been found that discharges between 200 and 1000 m^3/s cause sedimentation (Schettini 2002). Due to deepening of the harbour area for development, the basin has been attracting higher and higher sediment. This inherently resulted in more and more maintenance cost (Schettini 2002). Sedimentation ceases at about 1000 m^3/s because high flow velocities don't allow sediment to settle. Hence sediment that enters the basin will also leave the basin. Maintenance due to sedimentation is done since too much sedimentation will render shipping impossible in the harbour area.

1.1.3 Scour

When the discharges are high, problems with erosion start to occur. Locally high flow velocities cause deep scour holes. In the floods of 2008 and 2011 entire quay walls have collapsed due to very deep scour holes at the base of those quay walls. The problem with scour is in fact the opposite of the sedimentation problem. Therefore the solution for one of them could work adversely for the other. Scour is induced by high flow velocities, while sedimentation occurs when flow velocities are too low.

1.1.4 Salt intrusion

Salt intrusion up until today has been no serious problem yet. However, with a bypass that is meant to decrease the flow velocity drastically it can be expected that the salt intrusion will increase. This can become a problem. In the Itajaí-Mirim there is a water purification plant. If the salt intrusion will increase at its location, the process will become more expensive to purify water for use in the area.

1.2 Objective

The goal of this thesis is to give a first assessment of the impact of a bypass on flood risk, sedimentation, scour and salt intrusion. The following research questions will be the basis of this thesis:

- What are the changes in water level due to implementation of a bypass?
- What are the changes in sedimentation due to implementation of a bypass?
- What are the changes in scour due to implementation of a bypass?
- What are the changes in salinity dynamics due to implementation of a bypass?

This will be done in steps. These steps will result in the understanding of this complex system. The focus is on sediment transport and hydrodynamics. For that the water distribution, tidal propagation, salinity dynamics and water levels are investigated. The changes in these processes will be investigated. When these are understood, the step to the sedimentation behaviour can be made. No actual sediment transport model is used. However, the expected sedimentation behaviour has been assessed according to changes in bed shear stress in the system.

1.3 Approach

As said in section 1.2 the different processes has to be understood separately before the complete system behaviour can be analysed. This means that all processes need to be isolated in an artificial way to look at its behaviour in the old and new situation and compare them. This is only possible when using a type of model that can be modelled for the situation as in Itajaí.

Frist this will be done with a simplified model for the water distribution over the current branch and the bypass. This is to get an initial feeling for hydrodynamic behaviour in a bifurcating system. For the scour problem the data from previous models is used to get a sense of magnitude of this issue. The results of the distribution model and the scour analyses determined a bypass capacity. This bypass is used to determine the influence of a bypass on the system. This bypass is therefore a kind of arbitrary. Nevertheless this is a good way to assess the impact of a bypass in this situation. Fine tuning the bypass is only possible when more accurate data is available. And also one needs to know the consequences of a bypass implementation. However, the fine tuning of the bypass has not been done in this study.

The next step is modelling in Delft3D. At the start of this research a complete Delft3D model was available. This model described the current situation only. Therefore the current model has been expanded with the implementation of the earlier determined bypass.

This model is used to verify the results from the simplified models and make it possible to test hypotheses on the behaviour of the discharge distribution, tidal propagation and salinity dynamics. They are hard to predict by hand. All three are nevertheless important for the behaviour of fine sediment which is found in the Itajaí-Açu River. In this stage all the processes are treated isolated as well as in combination to get a grip on what happens with different processes.

With an evolved understanding of the system, changes in bed shear stresses can be understood. These changes in bed shear stress give insight in the new behaviour of sedimentation and erosion in the system.

The reason not to use this model straight away is that it was not calibrated or verified with the implementation of a bypass. It only described the current situation. When implementing a rigorous change such as a bypass, the calibrated system might be outside the range of calibration, even though it might give feasible results. The model is than rendered useless since the results might be far of reality without the user knowing. If an evolved understanding of the processes at play gives more insight the results can be evaluated more thoroughly on reliability.

1.4 Report outline

The structure of the report can be divided in two parts. Chapter 2, 3 and 4 are focused on the analysis of the existing situation and literature on bifurcations in estuarine areas. Chapter 5, 6 and 7 are focused on the analysis on the impact of the implementation of a bypass in the Itajaí-Açu River.

In Chapter 2 the current situation is described. These are the boundary conditions and system properties of the Itajaí-Açu River. With this chapter a first view on relevant aspects is shown.

Chapter 3 is a short summary of the literature study. In appendix I and II a more elaborate explanation on relevant processes and methods is given. It connects the theory to the system aspects in Itajaí relevant to the research in chapter 5.

Chapter 4 elucidates the models used. Both the simple study models as well as the behaviour based numerical software of Delft3D are explained and why they are used. Results from the simple models can be found in appendix III.

Chapter 5 treats the results of the research with Delft3D. The results are coupled to theory and the first conclusions are drawn.

Chapter 6 summarizes the results and conclusions from chapter 5. With these conclusions this thesis is ended in this section with recommendations for future research.

2 Current system description

This section will elaborate on the Itajaí-Açu River system. It will describe relevant system properties that are used in the investigation to look at the impact of the implementation of a bypass. Aspects as bathymetry, water level measurements, salinity measurements and sediment properties are evaluated. Especially the lack of detailed properties are. It needs to be shown that this information is qualified for this research or at least will not compromise the results.

Itajaí is located in the southern state of Santa Catarina, Brazil (light colored area in Fig. 2-1). Santa Catarina is an area with one of the highest living standards in South America. Inhabitants are mostly descendants of Portuguese, German and Italian origin (Itajaí 2013). The municipality of Itajaí is a wealthy area with the harbour as its economical heart. The city of Itajaí (Fig. 2-2), being the second harbour of Brazil regarding container throughput, is of significant importance.

Itajaí is located at the northern part of the Santa Catarina coast line at the mouth of the Itajaí-Açu. Most of the city is flat and near sea level. The river mouth is the entrance for the harbour area and is maintained for navigation.

The river has in principle two functions. One is the drainage of excess water from the watershed. This has resulted in high water discharges in the past en caused problems for a large area. The other function is the navigation for ships. The channel needs to be navigable. Meaning that with increasing sizes of ships the access channel has been deepened in the past. This has been attracting sediment in an increasing amount over time.

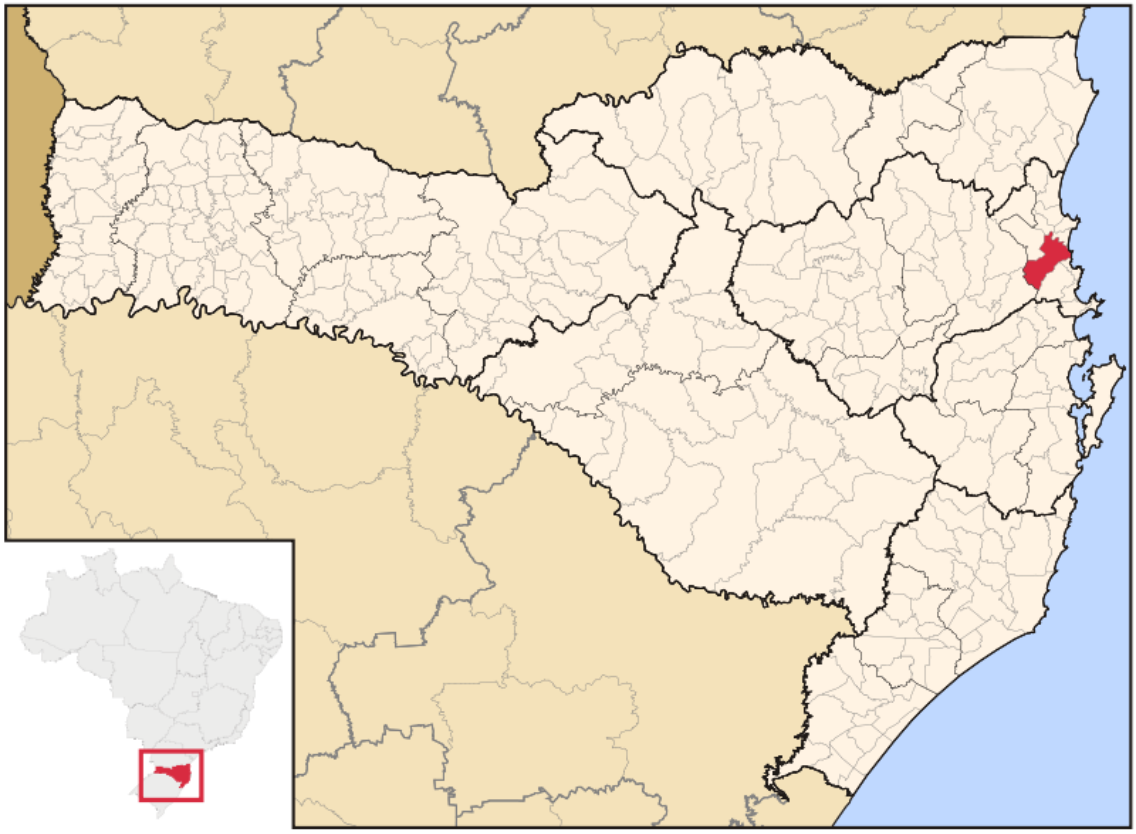

Fig. 2-1: Itajaí Municipality (2006)

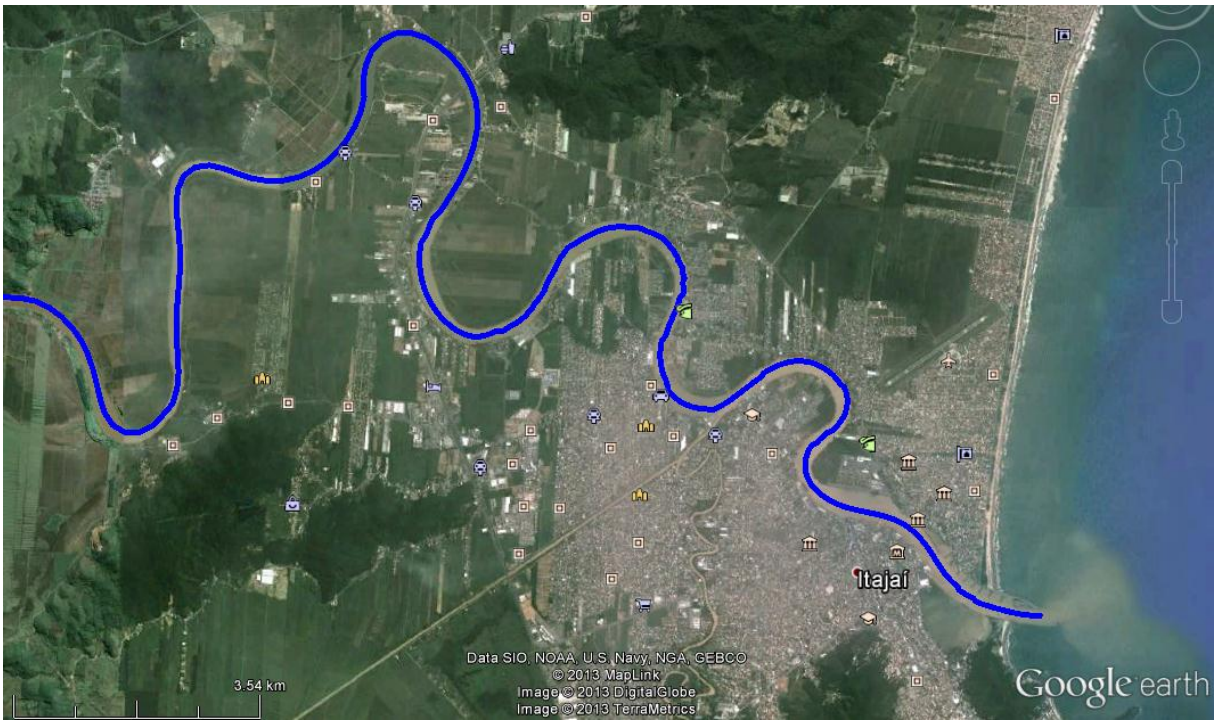

Fig. 2-2: Itajaí & Itajaí-Açu (Google 2013)

2.1 Itajaí–Açu River

The Itajaí-Açu River covers a watershed of around 15.500 km^2. Over time, discharge measurements have been done at Indaial, which is about 90 km upstream of the river mouth. The measurements were done by Agência Nacional de Energia Eléctrica. These measurements are at the Indaial station. These discharges are on average representing 72% of the discharge at the river mouth (Jansen 2000). The mean discharge is about 230 m^3/s, with low values around 40 m^3/s, high values around 2000 m^3/s and extremes around 7000 m^3/s. This shows that the river has very dynamic character.

It is the location of the harbour areas in Itajaí. It is therefore essential for the area in general. Below in Table 2-1 the extreme measurements of the past 30 years are given. This shows from the past 30 years the 10 most extreme discharges that occurred. Sometimes twice in two months' time (1992), but the quite periods between 1984-1992 and 2001-2008 shows that it is very unpredictable when the extreme events occur, especially when there is also no specific season that accounts for the extreme events.

It needs to be added that the measurements of 2008 and 2011 are not correct. This data is not from Indaial since it wasn't recording during the event. Therefore data from Blumenau is used although the water level recordings stopped as well for a few hours during the event. Therefore the extreme levels just before stopping are used. The discharges are there for lower than actual. The event of 2011 the recording stopped for 1.5 days. Which means the underestimation here is even bigger.

With the day to day measurements Table 2-2 gives insight on the return period of different discharges. The Weibull distribution was used to find these return periods. The distribution used is presented in Fig. 2-3.

Date	Max. day-average river discharge [m^3/s]
09/07/1983	7100
07/08/1984	7300
30/05/1992	5290
30/06/1992	4450
01/02/1997	3340
28/04/1998	3150
03/07/1999	3040
01/10/2001	4800
23/11/2008	4130
10/09/2011	4570

Table 2-1: Extreme values of discharge of the past 30 years (ARCADIS 2012d)

Return period [yr.]	Probability of Exceedance per day [%]	River discharge [m^3/s]
25	0.011	6400
50	0.005	7250
100	0.0027	8010

Table 2-2: Return time with according discharges (ARCADIS 2012d)

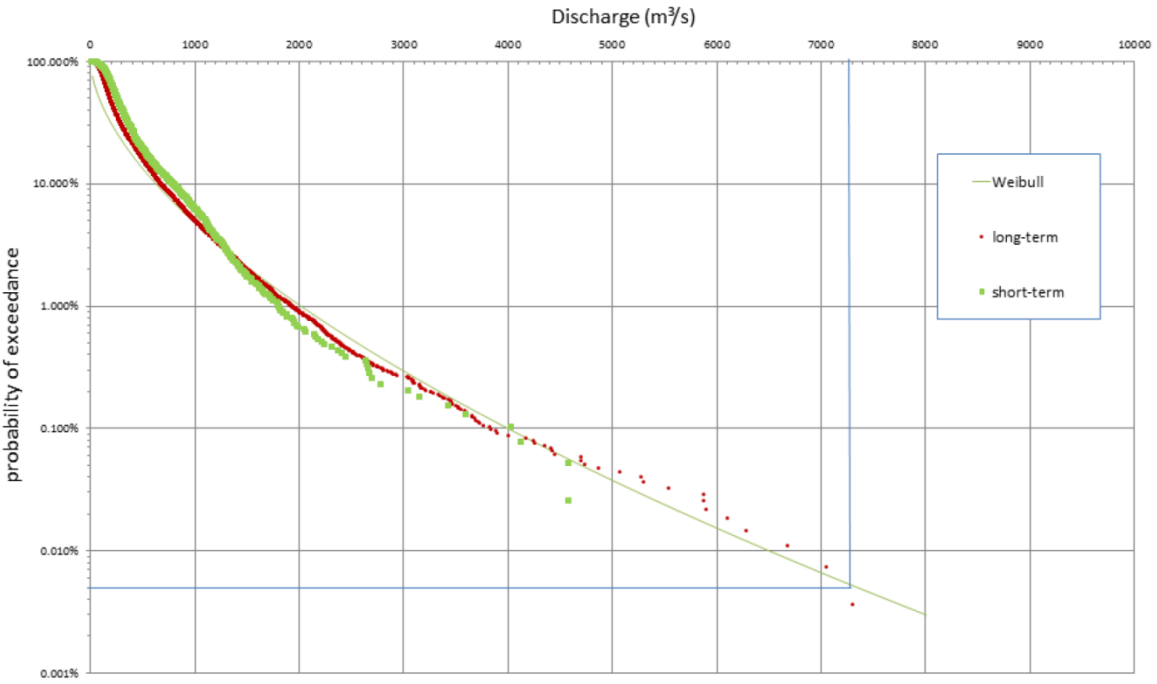

Fig. 2-3: Weibull distribution measured river discharges (ARCADIS 2012d), probability of exceedance per day

2.2 Channel dimensions & lay-out

The channel has been undergoing several changes in the past. The biggest influence has been the development of the harbour area. But also urbanisation on the river banks has restricted the river as it is today.

The river mouth has been stabilized in the 1930's with breakwaters. In the downstream part the river flow is controlled by groins by narrowing the cross-sectional profile. This has been done to increase flow velocities and with that reduce sedimentation or allow a greater depth to be achieved with the same maintenance effort. This is also visible in the Admiralty Chart in Fig. 2-4.

8 km upstream of the river mouth there is the confluence with the Itajaí-Mirim. In this branch there is a fresh water inlet. This puts restrictions on salinity in the area. This has been of interest in previous ARCADIS studies.

At the mouth, the width of the channel is about 190 meter wide. This increases to about 400 m at the harbour of Navegantes. After that the river varies between 140 meter and 220 meter and meanders upstream to cities such as Gaspar, Blumenau and Indaial. The natural depth is about 7 to 8 meters. It is therefore that it can be an important navigation channel to these upstream cities.

2.3 Bathymetry

The bathymetry in the area has been subject to change. Extreme events have changed it drastically in the past. Also the man-made changes that were executed for the harbour have had an impact. The harbour area is around 14 m deep while the un-dredged parts are at a natural depth of 7m-8m (ARCADIS 2012b). The transition from dredged to un-dredged is after roughly 4km from the river mouth. In Fig. 2-4 one can see the current bathymetry from the Admiralty Charts.

Something that should also be noted is that there are sand mining pits upstream in the river. The depths at those mining pits are much deeper than the equilibrium depth.

Sources for bathymetrical information are:

- Van Oord: trajectory of some 6.4 km from harbour to begin of access channel
- Van Oord: trajectory from harbour to 9.3 km upstream
- Community of Blumenau: the depths along the trajectory from upstream of the harbour of Itajaí to Blumenau, herewith the contour of the river banks are plotted as the 0m contour (surveyed with DGPS)
- Hidrotopo surveys listed in Table 2-3 (ARCADIS 2012a)

No.	Survey	Start date survey	End date survey
1	HDT-527-06 [200 kHz]	27-03-2008	01-04-2008
2	HDT-638-08 [200kHz]	27-11-2008	27-11-2008
3	HDT-731-11 [200kHz]	11-04-2011	26-04-2011
4	HDT-731-11 [200kHz]	14-11-2011	20-11-2011
5	HDT-704-10 [240kHz]	09-08-2012	09-08-2012
6	HDT-704-10 [240kHz]	26-09-2012	29-09-2012

Table 2-3: Bathymetric surveys considered in this study

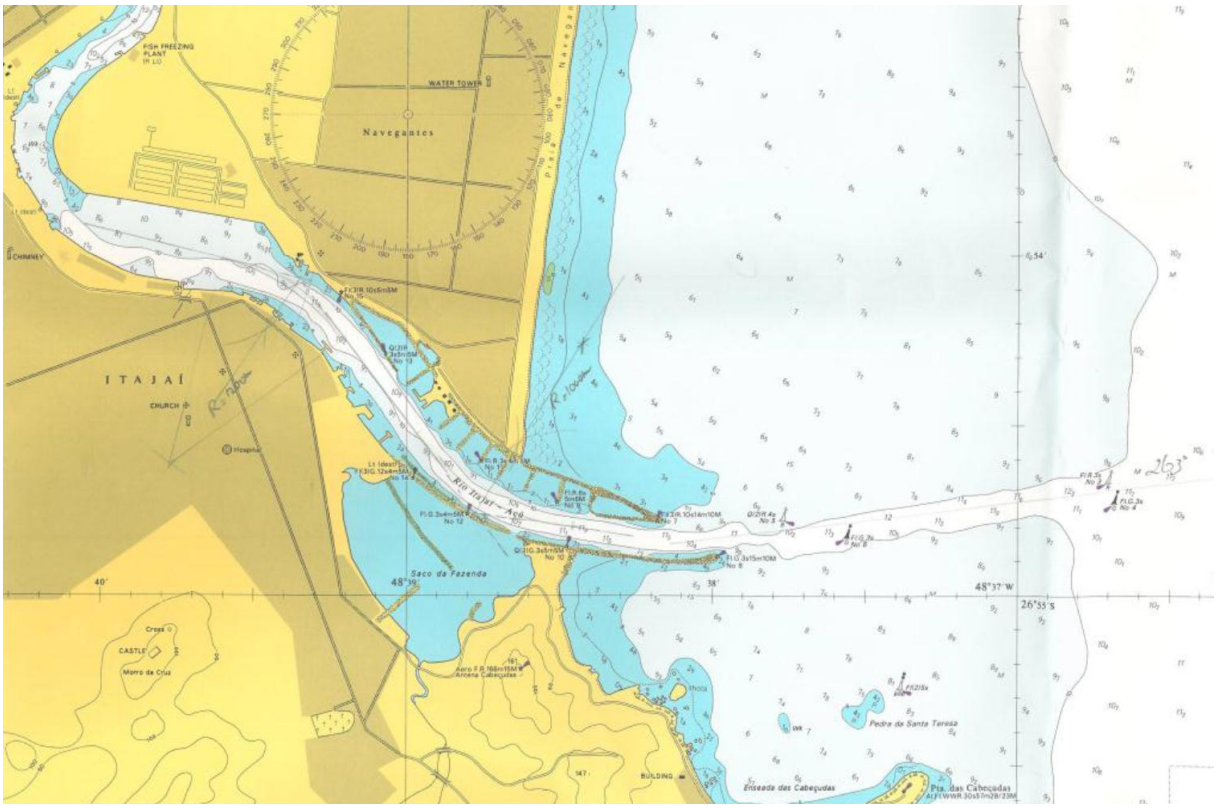

Fig. 2-4: Downstream section of Itajaí-Açu River (copy from Admiralty Chart no 500)

2.4 Tides & water level variations

For research in the past, measurements have been done on the water levels. For a period from 1999 to 2008 a time series of observations is available. This data is used for a tidal analysis (ARCADIS 2009a). In this period the highest water level is 1.91m above DHN/NR (=Chart Datum) and the lowest water level is 0.69m below DHN/NR. With an average level of 0.58m above DHN/NR, this is not only the tide but also due to meteorological influences.

With a tidal analysis the measurement signal is decomposed into a certain amount of harmonics. These harmonics combined describe the tidal signal, and originate from different sources such as the sun and the moon. But also friction causes harmonics, a so called over-tide, and it turns up in the full tidal signal as well. When these components are found with a Fourier analysis, the full tidal signal can be described by them. However, in reality a residue will remain in the signal that cannot be ascribed to tidal components. This is due to meteorological effects. A depression or wind set-up can cause a water level fluctuation that is not related to the tide but shows up in the signal. In Fig. 2-5 the measurement time series from January 1st until March 31st 2000 is shown. It is decomposed into the tidal components and the residue which represents the meteorological effects.

To come from a complete tidal signal to a set of tidal components in the form of harmonics one uses the following equation from the Fourier analysis. The analysis has been carried out by (ARCADIS 2009a).

$$h(t) = A_0 + \sum_{i=1}^{n} f_i * A_i * \cos(\omega_i * t + (v_0 + u)_i - g_i) \qquad (2.1)$$

With:

- $h(t)$ = water level at time t [m]
- A_0 = Mean water level [m]
- A_i = Amplitude of component I [m]
- f_i = amplitude factor of component I [-]
- ω_i = angular speed of component I [rad/s]
- $(v_0+u)_I$ = phase factor of component I [-]
- g_i = phase angle of component I [rad]

In Fig. 2-6 and Fig. 2-7 one can see the component decomposition from the tidal analysis. With this set of harmonics it is possible to make a forecast or hindcast that is required.

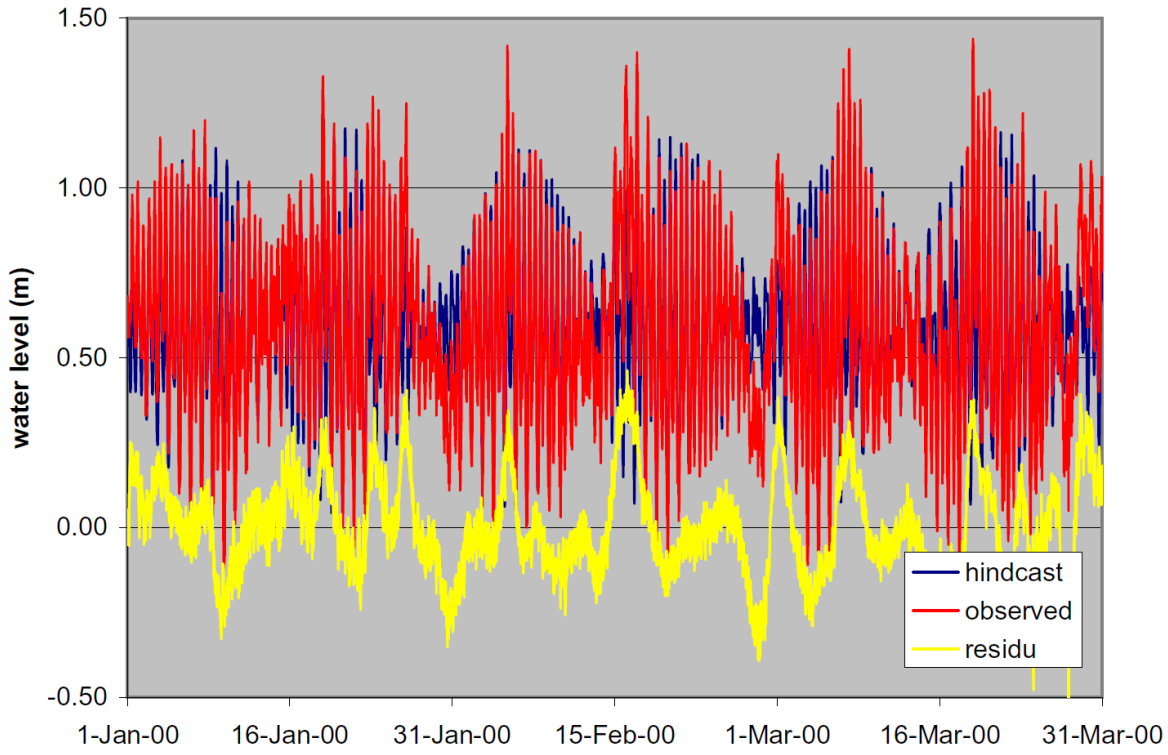

Fig. 2-5: Water level prediction and observation at Itajaí

Another source of information on water levels is the Admiralty Tide Table. In here the basic data on tidal water levels is given. Below in they are compared in Table 2-4. Eventually the tidal analysis is used as this represents results from local measurements and therefore is assumed more accurate.

Characteristic Level	Water level [m]	
	Admiralty Tide Table	Tidal Analysis
MHWS = Mean high water spring	1.00	1.09
MHWN = Mean high water neap	0.60	0.75
MSL = Mean sea level	0.6	0.58
MLWN = Mean low water neap	0.50	0.40
MLWS = Mean low water spring	0.20	0.21

Table 2-4: Tidal water levels. A.T.T vs. Tidal analysis

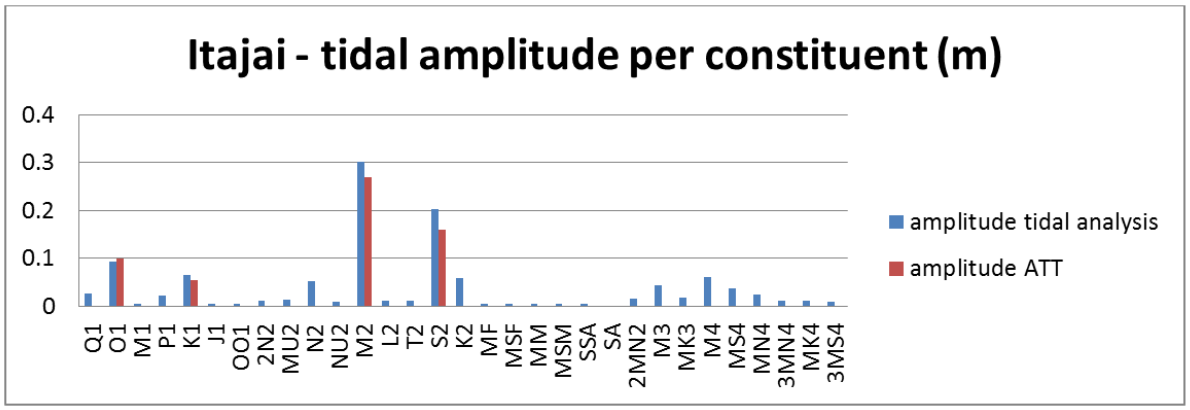

Fig. 2-6: Decomposed constituents tidal amplitudes and Admiralty tide table

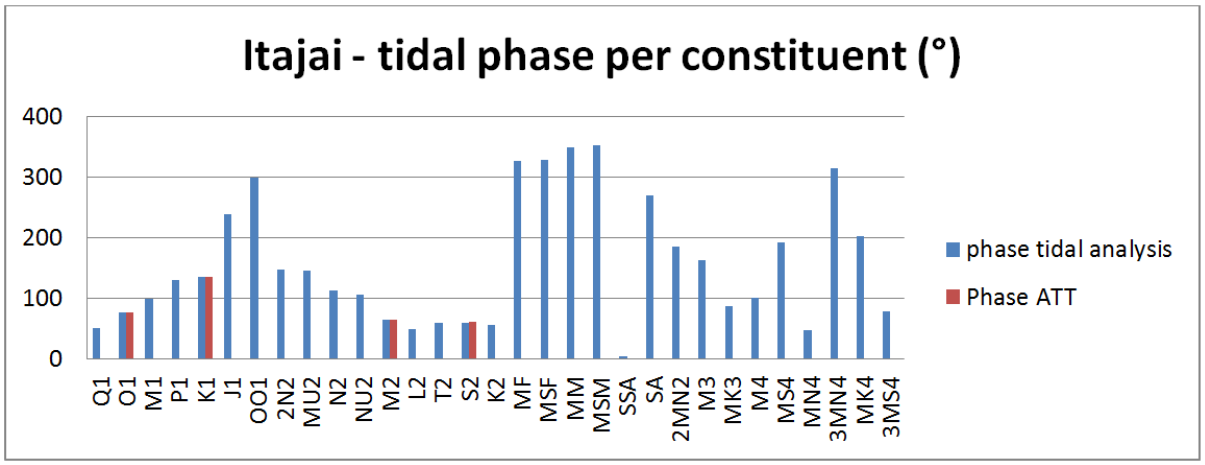

Fig. 2-7: Decomposed constituents tidal phases and Admiralty tide table

2.5 Salinity

A recent salinity intrusion study has been done to investigate the consequences of the harbour basin deepening plans. This study (ARCADIS 2009a) has shown that the salt intrusion will change due to deepening of the harbour basin, but is still strongly depending on the rivers discharge.

Fig. 2-8 (Brandt 2000) shows the position of the salinity intrusion during high water and low water measurements are from 7th untill 21st of jan 2000. One can see that with low discharges (< 200 m^3/s) the salinity intrusion can reach up until 18km up river and up to 30km up river when discharges drop below 100 m^3/s. When the discharge reaches over 1000 m^3/s the salinity intrusion has disappeared entirely since there is only water exiting the basin. The dynamics of this salinity intrusion are important for the so called gravitational flow than can induce a sediment importing process. This is further explained in section 3.3.2.

Another important issue here is an inlet for fresh water in the Itajaí-Mirim River. This is about 10 km upstream of the port of Itajaí. The salinity around this inlet cannot be too high to keep production costs within acceptable ranges. During measurements between 2001 and 2003 it is shown that with a discharge over 300 m^3/s the intrusion does not reach the confluence of the Itajaí-Açu with the Itajaí-Mirim (ARCADIS 2009a). There are no measurements available of the behaviour of the salinity intrusion in the Itajaí-Mirim.

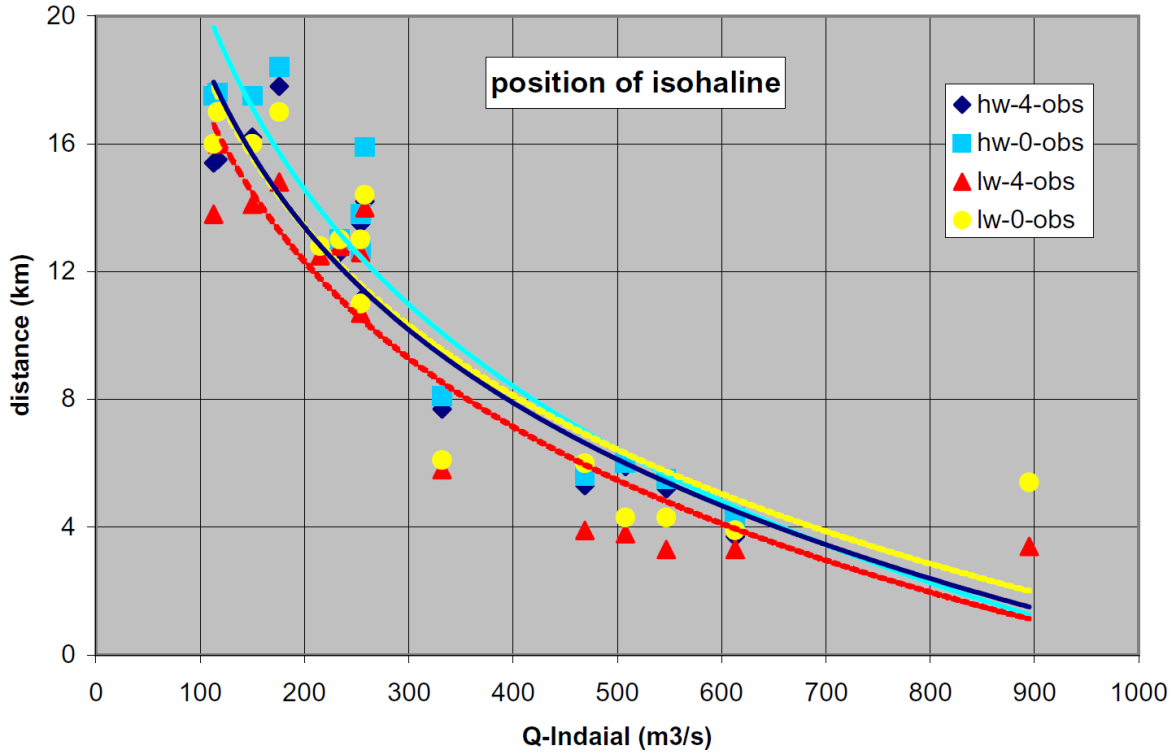

Fig. 2-8: Upstream position of salinity values of 0 and 4 psu during HW and LW

2.6 Morphology & sediment

Not much is known about the spatial distribution of the different subsoil layers besides some local information around the construction of the APMT1 and APMT2. In previous studies the properties of the subsoil at APMT2 were used. This terminal is located 2150 m upstream of the river mouth. Since this is a very local measurement it could be wrong for the entire area to use these subsoil properties. In Table 2-5 the properties related to depth are shown. The D_{50} and silt fraction have been estimated by comparing the soil appearance of the shallow and deeper layers and considering the known D_{50} and silt fractions of the sediment samples taken before (ARCADIS 2012c). From these samples it was concluded that a D_{50} between 10 µm and 30 µm is found in the harbour area (Cornelisse, Kesteren et al. 2000).

Level [DHN m]	Soil material
-12 to -16.5	Soft clay
-16.5 to -19.5	Loose silty sand
-19.5 to -21.5	Soft clay
<-21.5	Loose silty sand

Table 2-5: Subsoil properties at APMT2 quay wall

These figures have been used in an investigation near the APMT terminals. For that purpose it might suffice. But when considering a much larger area, thorough research could be required for more accurate results.

In Fig. 2-9 measured suspended sediment concentrations are plotted against the river discharge. A quadratic curve fits the data. This has been used in the past for sedimentation studies in this area

(ARCADIS 2005). A quadratic relation seems feasible when comparing the measurements with the quadratic line

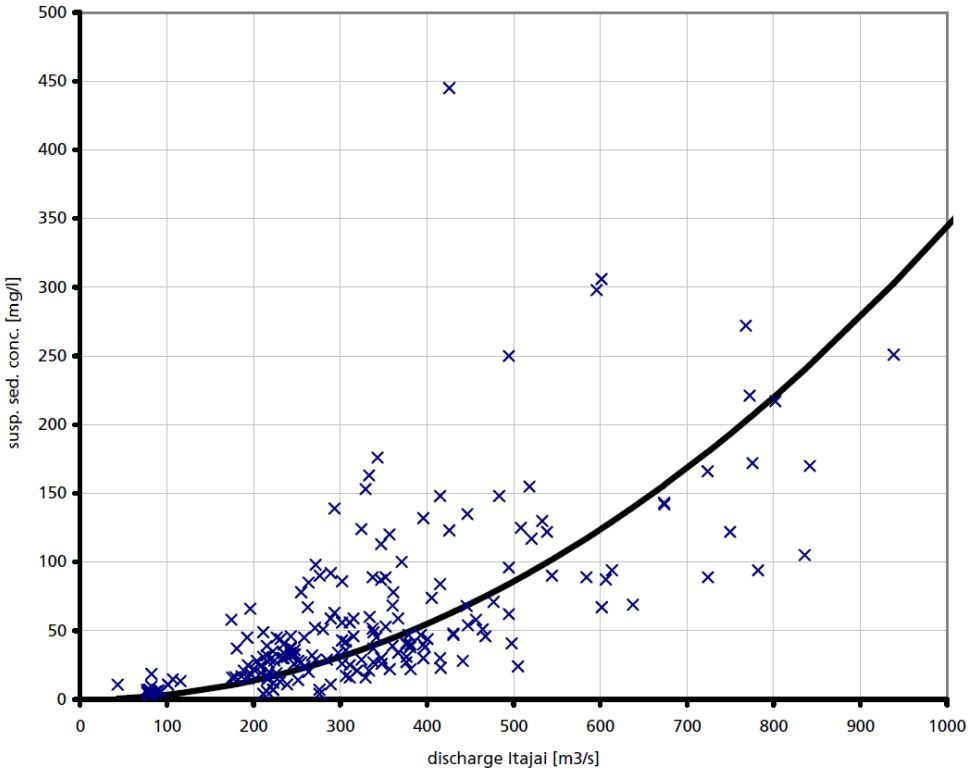

Fig. 2-9: suspended sediment concentrations vs. river discharge

In 2000 research has been done by Deltares on the sediment properties (Cornelisse, Kesteren et al. 2000). It was has shown that the sediment is fine and cohesive. Those properties have been the basis of previous studies and are considered in this thesis as well.

On the 8th of December 1999, a 25h field experiment has been executed to investigate the advective transport of salt and suspended particulate material (SPM) (Schettini, Ricklefs et al. 2006). This research has shown interesting results when considering the trapping efficiency along the river. In this research the river has been divided in three segments.

- The lower estuary (LE) (2 km upstream of the river mouth)
- The middle estuary (ME) (17 km upstream of the river mouth)
- The upper estuary (UE) (38 km upstream of the river mouth)

These sectors were divided like this because of the regime in those sector. This is a common way to do this since the separated sectors can be compared between estuaries. In the LE the marine waters prevail in general and have a large influence on the estuaries behaviour. When looking at the ME the tip of the salinity intrusion indicates its upstream boundary. The UE is the part where only the tidal signal has an influence on the flow but the salinity intrusion does not reach that far.

In these three sectors it is seen that the sediment transport decreases with 70 % over each sector boundary, meaning that there is a certain amount of sediment settling in the last two sectors. In the LE there is even sediment import from the inner shelf. These figures would indicate that the estuary

should be silting up and eventually close. Since this doesn't happen the conclusion is that episodic events are strong enough to re-establish the current profile time after time. The 25h measurements were done during a relative quiet period under mild conditions that fairly represents the day to day conditions.

From the results it becomes clear that the river discharge determines the direction of transport for both salt and sediment. A lower discharge means a larger transport inward. A high discharge means that transport is lower or even directed outward. At 1000 m^3/s all salt is flushed out (Schettini 2002).

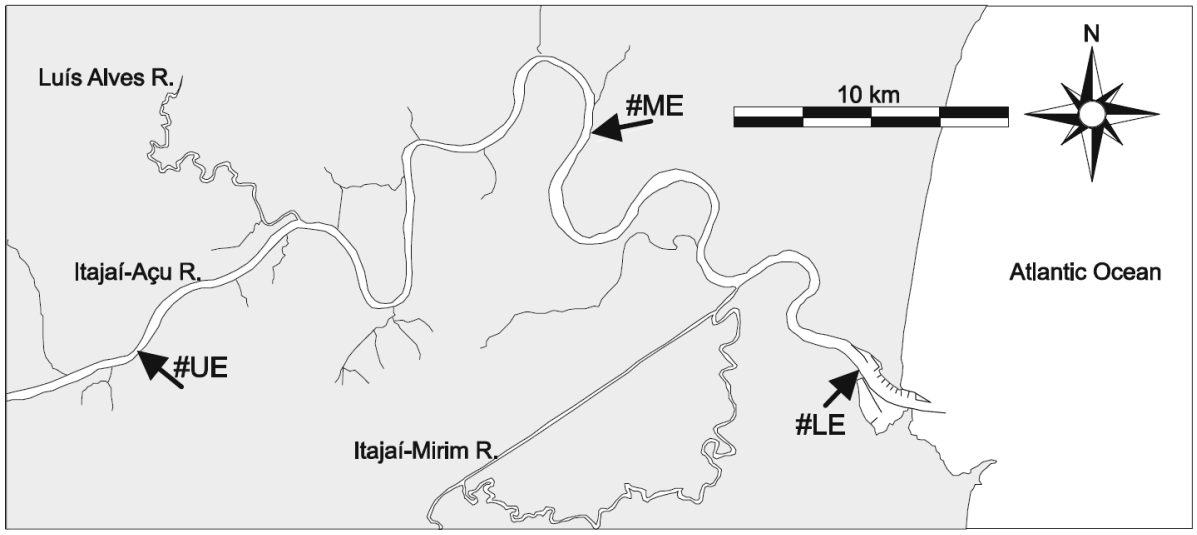

Fig. 2-10: The three indicated segments: LE, ME and UE (Schettini 2002)

2.7 Maintenance & dredging

Van Oord has executed the maintenance dredging for the past years. This gives an estimate of the amount of sediment that is settling in the current and previous situation. In appendix IX (ARCADIS 2009b) the figures are presented.

Van Oord did also numerous echo-soundings before every dredging cycle. For sedimentation results this is useless since there is no knowledge about the dredging result after the previous cycle. There is however one record of an idle period between 6th of August 2006 and 24th of September 2006. The soundings were done with two frequencies, respectively 33KHz and 210KHz. The lower frequency measures the top of the more dense mud layer which is considered to be consolidated soft mud. The top of the soft mud layer is measured with the higher frequency. The difference between the measurements of the high and low frequency shows the thickness of the soft mud. The low frequency measurements show the top of the dense mud layer and hence the bottom of the soft mud layer. The high frequency shows to top of the layer of the soft mud. Hence the two measurements with the two frequencies delineates the top layer which is the soft mud layer.

The deposition areas are visualized in appendix IX in Fig. 9-36 Fig. 9-37 Fig. 9-38 Fig. 9-39 (ARCADIS 2009b). The first thing that can be noticed is the deposition location for the two different sediment categories. The more dense mud (33kHz) is more upstream and the fluid mud (210 kHz) is more downstream.

It is clear that maintenance is already a big project due to large volumes of sedimentation. This is induced by the harbours expansion. The dredging figures do not give a straightforward image of the sedimentation behaviour. But some conclusions have been drawn by Van Oord by experience.

In general the largest depositions are during medium discharges. This means that very low discharges do not carry any significant amount of sediment (ARCADIS 2009a). It is also known that after high discharges there actually is erosion to be found. This is also concluded by (Schettini 2002). What is also recorded is that after long periods of lower discharges the next high discharge is loaded heavily with sediments. This is probably due to the fact that upstream during the low discharge, volumes of sediment have been deposited. In the end, the sediment will deposit in the channel unless the discharge is large enough to transport it out of the harbour basin area.

On average it can be said that in the earlier years of the harbour maintenance resulted in several hundred thousand cubic meters per maintenance cycle that was done irregularly over the years in the seventies, eighties and nineties. Between 1998 and 2006 maintenance volumes have risen to 1.5 million to 2 million per year. This the result of deepening of the harbour. This resulted in stronger attraction of sediment as the depth was further below equilibrium depth.

3 Concept of a river bypass

To get an understanding of the principles of a bypass in a coastal area, the general aspects of a river bypass will be addressed in this chapter. First the location will be presented. This gives the opportunity to place all theory into the perspective of the Itajaí-Açu River system.

Next, the basic schematization is given to address the relevant aspects shortly and the relevant aspects will be explained next. In that last section only the estuarine aspects are treated since they have the largest impact. For the more basic treatment of bypass aspects in a non-estuarine situation a description is given of a few relevant processes in appendix I. These processes are relevant in non-estuarine areas but not here as they are dominated by the estuarine processes. For a thorough understanding of a bypass this is however an interesting section for comprehension of a bypass in general.

3.1 Location of the bypass

The bypass itself is located about 11 km upstream of the river mouth. This is for several reasons. In Fig. 3-1 the position of the bifurcation point is shown with the red dot. From there on the river stretch downstream is covered by the bypass. The upstream part is also covered by the bypass since its influence diminishes when moving further upstream away from the junction. However from this point the major part of Itajaí is covered and also a significant section of the river upstream of the bifurcation point. Besides that, it is also a convenient spot since there is not so much housing in that area that would have to be removed.

Two other possibilities would be the next outer bend more downstream. But this would not cover much of the Itajaí area. Or the next upstream bend w.r.t. the chosen one. But that would mean a much longer bypass while not protecting a lot of additional populated area. Further, the route of the bypass is chosen arbitrarily. It has been chosen to be as short as possible to reduce excavation expenses. The only aspect that has been taken into account besides avoiding populated areas is a preference for low and flat areas.

Fig. 3-1: Bypass location

3.2 Basic aspects of a river bypass

Below in Fig. 3-2, a simplified schematization of a bifurcation is shown. A river branch splits up into two branches that end up in a lake in this case. The most complex part is the bifurcation. Around that point, rather complex processes are going on that determine the sediment distribution over the branches. This distribution determines the development of the system in time. Since in this situation fine sediment transport is the case here, one cannot look at transport capacity by flow alone, since fine sediment does not respond instantaneously to the behaviour of the hydrodynamics. Another important aspect is the fact that the bifurcation is in a estuarine area and is therefore also influenced by coastal processes such as tide and salinity. Tidal behaviour and salinity dynamics will change due to the bypass. For sedimentation it is also possible that a circulation of sediment will occur in the system.

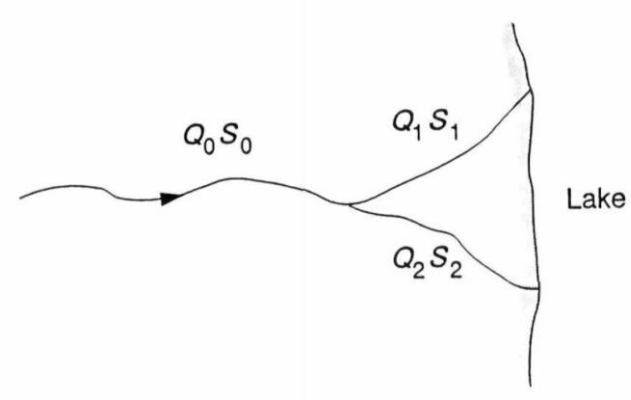

Fig. 3-2: Concept of a river bypass (Wang, Fokkink et al. 1995)

3.3 Influence of an estuarine situation

Additional to the non-estuarine aspects discussed in appendix I, the situation in Itajaí entails predominantly estuarine behaviour. This is explained by the two main contributors to this behaviour, which are: tidal behaviour and gravitational flow. This influences the hydrodynamics strongly. therefore also the sediment dynamics. As mentioned before the sediment behaviour can determine the sustainability of the bypass as it can increase maintenance cost.

In this section, four aspects are looked at that are relevant processes in an estuarine area for a sustainable channel. These are related to the tide, gravitational flow, salinity structure and fine sediment.

3.3.1 Tidal behaviour

Something relevant in the case of a tidal river is the interaction with the tide. A tidal wave can cause residual currents in shallow areas such as the river basin. These residual currents can be very small. They can average out but asymmetry than might still result in a residual sediment flow due to the non-linear response of sediment transport to flow velocities. This will be further explained here.

When a simple M2 tide is used with no additional components on the model's boundary it will render higher harmonics as well. In general only the M4 and M6 higher harmonics are relevant since others are significantly smaller and transport rates have shown to average out over a longer period of time (Bosboom and Stive 2011). The higher harmonics are mainly generated by interaction of the M2 component with the:

- bathymetry
- bottom-friction
- wave-current interaction

The reason why the combination of these components generates a residual sediment transport is due to asymmetry. The current in a progressive wave changes direction during the tidal cycle. When the current is stronger in one particular direction than in the other this will induce a residual transport rate. This is due to the non-linear behaviour of sediment transport with relation to flow velocity. To explain this process it is shown how bed-load transport due to a set of harmonics can be described analytically. Fine sediment transport is more complex and therefore coarse sediment is used for this explanation. Another assumption is a scenario where the residual flow is small. Conditions for this approach are described and shown to be reliable by (Kreeke and Robaczewska 1993). Residual flow could be a river discharge. This discharge needs to be small in comparison to the flow velocities induced by the tide. This is for simplifying terms of the M2, M4 and M6 velocity components later.

When the following transport formula for bed load is used:

$$S = c * |u^{n-1}|u \tag{3.1}$$

With:

- S = sediment transport [$m^3/m/s$]
- c = coefficient [$m^{2-n} s^{n-1}$]
- u = flow velocity [m/s]

With the coefficient n=3 for bed load, and no threshold for motion it can be combined with the formulation for the velocity signal:

$$u(t) = u_0 + \hat{u}_{M2} \cos(\omega_{M2} * t) + \sum \hat{u}_i * \cos(\omega_i * t - \varphi_i) \tag{3.2}$$

With:

- u_0 = the Eulerian residual flow [m/s]
- $\hat{u}_{M2}$ = the amplitude of the M2 tidal current [m/s]
- $\hat{u}_i$ = the amplitude of the other tidal current constituents [m/s]
- ω_{M2} = the angular frequency of the M2 constituent [rad/s]
- ω_i = the angular frequency of the other tidal current constituents [rad/s]
- φ_i = the phase lag between M2 and the other tidal constituents. [rad]
- t = time [s]

(Kreeke and Robaczewska 1993) have shown that when the M2 constituent is large compared to all other constituents and the residual flow, one can fill out equation (3.2) in equation (3.1) and arrive at the following equation:

$$\frac{S}{c\hat{u}_{M2}^3} = \tag{3.3}$$

$$\frac{3}{2}\frac{u_0}{\hat{u}_{M2}} + \frac{3}{4}\frac{\hat{u}_{M4}}{\hat{u}_{M2}}\cos(\varphi_{M4-2}) + \frac{3}{2}\frac{\hat{u}_{M4}}{\hat{u}_{M2}}\frac{\hat{u}_{M6}}{\hat{u}_{M2}}\cos(\varphi_{M4-2} - \varphi_{M6-2})$$

$\Phi_{m4\text{-}2}$ is the phase lag between M4 and M2 which is $\phi_{M4} - 2\phi_{M2}$. This can be explained by the following expression

If:

$$\eta(t) = a_{M2}\cos(\omega_{M2}t - \varphi_{M2}) + a_{M4}\cos(\omega_{M4}t - \varphi_{M4}) \tag{3.4}$$

And:

$$\omega_{M4} = 2\omega_{M2} \tag{3.5}$$

$$t' = t - \varphi_{M2}/\omega_{M2} \tag{3.6}$$

With:

- η = water level deviation in time [m]
- a_i = amplitude of constituent I [-]

Then:

$$\eta(t) = a_{M2}\cos(\omega_{M2}t') + a_{M4}\cos(2\omega_{M2}t' - (\varphi_{M4} - 2\varphi_{M2})) \tag{3.7}$$

Further, on the right-hand-side of (3.3) there are three terms. They all account for different contributions. The first term on the RHS mentions the transport due to asymmetry introduced by the wave-current interaction of the M2 component with a river discharge.

The second term is the contribution by interaction of the M2 and M4 component. It is obvious that the phase difference between M2 and M4 is determining how much and in what direction this term is contributing.

The third term is the interaction between M2, M4 and M6. The amount and direction is determined by the phase difference between M4 and M2 and M6 and M2.

What is also clear is that there is no term that describes the interaction between M2 and M6. This is due to the fact that whatever the phase difference is, there is no residual sediment transport. This is because the combined signal of M2 and M6 only shows saw-tooth asymmetry meaning that there is the same positive as negative signal for the combined signal meaning that when to the third (or higher) power there is no dominating direction that has the largest sediment transport.

The results can be visualized as follows in Fig. 3-3 with only an M2 and M4 combination. Only the M2 and M4 components are used to simplify the visualisation. Hence the angle φ is the phase difference between the M2 and M4 signal. The figure shows the combination of two harmonics combined. The continuous line is the M2 signal. The bold dashed line is the M4 component. And the fine dashed line is the signal of the M2 and M4 combined. The result of the difference in phase shows that the difference will determine the direction of the maximum velocity hence the residual transport of sediment.

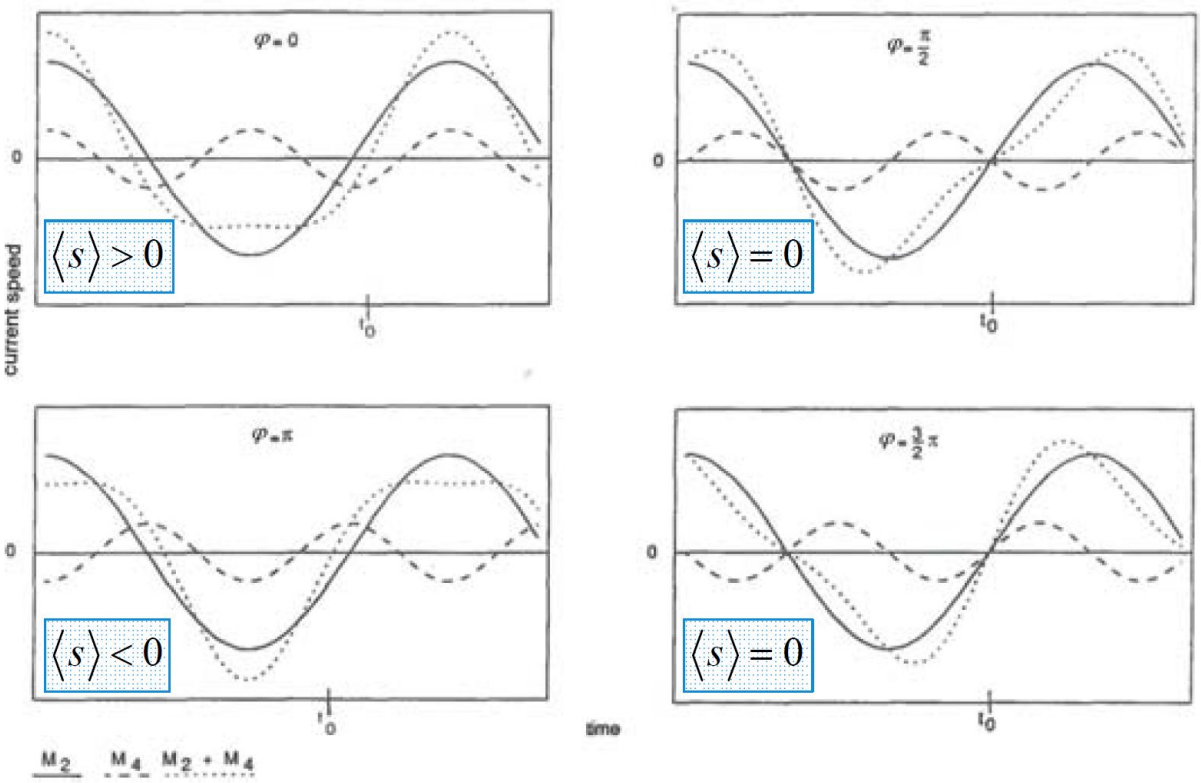

Fig. 3-3: Tidal asymmetry by M2 and M4 (Bosboom and Stive 2011), $\varphi = \varphi_{m4} - 2\varphi_{m2}$

The actual transport of sediment depends on the phase difference between the components as mentioned before. When the phase difference is π/2 or 3π/2 the residual transport is zero. When the phase difference is 0 the transport is in the positive x direction. And for the phase difference of π it is at its maximum in the negative x-direction.

During the research phase in this project it was found that tidal asymmetry changes. Change in tidal asymmetry is not significant due to another phenomenon that arises with a 2-channel tidal system. The theory behind this other phenomenon will be elaborately explained in section 5.3.

The tidal behaviour of the Itajaí-Açu system is important. The general influence of a tidal signal on sediment transport has been explained in a general way. But since this system is coping with fine sediment the asymmetry is even more important.

3.3.2 Gravitational circulation

In this system, fresh and salt water meet. The two water bodies are not strictly separated. Due to turbulence the two water bodies will tend to mix, but density difference will tend to keep the two water bodies separated. When salt water is put in a tank with fresh water the salt water will settle below the fresh water due to a higher density. This means that the same will happen at the mouth of a river. The salt water will move under the fresh water. How far upstream the salt water can move depends on the river discharge. A high discharge can force the salt water out because of friction between the two water bodies passing each other. For a lower discharge one first needs to understand the balance of forces between fresh and salt water.

When one looks at different depth averaged densities along the length of the river one can see that the density is decreasing in an upstream direction. This means that when two virtually adjacent

water bodies have different densities there is also a different water level to keep a balance in forces. Fig. 3-4 below schematizes this. The water body on the left has a higher density (+Δρ). To keep F_1 and F_2 in balance the water level on the right (h_1) needs to increase (+Δh). The resulting forces F_1 and F_2 are equal now. But they do not act along the same working line. This results in a moment M. When salt water starts to flow inward from left to right this will shear the bottom. This bed shear stress is directed in the opposite direction of the incoming salt water flow. Hence the total bed shear force acts in the same direction as F_1. The faster the flow the more bed shear occurs. Hence the incoming flow is depending on the equality between F_1 and F_2.

During lower discharge something changes. Due to a lower discharge the gradient of the water surface is lower. As the fresh water body requires an additional height (=Δh) the lack of height is compensated with salt water under the freshwater. At the sea mouth salt water is predominantly present and only a thin layer of fresh water is on top. As the water level rises along the river less salt water is present under the fresh water. Every step further upstream the water level rises and the salt water layer thins out. This explains how a low discharge results in a deeper intrusion. During low discharges the gradient is low. Hence it requires a longer distance along the river to aquire the required height (=Δh).

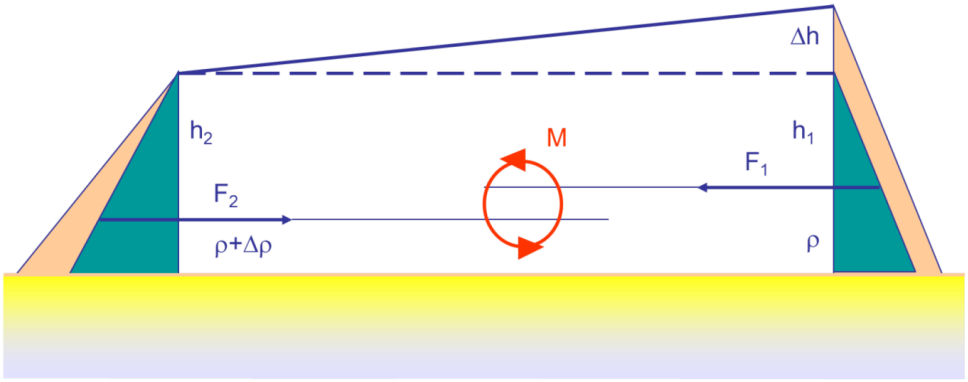

Fig. 3-4: Gravitational flow (Savenije 2006)

Since a flow will result from a stationary situation it means that the fresh water flowing out is shearing the salt water body on the interface. Mixing of these two layers means that the saline water particles on top of the salt water body are affected and become less salt, hence less dense. They will rise and end up in the outward flowing fresh water body. The displaced saline water particle is than replaced by more salt water flowing inward. It is clear that the outflowing freshwater causes an inflowing salt water volume. This is within the salt water body. This salt water body is positioned at the bottom. While the fresh water body is positioned at the top of the salt water body. Since it is known that the highest sediment concentrations are in general at the bottom this means that even though the inflowing salt water is close to the fresh water in volume it doesn't match it in sediment concentration. This can result in a net inflow of sediment.

This phenomenon is the strongest with a high salinity gradient. Hence a short salt water body yields a stronger gravitational flow. (Savenije 2006) has found that gravitational flow is the strongest in small prismatic channels. A wide estuary for example has a low salinity gradient because the sea water can move in much further before it starts to mix with fresh water. The transition to fresh water

is much longer. In the case of a river, the transition from fresh to salt water is much shorter. Here the gravitational circulation is in general dominant (Savenije 2006).

It is known that the salt intrusion can get as far as 30 km upstream of the Itajaí-Açu River mouth during the right conditions. This means that gravitational flow is influencing the river for a long distance. Because the new 2-channel system distributes the "outflow" it is possible that the impact of heavier salty sea water increases strongly. Another thing is that with a two channel system one cannot think of it as being a serial chain of cross-sections. Now it has a parallel part between the bifurcation and the sea. The depth and width integrated force on the mouths of both channels due to density differences can differ so much that flow could reverse in one of those channels considering a tidal averaged flow. This can be explained differently as well.

When looking at Fig. 3-4 and consider this for both channels one channel might require a larger Δh at the bifurcation than the other to be in equilibrium with the density difference induced force at the mouth. This is impossible since at the bifurcation the water level is the same for both channels. Hence a lower Δh than required for one channel, to be in balance with the density induced force, can result in a net force that is directed upstream if the driving water level gradient is not strong enough anymore to resist the opposing density induced force. This is indeed found during low discharges in the current branch. During low discharges the forces on the two mouths is rather large compared to friction. Hence a difference between those two forces can strongly influence the distribution at the bifurcation point. When friction forces are very it actually happens that the difference in density induced forces on the mouths is so large that averaged over a tidal cycle water flows in an upstream direction in the current branch.

3.3.3 Salinity structure

To have a proper understanding of gravitational flow it is important how the fresh and salt water bodies are in balance. This can be done by looking at the salinity structure. The salinity structure explains how the interface between the two water bodies behaves and how energy is exchanged along with diffusion and advection of salt.

Flow ratio

(Simmons 1955) proposed a classification based on the ratio of the tidal prism and the cumulative river discharge during a tidal cycle:

$$P = \frac{u_f}{u_t} \tag{3.8}$$

For the river flow velocity:

$$u_f = \frac{Q_r}{A_r} \tag{3.9}$$

With:

- Q_r = river discharge [m^3/s]
- A_r = cross-sectional area of the river [m^2]

For the tidal flow velocity the root-mean-square of the tidal current peak velocity:

$$u_t = RMS\,(U_t) = \frac{U_t}{\sqrt{2}} \tag{3.10}$$

With:

- u_t = root mean square of tidal flow [m/s]
- U_t = tidal flow amplitude [m/s]

The following domains of P belong to different salinity structures:

- If $P < 10^{-2}$ system is well mixed
- If $P > 10^{-1}$ system is stratified

Estuary number

An estuary number can be formulated as follows:

$$Ne = \frac{PF_m^2}{TR} \tag{3.11}$$

- If Ne > 0.1
- If Ne < 0.1

With:

- P = tidal prism [m^3]
- T = tidal period [s]
- R = river discharge [Q^3/s]
- F_m = densimetric Froude number [-]

The densimetric Froude number is formulated as follows:

$$F_m = \frac{u_f}{\sqrt{g\left(\frac{\Delta\rho}{\rho}\right)h}} \tag{3.12}$$

The densimetric Froude number is based on relative gravitational pull and not on the complete gravitational pull. If a parcel is in an environment with the same density, it acts as weightless. The formulation of the densimetric Froude number originates from the Richardson number (Ri). This formulation shows the relation between kinetic and potential energy:

$$Ri = \frac{gh}{u^2} \tag{3.13}$$

Or:

$$Ri = \frac{1}{Fr^2} \tag{3.14}$$

When looking at a submerged particle it has a different kind of potential energy than would be expected in a vacuum. The Richardson number can be rewritten with a relative gravitational pull:

$$Ri = \frac{\sqrt{g\left(\frac{\Delta\rho}{\rho}\right)h}}{u_f^2} \tag{3.15}$$

With:

- $\Delta\rho$ = density difference between fresh and salt water [kg/m^3]
- ρ = density of the fresh water [kg/m^3]
- u_f = Cross-sectional averaged flow = average river flow [m/s]
- h = depth [m]
- Ri = the Richardson number [-]
- u = flow velocity [m/s]
- g = gravitational acceleration [m/s^2]

Since the potential energy of a parcel in a fluid with equal density is 0, the measure of density-difference can be seen as a factor of potential energy. If the Richardson number is much smaller than one, the density differences are negligible compared to the velocities. This tells us that the density differences that would keep fluids from different densities separated is too small compared to the mixing action of the flow. If the number is unity or even larger this means that the density differences are large compared to the mixing flow. This way the density differences separate the two fluids by gravity.

Stratification number

(Ippen and Harleman 1961) investigated the effect of tidal energy dissipation. More energy dissipation means more energy used for mixing. Therefore inefficiency stands for mixing. The energy transport through a cross-section is:

$$P_x = -cbg\rho A_0^2 \sinh(2\mu x) \tag{3.16}$$

With:

- P_x = Rate of transport of tidal energy [J/kg]
- c = wave celerity [m/s]
- b = cross-section with [m]
- g = gravitational acceleration [m/s^2]
- ρ = density [kg/m^3]
- A_0 = tidal amplitude at the mouth [m]
- μ = damping coefficient [N s/m]

The amount of dissipated energy per mass of water is

$$G = \frac{P_{x_1} - P_{x_2}}{\rho bh(x_1 - x_2)} \tag{3.17}$$

Opposed to dissipation there is another process. When a freshwater parcel moves seaward it gains weight by mixing with heavier salt water. This gives it an increase potential energy. This increase of potential energy per mass of water is formulated as:

$$J = \frac{g\left(\frac{\Delta\rho}{\rho}\right) hu_f}{L} \tag{3.18}$$

(Ippen and Harleman 1961) stated that stratification is represented by the ratio of (3.17) and (3.18). The ratio of gains and loses give an estimation of the eventual salinity structure.

(Prandle 1985) found that similarly a method that described these gains and losses over an entire estuaries length. The stratification number according to (Prandle 1985):

$$S_t = \frac{G}{J} = \frac{0.85kU_tL}{\left(\frac{\Delta\rho}{\rho}\right)gh^2u_f} \tag{3.19}$$

- If S_t < 100 system is stratified
- If 100 < S_t < 400 system is partially mixed
- If S_t > 400 system is well-mixed

With:

- S_t = stratification number [-]
- k = friction coefficient [-]
- U_t = amplitude of tidal flow [m/s]
- L = estuary length [m]
- $\Delta\rho/\rho$ = ratio of density difference ($\rho_{salt} - \rho_{fresh}$) and freshwater density [-]
- h = depth [m]
- u_f = depth mean current [m/s]

3.3.4 Fine sediment transport in a tidal river.

In the case of Itajaí it is important to be aware that the system's sediment consists mainly out of fine sediment. Fine sediment means that more processes play a role than just transport capacity by water flow. Fine sediment transport rates in a tidal river are strongly influenced by:

- Flow and residual flow directions in combination with the lag effect
- Flocculation of cohesive sediments

Fine sediment does not respond instantaneously to flow changes. This makes it impossible to average out flow velocities and directions. These hydraulic transport directions and distributions of a system might be different than that of the sediment transport. The best way to look at the hydro-dynamics of a system is by decomposing the most important factors of water movement and residual movement. With these decomposed a qualitative prediction can be done on sediment transport. Important hydrodynamics for fine sediment are:

- River flow
- Gravitational circulation
- Tidal asymmetry

River flow is the most straightforward of these three. It is the net result of water export by the river. With steady flow the approach is relatively straightforward. However, cohesive sediment has a threshold level of bed shear stress to be mobilized. And besides that the tidal flow causes a non-steady flow in the river. Related to the non-linear relation between sediment and flow this results also in a more complex view on sediment transport.

The second is circulation due to density differences. This is due to the density difference of fresh and salt water. The water coming down the river is not as heavy as the water from the sea. This is previously explained in section 3.3.2.

Another important aspect for sediment transport is tidal asymmetry. This is a result of different harmonics that result in a net water flow that could for example be the river flow. Sediment however responds non-linear to flow velocities. This non-linear response can result for example in a net transport for sediment while the hydrodynamic movements are averaged out to zero.

Another influence on fine sediment behaviour is cohesion. Flocculation occurs with this kind of sediment in a saline environment. This means that instead of separate grains there are particles "sticking" together. In this way high porosity is possible. Relative very low densities can occur. Relative density is how dense a volume is when submerged. If a volume consist mainly out of water due to large pore, as with flocculated particles, it's density is not much higher than water, hence a rather low relative density occurs. This is a reason why fine sediment does not obey Stokes law regarding falling velocity. Hence the falling velocity depends on how the fine sediment flocculates.

In section 3.3.1 the response of sediment has been explained. This is in fact the response of course sediment. Since the situation in Itajaí entails fine sediment it is important to know what the implications are with fine sediment in combination with a tide.

As mentioned before fine sediment does not respond instantaneously. The behaviour is similar to diffusion. A relaxation time scale, an equilibrium concentration and a current concentration determine the rate of change of the concentration. The equilibrium concentration is a property that is determined by flow and sediment properties. Hence this can change over time (time dependent flow) and over space (different sediment types distributed over the system and the hydrodynamic behaviour changes from place to place). In a formula it can be stated as follows:

$$\frac{dc}{dt} = \frac{1}{T_{eq}}(c_{eq} - c) \tag{3.20}$$

With:

- t = time [s]
- T_{eq} = relaxation time scale [s]
- c_{eq} = equilibrium concentration [kg/m^3]
- c = concentration [kg/m^3]

Below an arbitrary solution is shown in Fig. 3-5. In there the over the tide four different variables are shown. The flow velocity (u), the equilibrium concentration (c_e), the occurring concentration (c) and the critical velocity (u_c) at which sediment starts to erode or settle (these threshold velocities for erosion and sedimentation are in general not equal). The phenomenon of the concentration lag from instantaneous response is called the lag effect. The result becomes clear when looking at the example given in Fig. 3-5. Here the high water slack (HWS) duration is longer than the low water slack (LWS). HWS means the time that it takes of flow reversal from flood to ebb. Flood meaning rising water and ebb meaning falling water. The fact that the water is standing still for a longer time during high water means that it is settling more at that moment. At LWS the flow reversal doesn't take that long. And when the flood flow starts again the suspended sediment concentration hasn't dropped as much meaning that it is carrying more sediment in the flood direction. It is obvious why this

phenomenon does not apply for coarse sediment. Slack is not necessary for coarse sediment to settle due to the instantaneous reaction of the particles. So difference in slack duration is of no influence for coarse sediment, but very important for fine sediment.

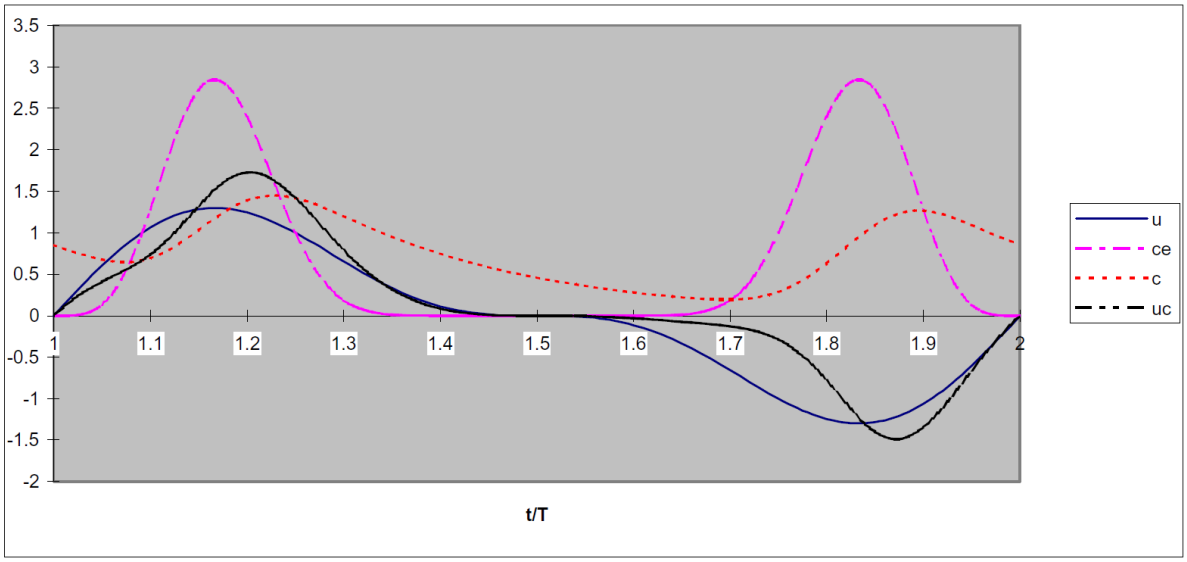

Fig. 3-5: Result of lag effects with fine suspended material (Wang, Jeuken et al. 1999)

In the Itajaí-Açu River the main sediment component is fine sediment. As described in this section and in section 3.3.2 is important to understand the implications of fine sediment in a system as in Itajaí.

In the past research has been done on the sediment properties in the Itajaí-Açu by (Cornelisse, Kesteren et al. 2000) . As mentioned about fine sediment there is a lag effect that is one of the causes of the difference between water transport and sediment transport rates. The research done in the past was based on a physical analysis of four samples from the Itajaí-Açu-river. The conclusion was that the grain size distribution has a D_{50} between 10µm and 30µm. Since it is fine sediment the important aspect is settling velocity. For the relationship between particle size and settling velocity a model by (Winterwerp 1999) was used. The settling velocity is determined to be in between 0.05 mm/s and 0.2 mm/s.

For the sediment erosion and sediment accretion rate there are the following formulations. For accretion:

$$\frac{dm}{dt} = m_e(\tau_0 - \tau_e), \qquad for\ \tau_0 > \tau_e$$
$$\frac{dm}{dt} = 0, \qquad for\ \tau_0 \leq \tau_e \tag{3.21}$$

With:

- dm/dt = rate of erosion [kg m^{-2} s^{-1}]
- m_e : typically has a value of 0.002 [kg N^{-1} s^{-1}]
- τ_o = occurring bed shear stress [N/m^2]
- τ_e = threshold level of bed shear stress to initiate erosion [N/m^2]

In Fig. 3-6 one can see how this formula relates to measured data. The dashed lines indicate the limits of scatter in the experimental data (variation of m_e). For sedimentation a similar approach is used as a formulation of mass rate of sedimentation related to difference of occurring bed shear stress and threshold bed shear stress:

$$\frac{dm}{dt} = -\left(1 - \frac{\tau_0}{\tau_d}\right) C_b w_{50}, \qquad for\ \tau_0 < \tau_d$$
$$\frac{dm}{dt} = 0, \qquad for\ \tau_0 \geq \tau_d \tag{3.22}$$

With:

- C_b = Near-bed concentration [kg/m^3]
- w_{50} = median settling velocity [m/s]
- τ_o = occurring bed shear stress [N/m2]
- τ_d = threshold bed shear stress for deposition [N/m2]

Typically the settling bed shear stress threshold level is half of the erosion bed shear stress threshold level and is in between 0.06 N/m^2 and 0.10 N/m^2. However they are not directly related and need to be determined with tests.

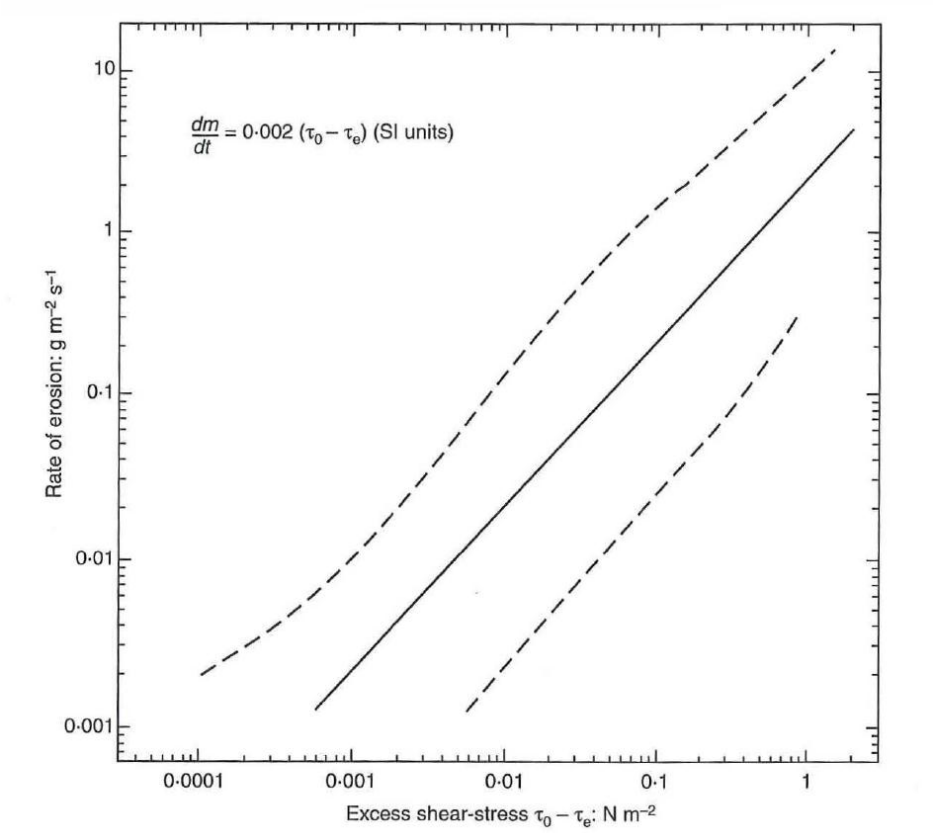

Fig. 3-6: Rate of erosion in currents as a function of excess bed shear-stress (Delo 1988).

3.4 General conclusion for Itajaí-Açu

All the aspects summed up can have a significant influence on the system together. Especially the gravitational flow and the changes to the tide in the river can cause a drastic change to the behaviour of the system.

Another important step in every form of analysis is to keep in mind that sediment transport is not responding the same as the water discharge. Specifically in this case due to the non-instantaneous response of fine sediment.

4 Models

This research report is based on theory and model results. The start has been made with a theoretical literature study. The next step after the literature study has been to build a simple model or method to determine the required capacity of the bypass. This was done in a very rudimentary way. This had two advantages. First of all the models gave insight in the behaviour of the system in a simplified way. The second advantage is the speed with which a bypass can be determined. That was of great importance since it was not the main question to find an optimal solution.

The next phase was using the new situation as found with the simple models to investigate its new behaviour. The comparison between old and new is done in stages. Separate processes are identified as the most important ones. These are investigated thoroughly as isolated processes and as combinations. This has been done with Delft3D. This is a numerical simulation programme that is able to simulate complex behaviour step by step in time. This allows a user to calibrate the parameters in such a way that it behaves according to the current situation so that it is calibrated en the next step is than that it can be applied to a slightly changed situation to see what the new behaviour is.

This section will elaborate on the use of these models and give their description how the details of each model work. In this report however, there the focus is on the results from Delft3D. The methods and results from the simple models can be found in appendix III. A short explanation is given here.

4.1 Simplified models

Two methods have been used in this thesis. One was specifically meant for determination of the water level along the river axis. This was done with the Bélanger formula. Another method was to look at flow velocities during high discharges. In the past during extreme events high flow velocities have caused scour holes that have led to the collapse of quay walls in the Itajaí harbour. Eventually the last method demanded the largest capacity from the bypass. The bypass had to transport a very large portion of the total discharge to prevent extreme scour in cases of one in 50 or 100 years floods. The conclusion is that the bypass is 300 meters wide and 7.6 meters deep. The depth is determined by the depth at the bifurcation point. It cannot be deeper than the river since that would not add to the capacity of the bypass. With this depth the width of 300 meters is found to meet requirements of a reduction of 70% of discharge in the current branch. This requirement comes from the scour model. Another requirement is that it leads rather straight to the sea without going through too much urban area. The requirement of being as short as possible is to keep the resistance in the bypass low. With a higher resistance the bypass needs to be wider to attain the same capacity. Detailed results from this preliminary research can be found in appendix III.

4.2 1D models

A part of the literature study done for this thesis, covered some research on existing 1D models. The theory they were based on and the short comings of the models gave a useful understanding of the difficulty of how to relate theory to reality. In appendix II the theory and conclusions can be found. It shows the extent of the possibilities of 1D models. The evolution with newer models showed the desire for improvement and the arguments why. That made it possible to understand why or why not use 1D models. The main reason for 1D models is that they are focussed on one process that dominates the development or already depend on the equilibrium of the system. The

first might be very of the actual processes that are at play. And the second requires an understanding of the system that one is actually looking for. Hence the behaviour based 3D model gives more reliable output. Albeit that the processes that are simulated have to comply with the theory.

4.3 Delft3D

Delft3D by Deltares is numerical modelling software for behaviour based simulations. Due to the complexity of the Itajaí-Açu system a comprehensive model was required. In the past Delft3D has been used by ARCADIS for projects in Itajaí before. The existing model has been improved several times by ARCADIS for project purposes. The first version of the Itajai-Açu model has been set-up in 1993 by ARCADIS. The latest setup was calibrated in 2009. Results of this set-up and calibrations can be found (ARCADIS 2009a). It has shown to be rather accurate. This model has been used to model the salt intrusion for a planned harbour expansion in the Itajai harbour area. It has been calibrated on the current measured salt intrusion. Besides the salt intrusion it has also been calibrated on sedimentation behaviour in the harbour area. Since the dredged volumes are known it was possible to calibrate this model as well on sedimentation and erosion behaviour based on a one year climate and conditions. However, for this investigation actual sediment behaviour has not been modelled.

Since the questions in this thesis require a detailed understanding of the processes in the Itajaí-Açu River a numerical model such as this Delft3D model was used.

In this way it was possible to separate and combine the different processes that determine the discharge distribution, water levels, tidal flow, salinity dynamics and bed shear stress. The input and properties of the model as it has been set-up will be explained in this section

4.3.1 Model grid

The grid covered the river until 70km upstream from the river mouth. This was done to be able to model the salinity dynamics and water levels in the system properly. It was calibrated in a 3D set-up for the correct representation of the current salinity dynamics. Next to that it has been calibrated to measured water levels along the river further upstream.

For this project the grid had to be adapted to fit in the bypass. There are two possibilities to attach two grids together. One of them is by boundary decomposition. And the other would be simply extending the current grid with grid cells. Both have disadvantages and advantages.

When simply extending the current grid with additional grid cells this would mean that a specific row index of the grid matrix of the bypass had to connect to the same row index of the matrix at sea. This is a problem since at the bifurcation the two rows that connect the bypass and the current river are a few kilometres separated when getting to the sea. This is shown in Fig. 4-1. The bypass there for had to be extended not only in the direction of the sea but also extended in rows to the north without moving to the north. Below the method used is shown in Fig. 4-2. Additional cells are added over a length before the bifurcation. And afterward the upper rows are removed from the current river branch.

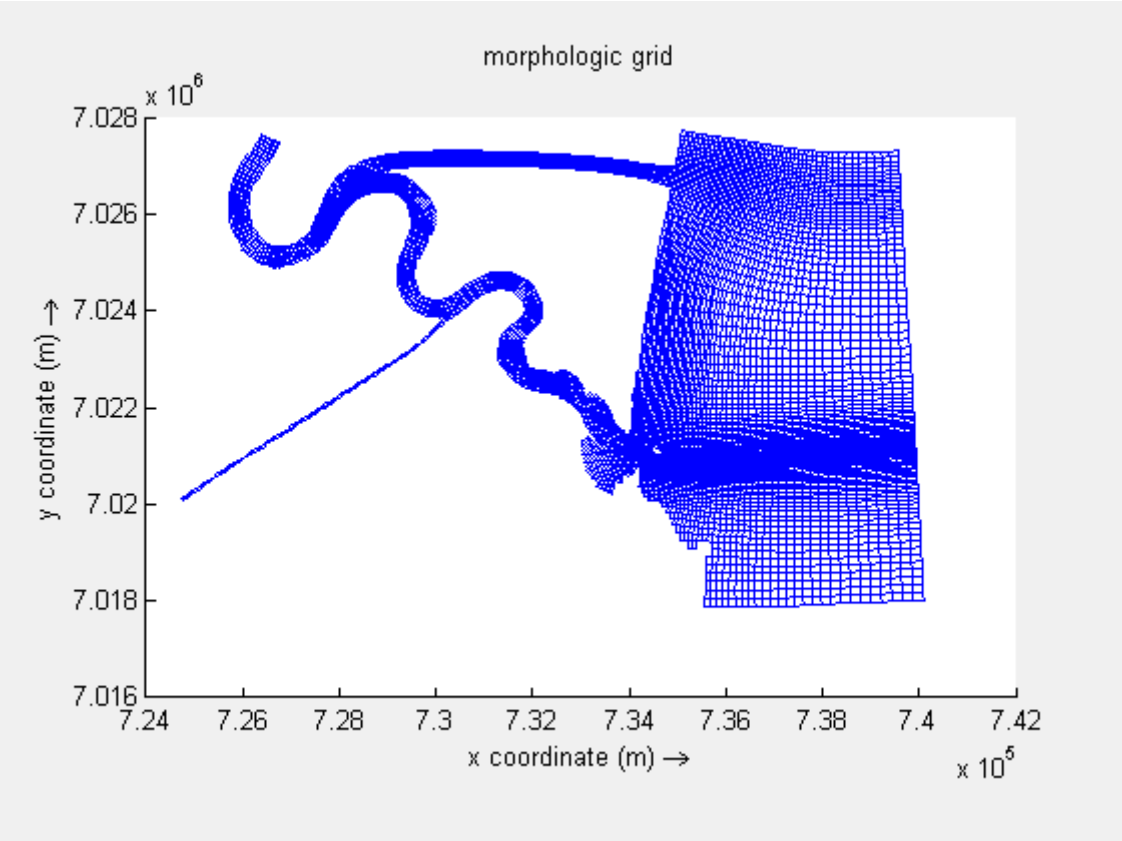

Fig. 4-1: Computational grid of the bypass

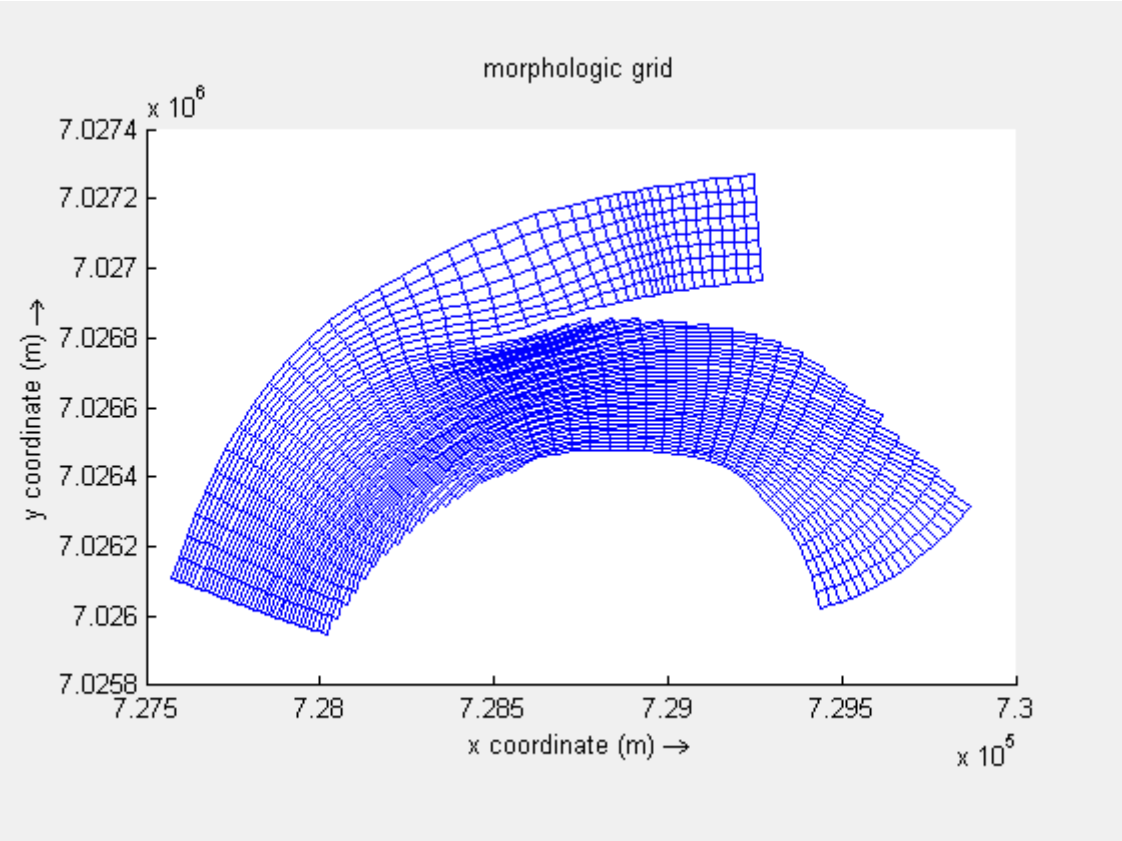

Fig. 4-2: computational grid at the bifurcation

This is a very work intensive method. Especially when fine-tuning the grid for numerical accuracy. Another method that would prevent this is boundary decomposition. This makes it possible to connect two different grids regardless what the index is of adjacent cells at the grid interfaces. Both grids are computed separately using each other's boundaries as boundary conditions. This method would mean that both domains are computed parallel. Hence this is only computationally efficient if both domains have the same size. This is not the case here. Efficiency is therefore a reason not to choose boundary decomposition.

To be able to make a justified comparison between the old and new situation the grid for the bypass is used for the current situation as well. The bathymetries of the bypass and the current scenario would then be interpolated on the same grid. This way observations and numerical errors should remain the same.

For the model that will calculate the scenarios with salinity a 3D model was required. Since that was already set-up in the past in a 20 layer grid this is used here as well.

Something to keep in mind is the high courant number in the grid refinement area around the bifurcation. They vary from 5 to 10 and in some place near 15. The high courant numbers are caused by the very small width of the cells in combination with large depths. Since it can be assumed that at these high discharges it is possible that the water flow follows the cell direction. What has to be kept in mind is that the highest values are found inside the current river branch in a location where the water will follow the length direction of the cells anyway. The dimensions of the cells differ very much depending what direction is considered (x or y) and if it is near the bifurcation grid refinement. Lengths outside the refinement are in the order of 25 m to 110 m. Inside the refinement the lengths range from 7m to 70 m as the differences between length and width of these cells are large.

For stability the orthogonality and smoothness are relevant. The orthogonality condition was kept at a maximum of 0.02 for wet cells. The smoothness limit was set at 1.2 for the wet cells.

4.3.2 Bathymetry

For the numerical model the latest bathymetry is used as supplied before to ARCADIS. This is shown below. Important to notice is that greater depth in the harbour area than used in the simplified models. In the harbour a depth of about 14m is found. In Fig. 4-3 the bathymetry data of the major part of the model is shown.

The sources of this information are:

- Van Oord: trajectory of some 6.4 km from harbour to begin of access channel
- Van Oord: trajectory from harbour to 9.3 km upstream
- Community of Blumenau: the depths along the trajectory from upstream of the harbour of Itajaí to Blumenau, herewith the contour of the river banks are plotted as the 0 m contour (surveyed with DGPS)
- Hidrotopo surveys in 2008 – 2012 for harbour and access channel

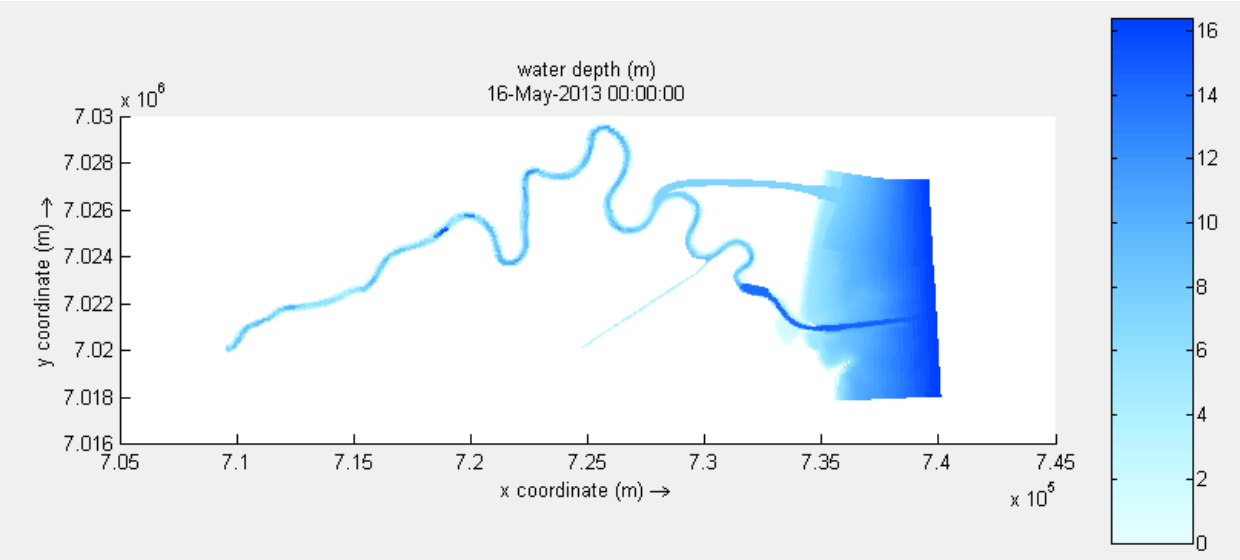

Fig. 4-3: Bathymetry used in model

4.3.3 Hydraulic boundary conditions

The hydraulic boundary conditions are based on two aspects.

- River discharge
- Tide

Waves are not taken into account in this case. Waves are not relevant for the behaviour of the entire system since their area of influence is only at the river mouth. Especially since it would mean a lot of extra computational time it has been neglected as has been done in previous studies as well by ARCADIS.

For the investigation there were three discharges chosen. They are selected to get a variety that represents different conditions that typically occur and are as follows:

- 150 m^3/s
- 230 m^3/s
- 1000 m^3/s

150 m^3/s is a discharge that prevails for most of the time during a dry year and 230 m^3/s is the overall average discharge according to (Schettini, Ricklefs et al. 2006). Another survey showed that the river turns into full fluvial mode above 1000 m^3/s (Schettini and Toldo 2006). Full fluvial means that there is no flood flow anymore. At high water the flow stands still but does not flow in an upstream direction anymore. This also means that the river flushes out all salt intrusion. For salt intrusion it is interesting to see how far the salt water body will move upstream when a similar discharge is applied in the situation with a bypass.

The occurrence of the three discharges is derived from the same distribution shown previously in Fig. 2-3. Exceedance probabilities on a given day are respectively: 70%, 50% and 5%, respectively. These discharges will be applied in a stationary time series since these discharges can last for a longer time. Extreme discharges are more sensitive to fluctuations over time.

Another hydraulic boundary condition is the tide. A tidal signal can be a very complex sum of components. For the research part of the propagation of the tide upriver and the influence of the tide on the water distribution a simplified M2 tide is used. This component is set as boundary condition on the sea side boundary. What can be noticed is that there is no phase difference between the two edges of the boundary. Earlier models did use this phase difference. It did however induce a cross current that is in reality not as strong as was found with the model. The cross current in Itajaí is blocked by a rocky outcrop south of Itajaí. This prevents a flow in a lateral direction.

4.3.4 Salinity

Values used in the past for salinity in models are 32 psu for the salt sea water and 0.01 psu for fresh river water. These values were used in the salt intrusion study done by ARCADIS (ARCADIS 2009a). This is also the model that has been expanded and calibrated the most extensive. For the modelling of salinity it is required to run the model in 3D mode as mentioned earlier. In this model the salt water body is realistically represented by application of the K-epsilon turbulence model generating a vertical viscosity and diffusivity value of 1.0e-4. For horizontal viscosity a value of 2.0 is used and diffusivity 10.0.

4.3.5 Bottom roughness

When doing research on the bottom roughness it was important to realize that investigations until now have been done with fairly common circumstances or extreme circumstances. Since high flow velocities can result in a lower bottom roughness (Rijn 2007a) it might require additional research. High velocities can streamline the bottom profile as obstructions are transported away and reforming dunes into drop shaped bodies that allow for smoother flow. On the other hand the extreme velocities could cause ripples and dunes on the bottom as well. This kind of behaviour is hardly investigated in Itajaí so far and can have a strong influence on the systems behaviour. As this is overlooked the calibration that has been done so far can be wrong as it compensates the complete roughness to match its behaviour while in different place specific smoothing of roughening might have taken place due to extreme flow velocities.

The research done so far with numerical models have been using rather low values for bottom roughness (White Colebrook values ranging from 0.5 at upstream boundary until as low as 0.001 at the downstream section) (ARCADIS 2009a). It is very common to use the bottom roughness as a calibration parameter. And this is also done here, keeping the values within feasible ranges.

4.3.6 Sediment & morphological input

Although eventually no assessment was done on a complete sediment transport model. This is due to time restrictions. However some research has been done on the exiting model. This information is indispensable for future research. A short explanation of considerations is given here.

For input of the sediment parameters, it is important to realize that the information available is limited. The original model has been calibrated on the climate of a year in combination with dredging figures. This means that the model has been simulated for a year with different parameters that were adjusted until the model results showed the same accretion volumes as was found in reality in that same year. For the subsoil distribution upstream of the harbour no information is available. This is an aspect that might be worth researching more thorough.

The calibrated model uses the new van Rijn formulation from (Rijn 2007b). This module has recently been implemented in Delft3D. This module is specifically able to work with the fine sediment diameter as found in Itajaí-Açu. Since there is no precise information about the entire area on sediment sizes and distribution this was used as a calibration factor previously (ARCADIS 2012a). An extensive explanation of this new formulation can be found in (Rijn 2007a) and (Rijn 2007b). A short description is given in Appendix VI.

Morphological updating is not used. This would interfere with the influence of the bypass as it is implemented. If that happens the effects would not be separable anymore from the processes that are analysed.

4.3.7 Time step assessment

When using a model it is important to know if it is accurate. With numerical models that can be in spatial resolution. Another form of accuracy of a model is the time step. A small time step is obviously more accurate but computationally costly. The way that this could be assessed by Delft3D is with QUICKIN. This is a module that allows users to create and asses many different spatial inputs. One of them is the Courant number. The courant number is a measure of numerical stability. This is however different per numerical scheme that is used to calculate every time step.

The first comparison was done with the scenario of 1000 m^3/s with a static sea level. This is simulated with a time step of 30 s and 6 s. Especially in the area of the bifurcation where high courant numbers are found. This is due to the grid refinement that is the result of the implementation of that bypass. The extra grid cells were required as explained in section 4.3.1. The courant numbers that are related to the two different time steps are rather large:

- 6 s: outside grid refinement: 3-7, inside grid refinement: 5-12
- 30 s: outside grid refinement: 12-38, inside grid refinement: 25-80

These courant numbers are determined for each cell depending on the shortest dimension in either x-direction or y-direction:

$$CFL = \sqrt{g * h} * \frac{\Delta t}{\min(\Delta x, \Delta y)} \quad (4.1)$$

With:

- g = gravitational acceleration [m/s^2]
- h = water depth [m]
- Δt = time step [s]
- Δx = cell length [m]
- Δy = cell length [m]

In general the CFL (Courant-Friederichs-Lewy) number should never exceed a value of 10. However in situations with rather small variations in both time and space it can be taken substantially larger (Delft Hydraulics 2005). It can be concluded that a time step of 30 s will most likely be too large for some scenarios. It is therefore not used in simulations. The conclusion was that a time step of 12 s would suffice in most scenarios and 6 s when a higher accuracy is required.

In Fig. 9-23 appendix V the results are shown of the time step difference results of a 6 s time step and a 30 s time step. The difference is a slightly over 1%. With a time step of 6 s the discharge through the bypass is 609 m^3/s and with a time step of 30 s the discharge through the bypass is 618 m^3/s. This can be explained by the idea that water particles "skip" more grid cells during one time step. This means that the bathymetry is unable to steer the parcels accordingly. The result is that a parcel can pass an obstacle in one cell and not be influenced by it. Normally the influence of one grid cell is not that large. But when large depth variations are found, that have a lot of influence in the flow this could be a problem. Since this is not the case here the results between 30 s and 6 s are not that large. However, since it produces some uncertainty a time step of 12 seconds is chosen to make the computations less extensive.

The velocity differences between 6 s and 12 s are shown appendix V for 150 m^3/s discharge and 230 m^3/s discharge. The differences are in the order of tenths of millimetres per second. The velocities are depth averaged. It is clear that the low flow velocities are hardly influence by a doubled CFL value.

4.3.8 Numerical parameters

All numerical parameters are listed below in Table 4-1

Parameter	Value
Roughness	
Roughness formula	White-Colebrooke
Roughness value	0.001 m - 0.5 m
Viscosity	
Horizontal eddy viscosity	2 m^2/s
Horizontal eddy diffusivity	10 m^2/s
Background vertical eddy viscosity	1e-4 m^2/s
Background vertical eddy diffusivity	1e-4 m^2/s
Model for 3D turbulence	k-Epsilon
Time step & Domain	
Time step	12 s
Courant number (outside grid refinement)	5 [-]
Courant number (inside grid refinement)	10 [-]
Grid size in general	25 – 110 m
Grid size in bifurcation area	7 - 70 m

Table 4-1: Model parameters

5 Research on hydrodynamics, salinity and bed shear changes

In the research section the investigation is focused on the consequences of the implementation of a bypass in the situation of Itajaí. The subjects of interest in the Itajaí area are:

- Flood risk
- Erosion
- Sedimentation

5.1 Introduction

The purpose of the bypass is to mitigate problems with these aspects. However it is very well possible that the bypass can have a negative effect on one or two of them. On the basis of the preliminary research four research aspects were chosen. Changes regarding these aspects can have positive and negative effects. These four aspects will be addressed first. Below in Fig. 5-1 the different sections are mentioned as they are addressed as of now. There is the upstream section that remains the same in the current and as well as in the bypass scenario. Further downstream the system will split in the bypass and the current branch. The current branch is also the same in the current and bypass scenario. Both end up in the sea. The two branches then flow out into the sea approximately 5 to 6 kilometres away from each other.

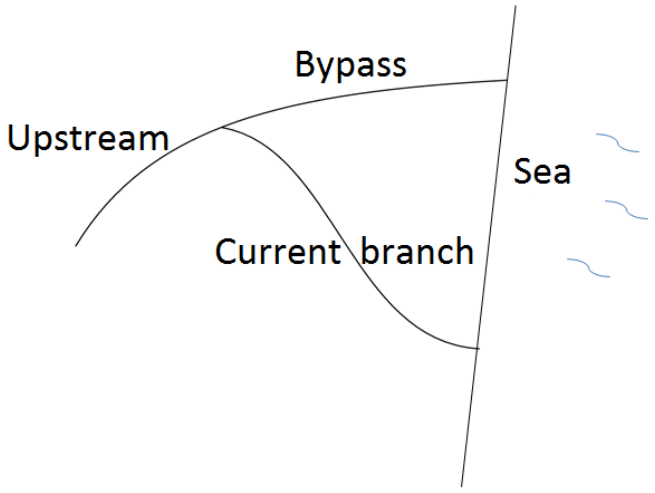

Fig. 5-1: Situation sketch of the Itajaí-Açu and the bypass

5.1.1 Discharge distribution

The discharge distribution is important to see how the bypass is coping with the total discharge. With the knowledge what steers this distribution over a range of scenario's the efficiency of the bypass can be assessed. The effect of the tide is included on this since it is expected to have a lot of influence on the distribution. It will be shown that the tidal flow has a large impact on the resistance of both channels. This changes with different discharges since the tidal flow does not change in both channels accordingly. This will result in a different average discharge distribution with different discharges while a method will be shown how this is constant when looking at a linearized combination of river flow and tidal flow resistance.

5.1.2 Water levels & tidal flow

With the goal to assess the mitigation on flood risk the water levels will be investigated as a result of the tide in combination with the river flow. The tide causes movement of the water in a vertical and horizontal manner. The implementation of the bypass is in fact the same as a widening of the current branch. This results in a larger capacity to move water. This is only true for the part between the bifurcation and the mouths. Upstream of the bifurcation there is no increase of capacity. Hence there is not additional storage surface for the tidal prism. If the increased capacity of the downstream section would be used fully it would mean that the tidal elevation range would triple as the capacity of the downstream section has tripled. This is unlikely to happen as flow velocities would increase in the upstream section strongly. This will not happen as friction forces increase quadratic with velocity. Hence through the current branch the discharge by tide will be much lower as a large portion will flow through the bypass. This decrease in velocity results in a reduction of friction force in the downstream section. This will in return result in a lower resistance for the entire system meaning that the tidal flow will slightly increase. Meaning that tidal flow will increase upstream as well as the tidal range. In the downstream section the tidal discharge will increase when considering the bypass and the current branch combined. Here the tidal elevation range will increase as well as the tidal prism has increased due to a slightly reduced friction force of the entire system by lower velocities in the downstream section

5.1.3 Salinity dynamics

The salinity dynamics will cause a change in interaction between fresh and salt water compared to a situation where both water bodies have the same density. The weight difference will cause a new balance of forces. The heavier sea water will resist the outflowing fresh water. However, since the two mouths are not of the same size this force will be different, resulting in an additional term in the momentum equation. This term will have a significant influence during lower discharges. At higher discharges the constant imbalance caused by the density difference in the momentum equation relatively diminishes since the system responds in a quadratic way to flow velocity regarding flow resistance.

5.1.4 Bed shear stress

The bed shear stress is an important indicator of the sedimentation / erosion behaviour of the system. With an understanding of that, a first assessment can be done. With the acquired knowledge on the flow due to the discharge distribution, the tidal flow and salinity dynamics the changes in bed shear stress can now be understood.

5.2 Discharge distribution

Water flows along the path with the least resistance. With two branches from the bifurcation to the sea it is therefore relevant to find out what the difference in resistance is between the two branches. Since there is the influence of the river discharge and the tide this section is split up in two. First the situation without the tide will be assessed. After that the scenario with the tide will be compared. The differences will than clarify the influence of the tide.

5.2.1 Theory & hypotheses

First in this section the general situation will be described. This relates to the tideless scenario This is the basis that will lead to the theory around the tidal scenario.

Stationary scenario

The way to look at this in a theoretical way is starting with the momentum balance. This is the basis of both the situation with and without the tide. The momentum balance is as follows:

$$\frac{\partial Q}{\partial t} + \frac{\partial}{\partial x}\left(\alpha \frac{Q^2}{A}\right) + gA\frac{\partial \zeta}{\partial x} + \frac{gQ|Q|}{C^2 Ah} = 0 \tag{5.1}$$

With:

- Q = discharge [m^3/s]
- t = time [s]
- x = distance in longitudinal direction [m]
- A = cross-sectional surface [m^2]
- g = gravitational acceleration [m/s^2]
- ζ = water level deflection [m]
- C = Chézy coefficient [$m^{0.5}$ /s]
- h = water depth [m]

Several of these terms can be neglected under certain situations. With this, equation (5.1) can be strongly simplified for better understanding. This gives insight in the results coming from the complex Delft3D model. The assumptions to justify the simplifications will be mentioned first. The assumptions will first be explained for the tideless situation. The tidal scenario continues with the same assumptions:

- The depth remains constant independently of the discharge. Along with that the width of both channels is kept constant as well. These assumptions can be justified with the knowledge that with low discharges the water level hardly changes. For a change in width the water level has to change so this is automatically true as well. This than leads to the assumption that is required. With a constant cross-section there is a linear relation between discharge and velocity. This means that u=Q*p. With p the reciprocal of the fixed cross-sectional area
- In the momentum balance the second term can also be neglected. This means that the channel needs to be prismatic. For the bypass this is certainly true. For the current branch this is not strictly true. The harbour for example has a different cross-section than the rest of the current branch. It is found in the end this doesn't influence the results very much during high discharges.
- The first term in equation (5.1) can also be neglected. The fluctuations of flow in all branches over time are very small. The velocities are of much bigger influence than the change of these velocities due to the duration of the tidal cycle. For the non-tidal situation there is no change at all. And this is in this tideless scenario obviously justified since the discharge is stationary.

With these assumptions equation (5.1) can be written as:

$$gA\frac{\partial \zeta}{\partial x} + \frac{gQ|Q|}{C^2 AR} = 0 \tag{5.2}$$

Which in return can be written into

$$Q^2 = C^2 * (B * h)^2 * h * i \tag{5.3}$$

With:

- Q = discharge [m^3/s]
- C = Chézy coefficient [$m^{0.5/s}$]
- h = water depth [m]
- B = channel width [m]
- i = the water level gradient [-]

So:

$$Q = C * B * h^{\frac{3}{2}} * \sqrt{i} \tag{5.4}$$

This can be used for both branches as follows:

$$Q_i = B_i C_i h_i^{\frac{2}{3}} i_i^{\frac{1}{2}} \tag{5.5}$$

The mass balance reads:

$$Q_0 = Q_1 + Q_2 \tag{5.6}$$

And the geometrical relation reads:

$$i_1 * L_1 = i_2 * L_2 \tag{5.7}$$

With:

- L_i = length of channel i [m]

When one combines equation (5.5), (5.6) and (5.7) one can write the discharge for the two separate branches as follows:

$$Q_1 = \frac{\beta_1 * h_1^{\frac{3}{2}}}{\beta_1 * h_1^{\frac{3}{2}} + \beta_2 * h_2^{\frac{3}{2}}} * Q_0 \tag{5.8}$$

$$Q_2 = \frac{\beta_2 * h_2^{\frac{3}{2}}}{\beta_1 * h_1^{\frac{3}{2}} + \beta_2 * h_2^{\frac{3}{2}}} * Q_0 \tag{5.9}$$

With:

$$\beta = B_i C_i L_i^{-\frac{1}{2}} \tag{5.10}$$

This shows that when the depth and β remain the same the ratio between Q_1 and Q_2 The lengths of both channels won't change obviously. The last condition is that the friction term (4^{th} term in equation (5.1)) stays dominant.

Tidal scenario

As mentioned previously the time dependence due to the tide can be neglected due to slow changes. Although these changes are slow they are large. Therefore the resistance term changes drastically over time since this is a quadratic function of flow velocity. To be able to cope with the effect of this quadratic term it can be linearized over a tidal cycle. This is done by integrating the total flow of the river and the tide during over a tidal cycle and dividing this by the duration of the tidal cycle. The result over a tidal cycle are the same for the non-linearized and the linearized formulation. This is called the effective discharge and is formulated as follows:

$$Q_{eff} = \sqrt{\frac{1}{T}\int_0^T Q|Q|dt} \tag{5.11}$$

With:

- Q_{eff} = effective discharge [m^3/s]
- T = tidal period [s]

The function for flow in the channels can be described as a part from the river discharge and a part from the tidal flow. This can be formulated as follows:

$$Q(t) = Q_0 + \hat{Q}\cos(\frac{2\pi t}{T} - \phi) \tag{5.12}$$

With:

- $Q(t)$ = time function of discharge {m^3/s]
- Q_0 = average discharge [m^3/s]
- t = time [s]
- T = tidal period [s]
- φ = phase angle [rad]

When integrating this and averaging as explained before the result is as follows:

$$Q_{eff} = \sqrt{Q_0^2 + \frac{\hat{Q}^2}{2}} \tag{5.13}$$

5.2.2 Results

The results from Delft3D have shown that the distribution is not friction dominated during low discharge and no tide. It is clear that in that scenario the assumptions are not valid. However this was a pure theoretical scenario without tide. The tidal scenario shows that with a tide the situation is always friction dominated. The effective discharge shows a constant distribution during al discharges. The influence of the tide on the distribution is clear as can be seen in Fig. 5-2. As with the tideless scenario the distribution deviates from a constant value. As with higher discharge the tidal flow reduces and the effective discharge is completely determined by the discharge and hence the three lines of the tideless average, tidal average discharge and the tidal effective discharge converge to the same distribution at high discharges.

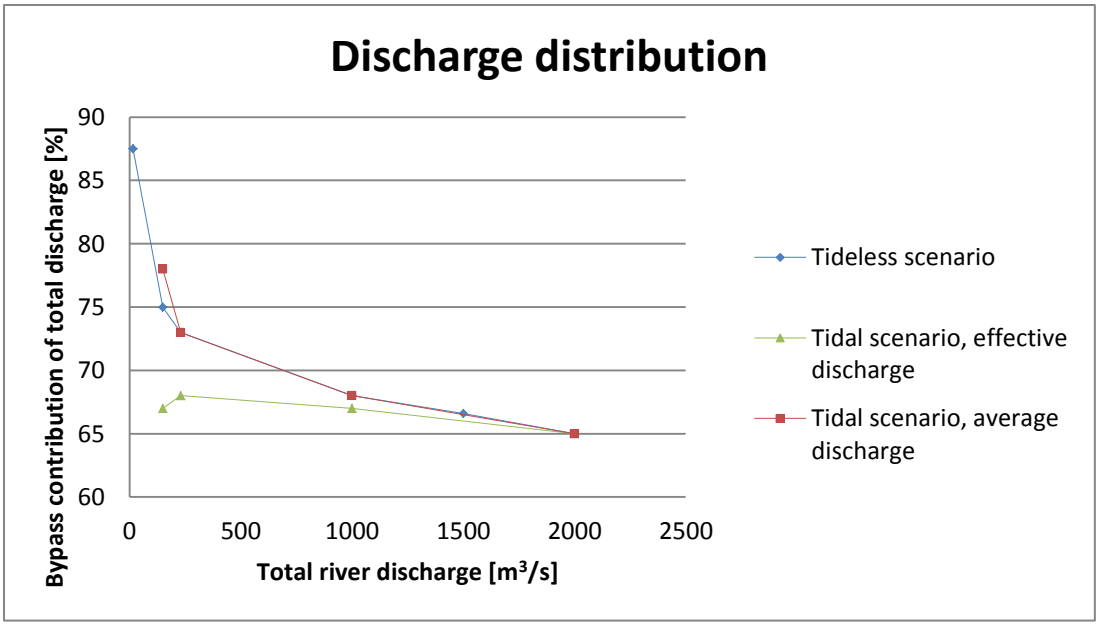

Fig. 5-2: Discharge distributions, bypass part of the discharge

If it is not relevant what determines (e.g. tide or river flow) the effective discharge the result of the distribution should be the same during springtide. In Fig. 5-3 the part flowing through the bypass as effective discharge is shown for the average tide and for the spring tide. It shows a practically equal distribution. Roughly 65% flows through the bypass and 35% flows through the current branch. This is the distribution for the effective discharge. For higher discharges this is the average discharge. When the river flow starts to dominate the tidal flow and hence the effective discharge is predominantly determined by the river flow.

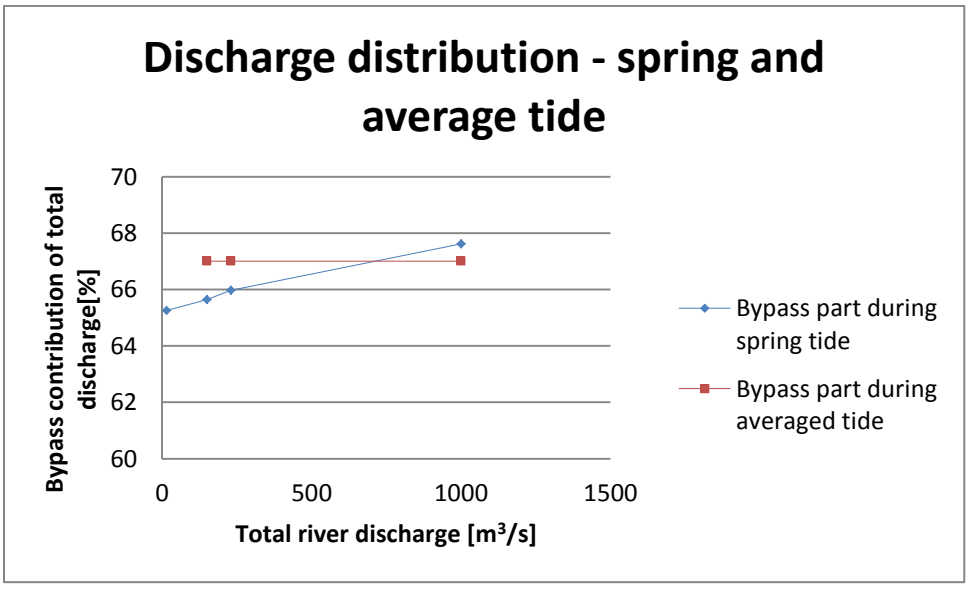

Fig. 5-3: Bypass part of effective discharge during springtide and average tide

5.2.3 Conclusion

With the results found it can be said that the assumptions at the beginning of this section that resulted in equations (5.8) and (5.9) are valid under certain conditions. For high discharges there is a fixed distribution. For the tideless scenario it means that the river flow needs to be rather high for

the friction term to be dominant in the momentum balance. With a tidal scenario there is always friction dominance due to the combination of river flow and tidal flow. However, for the average flow (the effective river discharge) distribution to approach the fixed distribution value it requires to dominate the tidal flow. This is during high river discharges. During high discharges the tidal flow has hardly any part in the effective discharge. Hence the river can be considered to be the only contributor to the effective discharge.

It is clear that the distribution is predictable for high discharges. During high discharge the friction distribution dominates all other influences. As it is known that the friction of both channels keeps the same ratio the distribution will remain the same as well.

This fixed distribution is of importance in the next section when looking at origin of the tidal wave into the upstream section. It will be shown that the tidal wave in the upstream section originates from both the current branch and the bypass. Both branches contribute to this tidal wave in the ratio as found here of the fixed distribution.

5.3 Water levels & tidal flow

The new tidal behaviour in the system is a result of an entire new system. With an extra mouth at the sea side more water can flow in. A condition for this extra water to flow in is that it can be stored in the entire basin behind the inflow. The result is that since the resistance for the flow entering is lowered with the extra channel, the amplitude of the tidal flow will increase. However in combination with the upstream section that still has the same capacity the total response is more complicated.

5.3.1 Theory & hypotheses

The basin storage can be formulated in the basin storage equation. This is in 1D form:

$$B\frac{\partial \zeta}{\partial t}+\frac{\partial Q}{\partial x}=0 \tag{5.14}$$

It states that the vertical movement of the water surface between two cross-sections is in balance with the difference in discharge between these two cross-sections. If more water flows in this space between two sections than out, the water level rises and vice versa. So when the tidal flow amplitude increases the tidal flow differences between cross-sections increases as well. Therefore the tidal movement of the water level increases also.

As mentioned in section 5.2 the resistance and effective discharge have a direct relation. The combination of the resistance of both channels has therefore a constant relation as well. When considering the bypass situation as just a widening of the current channel and not as two channels it is obvious that the resistance decreases. When driving forces remain the same, such as the tide and the river discharge, the resulting response of the system will increase with a lower resistance. This increase in water movement will result in a higher resistance. This limits the increase of the response.

Another aspect is the increase of the “effective” channel width between the sea and the bifurcation. The combined channels are different from the current channel alone. If the current situation is schematized as follows as a prismatic channel:

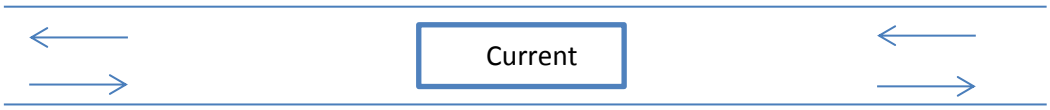

Fig. 5-4: Schematization of current system, single channel

The bypass scenario can be schematized as a wide channel from the sea to the bifurcation where it narrows into the upstream section. The wide channel is a schematization of the combined current channel and the bypass. In a schematization this would visualize as:

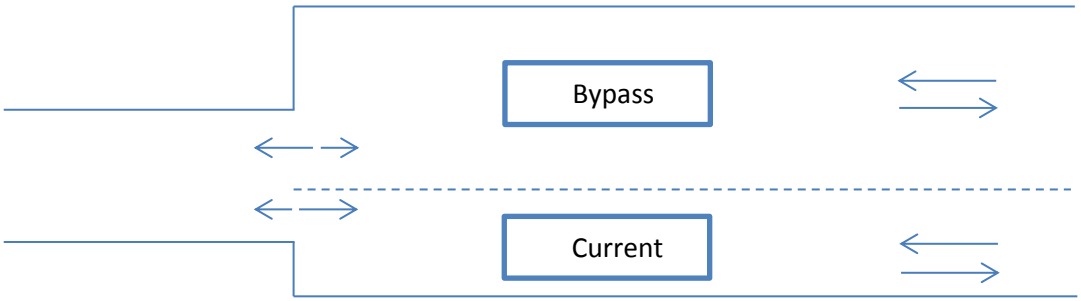

Fig. 5-5: Schematization of bypass system, dual channel

As one can expect the tidal flow in the current channel cannot remain the same parallel to the bypass discharge (which would also be larger than the current channel's discharge) as this would flow combine into the upstream section. If this would happen the tidal range of the water level would increase drastically as can be understood from the basin storage equation (5.14). All water from the bypass and the current channel needs to be stored in the system which consists of the bypass, the current channel and the upstream section. Although the storage capacity has increased with the addition of the bypass it hasn't increased with the same amount as the increase of transport capacity by the addition of the bypass. Hence the discharge combined of the bypass and the current branch will be in the same order as was discharge solely by the current branch in the current situation. Hence the tidal discharge in the current branch will diminish. As a large portion of the tidal discharge will flow through the bypass. The theory behind this is similar to the theory of section 5.2 on discharge distribution. Only the direction has changed. The distribution is based on friction which is much lower in the bypass than in the current branch.

Additional to the low flow velocities there is a decrease of total resistance of the system. As the same amount of tidal discharge would flow through the system the flow velocities in the current branch and the bypass are rather low. Hence the friction force in these two are low. For the current branch one can say that with the same tidal discharge the flow velocities are lower. Hence the tidal prism will slightly increase as with the same tidal forcing flow velocities will increase until the forcing is matched by friction. For that flow velocities in the downstream section will increase, and hence also in the upstream section. This will result in a slightly higher tidal discharge (for the downstream section the combination of the bypass and the current branch) and a larger tidal elevation range.

5.3.2 Results

All results from this section are from the Delft3D model. In Fig. 5-6 the tidal flow amplitude in the current branch just downstream of the bifurcation point is shown. This is done for the current

situation without bypass, and the situation with the implemented bypass. This is related to the complete river discharge from the upstream section.

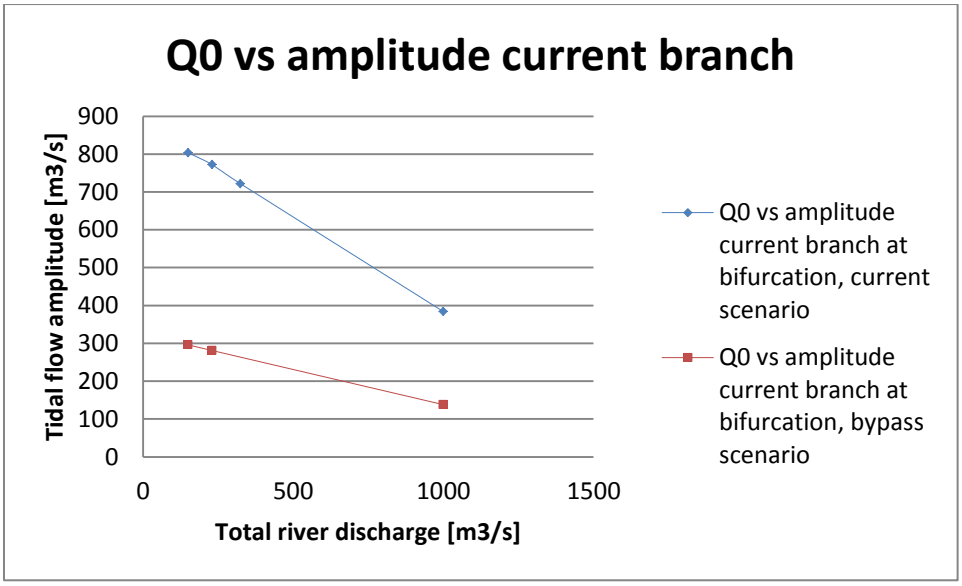

Fig. 5-6: Tidal flow amplitude vs. river discharge

The reduction is very clear to see. This can be related to the increased downstream capacity theory from the introduction of this section. As can be seen below in Fig. 5-7 there is a constant ratio between the amplitude in the current and bypass scenario regardless of what the river discharge is. The reason for this reduction is the downstream overcapacity as explained before. As can be seen the tidal wave is reduced to about 35% in the current branch. This is similar as was found for the discharge distribution for the current branch. This can be explained as follows. As with the river flow the tidal flow is the same when it comes to friction only the direction changes. When considering high water the flow is in an upstream direction. Considering the upstream section and the downstream section as a basin it is filled by the two mouths. The water flowing through the bypass and the current branch is filling the upstream section. As the resistance of the bypass is much lower than from the current branch more is flowing through the bypass. The theory behind this is the same as with the river discharge distribution from section 5.2. Hence the reduction is also the same no matter what tide occurs as the same tidal forcing is applied on both mouths. This can be seen in Fig. 5-7

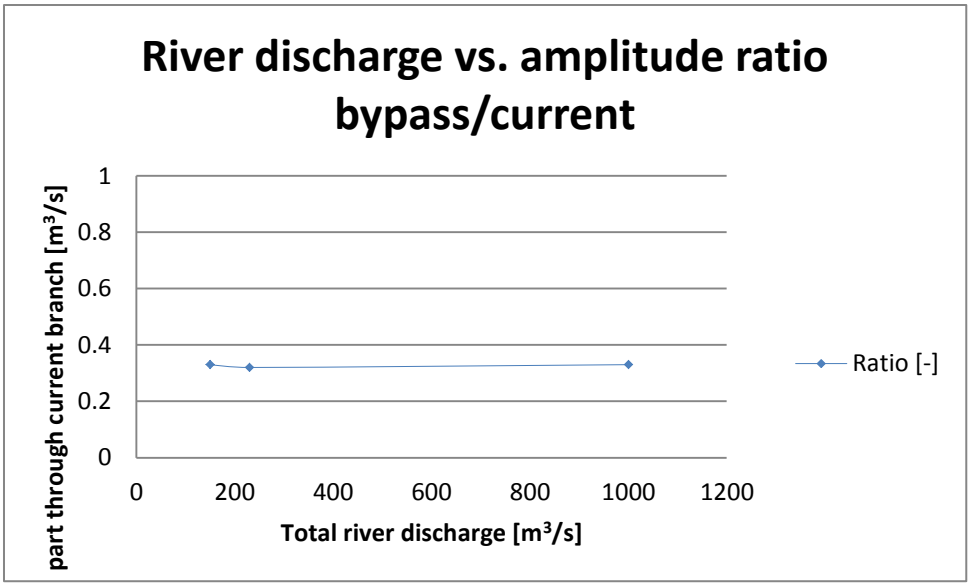

Fig. 5-7: River discharge vs. ratio amplitude current and bypass scenario

Parallel to this the theory of the increased capacity in the bypass should yield the same result with a different amount of reduction as the contribution of the bypass is larger than of the current branch. This would mean that 65% of the upstream tidal discharge would come from the bypass. This was found in section 5.2 with the discharge distribution. As mentioned before this is the same principle but in a different direction. This means that there is a reduction of tidal discharge in the bypass as well. However there is no current situation for the bypass as it doesn't exist today. Therefore an assessment is made within the Delft3D model by closing of the current branch as can be seen in Fig. 5-9. And compare this with the results from the complete system. The results are basically the same as with the current branch. This confirms the result of the "bottle neck" formed by the upstream section. This slows down flow velocities in the downstream section far below the discharge they would carry if there wouldn't be such a bottle neck. The comparison between the artificial current situation for the bypass as a single channel and the bypass in the dual channel system can be found in Fig. 5-8.

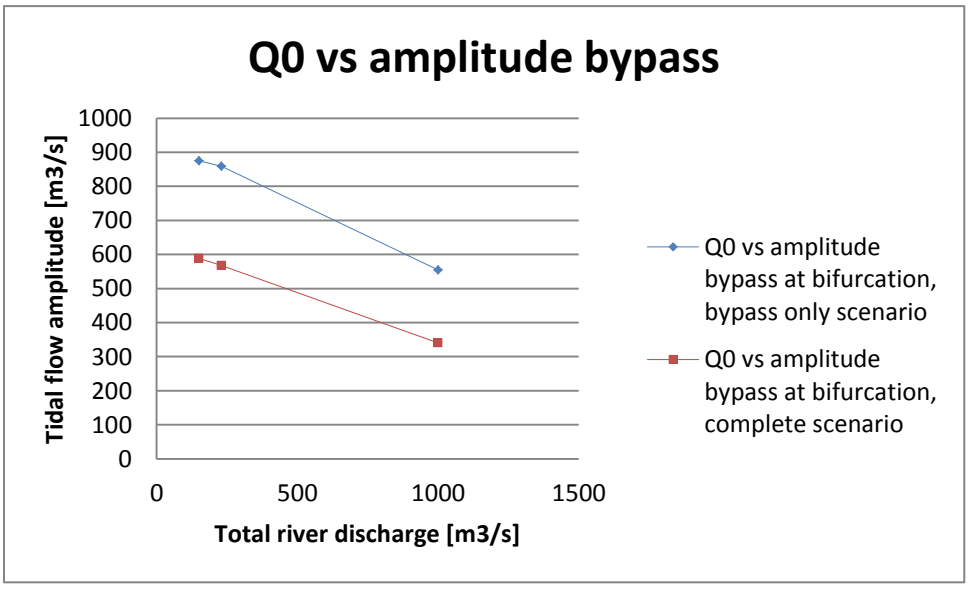

Fig. 5-8: Tidal flow amplitude vs. river discharge

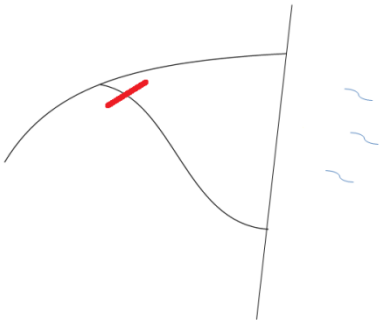

Fig. 5-9: Bypass only schematization

Besides the effect on the tidal flow that is reduced in the bypass scenario in the current branch and the bypass, there is also the increased tidal elevation. Due to the increased tidal prism as a result from the slightly lower friction of the system high water and low water will have a slightly larger difference. This can also be understood by equation (5.14). The first term will increase as during the same tidal period the difference between high and low water increases. Hence the derivative will increase this is due to the second term that indicates the gradient of discharge over the length of the basin (the downstream and upstream section combined).

This will this result differently during different discharges. As one can see in equation (5.15) for the effective discharge there is a non-linear relation between river discharge and tidal discharge that result in an effective discharge which in return is related to the total resistance by the combination of tidal and river discharge. This means that the resistance reduction of the complete system by the addition of the bypass will be compensated by an increased tidal flow as explained earlier. However during high river discharges the contribution by tidal discharge to friction is very low as the flow is dominated by the river discharge. Hence during high river discharges the tidal flow needs to increase more to compensate for the friction reduction by the bypass. This can be seen in Fig. 5-10. It shows the increase of the tidal range along the river axis in % (x=0 starts it the current branch's mouth and runs up the upstream boundary of the model

$$Q_{eff} = \sqrt{Q_0^2 + \frac{\hat{Q}^2}{2}} \tag{5.15}$$

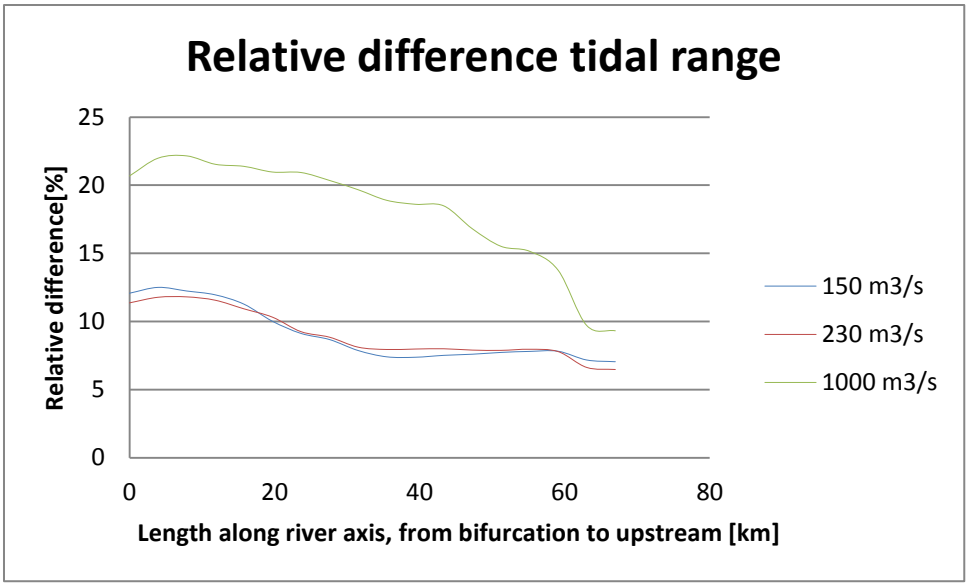

Fig. 5-10: Relative difference of tidal range between current scenario and bypass scenario

What is clearly visible is the relative large increase of tidal amplitude for a high discharge. This is explained earlier.

Something important for this investigation is to look at extreme scenarios. During for example a discharge that occurs once every 50 years the bypass should decrease the water level significantly to be of use. The once in a 50 year event is a river discharge of 7250 m^3/s. In Fig. 5-11 the water levels along the current branch from the mouth (x=0) all the way upriver are shown for both the current scenario and the bypass scenario with this discharge. It shows that around the bypass it works very well. With a decrease of 2-3 meters at the bifurcation point it shows a significant lowering of the average water level.

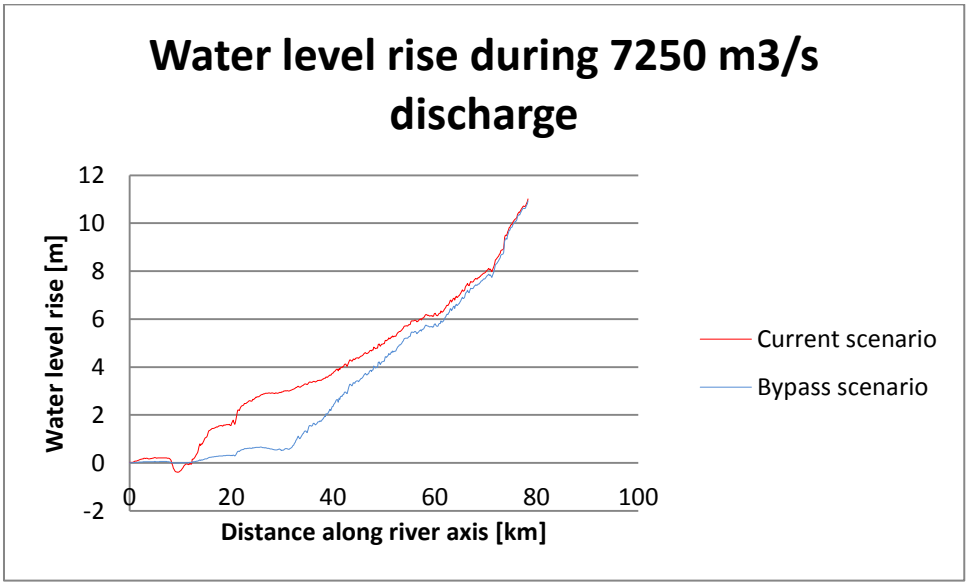

Fig. 5-11: Water level during river discharge of 7250 m^3/s in current scenario and bypass scenario

What is interesting to know is how this affects certain locations. Therefore three locations are chosen that can be seen below in Fig. 5-12. Location one is at the upstream end of the harbour. Close

to the sea but not at the mouth. At the mouth the sea conditions will prevail. Location two is at the bifurcation point. This is where the largest effect will be found. Location three is The first larger city along the river to be found upstream of Itajaí. The effects there are relevant to know.

Fig. 5-12: Location one, two and three along Itajaí-Açu

For these locations the maximum and average water level were assessed as well as the new tidal elevation amplitude since it is clear that it has increased.

In Fig. 5-13, Fig. 5-14 and Fig. 5-15 the changes are shown for the three different locations regarding maximum water level, average water level and tidal amplitude respectively.

Everywhere the average water level has lowered. Higher discharge results in a larger decrease in water level. This is the bypass working better with an increasing upstream discharge. Obviously the distance to the sea and the bifurcation are also relevant for this lowering. The further away the less the influence of the bifurcation is noticeable. At sea the influence is the smallest since the influence of the sea level prevails here. Closer to sea means sea conditions are prevailing.

When looking at the maximum water level one can see that this is the result of the average water level and the amplitude. For location one and location two the amplitude increases with an increased discharge. This is explained previously with the relative small contribution of the tidal flow to the resistance so the tidal flow can increase there. However at very high discharge the increase of the tidal flow becomes smaller at location three. This is only in an absolute way. Due to the fact that location three is very far upstream the influence of the tide decreases rapidly. When the tidal movement is very small a change of a few centimetres can be large. The relative change was shown previously in Fig. 5-10 along the upstream section between the bifurcation and the upstream boundary of the model. Location three is about 45 km upstream of the bifurcation. So although the amplitude diminishes at higher discharges it still is a relative increase with increasing discharges. More important at location three is the reduction of the average water level since this contributes much more to the flood risk problems here than the additional tide. What is shown is that the decrease of water level is noticeable. And also here the difference between the old and new situation increases are positive results for the bypass.

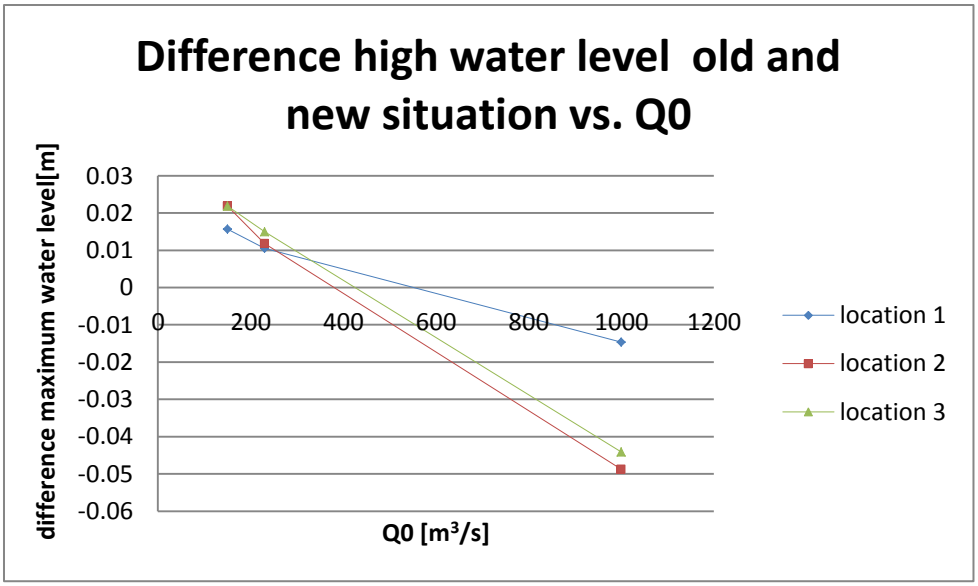

Fig. 5-13: Δh, water level plotted against total river discharge vs. Q0, loc. one, two and three

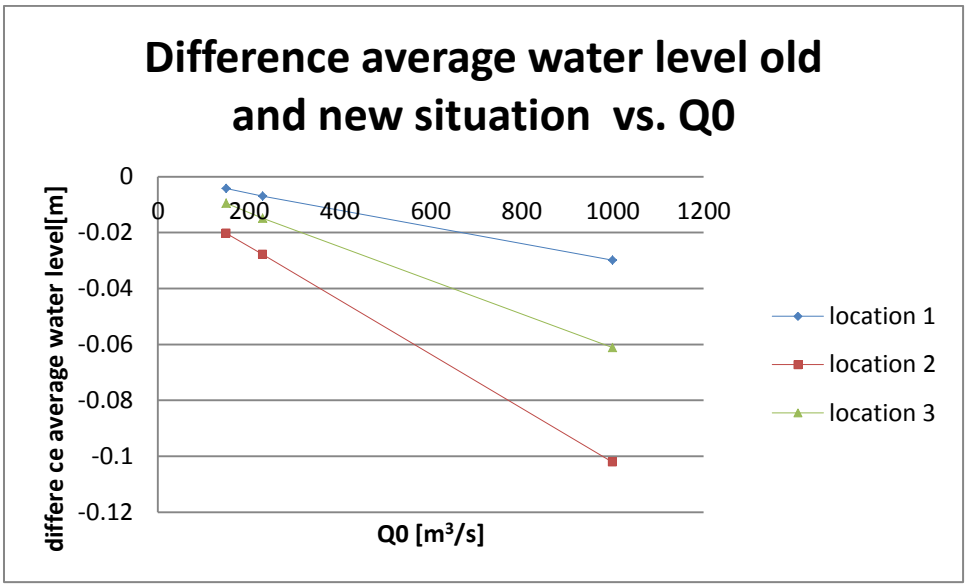

Fig. 5-14: Δh, average water level vs. Q0, loc. one, two and three

Remarkable is the strong increase of amplitude in location two. The exact reason behind this is unknown. Possibilities are partial reflection as a result of the narrowing from the bypass and current channel combination into the much narrower upstream section. Another possibility is tidal asymmetry or local effects that amplify the tidal response. Multiple reasons have resulted in a non-conclusive explanation about this phenomenon. However it can be said that the resulting larger tidal amplitude is not really significant as the lowering of average water level is stronger at higher discharges as can be seen in Fig. 5-13.

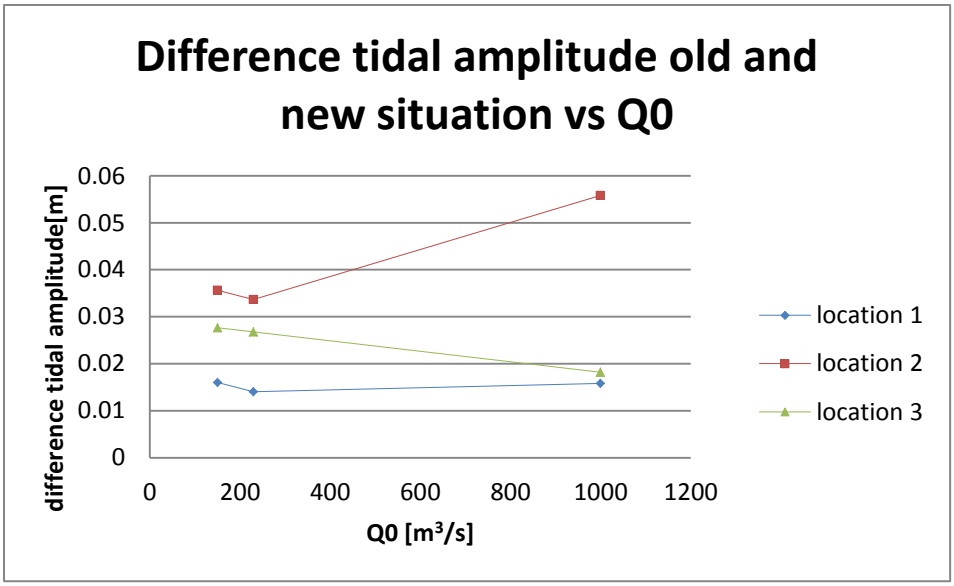

Fig. 5-15: Δa, tidal water level amplitude vs. Q0, loc. one, two and three

Another aspect to look at with fine sediment is high water slack (HWS) and low water slack (LWS). As explained in section 3.3.4 this very relevant. As it is now known that the tidal flow amplitudes have diminished in the bypass scenario the slack periods have increased as well.

In Fig. 5-17 and Fig. 5-18 the slack durations for low and high water are given for the current scenario and the bypass scenario. These are measured at nine cross-sections in the current branch and the upstream section. Cross-section one is at the mouth and cross-section four is just downstream of the bifurcation. five through nine are in the upstream section. The locations are numbered and shown in Fig. 5-16.

Slack is defined as the period where the discharge through a cross-section is between -50 m^3/s and 50 m^3/s. This is why the 1000 m^3/s discharge is not assessed since it has no slack period in either cross-section.

Fig. 5-16: Positions of cross-sections in current branch

What is now clear is that HWS and LWS have increased drastically in the current branch. This is covered by cross-section one through four. This is as expected in line with the decreased tidal amplitudes. The effect of increased slack period means that during both HWS and LWS more sediment can settle. But since the LWS duration, that used to be slightly longer than the HWS duration, is now much longer than the HWS duration, more sediment export can be expected. This is a secondary effect besides the more direct advective transport by mean flow.

Another thing to be seen is the shortened HWS in the upstream section. LWS has remained roughly the same. This shows that the slight increase of the tidal flow amplitude in the upstream section has a small effect. Nevertheless, the upstream section has become more sediment exporting. This is not as much as in the current branch.

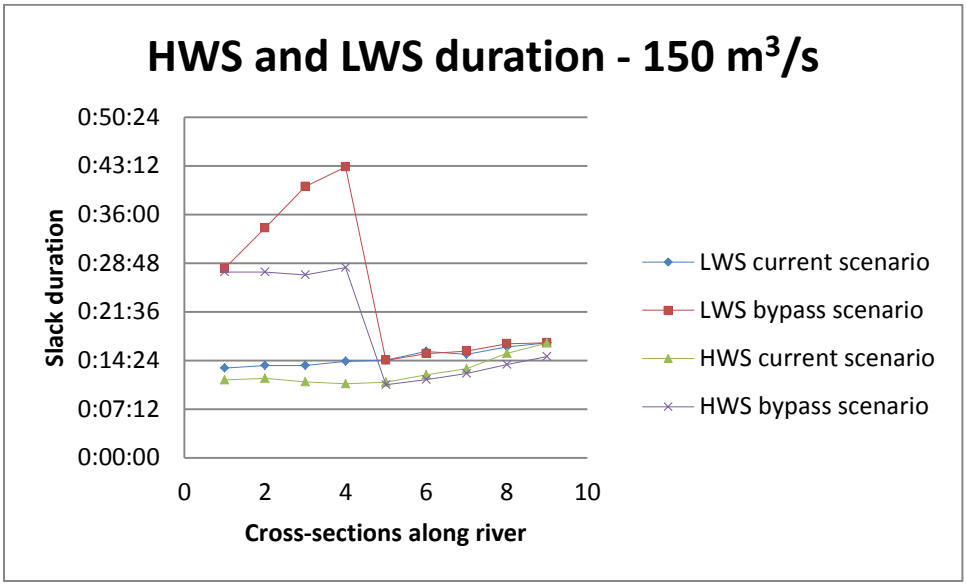

Fig. 5-17: Duration HWS and LWS 150 m^3/s

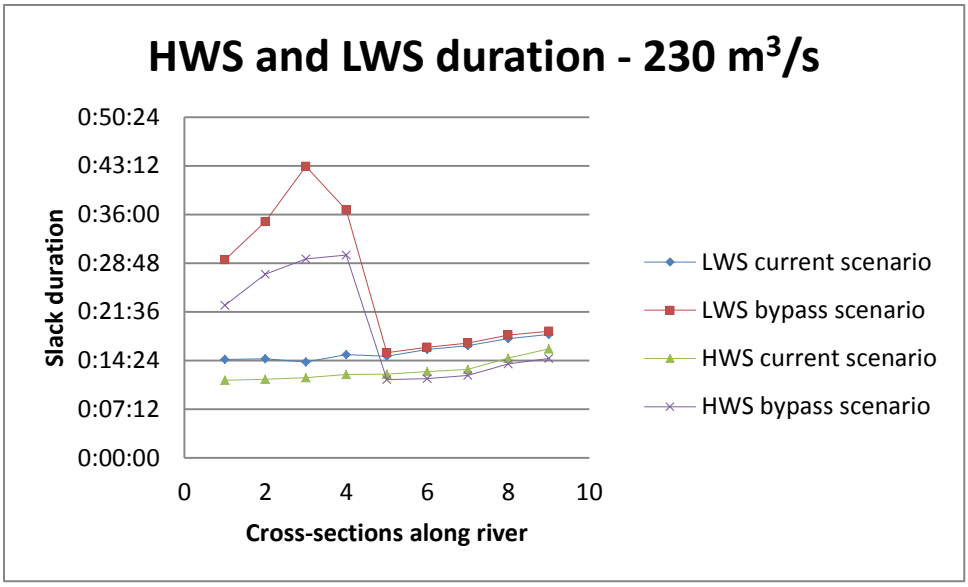

Fig. 5-18: Duration HWS and LWS 230 m^3/s

What would be the total result of sediment transport due to the LWS-HWS difference is unclear. This strongly depends on the sediment concentration during HWS and LWS. Since this again depends on events prior to that this is very unpredictable. After high discharges sediment concentrations can remain high for a while even during lower discharges. This is related to the non-instantaneous response of fine sediment to flow changes. This makes the correlation between flow slightly lower.

5.3.3 Conclusions

Clear from the investigation on the difference of tidal behaviour are a few aspects that are important:

- Change in tidal flow
- Change in tidal elevation range
- Change in HWS and LWS

With the change in tidal flow the main conclusion is that during low to average discharges, the system has more tidal action upstream of the bifurcation causing most likely more sediment transport. Downstream of the bifurcation the tidal action will diminish due to the bypass. This means that potentially increased sediment transport in the upstream section will decrease severely here. Therefore large sedimentation can be expected in both the current branch and the bypass. Although the sedimentation volumes in the current branch will be the largest since the tidal flow amplitude has been reduced the most.

The increased tidal range is been shown the be a result from the reduced friction in the downstream section. The increase in tidal range is remarkable but is not of any interest when considering flood risk. During low discharges the increased levels of high waters are not normative for flood risk. During high water the water levels reach much higher levels. At that point the tide has hardly to no influence anymore on water levels. It is than completely determined by the river discharge. Since it is now known that at higher discharges the bypass functions better when looking at water level decrease it can be said that the increase in tidal range has no negative effect at all.

The last aspect is the change in slack time durations. The first to be said is that it is hard to say what the effect will be of the ebb or flood dominance of slack duration. But Due to the bypass the slack periods have increased severely in the current branch. This is explained by the decreased tidal amplitude. With a lower amplitude the zero-crossing takes longer. This phenomenon abruptly disappears in the upstream section. Here the tidal flow amplitude has increased slightly. It can be seen that the HWS has decreased a bit and the LWS as remained the same. So the upstream section is showing the same kind of change as the current branch albeit in a much weaker form. Since it is hard to predict what the result will be of the different slack durations it is recommended to look at this with a full sediment transport model. This will require more investigation of sediment properties further upstream.

5.4 Salinity dynamics

In an estuary density currents occur. These are responsible for the fact that the average water movement changes maybe only slightly while changes at certain depths can be significant. Sometimes differ from direction at different depths. This has large consequences for the bottom shear stress and hence also for sediment transport. That is why it is good to know how this system acts with and without heavier salty sea water.

5.4.1 Theory & hypotheses

The basics of salt dynamics are the result of the density difference. This has two different consequences. One is from a hydrostatic point of view. At equal water levels a salt water body exerts more hydrostatic pressure than fresh water. This means that although at equal water level there is a resulting force pushing towards the freshwater.

Besides the hydrostatic pressure there is also a dynamics aspect. During the encounter between fresh and salt water the density difference causes them to separate. The lighter fresh water will flow over the heavier salt water. However, friction between them causes them to mix. Salt water entrains in the freshwater and is than exported along with the exiting fresh water. This entrained salt water is replaced by more salt water coming from the sea. This is the gravitational flow as explained in section 3.3.2. The difference in density in combination with kinetic energy determines how well the two water bodies will mix.

Hydrostatic pressure difference

The driving force behind the gravitational current is the density difference as mentioned before. This difference is a force that was not included in the momentum balance so far since salinity was not included. First to explain one considers a static scenario where the water does not move and imagine a dividing interface between the fresh and salt water a resulting force arises. The integrated force over the interface would be as follows:

$$F = \frac{1}{2}\Delta\rho h^2 * B \tag{5.16}$$

With:

- F = resulting force [N]
- $\Delta\rho$ = density difference [kg.m^3]
- h = water depth [m]
- B = channel width [m]

A visual schematization could be seen as follows since it is to the highest power. The red triangle is the hydrostatic pressure distribution over depth for the salt water body. The blue triangle is the smaller hydrostatic pressure distribution over depth for the fresh water body. The resulting force is schematized as the purple triangle. This is the small difference distributed over height.

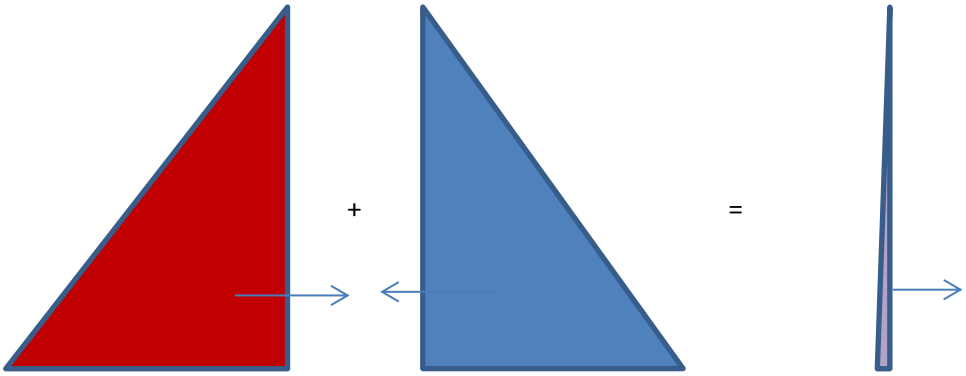

Fig. 5-19: Schematization of hydrostatic forces. Red salt water, blue fresh water, purple resulting force

What is clear is that the depth is the most relevant in this formulation. What happens in a single channel is that to equal the force the water slope rises in the fresh water section to equalize the balance of forces. With a two channel configuration as here with an implemented bypass this would mean that the water level in the other channel would rise as well. If the opposing force of salt water at the second mouth is not as strong the distribution will change. This can be shown as follows with the simplified momentum balance in equation (5.2), with S the term for the density induced force, into:

$$gA\frac{\partial \zeta}{\partial x} + \frac{gQ|Q|}{C^2 Ah} + S = 0 \tag{5.17}$$

With:

- g = gravitational acceleration [m/s^2]
- A = cross-sectional surface [m^2]
- ζ = water level deflection [m]
- x = longitudinal distance [m]
- Q = discharge [m^3/s]
- C = Chézy coefficient [m$^{0.5}$/s]
- h = water depth [m]
- S = resulting force from density difference [m$^{3.5}$ s^{-3}]

It can be expected that at low discharges the friction term in this equation will not be dominant. However, since the resulting force on both channels mouths are constant independent from the discharge the density difference term will become insignificant. So at low discharges the consequences will be the clearest.

Salinity structure

Due to the interaction between the intruding salt water and outflowing freshwater a certain structure arises. This structure is a result of the density current that arises when the density

differences are large enough, the lost energy of the tide over the estuary and the fresh water river discharge. Possible structures are:

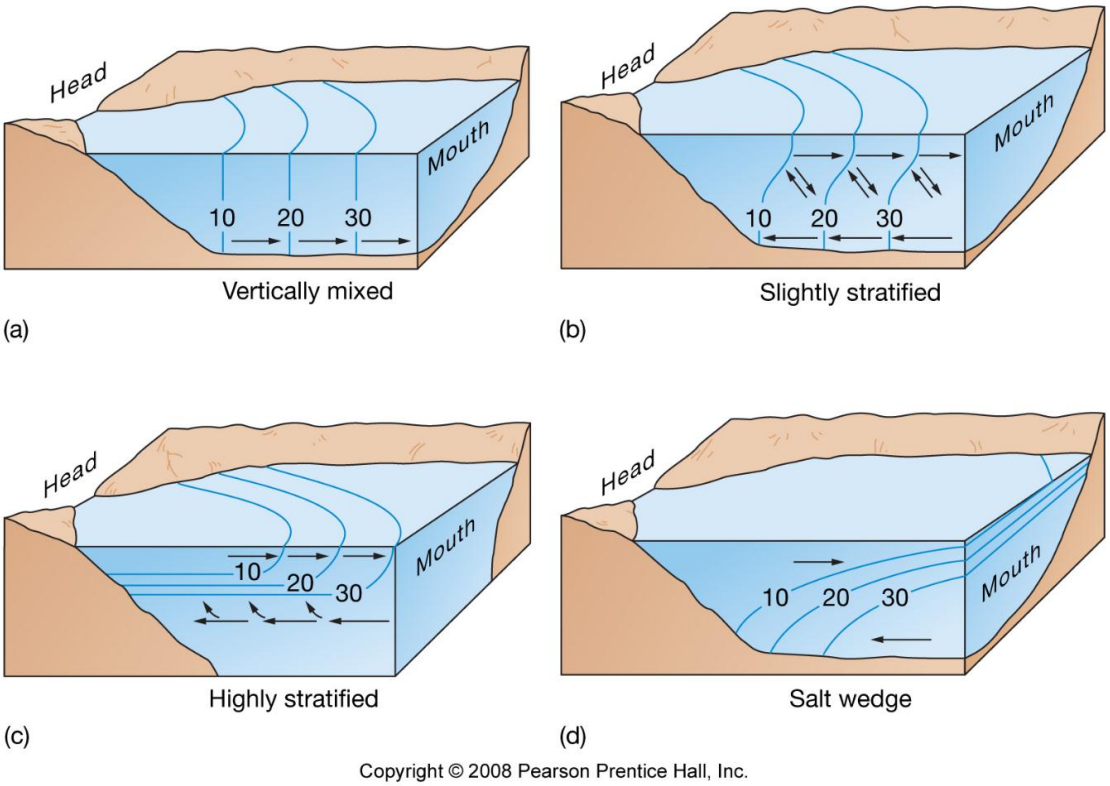

Fig. 5-20: Categories of salinity structures

To predict the actual structure there are several formulations that can give a prediction depending on several parameters of an estuary. These are explained previously in section 3.3.3.

5.4.2 Results

As introduced in the previous section there are two aspects that will be treated. Both the static and the dynamic approach will be explained as they have different effects.

Hydrostatic pressure differences

The result of an interface between a fresh and salt water body is that in the momentum equation friction might not be the dominant term anymore. Hence the distribution is not determined by friction anymore especially during low discharges. Both mouths endure more resistance due to heavier sea water as explained earlier in this section. Since it is most unlikely that the force applied on both mouths is equal equation (5.17) will not return in the form of equation (5.2). When equation (5.17) is applied for both the current branch and the bypass and related the following can be said.

$$g\left(\frac{\partial\zeta}{\partial x_1}+\frac{Q_1|Q_1|}{C_1^2A_1^2R_1}-\frac{\partial\zeta}{\partial x_2}-\frac{Q_2|Q_2|}{C_2^2A_2^2R_2}\right)=S_2-S_1 \tag{5.18}$$

With:

- S_1 resulting force from the density difference at the bypass mouth

- S_2 resulting force from the density difference at the current branch mouth.

From equation (5.17) is clear that when S_1 and S_2 are equal or when both very small compared to the second and fourth term the density difference is not changing much about the distribution. However the first situation of S_1 and S_2 being equal is not to be expected. The second situation where S_1 and S_2 are small compared to the discharge is only possible at high discharges. S_1 and S_2 are constant so they will relatively diminish compared to the discharge automatically with an increasing discharge.

The assumption of S_1 and S_2 to be constant requires the depth to be constant. Which is only true if the tidal elevation is rather small compared to the depth. Besides that also a constant channel width is required. This is automatically true as well if the depth can be assumed constant. Another last requirement is a constant density difference. If all these requirements are met S_1 and S_2 are constant. These assumptions are the same as for the assumptions made in section 5.2. Another assumption that was required for this schematization is that the fresh and salt water bodies encounter at a vertical plain that keeps them separated. This is not true. In reality the density has a gradient when looking at a depth averaged density along the river axis. This is due to the fact that the salt water body is position under the freshwater body and thins out further upstream. This is how the depth averaged density gradually decreases further upstream. However for the principle of looking at density induced force this simplification of one vertical plain is practical for understanding purposes without deviating to much from results from the model as will be shown later on.

The expectation of the salinity term in equation (5.17) to have a strong influence is indeed found with the results. Fig. 5-21 shows the part of the tidal-average river discharge that flows through the bypass through a cross-section just downstream of the bifurcation. The blue line shows part of the total flow that is discharged through the bypass when simulating without salt and the red line shows the results from the simulations with salt. It is clear that the adding salt to the simulation has consequences. At low discharges it can even occur that on average more water flows downstream through the bypass than supplied by the river upstream. This means that the current branch is on average flowing in an upstream direction.

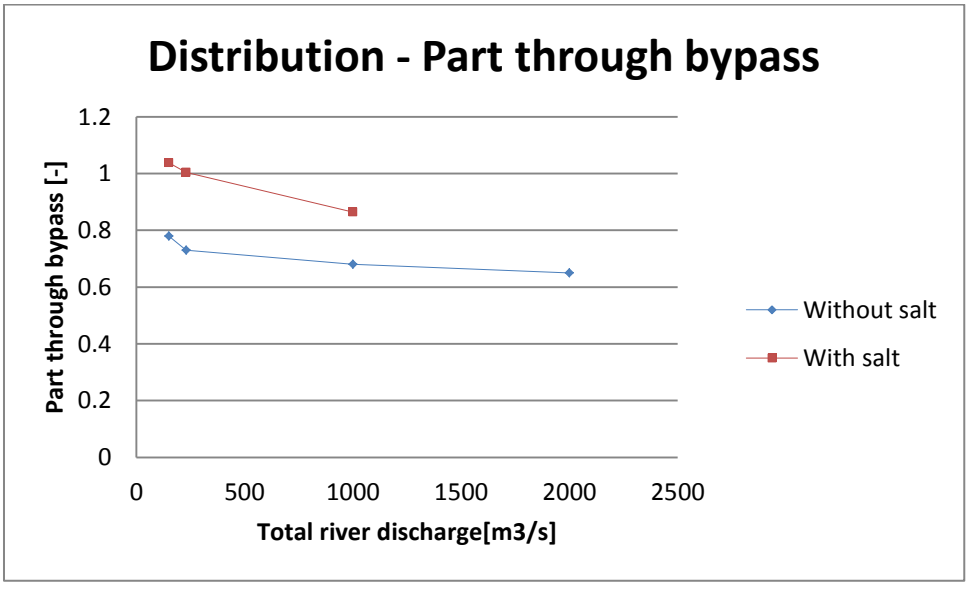

Fig. 5-21: Distribution at bifurcation, part flowing through the bypass.

The cause of this can be found in the difference of the geometry of the two mouths. As it is clear from equation (5.16) depth is the most important parameter in this since it is quadratic. Since the current branch's mouth is 14.6 m deep and the bypass only 7.6 m, it is clear where this phenomenon is coming from. Due to the much higher hydrostatic pressure that is applied from the sea land inward at the current branch's mouth the resistance is much larger for water to exit through the current branch than through the bypass. At low discharges the resistance of the bypass is so much lower that the density induced force at the river mouth is so dominant over the flow through the current branch that the average flow is from the sea towards the bifurcation. Fig. 5-21 does also show that the saline simulation tends to converge in the end towards the same distribution as found in the simulations without salt. This supports the theory that at high discharges friction will again dominate. However at low discharges salinity will have a very large intrusion length since there is hardly any flow to resist it or even an upstream flow can arise at very low discharges.

Salinity structure

The three aforementioned mentioned methods in section 3.3.3 to predict the salinity structure have the following results with the given hydro dynamic en geometrical information from the model. Based on the results and the understanding of the methods the results were useful or regarded as useless depending on their applicability to the Itajaí-Açu River system. This will be done per method.

Flow ratio

The first method is based on the ratio of river flow and tidal flow. For this the discharges are used with the assumption that the depth and width of the channels are constant. This assumption has been made before. The results from this method are as follows:

$Q_{0,total}$ [m^3/s]	Q_1 [m^3/s]	Q_2 [m^3/s]	$Q_{d,1}$ [m^3/s]	$Q_{d,2}$ [m^3/s]	P_1 [-]	P_2 [-]
150	155.6	-5.6	521	242	0.384 (stratified)	0.031 (partially mixed)
230	230	0	511	217	0.579 (stratified)	0.077 (partially mixed)
1000	863.9	136.1	327	107	3.132 (stratified)	1.152 (stratified)

Table 5-1: Salinity structure, results from method one

The column of P_1 gives the qualification of the salinity structure of the bypass. The column of P_2 gives the qualification of the salinity structure of the current branch. The results will be compared to the Delft3D model results later this section.

Estuary number

The second method is more elaborate than just the ratio of tidal flow and river flow. Besides this ratio density differences are also taken into consideration. The densimetric Froude number is a measure of the ratio between relative potential energy and kinetic energy. The tidal prism is based on the tidal flow amplitude of the M2 component which is practically all of the tidal flow in this model. The tidal prism is determined than as follows:

$$\int_{T_{HWS}}^{T_{LWS}} A sin\left(\frac{2\pi t}{T}\right) = A * \frac{T}{\pi} \tag{5.19}$$

The results for this method are as follows:

$Q_{0,total}$ [m^3/s]	P_1 [m^3]	$F_{m,1}$ [-]	T_1 [s]	R_1 [m^3/s]	Ne_1 [-]	Structure
150	8.15e6	0.06135	44700	155.6	4.410e-3	(stratified)
230	8.03e6	0.09100	44700	230.8	6.442e-3	(stratified)
1000	5.55e6	0.34061	44700	863.9	1.667e-2	(stratified)

Table 5-2: Salinity structure for bypass, results from method two

$Q_{0,total}$ [m^3/s]$_I$	P_2 [m^3]	$F_{m,2}$ [-]	T_2 [s]	R_2 [m^3/s]	Ne_2 [-]	Structure
150	6.07e6	0.00243	44700	9.4	8.527e-5	(stratified)
230	5.77e6	0.00574	44700	22.2	1.911e-4	(stratified)
1000	4.12e6	0.06101	44700	236.1	1.453e-3	(stratified)

Table 5-3: Salinity structure for current branch, results from method two

A problem with this method is the very low or even negative discharge through the current branch at low upstream river discharges. Due to the use of the densimetric Froude number that bases its kinetic energy on the river flow the estuary number becomes very low even though a high tidal amplitude can cause quite some mixing. However this low densimetric Froude number results in a very low estuary number. This is to be expected due to low tidal flow amplitudes as can be seen in equation (3.11). Since the tidal amplitude is rather high to very high compared to the river flow in the current branch the result should be a mixed structure. This is why this method is not working well in this system.

Stratification number

This method is based on energy dissipation that is used for mixing processes and results in a well-mixed system or with a more efficient estuary with little loses in a stratified system. Another process at play is the conversion of energy into heat which does not necessarily contribute to mixing. Both (Ippen and Harleman 1961) and (Prandle 1985) consider the forcing density difference and the potential energy. (Prandle 1985) considered energy dissipation over the length of the estuary in relation with the ratio of tidal flow and river flow. However the length of the estuary is difficult to determine in this situation. There are two entries (mouths) into the system. And there is one basin to be filled behind these two entries. Therefore the upstream section is split in two. For this the results from section 5.3 are used. When one remembers that 1/3 of the tidal prism is coming from the current branch and 2/3 from the bypass one can state that 1/3 of the upstream length “belongs” to the current branch and 2/3 to the bypass. The upstream model boundary is 65 km upstream of the bifurcation. Both branches have their own length as well for their own adapted estuary length. The results from this method are shown below:

$Q_{0,total}$ [m^3/s]	$S_{t,1}$ [-]	Structure
150	36.6	(stratified)
230	24.3	(stratified)
1000	4.5	(stratified)

Table 5-4: Salinity structure for bypass, results from method three

$Q_{0,total}$ [m^3/s]	$S_{t,2}$ [-]	Structure
150	269.4	(partially mixed)
230	163.7	(partially mixed)
1000	7.3	(stratified)

Table 5-5: Salinity structure for current branch, results from method three

The results from this method look more feasible. In the next section the similarities with the Delft3D model will be explained.

Delft3D model results

The Delft3D model showed good similarities with the first and the third method. The second method did not qualify for reasons explained previously due to low or negative discharges.

In Fig. 5-22 through Fig. 5-25 the visualization is shown of the comparison of the intrusion in the current scenario and the bypass scenario. What was expected from method one and method three explained earlier can be seen. The partially mixed structure is indeed found in the current branch. In the bypass the system looks more layered. At higher discharges the bypass gets a very distinct layered structure. The current branch is only at high discharges stratified. Until then the structure is partially mixed.

Another result is a very strong increase of salinity in the current branch. This can be a problem. When looking at the point of the Itajaí-Mirim bifurcation sever intrusion reaches now until there. In the Itajaí-Mirim there is a water purification plant. Increase of salinity there would increase operational cost.

The residual flow due to the larger hydrostatic water pressure at the current river mouth causes the larger intrusion. It is therefore undesired to have an open bypass at low discharges since the water is than pushed from the current branch mouth to the bypass mouth. This causes an increase of the salinity levels. What also enhances the intrusion is the lower discharge through the current branch due to the partial diversion of river discharge through the bypass.

In Fig. 5-22 one can see that at low discharges during flood the intrusion is beyond the bifurcation. This is the low discharge scenario of 150 m^3/s. The results for the 230 m^3/s and 1000 m^3/s scenarios can be found in appendix XI. This is the case for both the current branch as in the bypass. The structure in both branches is different. One can see that in the bypass the structure is much more stratified than in the current branch. The upper part is showing the current branch how the salt intrusion behaves in the bypass scenario. The middle part shows the salt intrusion in the bypass.

In Fig. 5-23 and Fig. 5-25 the comparison is visualized. With the current situation shown in the upper part and in the middle the difference between the current scenario and the bypass scenario are shown.

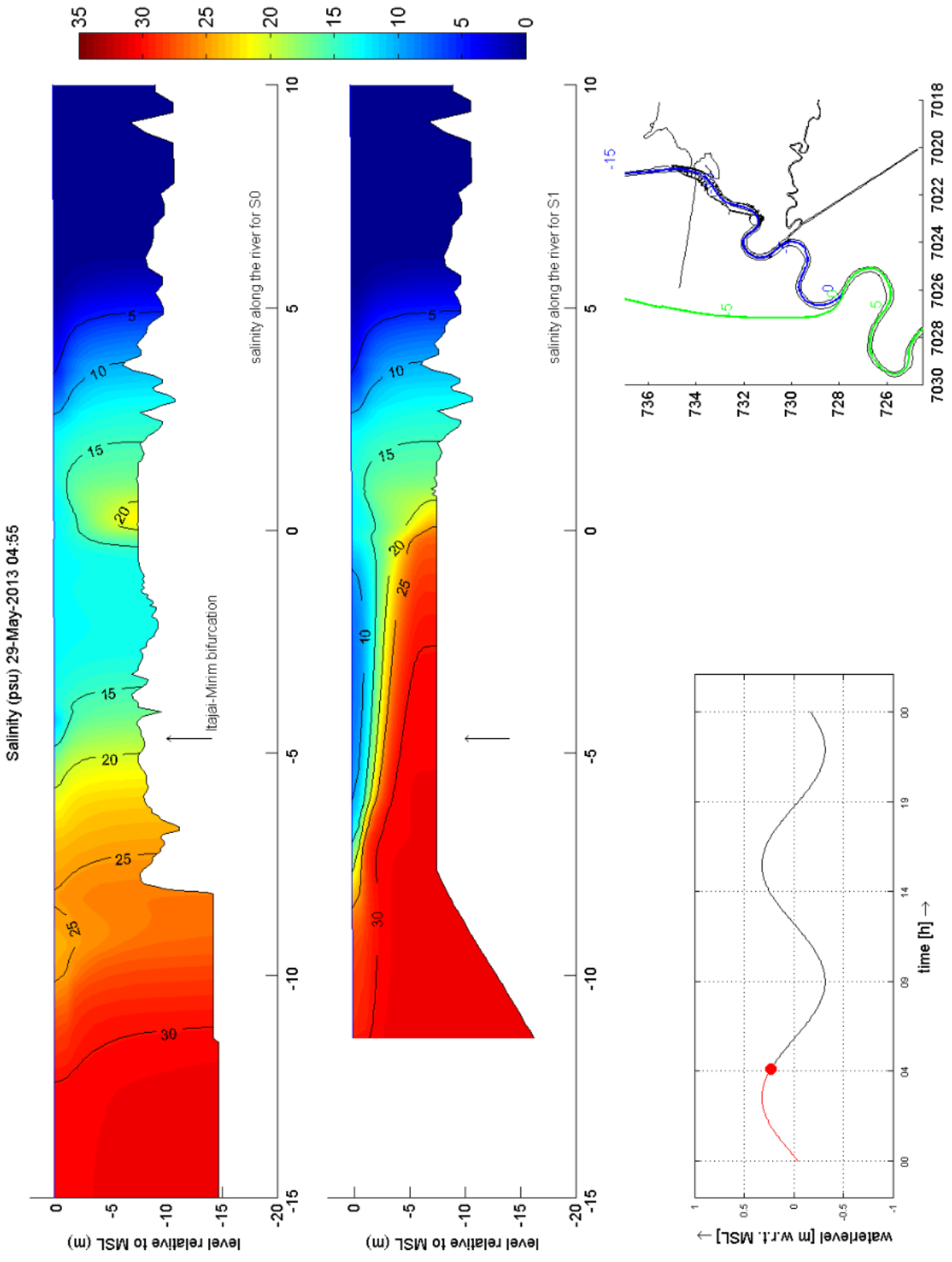

Fig. 5-22: Bypass scenario, salt intrusion during flood, 150 m^3/s

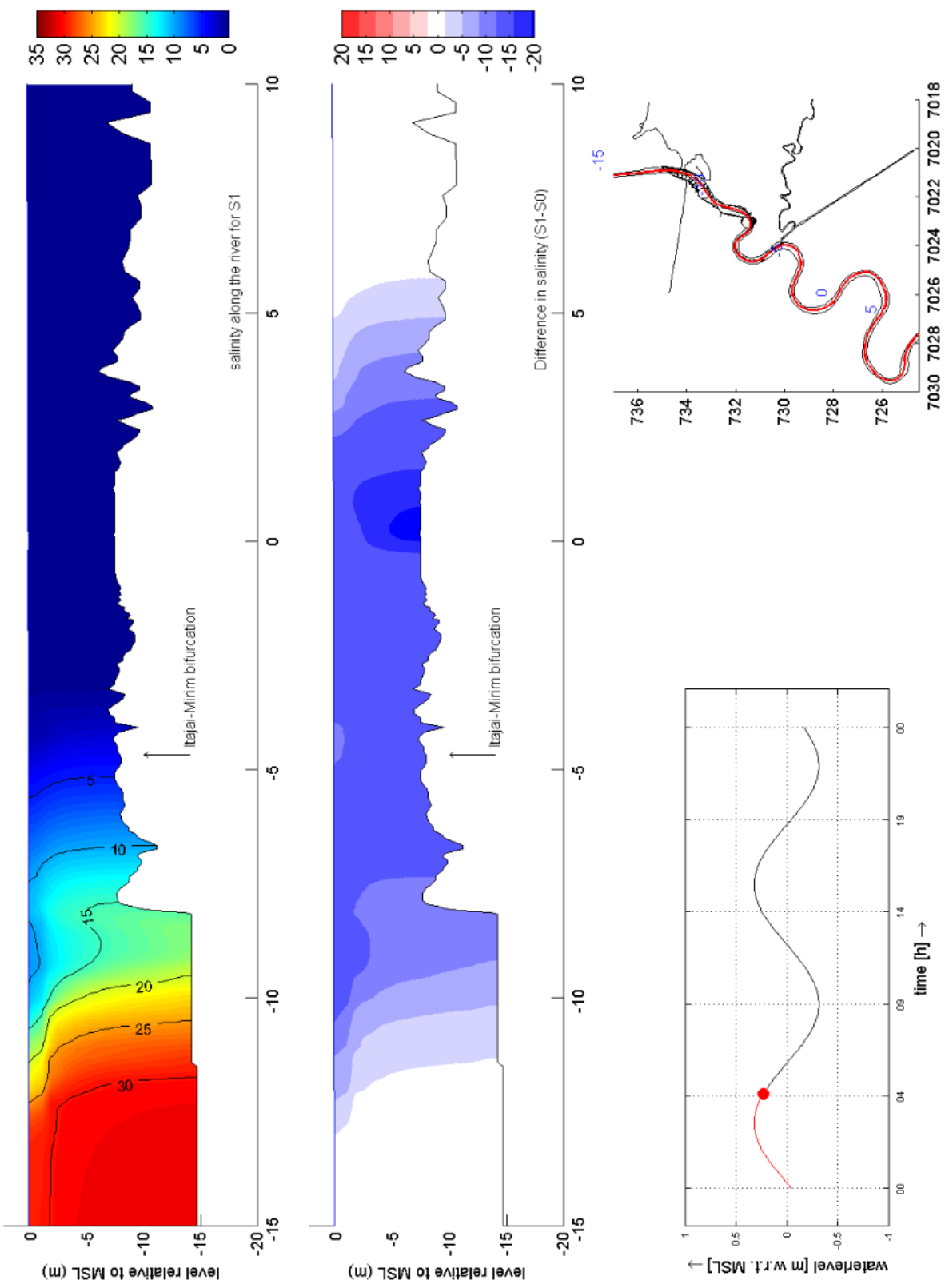

Fig. 5-23: Salt intrusion current situation and difference during flood, 150 m^3/s

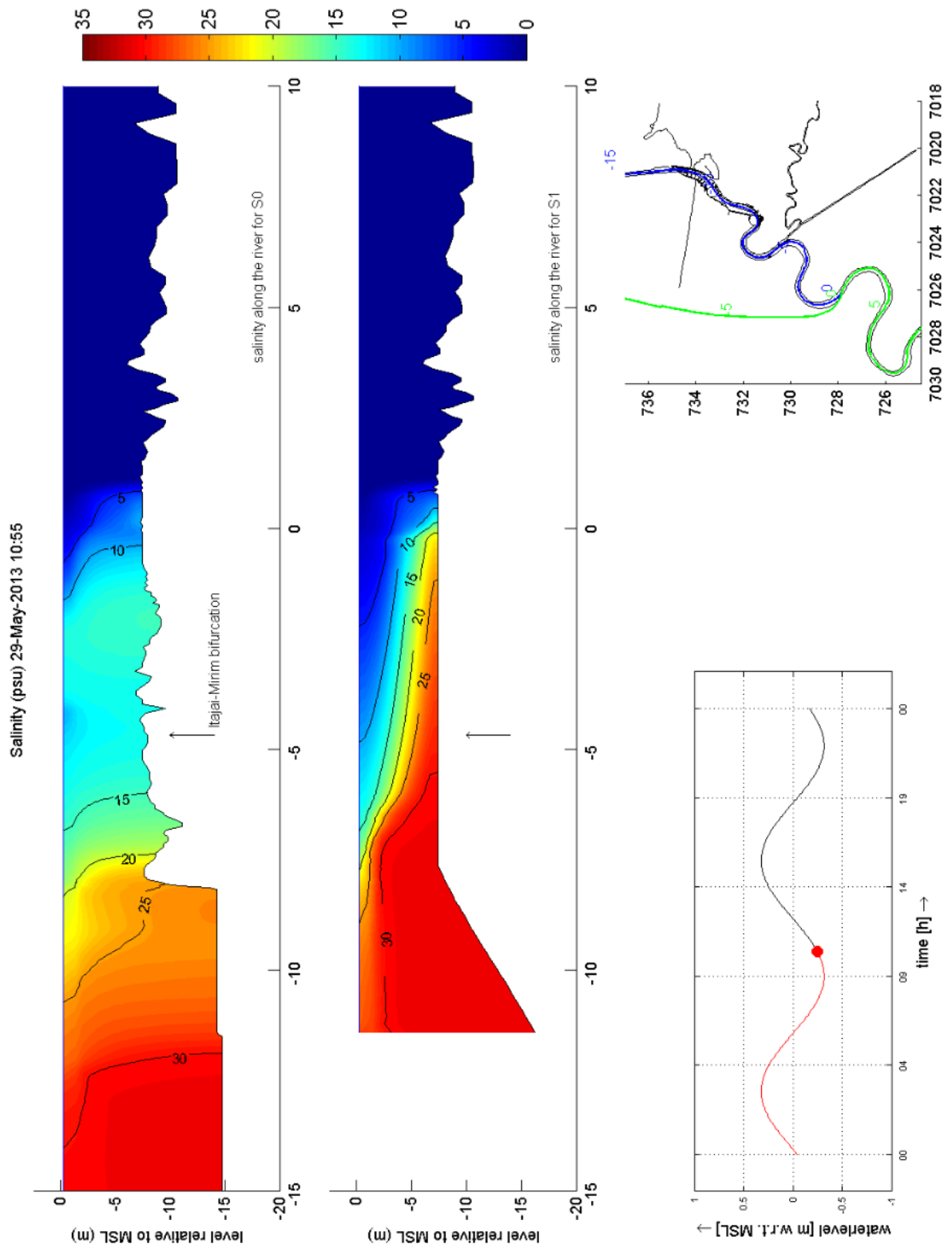

Fig. 5-24: Bypass scenario, salt intrusion during ebb, , 150 m^3/s

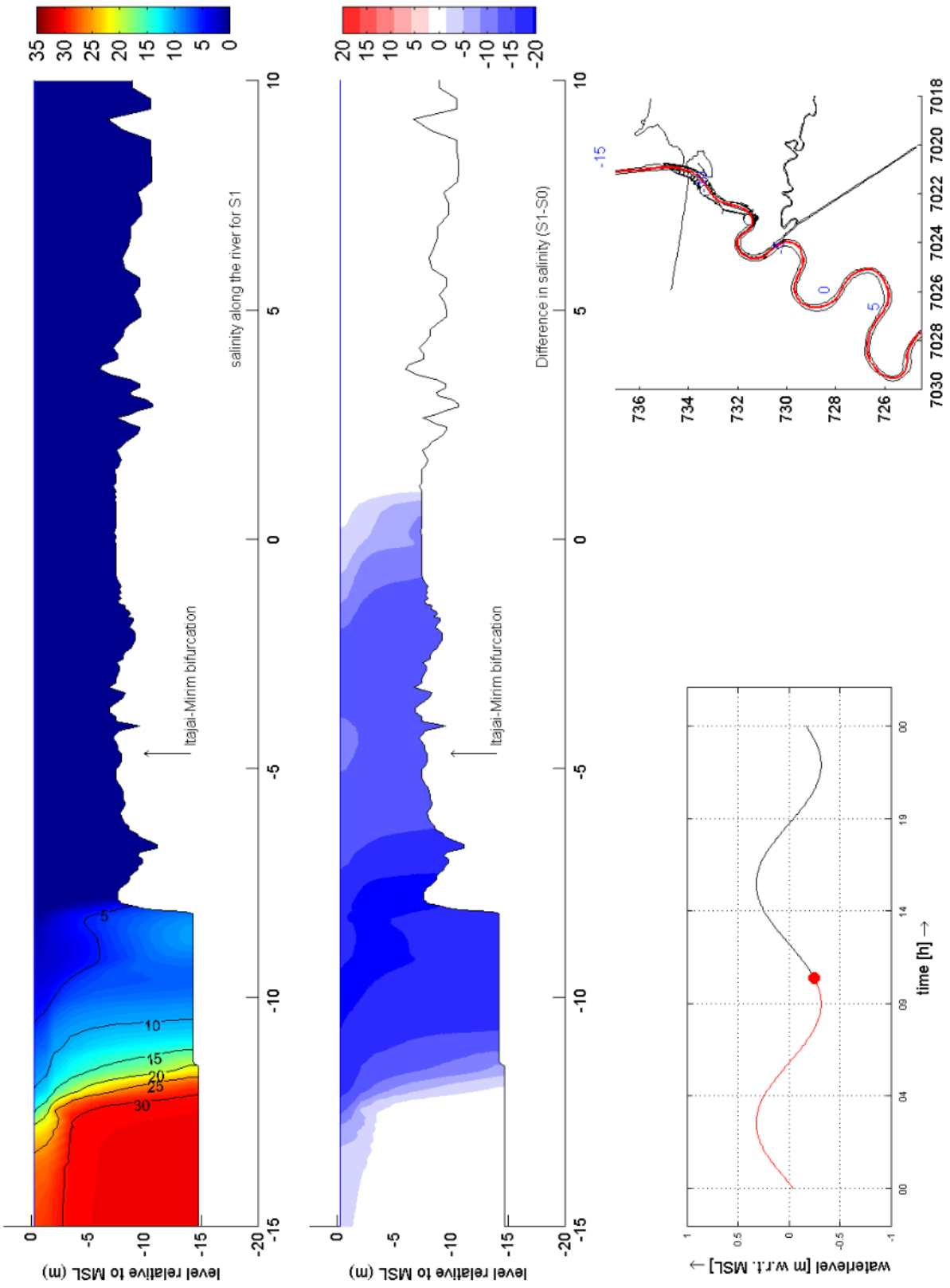

Fig. 5-25: Salt intrusion current situation and difference during ebb, 150 m^3/s

Another phenomenon that is found is the decrease of the tidal flow amplitude when comparing the simulation with and without salinity. As mentioned for the third method use was made of the idea of energy dissipation. This is induced by flow that moves over a rough bottom or two water bodies moving along each other in a different direction.

This movement in different directions does occur when salt water moves in and fresh water moves out with a mixing layer in between. The larger this mixing layer the more friction the two have. This shows the magnitude of mixing. In Table 5-6 and Table 5-7 the reductions are shown. The reduction in the bypass is larger at low discharges with about 10%. At higher discharges this decreases. This is when the mixing layer decreases and the stratification increases strongly. For the current branch this is different. Here the reduction remains 10%. This can be seen as the mixing that is still visible at higher discharges.

Q_0 [m^3/s]	Amplitude with salt [m^3/s]	Amplitude without salt [m^3/s]
150	573	643
230	564	625
1000	390	403

Table 5-6: Tidal flow amplitude for bypass at mouth

Q_0 [m^3/s]	Amplitude with salt [m^3/s]	Amplitude without salt [m^3/s]
150	427	470
230	405	459
1000	290	332

Table 5-7: Tidal flow amplitude for current branch at mouth

5.4.3 Conclusions

For the salinity dynamics two aspects have been analysed

- Static momentum balance between fresh and salt water
- Salinity structure

As concluded the parallel system of the two channels is during low discharges very sensitive for the density difference between fresh and salt water. At very low discharges it is even found that the density difference induced a residual current in an upstream direction through the current branch. This additional water is discharged through the bypass. However this will cause a tremendous increase of salinization in the current branch as salt water is on average transported in an upstream direction. The result can be severe as the purification plant in the Itajaí-Mirim branch might be having to deal with higher production cost or more downtime.

For the salinity structure it was found that the current branch behaves slightly stratified in the current scenario under average conditions. This stratification increased with the implementation of the bypass due to the discharge reduction through the current branch. This lower discharge does decrease the saline gradient which means a reduction of entrainment of the salt water particles. This way less salt water from the sea will flow in an upstream direction over the bottom. Hence this change does cause a further intrusion of salt but it reduces bed shear stress in an upstream direction.

The salinity structure in the bypass is different. Here there is a much more stratified structure to be found. Although the tidal discharge is larger in the bypass than in the current branch the river discharge through the bypass is relatively much larger. This large discharge is enhance by the average upstream flow through the current branch. Hence a stratified structure is reasonable.

5.5 Bed shear stress

Bed shear stress is an indication of the erosion / sedimentation patterns that will arise due to hydrodynamics. The occurring bed shear stress un combination with the suspended load concentration determines whether erosion or sedimentation will take place. The actual current determines the transport direction. The flow direction can differ over depth as can the concentration. Hence for transport it can be a very difficult to describe the transport in a qualitative way.

5.5.1 Theory & hypotheses

The previous four research areas, discharge distribution, water levels, tidal flow and salinity dynamics, have shown how hydrodynamics change due to the bypass implementation compared to the current situation. Some of those conclusions are relevant to postulate the hypotheses for the analysis of the results of the bed shear stress. The relevant results will be summarized first.

With the research on the discharge distribution it was found that the system is not friction dominated during low discharges. This means that bed shear stress is also low. At low discharges the amount of water flowing through the current branch is very low. This decreases the bed shear stress drastically. At higher discharges the distribution is 35% for the current branch and 65% for the bypass. If discharge reduces to 35% the bed shear stress reduces to roughly 12% since bed shear stress is quadratic related to flow velocity. This means that the erosion problem is most likely to be handled very well with the bypass at high velocities. However, at low velocities the flow velocities end up in the sedimentation range.

The change in tidal flow will have a large impact on the bed shear stress. In the current branch the tidal flow amplitude has diminished. The result is that the tidal induced bed shear stress has diminished even stronger due to the quadratic relation. The upstream section that is the bottleneck for the downstream section is the cause of this as explained in section 5.3. For the current branch this means a strong reduction of bed shear stress. For the bypass there is no comparable situation. However the Delft3D model has shown that the same effect arises there as well as a consequence of the tidal flow reduction when modelling the situation with only the bypass open. This is then compared with the modelled two channel scenario. These lowered tidal flow amplitudes have a very large effect on the bed shear stress.

In the section upstream of the bifurcation the tidal movement has increased due to the increased tidal prism caused by the lowered friction in the downstream section. Due to this increased tidal prism the tidal range of the water level elevation increases. A higher high water and a lower low water is the result. This drives a stronger tidal flow for the upstream section as more water is displaced between high and low water. This increase will cause an increase of bed shear stress. A result of this increased bed shear stress is that upstream more sediment can be mobilized by the tide. This mobilized sediment will be transported in suspension by the river discharge towards the section between the bifurcation and the sea where carrying capacity has diminished. If that happens this will become a severe sedimentation problem.

The salinity dynamics in this system have shown to have a large impact. The residual flow that arises due to the difference in hydrostatic pressure on the two mouths at low discharges is a very important realisation. But also the tidal damping due to energy dissipation by friction between the

fresh and salt water body causes a slight reduction of bed shear stress by the tidal flow. However this is less noticeable downstream since there are two processes at play in at the mouth area. The tidal decrease is noticeable everywhere. But at the mouth area there is also the two directional flow due to gravitational flow. This gravitational flow induces a change in bed shear stress as well. The result of the decreased tide and the gravitational flow is hard to predict. Bed shear stress in the mouth area can increase, decrease or hardly change. Further upstream where the gravitational flow has diminished the reduction of the tide will dominate. Hence further upstream less bed shear stress will occur.

Now the following hypotheses can be formulated:

- The discharge distribution reduces the flow through the current branch. At low discharges this is even more so than during high discharges. This reduction will reduce the bed shear stress.
- The tidal flow is responsible for most of the bed shear stress. Tidal flow is during day to day conditions dominant to river flow. Hence change in tidal movement has the biggest impact. The increased transport capacity of the bypass and the current branch combined in combination with a much less increased tidal prism results in a diminished tidal flow which in return paralyzes the downstream section to transport sediment.
- Upstream of the bifurcation the bed shear stress will increase due to the increased tidal flow by the increased tidal prism This is opposed to what happens downstream. In this upstream section nothing has changed with the cross-section. So an increased tidal prism results in higher tidal flow velocities.
- Salinity in the model induces three changes in the system. One is the increase of resistance in the current branch relative to the bypass. This will reduce the average velocity in the current branch. The second change is the gravitational flow. This will cause bed shear stress. The third change is the reduction of the tide due to dissipation. A reduced tide results in reduced tidally averaged bed shear stress.

5.5.2 Results

The results will be treated per hypotheses. Starting at the tideless scenario towards the influence of the tide and then the influence of salinity on bed shear.

Tideless scenario

The first step is to assess what the new stationary distribution changes about the bed shear stress. Fig. 5-26 shows the difference between the bypass scenario and the current scenario with a 150 m^3/s discharge. It shows that the differences are small. However this is in the same order of magnitude of occurring bed shear stress in the current situation. The reduction is at some point almost 0 N/m^2.

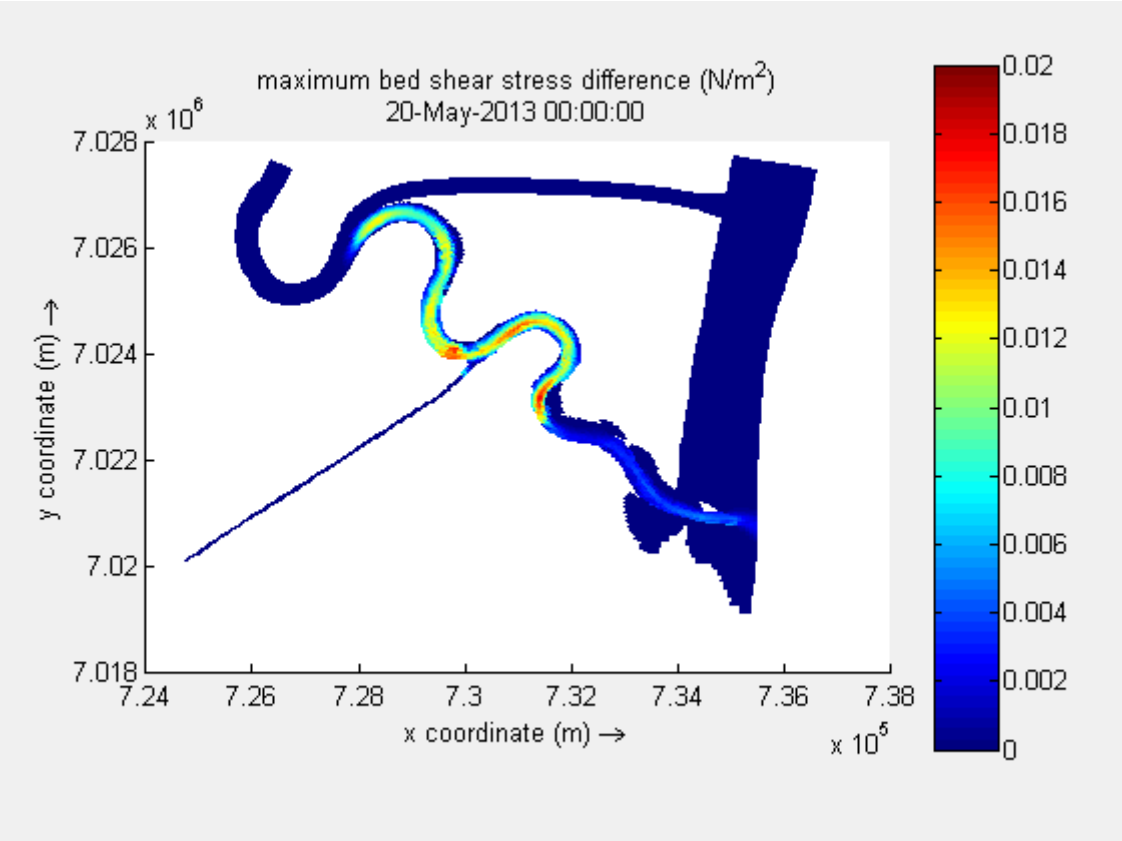

Fig. 5-26: Difference current - bypass scenario, stationary flow 150 m^3/s

In Fig. 5-27 one can see the difference between the bypass and current scenario during a 230 m^3/s discharge. Here the differences are much bigger. However, these differences are again in the same order of magnitude as the occurring bed shear stresses in the current scenario. The same can be seen in Fig. 5-28 with a discharge of 1000 m^3/s.

This can be explained with the quadratic relation between bed shear stress and flow velocity:

$$\tau_b \propto u|u| \tag{5.20}$$

With:

- τ_b = bed shear stress [N/m^2]
- u = flow velocity [m/s]

When velocities are reduced in the current branch to 20% to 35% (remaining part for the current branch during low and high discharges respectively) the bed shear stress reduces to 4% to 12 % respectively. This is in agreement with the results from the model.

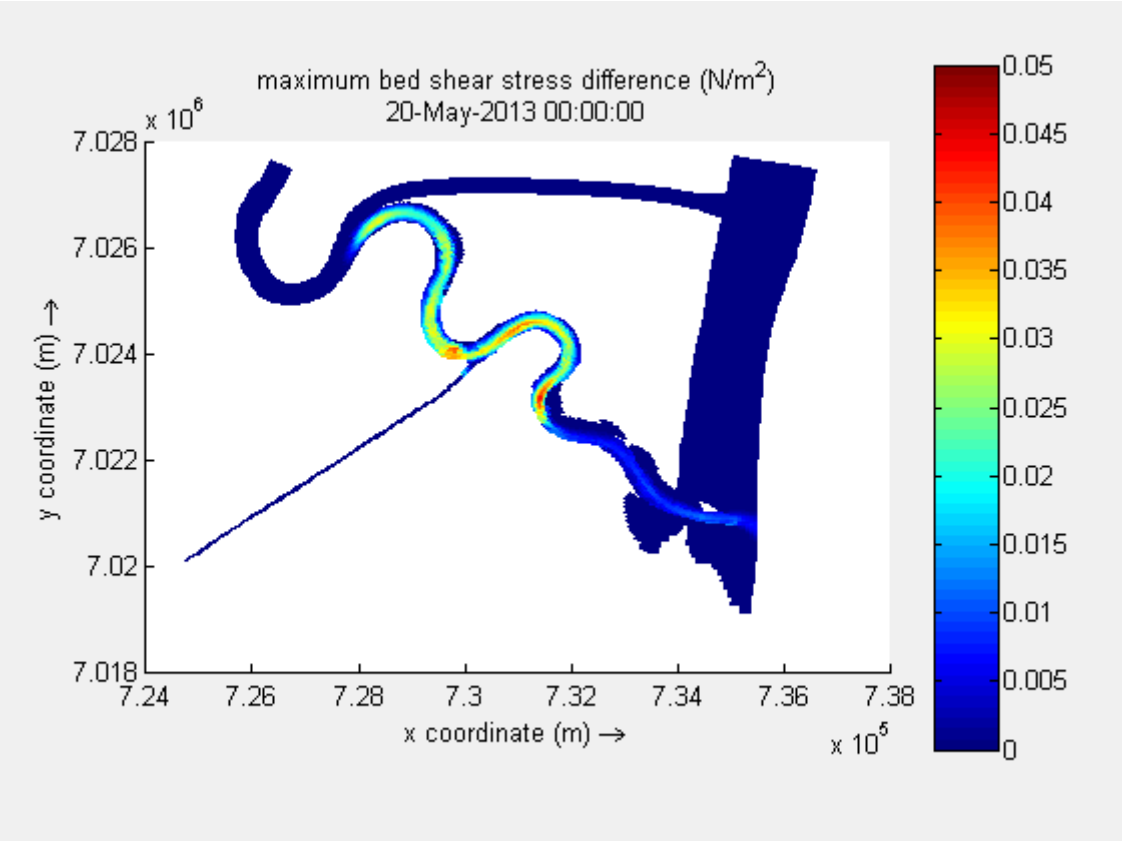

Fig. 5-27: Difference current - bypass scenario, stationary flow 230 m^3/s

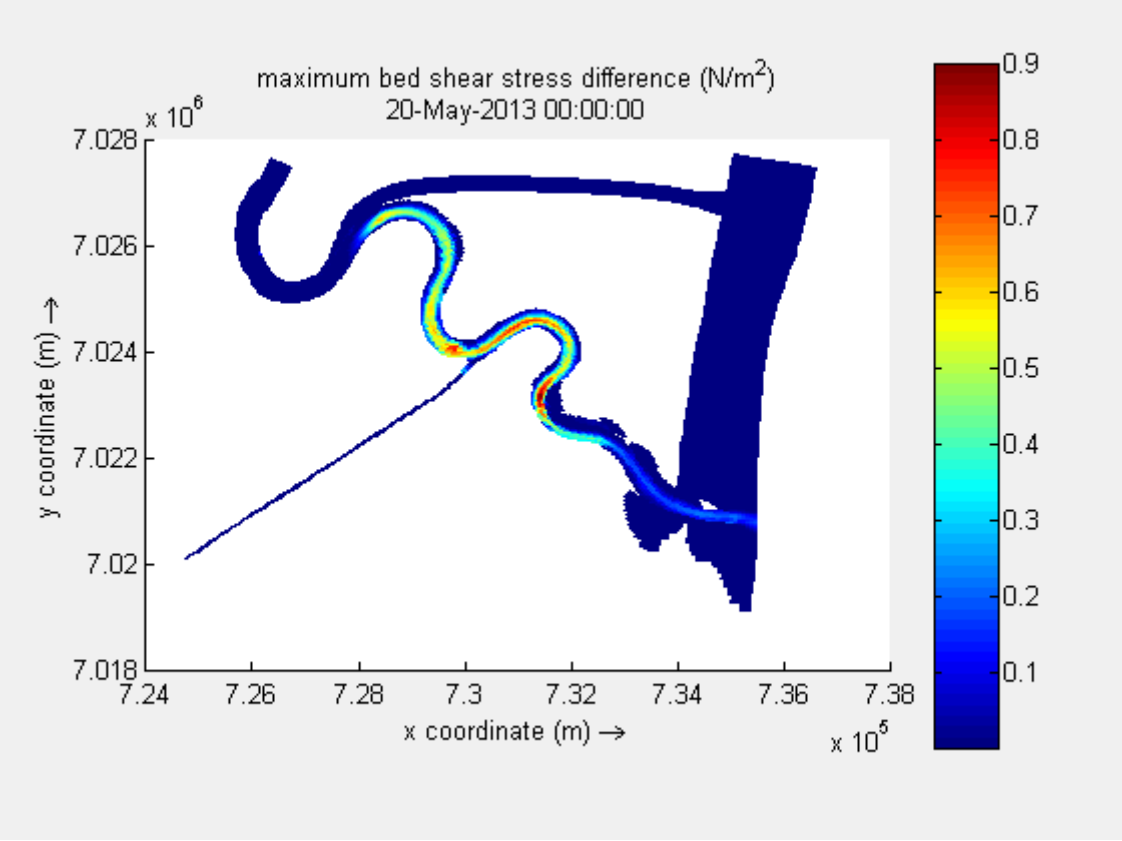

Fig. 5-28: Difference current - bypass scenario, stationary flow 1000 m^3/s

Ebb and flood scenario

For the tidal scenario it is interesting to see what the result is during ebb and flood. The direction was chosen not to be relevant since fine sediment does not respond instantaneously to water flow changes. The transport direction depends on the concentration over height and the direction distribution over height. Especially near the mouth where the flow can flow inward at the bottom and outward at the surface it is hard to say what happens by looking at depth averaged concentrations and velocities. The change in bed shear stress does give insight whether erosion or sedimentation can be expected to increase or decrease, although this would neglect consideration of the concentration of suspended load.

In Fig. 5-29 through Fig. 5-32,the bed shear stresses during ebb and flood are shown for 230 m^3/s. The results of 150 m^3/s and 1000 m^3/s are shown in appendix X. What was to be expected for the bed shear stress due to the diminished tidal flow has indeed happened. As one can see the bed shear stress has diminished in the current branch in the bypass scenario. Especially during ebb the decrease is large. It needs to be noted that during flood in the 1000 m^3/s discharge the bed shear stress is at a minimum since it is at minimal velocity at that moment as there is no flow reversal anymore hence no zero-crossing for the velocity signal.

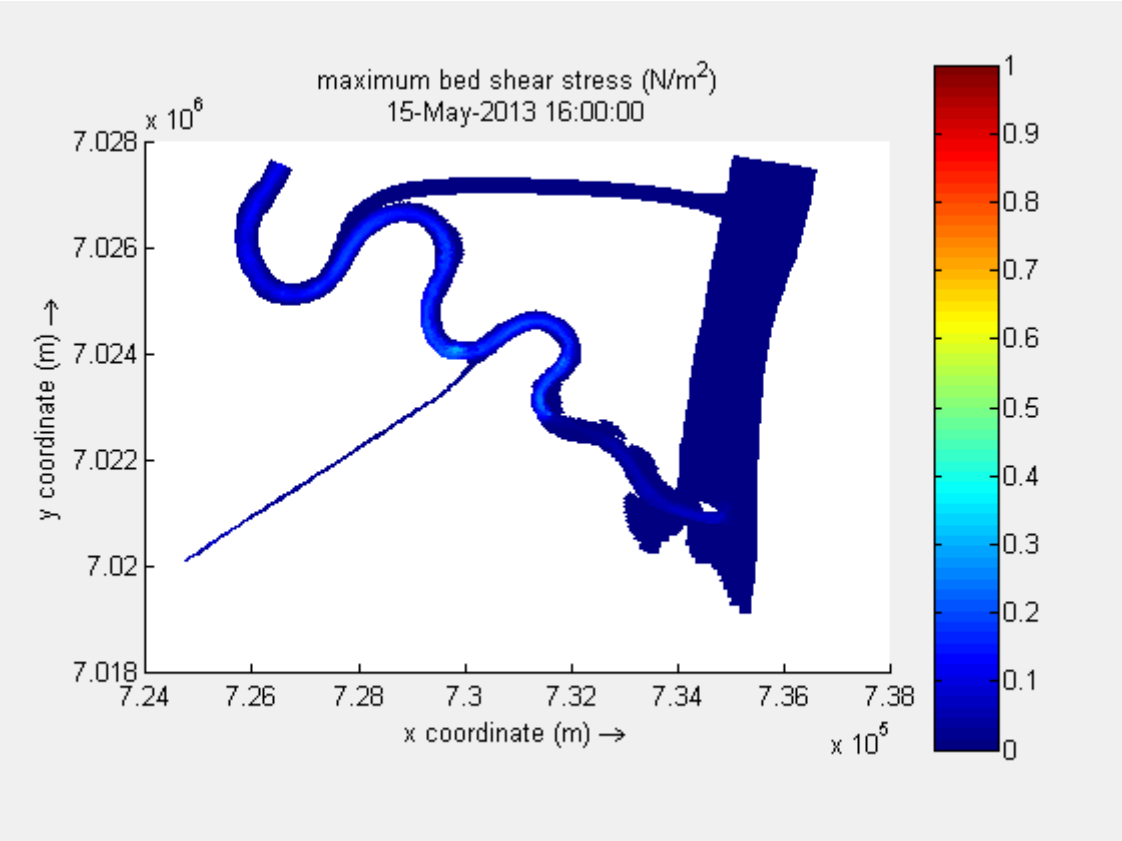

Fig. 5-29: Bed shear stress, 230 m^3/s, flood, current scenario

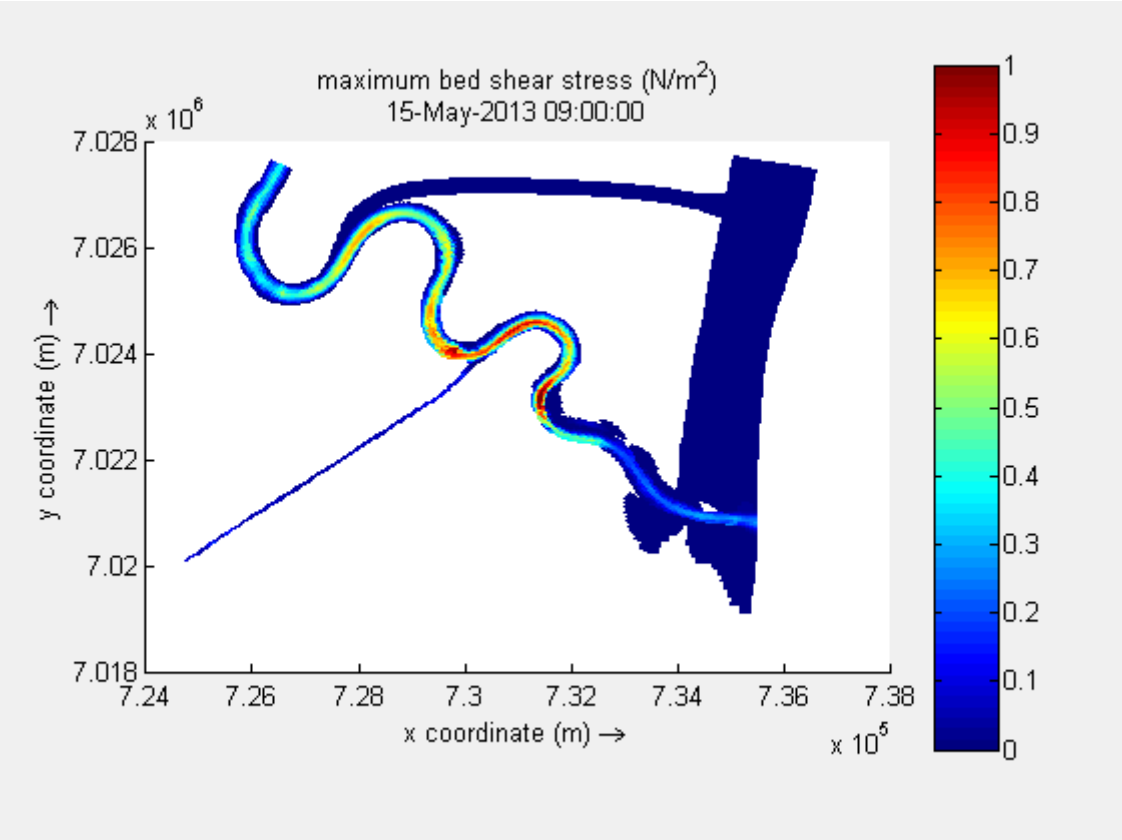

Fig. 5-30: Bed shear stress, 230 m^3/s, ebb, current scenario

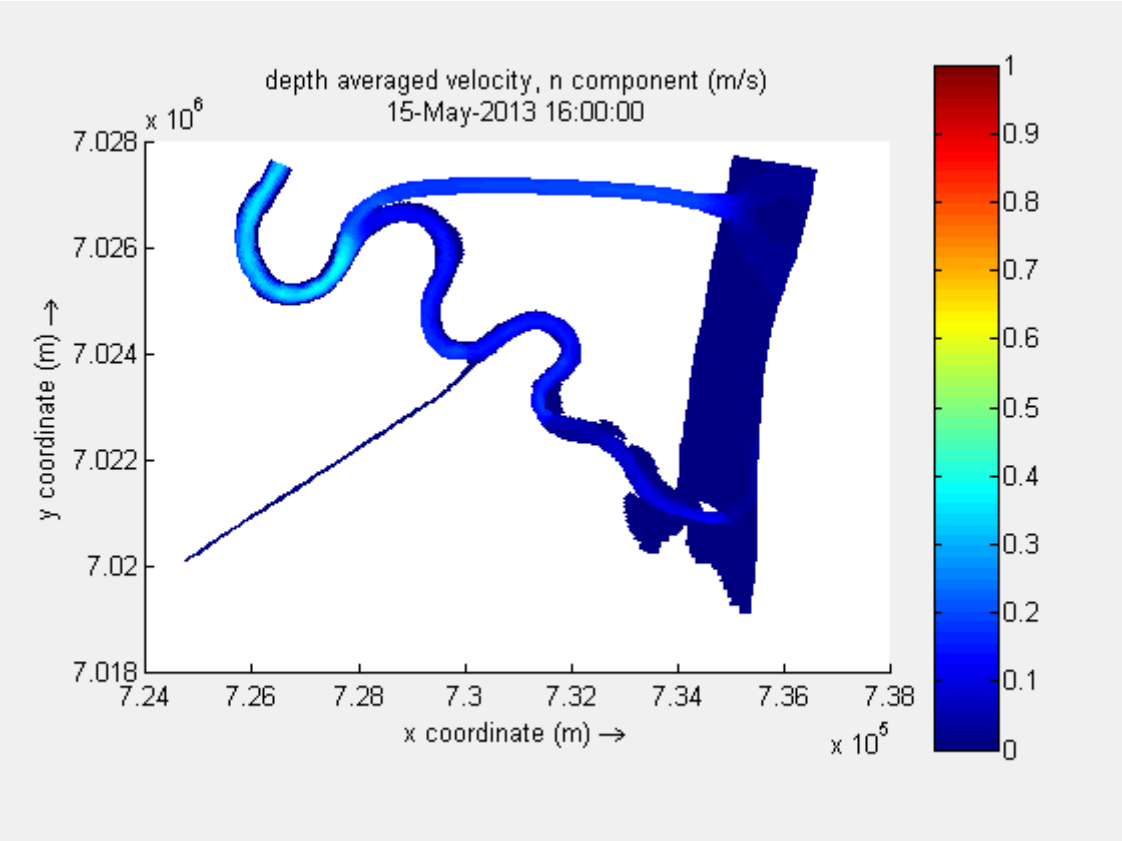

Fig. 5-31: Bed shear stress, 230 m^3/s, flood, bypass scenario

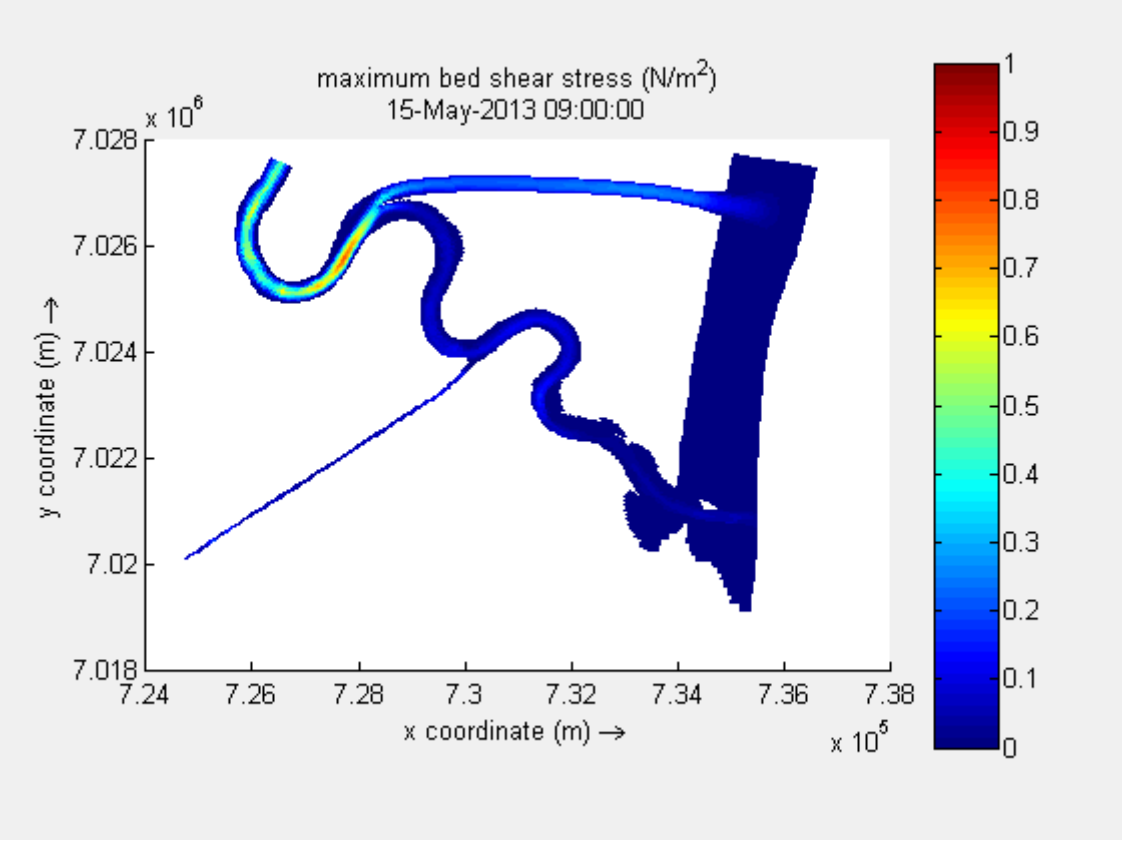

Fig. 5-32: Bed shear stress, 230 $m^{3/}s$, ebb, bypass scenario

To assess the impact in more details two locations have been chosen to take a closer look at the change in bottom shear stress. The first location is just downstream of the bifurcation in the current branch. Here the result of the reduced tidal flow should be the clearest. The second location is in the harbour basin.

Below in Fig. 5-33, Fig. 5-34 and Fig. 5-35 the results are shown of the bed shear stress directly downstream of the bifurcation point in the current branch. This is done for the bypass scenario with the blue line and the current scenario with the red line. As can be seen there is a very strong response to the tidal flow decrease. Since bed shear stress is quadratic related to velocity the reduction to 35% of the tidal flow amplitude should result in about 12% reduction of bed shear stress. This can indeed be seen below when correcting for the average flow by river discharge. When looking at the high peaks one can see that during ebb flow the bed shear stress is higher. This is only clear in the current scenario. In the bypass scenario the average river discharge has been reduced down to 25%. Hence it does not cause a big difference between maximum bed shear stress at maximum ebb flow and maximum flood flow.

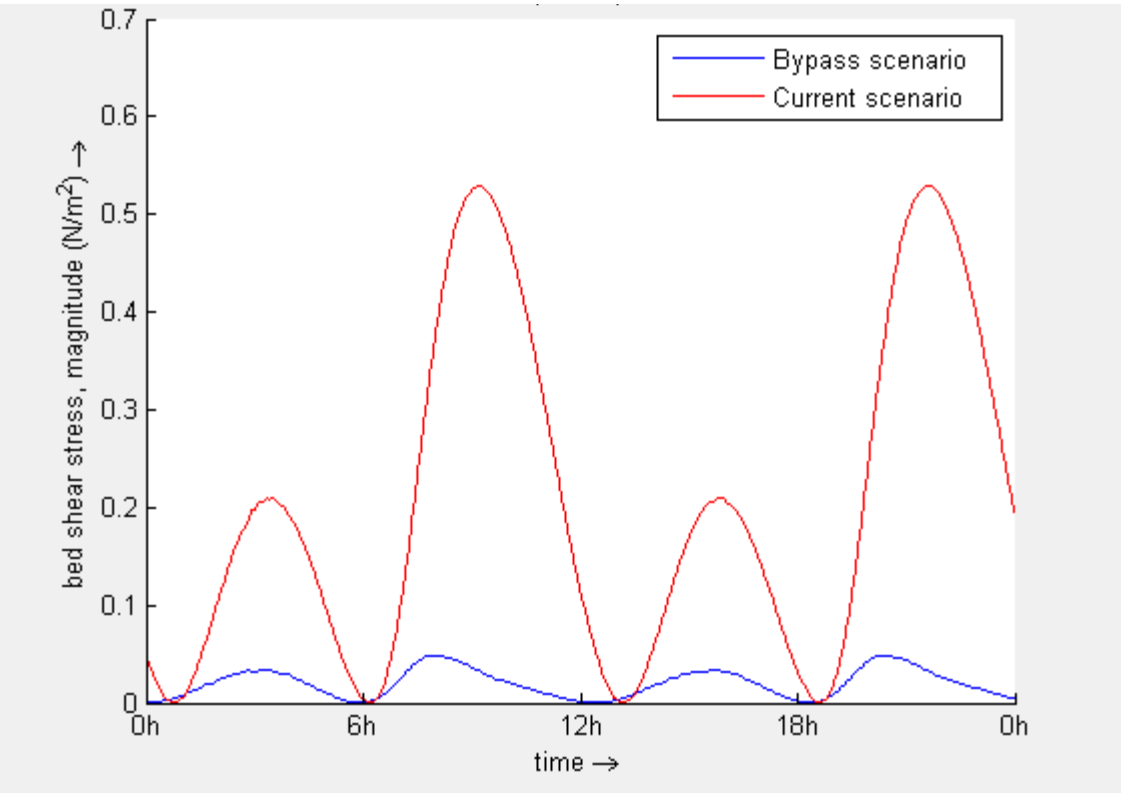

Fig. 5-33: Bed shear stress directly downstream of bifurcation point in current branch, 150 m^3/s

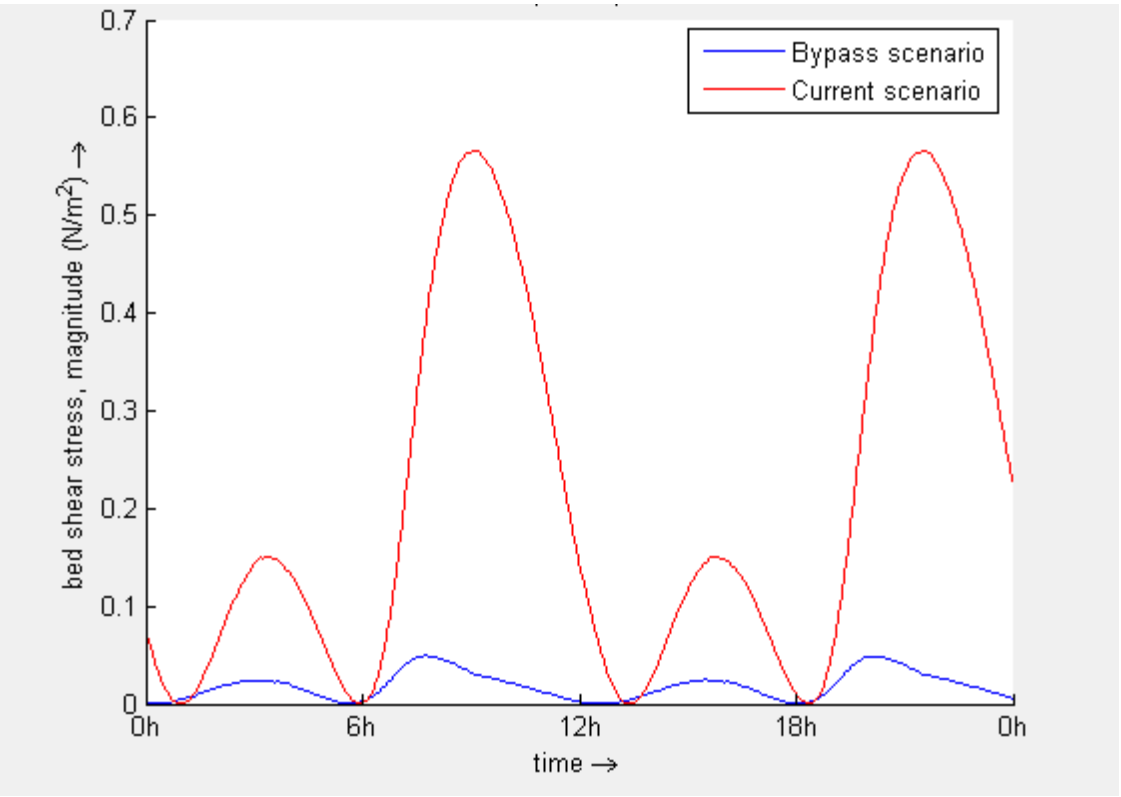

Fig. 5-34: Bed shear stress directly downstream of bifurcation point in current branch, 230 m^3/s

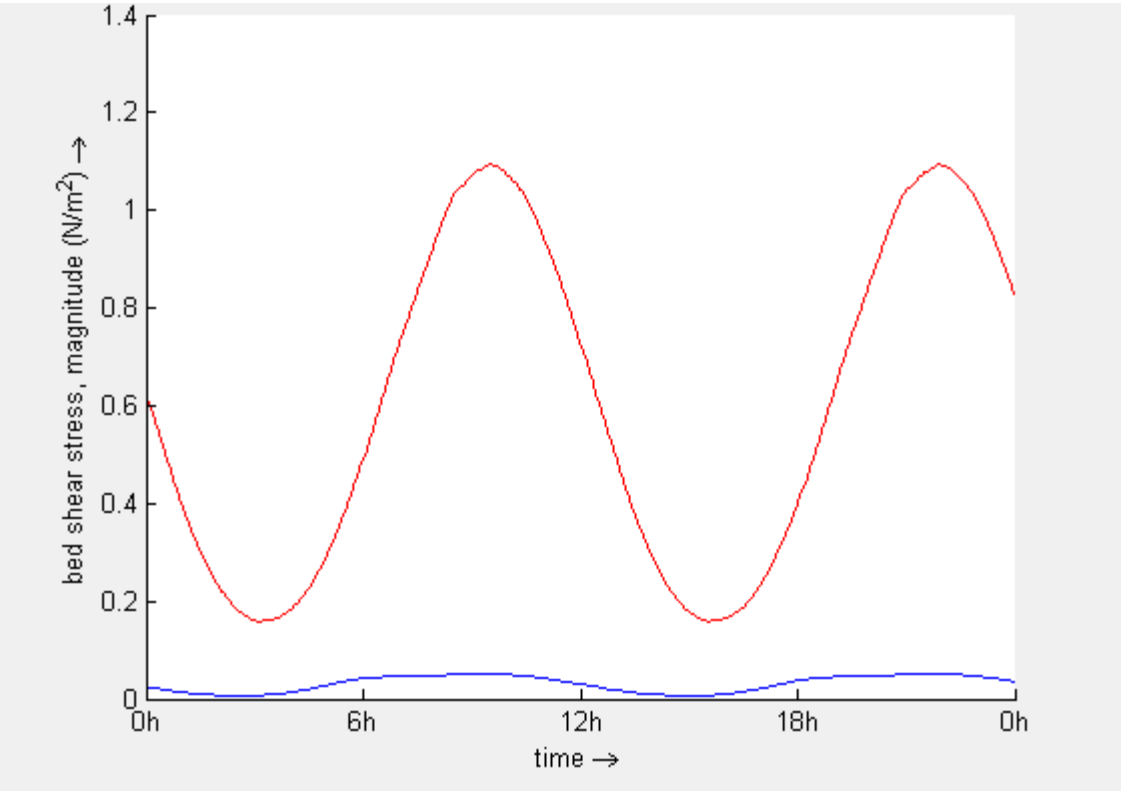

Fig. 5-35: Bed shear stress directly downstream of bifurcation point in current branch, 1000 m^3/s

The results in the harbour basin are from an observation point in the middle of the harbour basin. In Fig. 5-36, Fig. 5-37 and Fig. 5-38 these results are shown. Especially during flood flow the

result is less strong as with the observations more upstream at the bifurcation point. This is due to the fact that the effect of the Itajaí-Mirim is taken into account as well here. This river branches into the Itajaí-Açu between the two shown observation points just upstream of the harbour basin. This branch adds roughly 10 % of the total upriver discharge to the flow in the Itajaí-Açu River. This induces a higher bed shear during ebb and a lower bed shear during flood flow. When looking at the values of the peaks and comparing them for both observation points one can see that the bed shear is much lower in the harbour basin. This is due to the larger depth in the basin.

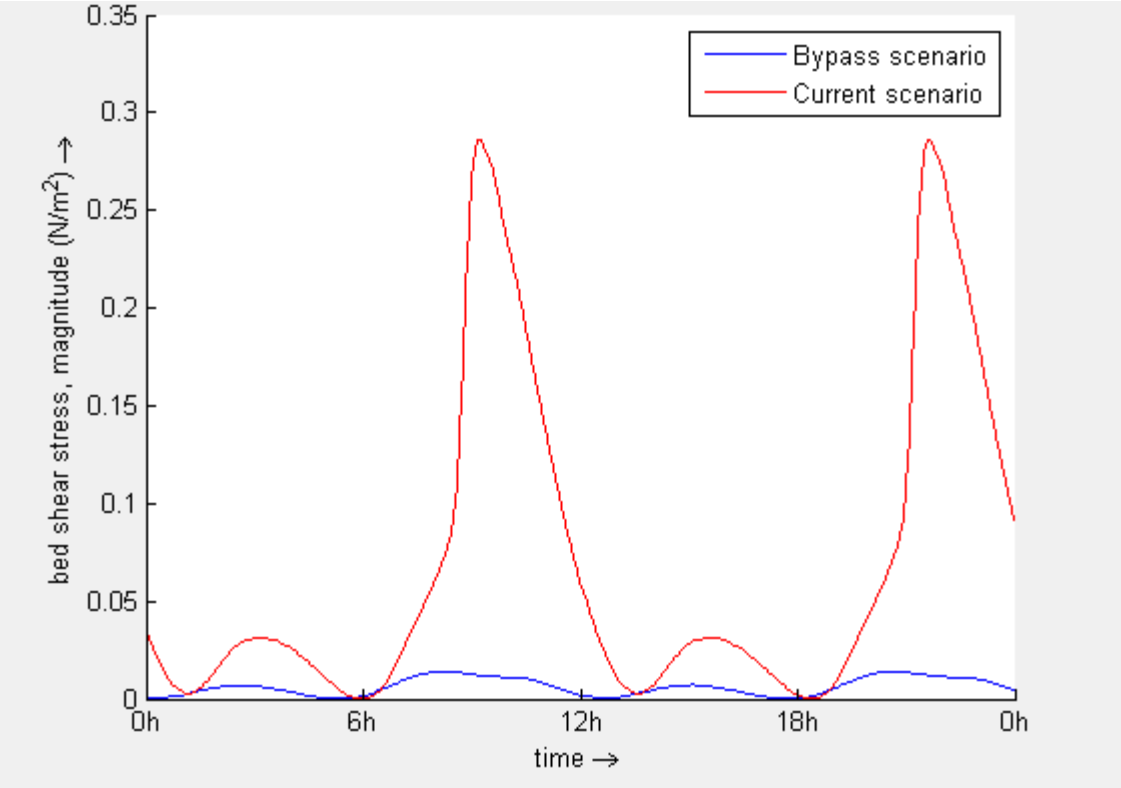

Fig. 5-36: Bed shear in harbour basin, 150 m^3/s

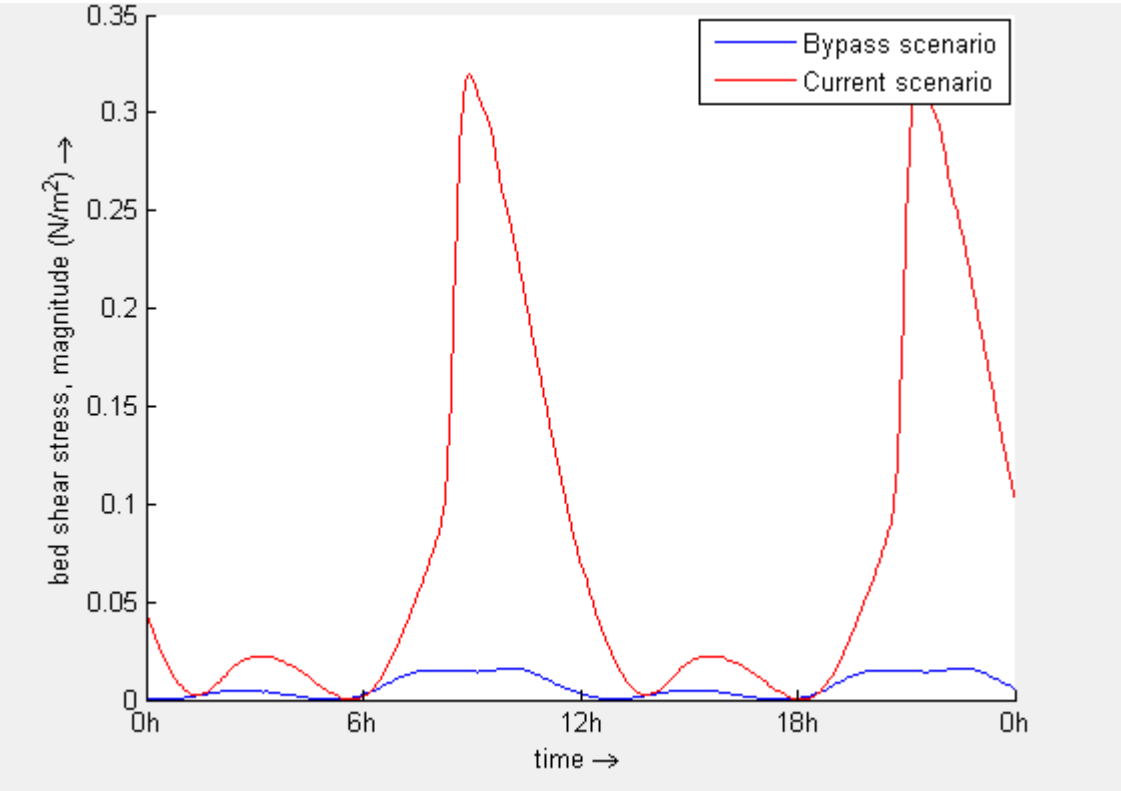

Fig. 5-37: Bed shear in harbour basin, 230 m^3/s

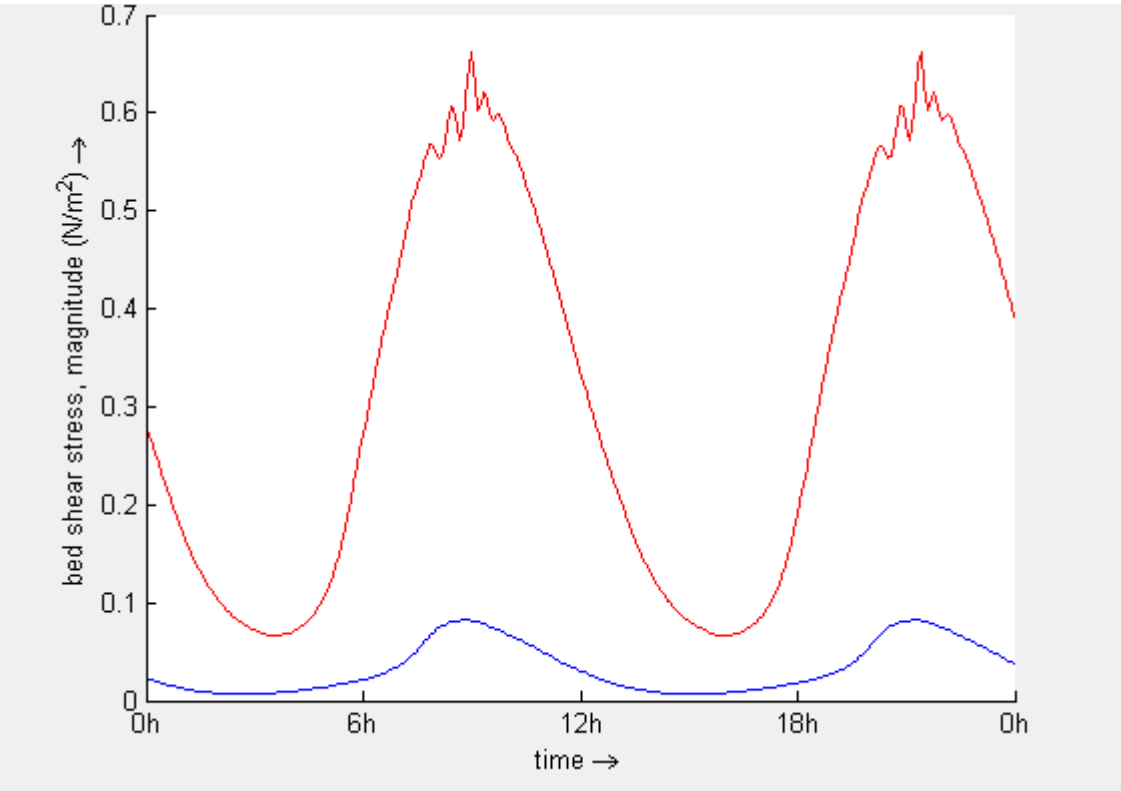

Fig. 5-38: Bed shear in harbour basin, 1000 m^3/s

Increased upstream bed shear stress

Due to the increased tidal prism for the entire system and an increased effective cross-section downstream, different changes occur upstream compared to downstream with the tide. In the upstream section the bed shear stress should increase. This increase is due to the increased tidal prism in combination with a cross-section that has remained the same. The increase of the tidal prism is only small as the friction is only reduced in the downstream section. An important thing is that this would induce an increase of sediment transport due to increase mobilisation capacity. While on the other hand the carrying capacity downstream of the bifurcation has decreased.

In Fig. 5-39 through Fig. 5-42 one can see the average tidal bed shear stresses for 230 m^3/s. In appendix X one can find the results for the 150 m^3/s and 1000 m^3/s scenarios. The change is indeed visible but indeed not as clear as downstream of the bifurcation. So it will most likely contribute to accretion directly downstream of the bifurcation.

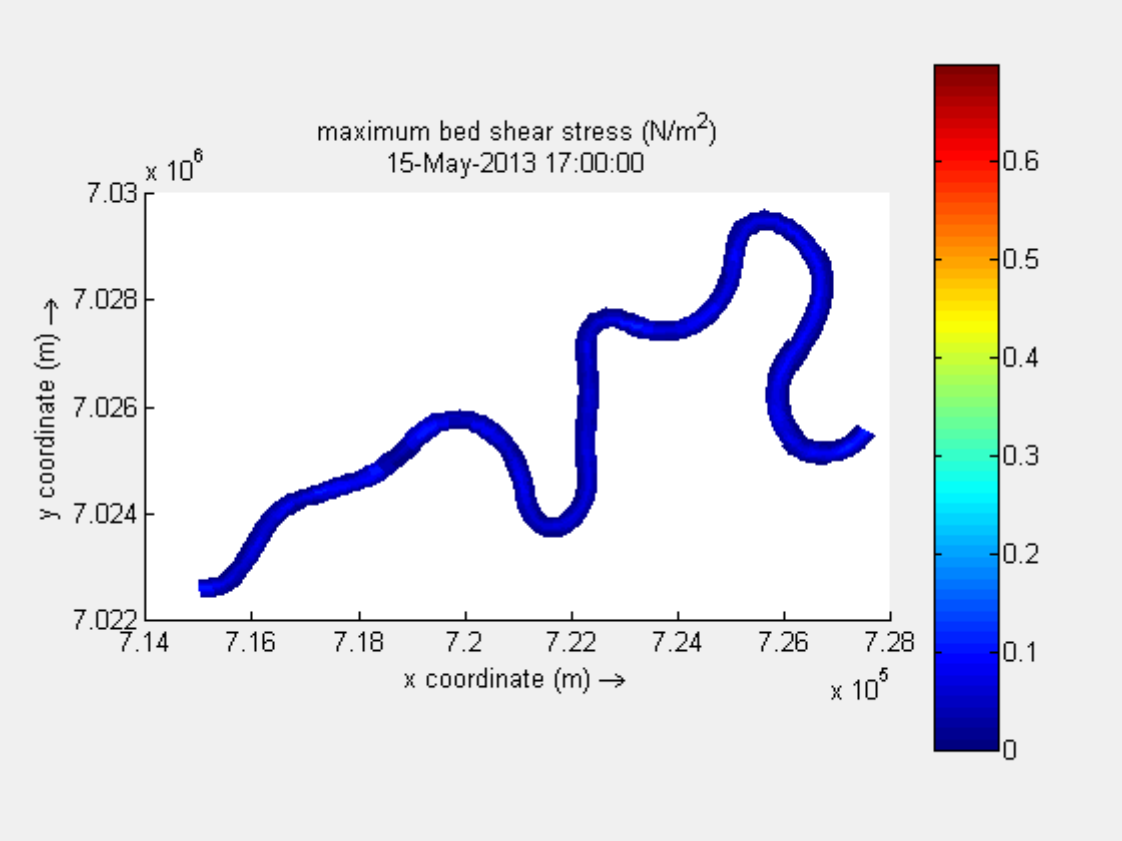

Fig. 5-39: Bed shear stress. 230 m^3/s, flood, current scenario, upstream section

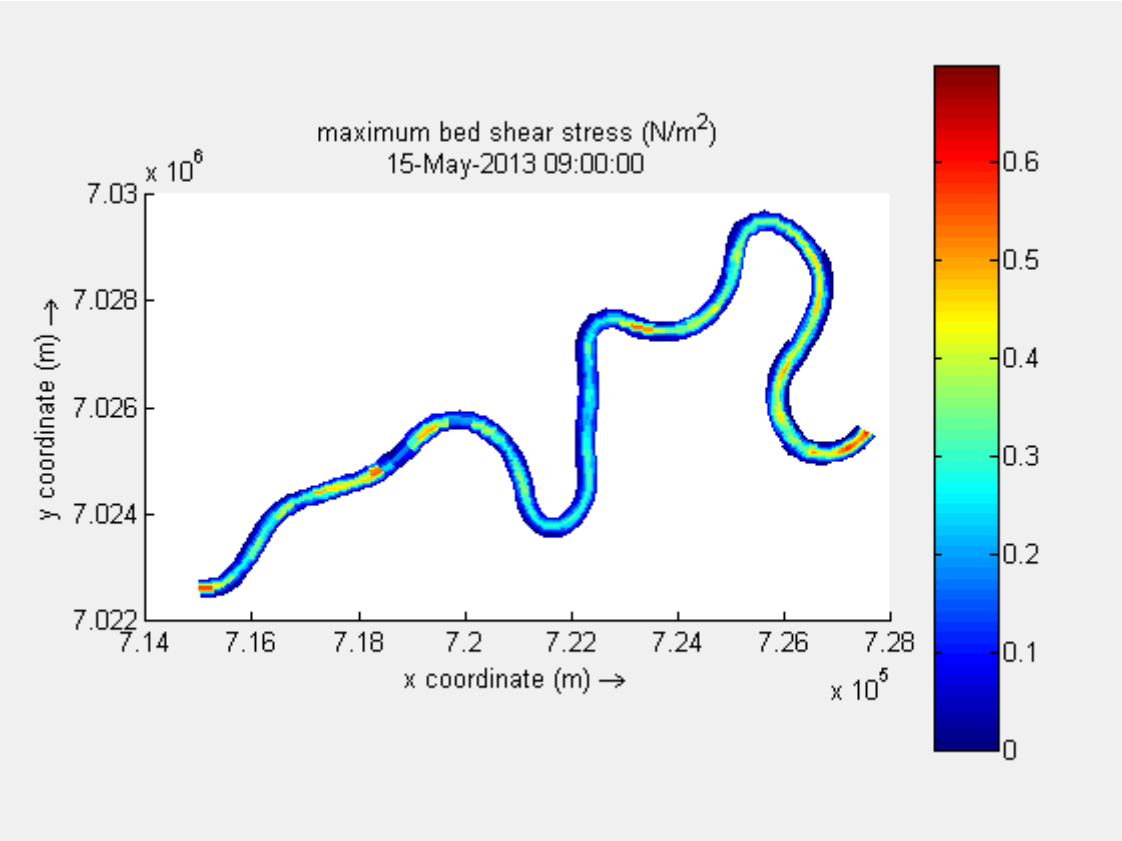

Fig. 5-40: Bed shear stress. 230 m^3/s, ebb, current scenario, upstream section

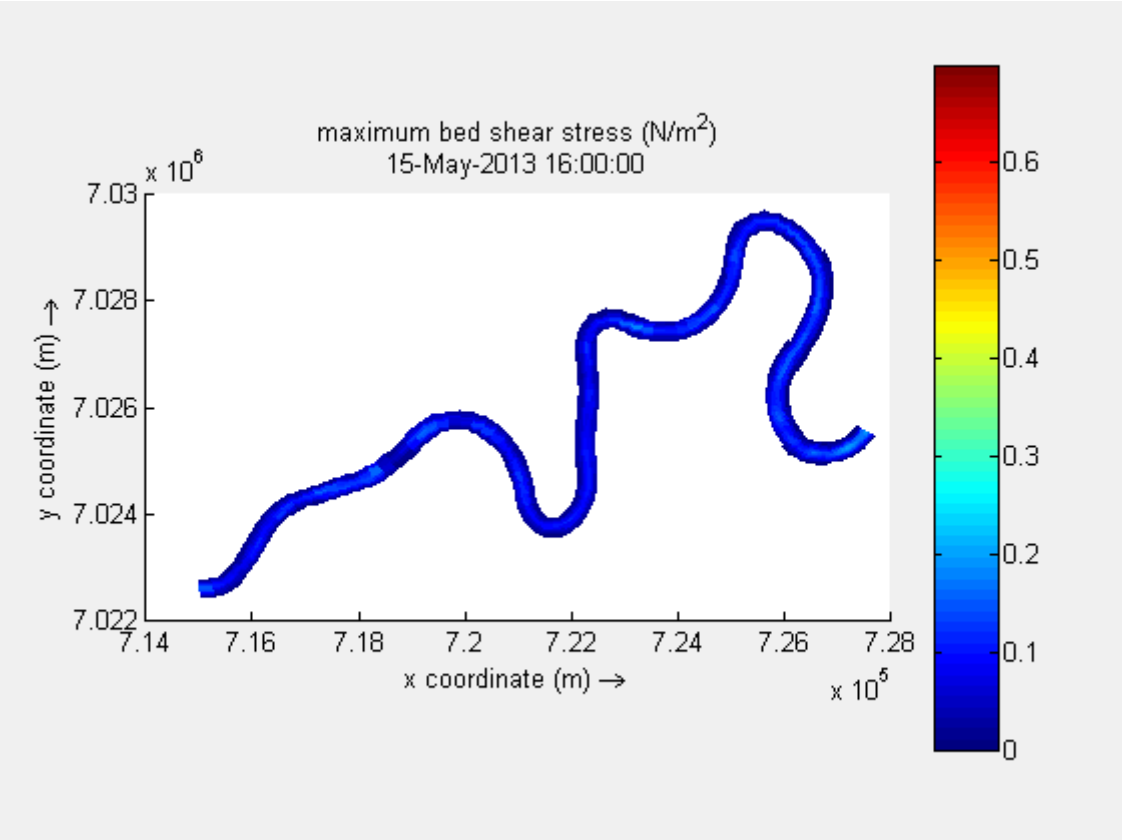

Fig. 5-41: Bed shear stress. 230 m^3/s, flood, bypass scenario, upstream section

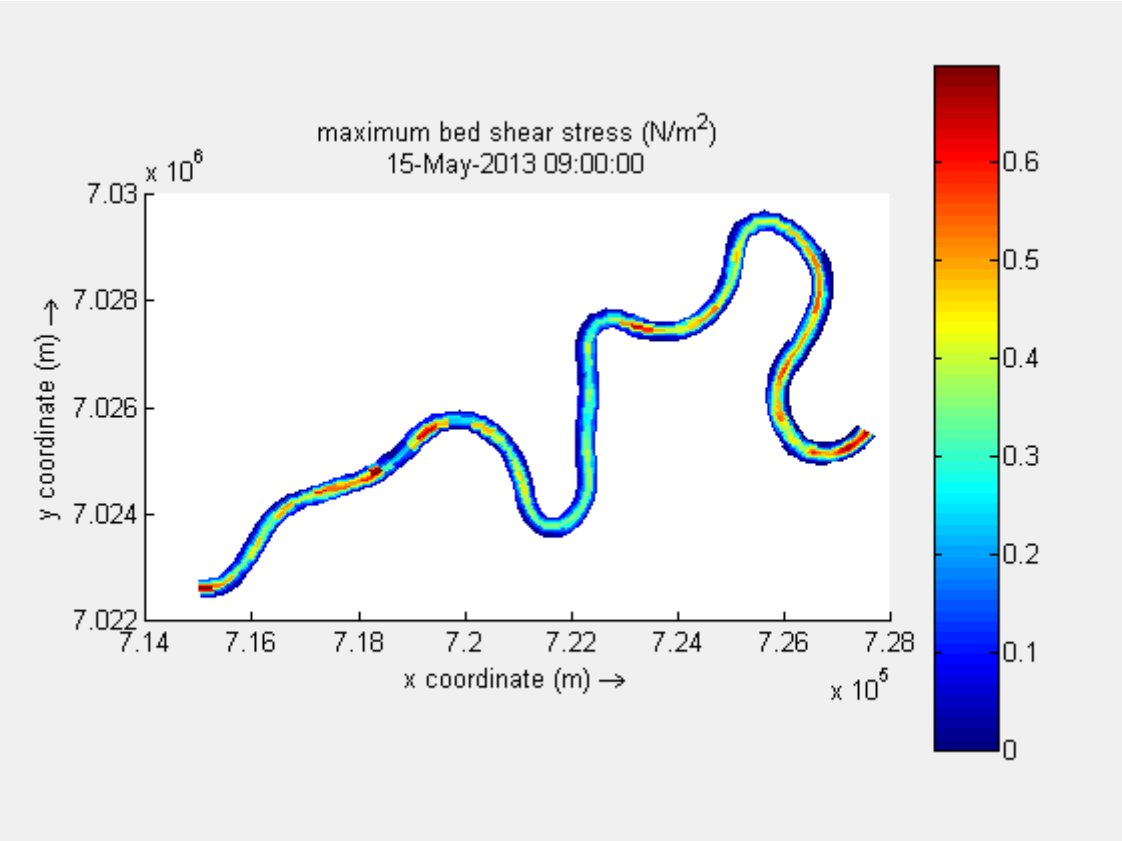

Fig. 5-42: Bed shear stress. 230 m^3/s, ebb, bypass scenario, upstream section

Salinity simulations

In the previous section on salinity dynamics it became clear that the influence of salt water is rather large. Especially during low discharges the tidal flow reduces but also the distribution changes. Next to that the gravitational flow will induce a change on bed shear stress that is the strongest near the mouth.

In Fig. 5-43 and Fig. 5-44 the differences are shown for a low discharge and a high discharge averaged over a tide. This gives an indication of the total result of the tide. The results are rather complicated. To explain the figures one needs to know that blue colours are negative values. This means that including salt means in increase in bed shear stress. Red colours mean positive values. This means that including salt means a decrease in bed shear stress.

For low discharges the differences are easy to explain. Between the Itajaí-Mirim and the current branch's mouth there is an increase of bed shear stress. This is most likely due to the gravitational flow. This part of the system is so deep that a strong density current can arise if enough salt water is entrained in the outflowing fresh water. This creates the gravitational flow.

Further upstream in the current branch there is a reduction of bed shear stress. Upstream there is not so much influence of the gravitational flow. Here the reduction of the tidal flow amplitude is noticeable. A decreased amplitude means less average bed shear stress. Besides the reduced tidal amplitude there is also the reduced average flow due to the resistance by the density difference at the current branch's mouth compared to the resistance at the density difference at the bypass mouth. This phenomenon has thoroughly been explained previously in section 5.4.

In the bypass there is a slight reduction of bed shear stress during low discharges. Even though the river discharge part that goes through the bypass is increased due to the salt induced resistance at the current branch's mouth, the average bed shear stress has decreased. This is because the tidal contribution to the flow, which when tidally averaged coincides with the effective discharge, is by far the largest. Hence the decrease of tidal amplitude is larger than the increase of flow induced by the net upstream flow through the current branch. Therefore there is, averaged over a tidal cycle, a decrease of bed shear stress.

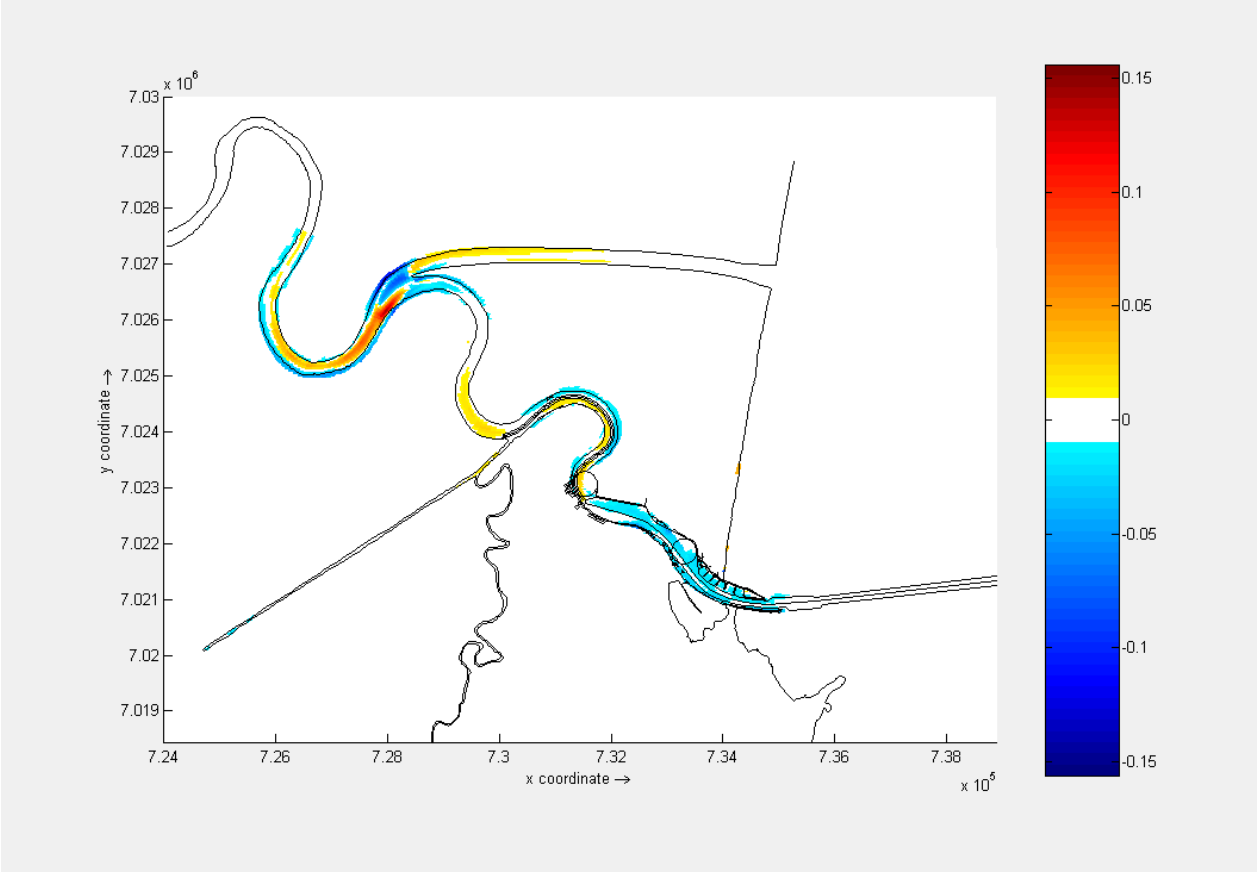

Fig. 5-43: Difference bed shear stress, "no salinity" minus "with salinity", 150 m^3/s

When moving on to the high discharge scenario some things have changed. In the current branch the gravitational flow has increased. Hence there is an increased bed shear stress. This is due to an increased flow through the current branch. This makes it possible to increase entrainment of salt particles. When more salt particles are exported by exiting fresh water, more salt water flows in over the bottom increasing the bed shear. If this happens it will happen over a shorter length. This can indeed be seen in Fig. 5-44. The bed shear has increased but the length over which this happens is shorter compared to the low discharge shown in Fig. 5-43

Another thing that is shown is that the reduction of bed shear further upstream just downstream of the bifurcation in the current branch still occurs at high discharges. This is still due to the reduced average discharge and the reduced tide. Both are the governing water motions at that point. Since they are both still reduced, the bed shear stress should also reduce.

A new phenomenon occurs in the bypass. Where at low discharge the entire bypass has less bed shear stress or the same amount, this has changed at high discharges. At the upstream end of the

bypass the bed shear stress has increased when simulating with salt. This is due to the fact that river flow dominates the water movement here and not the tide anymore. Although the tide has decreased in amplitude due to salinity induced damping the average river discharge through the bypass has increase also due to the stronger resistance at the current branch's mouth. Since the flow at this point is dominated by the average river flow and not by the tide anymore, it is clear that the increase of the average river flow is stronger than the decrease of tidal amplitude. Both effects have the same origin but the effect of river flow is dominant over tidal flow at these discharges. At the mouth the gravitational flow and the river flow are more or less in balance. Since the bypass channel is not so deep the gravitational flow is not as strong as in the current channel for example. However due to the opposing direction of gravitational flow compared to the river flow the bed shear stress could decrease especially since the tidal flow also has decreased due to energy dissipation. All put together there are a lot of insecurities on this part which process is dominant. This makes this part very sensitive to input errors. This is valuable information when interpreting output from a model.

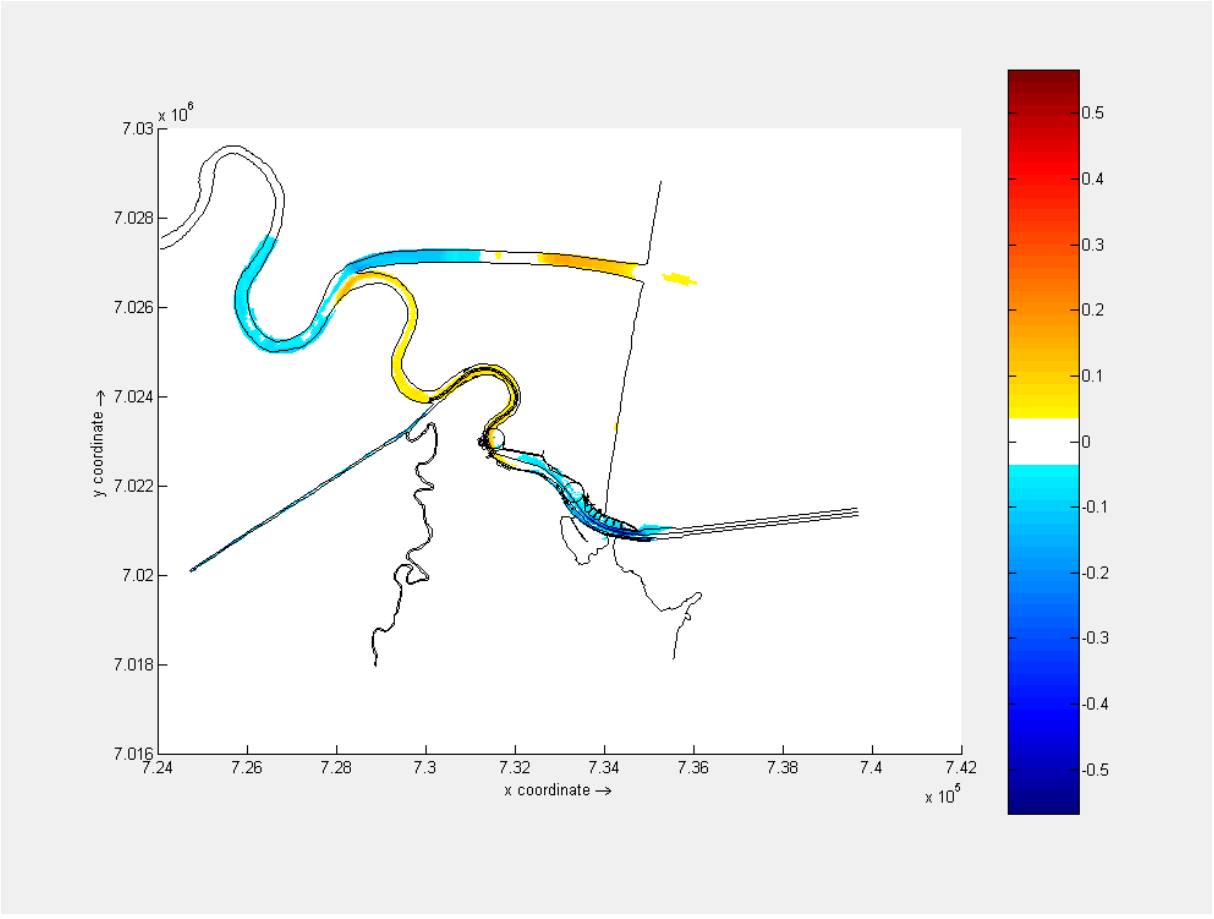

Fig. 5-44: Difference bed shear stress, "no salinity" minus "with salinity", 1000 m^3/s

5.5.3 Conclusions

This section on changes of bed shear stress is divided in four parts:

- Changes in a tideless scenario
- Changes in a tidal scenario in the downstream section
- Changes in a tidal scenario in the upstream section
- Change due to salinity

For the tideless scenario it has been seen that the reduction of bed shear stress in the current branch relates according to the quadratic friction law to the reduced flow velocity. However the stationary tideless scenario is not realistic. Hence the tidal scenario was the next step.

In the downstream section it was interesting to see what happens during ebb and flood regarding bed shear stress. Due to the diminished tidal flow amplitude, due to the increased combined cross-section of the current branch and the bypass, the bed shear during ebb and flood has diminished as well. When looking at the location it is clear that accretion is most likely to happen directly downstream of the bifurcation. This is amplified by the results found in the upstream section.

In the upstream section the tidal action has increased. The result might be that more sediment will be transported towards the downstream section from which it is now known that the sediment carrying capacity has decreased.

A change due to the combination of the bypass and salinity is the decreased gravitational flow. Since there is less entrainment there is less inflow of salt water. Hence less upstream directed transport by gravitational flow can be expected. However. During low discharges it was found that there is a depth averaged net import flow through the current branch due to the imbalance of density difference induced forces at the two mouths.

An important conclusion on the salinity dynamics is that the system is very sensitive to this. As for example the entire average direction of flow can change in the current branch during low discharges it can be a fall pit if implications of simulation mistakes are overlooked. Also the changes in bed shear stress in the bypass change gradually over higher discharges. The differences are small but can have large impact on maintenance as these processes are slow but persistent.

6 Conclusions

In this section first the conclusions and answers regarding the research questions of this thesis will be drawn, being:

- What are the changes in water level due to implementation of a bypass?
- What are the changes in sedimentation due to implementation of a bypass?
- What are the changes in scour due to implementation of a bypass?
- What are the changes in salinity dynamics due to implementation of a bypass?

Along this track the findings gave insight in the functionality of a bypass. Therefore secondly in this chapter the conclusions regarding the functionality of the bypass with a mobile closure will be drawn.

6.1 Conclusions regarding the four objectives

In this section the results from the investigated research areas are related to the objectives. This gives the answers to the four different objectives of this research.

Flood risk

As was explained in the results is that the bypass functions rather well during high discharges. With the increased capacity the bypass diverts such a large portion of water that the discharge through the current branch has dropped significantly to about 35 % of its current discharge. This way the flood risk problem is reduced significantly. As was found with the water levels during the once in 50 years occurring discharge of 7250 m^3/s the water levels relative to MSL decrease around the bifurcation point from +3 m to +0.5 m which is significantly. The influence of the bypass is noticeable over tens of kilometres further upstream. But in the end will diminish as the distance of influence is limited. Further upstream other measures will need to be taken.

It can be said that the bypass performs very well at the reduction of flood risk in the Itajaí area.

Sedimentation

With the research on sedimentation no use was made of a complete sediment transport model. Hence an assessment is made on the basis of change of bed shear stress. Bed shear stress mobilizes sediment if it is strong enough or oppositely if the bed shear stress is to low it will allow suspended sediment to deposit.

It was found that the diminished tide in both the bypass and the current branch will cause a drastic decrease of bed shear stress in both channels. This is only during low discharges when the river flow is not significantly contributing to the bed shear stress compared to the tidal flow. The upstream section on the other hand will endure increased tidal flow due to the increased tidal prism. It was found that the bed shear stress in the upstream section has increased in the new situation. Hence it can be expected that more sediment will be mobilized upstream and when it arrives at the bifurcation the tidal flow will decrease when it enters either the bypass or the current branch. The consequence is that large scale sedimentation will occur directly downstream of the bifurcation point.

During high discharges the change in the tide is not relevant for the mobilization of sediment. In that case the river flow will be the “mobilizer” and the “transporter” for sediment. There should be a

threshold discharge level at which an opened bypass will not cause sedimentation anymore. Currently it is found that in the current branch no sedimentation occurs at a discharge level of 1000 m^3/s. When with an opened bypass 1000 m^3/s flows through the current branch this means that roughly 3000 m^3/s flows through the upstream section. When considering the suspended sediment concentration curve seen in Fig. 2-9 one understands that the concentration is much higher. Hence the simple comparison of opening the bypass as long as more than 1000 m^3/s flows through the current branch is invalid. With these higher concentrations then in the current situation a higher flow velocity will be required to avoid sedimentation. The threshold level of (currently) 1000 m^3/s will therefore increase. A more precise sedimentation study is required to find this threshold level. In section 6.2 a more elaborate conclusion will be drawn on the functioning of a dynamic closure.

The main conclusion is that the bypass in principle has a negative influence on the sedimentation behaviour during normal day to day conditions. This is due to diminished tidal flow which is dominant during these day to day conditions. Only during more extreme conditions the sedimentation problem disappears as the tide has no significant influence anymore and the now dominant river flow is strong enough to transport all sediment without the tidal action. Apparently there is a threshold level where the river flow will be strong enough to compensate for the diminished tidal flow. It is important to investigate this threshold level to prevent sedimentation due to the bypass.

Erosion

As mentioned earlier no complete sediment transport model was used. However some insight in this matter was attained with analysis of the changes in bed shear stress. Erosion is occurring in general only during high discharges.

As a large part of the total discharge is diverted into the bypass the flow velocities in the current branch have decreased. When looking at the results from the bed shear stress it was found that the flow velocity reduction makes a significant difference for the bed shear stress. During extreme events the bed shear stress has dropped to levels that are encountered under less extreme conditions and are relatively harmless. This makes the diversion a solution to the erosion issues during extreme events.

When looking at sedimentation and erosion simultaneously it is now clear that the bypass has a positive influence during extreme events. But during day to day conditions the results can be very negative as accretion will be strongly enhanced.

Salt intrusion

The salt intrusion will increase due to the bypass. This is the result of the diversion of water through the bypass. This results in a more diffuse presence of the salt water body in the current branch as the tidal flow dominates. Another reason why the intrusion has increased is the net inflow or no flow due to the force applied on the two mouths of which the force on the current branch's mouth is much larger. Hence the denser sea water is pushing water in on average through the current branch and then it flows out through the bypass. This net upstream transport results in a much deeper salt intrusion which can have a negative effect on the water quality. The water purification plant in the Itajaí-Mirim river is for example will have to cope with increased salinity levels.

6.2 General conclusions regarding functionality of the bypass

In general it can be said that the bypass will function well for mitigation of flood risk and erosion problems. It was found that the bypass is less suitable during the day to day conditions. Hence it is a traditional trade-off between flood risk and erosion problems during extreme events on the one hand and sedimentation and salt intrusion problems during day to day conditions on the other hand.

A permanently opened bypass is ruled out in any case. This will induce an uneconomical amount of maintenance in the bifurcation area in both channels due to the reduced tidal flow in the downstream section. And also the salt intrusion will reach to far upstream with a permanent opened bypass during day to day conditions. Hence a dynamic closure is vital to an optimal functioning of the bypass. A dynamic closure means that it doesn't have to be opened or closed completely. A partial closure will divert a part of the discharge through the bypass. Lowering flow velocities in the current branch slightly but not too much to induce sedimentation. However. With a partially opened bypass highly concentrated suspended sediment flows into the bypass at a very low velocity since the bypass is very wide compared to the partially opened closure. Hence sedimentation will be inevitable. This decreases as the bypass has a smaller capacity as it is relatively less over dimensioned in that case with a partially opened closure. However this means that when the bypass will reduce flood risk and erosion problems less during extreme discharges. Hence a dynamic closure is not the perfect solution. Apparently there will always be a trade-off between safety and maintenance cost.

In Fig. 6-1 an example is shown of a large scale dynamic closure is shown. This is the Oosterscheldekering in the Netherlands. This closure actually closes during extreme conditions instead of open as would be required in Itajaí. However it shows an example of how to have such a large scale closure being able to open and close during extreme conditions.

Fig. 6-1: Oosterschelde kering, The Netherlands, (RTL 2013)

To summarize all arguments around the functionality of a dynamic closure is that the fine tuning will be a cost-based assessment. As risk is reduced, maintenance will increase. To keep maintenance within acceptable ranges a dynamic closure is required. And even with a dynamic closure the larger the capacity of the bypass the larger the maintenance effort but the lower the flood risk and erosion problems.

7 Recommendations

It is recommended to do more field measurements in the Itajaí-Açu River. This has been mentioned in previous research done with the Delft3D model as well. At this moment to few calibration parameters are available. Flow measurements will increase accuracy and reliability of the model.

A first assessment of arguments has been done on where to position the closure. Besides the location also the method of closing needs to be investigated. Since the bypass needs to be able to open just prior to an extreme event it is not allowed for the closure to fail to open.

Additional research on actual sediment transport is indispensable. This will give a clear picture of the maintenance cost with an implemented bypass. Maintenance cost is bound to increase with the bypass since there is more channel length to maintain. Also the fact that a non-maintained bypass channel would decrease its functionality during extreme events will motivate maintenance. Coastal processes will need to be assessed as well in the new situation. Sedimentation in the sea mouth is inevitable as lateral transport will sink down in a deep cross channel such as the bypass.

A cost estimation for construction and maintenance will be essential to show if the bypass is justified from an economical point of view as a solution to the flood risk and erosion problems. Looking at the cost of the last two disasters it is most likely a profitable solution on a relative short term.

The bypass will yield good results on erosion and flood risk issues. However it is inevitable that negative issues concerning sedimentation arise if the bypass is not closed during regular conditions. There it is recommended to implement a dynamic closure in the design. The conditions under which the bypass needs to be opened or closed need to be investigated. If this is done thoroughly it will save on maintenance cost.

An important recommendation is to look at the fine tuning of the bypass in combination with a dynamic closure. This will be a cost versus safety assessment. The partial closure will induce maintenance cost in the bypass. This can be reduced by decreasing capacity of the bypass. However that would result in less flood risk and erosion problem reduction. Hence it is a trade-off in cost. This is not straightforward to answer as all over the world the perception of the cost of risk is different.

The general recommendation as the main result from this report is to deeper investigate the bypass. So far the bypass concept yields good results and hence is a good suggestion to solve the flood risk and erosion problems that occur during extreme events.

8 Literature

(2006). Santa Catarina Municipality Itajai. www.wikipedia.org.

(2008). "Enchente Itajaí." Retrieved 19-9-2013, 2013, from http://jie.itaipu.gov.br/jie/files/image/27.11.2008/enchente_itajai.jpg.

ARCADIS (2005). Improvement of the access channel to port of Itajaí (report no. A1443R1r1), Alkyon.

ARCADIS (2009a). Salt intrusion study of the Itajaií-Açu, Brazil (report no. A1443R2r1).

ARCADIS (2009b). Sedimentation study, Port of Itajaí/Navegantes (report no. A2143R1r2).

ARCADIS (2012a). Restructering study, port of Itajai, Brazil (report no. C02031.002848.0600).

ARCADIS (2012b). Under keel clearance (ukc) study Itajai-max vessels, Itajai, Brazil (report no. A2848).

ARCADIS (2012c). Scour protection APM terminal Itajai, Brazil (report no. A2845R1r1).

ARCADIS (2012d). Extreme water levels in the port of Itajai, Brazil (report no. A2845R2r0), ARCADIS Nederland BV.

Bolla Pittaluga, M., R. Repetto and M. Tubino (2003). "Channel bifurcation in braided rivers: Equilibrium configurations and stability." Water Resources Research **39**(3): 1046.

Bosboom, J. and J. F. Stive (2011). Coastal Dynamics I: Lecture Notes CIE4305, VSSD.

Brandt, S. (2000). Salt wedge dynamics of the Itajaí-Açu estuary during a spring-neap tidal cycle, SC., Brazil.

Bulle, H. (1926). Untersuchungen über die Geschiebeableitung bei der Spaltung von Wasserläufen, VDI-Verlag.

CNN.com (2008). "Brazil death toll rises." CNN.com. from http://edition.cnn.com/2008/WORLD/americas/12/01/brazil.floods/index.html?iref=allsearch.

Cornelisse, J. M., W. G. M. v. Kesteren and J. C. Winterwerp (2000). Physical properties Itajai sediments.

Delft Hydraulics (2005). Delft3D-Flow user's manual: simulation of multi-dimensional hydrodynamic flows and transport phenomena, including sediments. Netherlands, WL Delft Hydraulics.

Delo, E. A. (1988). Estuarine Muds Manual, Hydraulics Research Limited.

Google (2013). Google earth.

Ippen, A. T. and D. R. F. Harleman (1961). "One-dimensional analysis of salinity intrusion in estuaries." Tehcnical Bulletin **No 5**(Committee on Tidal Hydraulics, Corps of Engineers, U.S. Army, Vicksburg).

Itajaí, P. d. (2013). "Prefeitura de Itajaí." from http://novo.itajai.sc.gov.br/.

Jansen, N. (2000). Site visit Itajai, report prepared for Van Oord Dredging and Marine Contractors (formerly: HAM).

Kleinhans, M. G., H. R. A. Jagers, E. Mosselman and C. J. Sloff (2008). "Bifurcation dynamics and avulsion duration in meandering rivers by one-dimensional and three-dimensional models." Water Resources Research **44**(8).

Kreeke, J. v. d. and K. Robaczewska (1993). "Tide-induced residual transport of coarse sediment: Application to the Ems estuary." Netherlands Journal of Sea Research **31**: 13.

Miori, S., R. Repetto and M. Tubino (2006). "A one-dimensional model of bifurcations in gravel bed channels with erodible banks." Water Resources Research **42**(11): W11413.

Mosselman, E. (2010). Lecture 6: River Dynamics - Bifurcations.

Prandle, D. (1985). "On salinity regimes and the vertical structure of residual flowin narrow tidal estuaries." Estuarine, Coastal and Shelf Science **20**: 615-635.

Rijn, L. C. v. (1993). Principles of Sediment Transport in Rivers, Estuaries, Coastal Seas and Oceans, IHE.

Rijn, L. C. v. (2007a). "Unified view of sediment transport by currents and waves. I: Initiation of motion, bed roughness, and bed-load transport." Journal of Hydraulic Engineering **133**(6): 649-667.

Rijn, L. C. v. (2007b). "Unified View of Sediment Transport by Currents and Waves. II: Suspended Transport." Journal of Hydraulic Engineering **133**(6): 668-689.

RTL (2013). "Veiligheid Oosterscheldekering." from http://www.rtlnieuws.nl/nieuws/binnenland/veiligheid-oosterscheldekering.

Savenije, H. H. G. (2006). Salinity and Tides in Alluvial Estuaries, Elsevier Science.

Schettini, C. A. F. (2002). Near bed sediment transport in the itajaí-açu river estuary, southern brazil. Proceedings in Marine Science. C. W. Johan and K. Cees, Elsevier. **Volume 5:** 499-512.

Schettini, C. A. F., K. Ricklefs, E. C. Truccolo and V. Golbig (2006). "Synoptic hydrography of a highly stratified estuary." Ocean Dynamics **56**(3-4): 308-319.

Schettini, C. A. F. and E. E. Toldo, Jr., (2006). "Fine Sediment Transport Modes in the Itajai-Açu Estuary, Southern Brazil." Journal of Coastal Research(39): 5.

Schiereck, G. J. (2010). Bed, Bank and Shore protection.

Simmons, H. B. (1955). "Some effects of upland discharge on estuarine hydraulics." Proceedings of the American Society of Civil Engineers **81**(792).

Vriend, H. J. d., H. Havinga, B. C. v. Prooijen, P. J. Visser and Z. B. Wang (2011). Lecture notes CT4346 River Engineering, TU Delft.

Wang, Z. B., R. J. Fokkink, M. d. Vries and A. Langerak (1995). "Stability of river bifurcations in ID morphodynamic models." Journal of Hydraulic Research **33**(6): 739-750.

Wang, Z. B., M. C. J. L. Jeuken and H. J. d. Vriend (1999). "Tidal asymmetry and residual sediment transport in estuaries." A literature study and applications to the Western Scheldt, WL| Delft Hydraulics report Z **2749**.

Winterwerp, J. C. (1999). The behaviour of high-concentrated silt suspensions. Delft, Technical University Delft. **PhD:** 172.

9 Appendices

I. Sediment and water distribution – non estuarine aspects

II. 1D morphodynamic models

III. Bélanger and scour model

IV. Flow velocities vs. discharges

V. Time step assessment

VI. Relevant processes of “van Rijn” sediment transport module

VII. Bottom influence on salt intrusion

VIII. Position of closure

IX. Maintenance dredging – numbers and figures

X. Bed shear stress – tidal scenario

XI. Salt intrusion

I. Sediment and water distribution – non estuarine aspects

The key aspects of a river bypass are the distributions of water and sediment. This determines the development of both branches. The division of water over the two branches can be very simple since that is determined by the water levels at both ends of both branches. Together with formulations for continuity, motion and a geometrical relation this is very straightforward. However, this assumes static water levels as boundary conditions for all branches and a fully symmetric bifurcation. In a coastal area, which is the case here, the boundaries are not static but are directly influenced by the tide. For convenience reasons the static boundary condition is assumed for now. In a later stage the more complex boundary conditions will be assessed instead. For the first step also non-cohesive course sediment is assumed. The complexity following from dynamic boundaries and sediment properties would not contribute to the general understanding of the system in this stage. So for now the simplified situation for the water distributions the mass balances can be stated as follows.

Mass-balance for water:

$$Q_0 = Q_1 + Q_2 \tag{9.1}$$

Water motion formulated by Chezy formula

$$Q_i = B_i * C_i * h_i^{\frac{3}{2}} * i_i^{\frac{1}{2}} \tag{9.2}$$

Geometrical relation

$$i_1 * L_1 = i_2 * L_2 \tag{9.3}$$

With:

- Q_0 = Discharge upstream of bifurcation [m^3/s]
- Q_1 = Discharge branch one [m^3/s]
- Q_2 = Discharge branch two [m^3/s]
- B_i = Width of branch one or two [m]
- h_i = Water depth in branch one or two [m]
- i_i = Bottom slope of branch one or two [-]
- L_i = Length of branch one or two [m]

Another difficult part is with the division of sediment. Basic models suggest that the distribution ratio of sediment and water over the two branches is equal. Meaning

$$\frac{S_1}{S_2} = \frac{Q_1}{Q_2} \tag{9.4}$$

With:

- S = sediment transport [kg/s]
- Q = discharge [m^3/s]

This could be true for some situations. But since the transport of sediment does not depend solely on discharge but on many other factors as well such as:

- Water depth
- Bottom resistance
- Channel width
- Residual currents due to tide and salt intrusion
- Non-linear distribution of sediment concentration over the water column

Besides the basic symmetric situation there are also 3D phenomena that can steer sediment concentrations in a certain direction other than one would expect on the average flow pattern. This means that the flow structure at the bifurcation can be so complex that it locally differs very much from the average result. Residual currents can cause sediment transport while the total result over the entire water depth is different. Some 3D and steering aspects are explained below to give insight in possible processes that could play a role.

The Bulle effect

The Bulle effect has been investigated with physical models by (Bulle 1926). He was the first one to describe this phenomenon. Due to the curvature of the flow a gradient will arise in the cross direction of the flow. Water is pushed to the outer bend of the flow. Since the flow is less strong at the bottom this means that the force outward for the flow at the bottom is less. The result is, since water cannot continue flowing to the outer bend that over the bottom the water will flow to the inner bend to compensate for the volume that is flowing to the outer bend at the water surface. Since the sediment concentrations are much higher at the bottom this means that there is a resulting sediment flow towards the inner bend. In Fig. 9-1 the net result is shown. The continued line is the flow at the water surface. The dashed line indicates a flow line that starts more to the left but due the Bulle-effect it ends at the right side. Considering that at the bottom the sediment concentration is much higher, this shows that more sediment can be imported into a channel than what could be expected based on the discharge distribution.

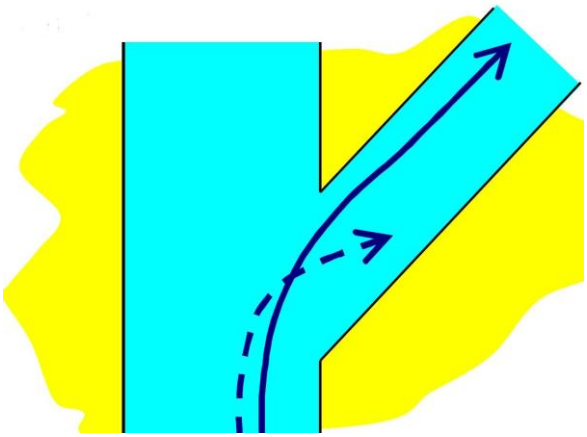

Fig. 9-1: Bulle effect (Mosselman 2010)

Gravity pull along bed slopes

Another aspect that occurs at the bottom is the bottom topography. When the bed is sloping down to the right in the situation shown in Fig. 9-2 this means that sediment tends to move slightly more to the right. Even though the flow that is carrying it might be in a straight line. The arrow shows the actual movement of a grain and the hatching indicates the slope. It is similar to a snowplough that moves straight but the angle of the blade pushes the snow to the side.

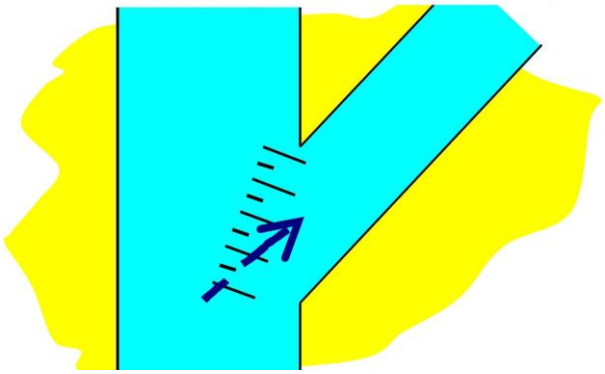

Fig. 9-2: Gravity pull along bed slopes (Mosselman 2010).

Asymmetrical flow approach

When a flow does not approach a bifurcation in a symmetrical way it can happen that the sediment distribution of the width of the flow is already distorted. The example in Fig. 9-3 and Fig. 9-4 is at the Pannerdensche Kop. In this specific situation there were initial problems with the stability of the bifurcation. As one can see below in Fig. 9-3 there is a small curvature in the channel just before the bifurcation. At that point the channel is the deepest at the outer bend because there the flow velocities are the highest. This is due to the greater radius with the same angular velocity. Compare this to a windmill. The outer tip of the blade moves faster than a more inward part of the blade but they turn at the same angular velocity. Since there is a non-linear relation between flow velocity and sediment transport this means that the outer bend will erode and be deeper than the inner bend. A higher flow velocity means also the capability of carrying more and heavier sediment. In Fig. 9-4 this is validated. One can see that at the part where it is the deepest also the coarsest sediment is found. Together this as reason to believe that the flow in the upper branch is richer in sediment load since the flow takes up sediment at the north part of the main flow just before the bifurcation. The flow does not have enough time to distribute the sediment homogeneously over the width of the channel. Therefore there will be a larger volume of sediment flowing into the upper branch than would be expected on the water distribution.

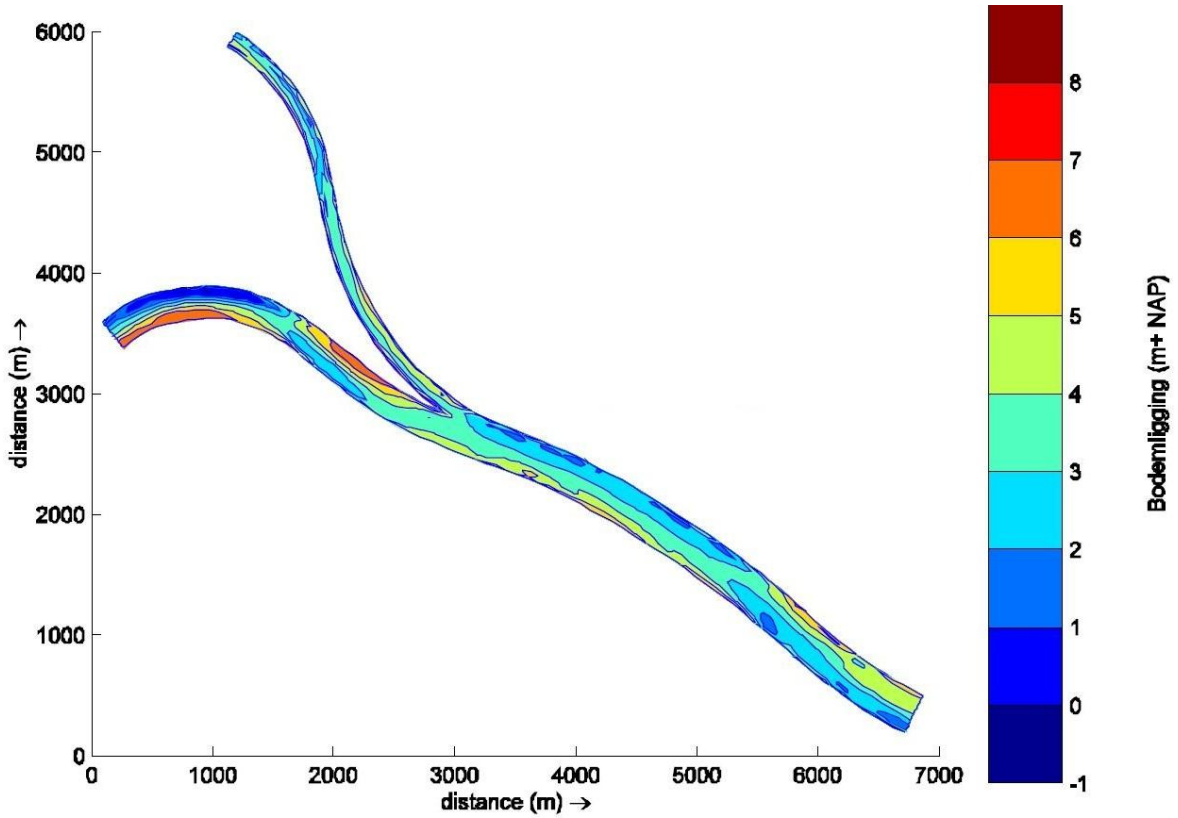

Fig. 9-3: Bathymetry at Pannerdense Kop (Mosselman 2010)

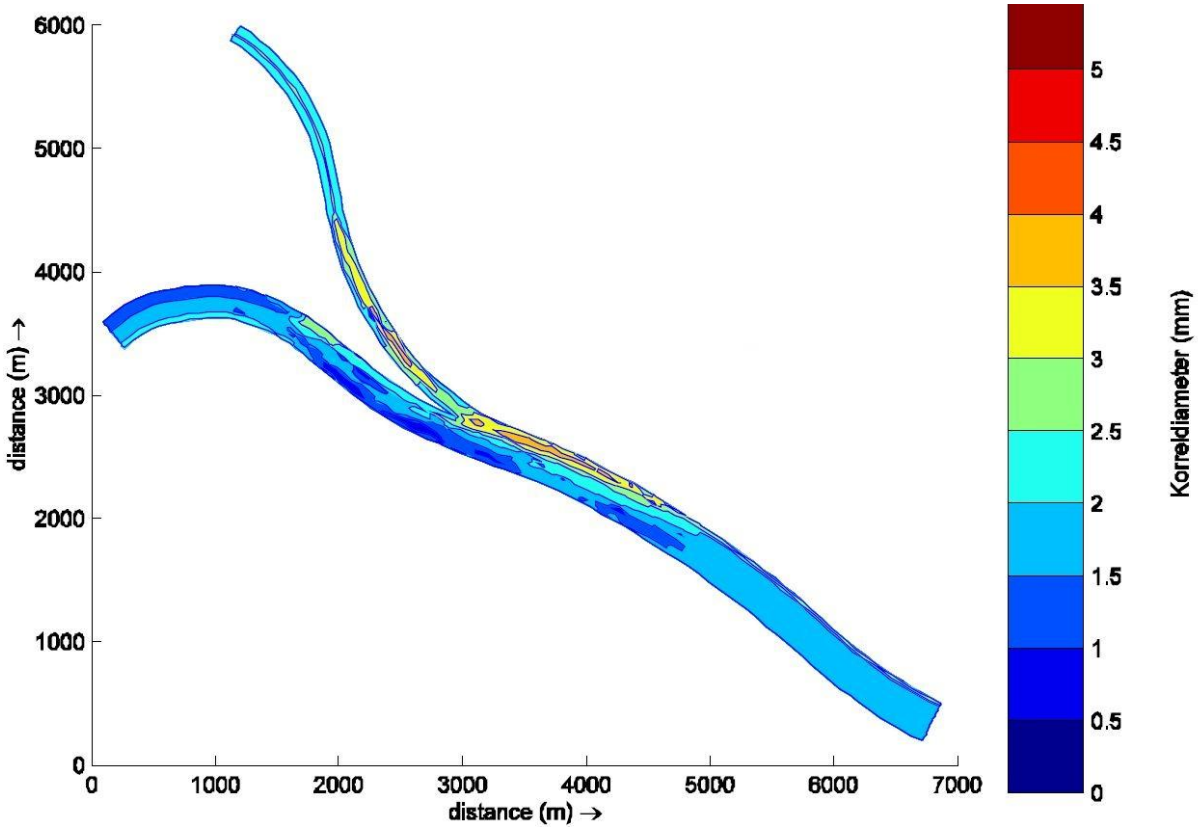

Fig. 9-4: Spatial granular distribution at Pannerdensche Kop (Mosselman 2010)

Flow separation

When a flow line passes a channel such as schematized below in Fig. 9-5 it might not be able to follow the bank contour lines and get separated. This only happens when the corner it passes is sharp. If this corner is smooth this will not happen. In this case the flow line will take a wider turn and reattach to the bank a bit upstream in the side channel. Between the sharp corner and the reattachment point an eddy will form. What will happen due to this eddy is that in the centre sediment will settle. This can be explained in several ways. The easiest to do this is remembering what happens to sugar in tea when you stir it. The result is that sugar ends in the centre of the eddy in the tea cup. A schematization of the actual process is shown in Fig. 9-6. This is actually the same as with the Bulle effect. The eddy is turning faster at the surface due to less friction than at the bottom. This means that the tea that is forced outward at the surface rises at the outside of the cup causing a hydrostatic pressure higher than at the bottom. Water will flow at the sides to the bottom. Resulting in a residual flow that circulates according to the yellow arrows. At the bottom this means transport to the centre. This is stronger than the centrifugal force due to the stirring that is acting as well on the sugar.

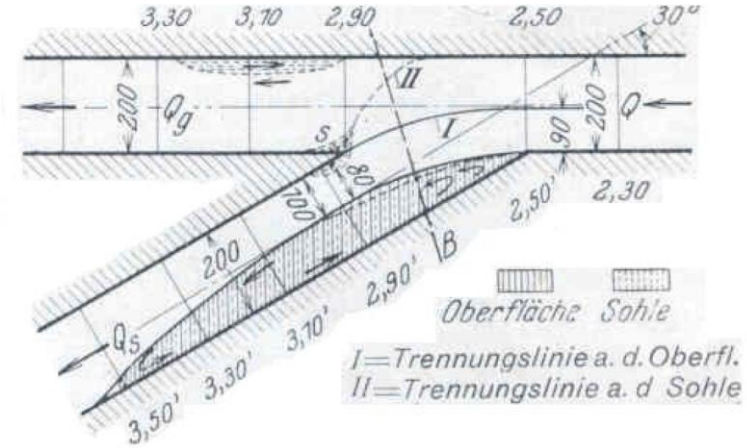

Fig. 9-5: Flow separation (Mosselman 2010)

Fig. 9-6: Particle motion due to hydrostatic pressure differences (Mosselman 2010)

Spiral flow in river bends

Spiral flow is a result of a transverse gradient in the water level produced by centrifugal force on the water body in a river bend. This causes the water level in the outer bend to be higher than the inner bend. This effect is the strongest at the level where the flow velocities are the highest. This is at the water surface since near the bottom the influence of friction is the strongest. So when the velocities are lower at the bottom the outward flow at the surface is compensated by inward flow at the bottom. When sediment transport is dominated by bed load transport this means that there is a residual flow for sediment to the inner bend. The direction of flow, water level and bottom shape is depicted in Fig. 9-7. The spiral flow has an opposite effect than the transverse slope of the river bed. Although the spiral flow does account in general for a transverse slope in a river bend due to sediment transport to the inner bend. The transverse slope therefore counteracts. When in equilibrium the net result will be zero, meaning that the inward transport is zero due to a transverse slope that is just steep enough to balance the inward flow. But when sediment and flow properties change equilibrium will change. Until the new equilibrium it is most likely that the either spiral flow or the slope effect will dominate. When looking at the location where the bifurcation would connect to the current river it is clear that there is almost no stretch of river to be found that is straight. Hence spiral flow is probably inevitable at the bifurcation.

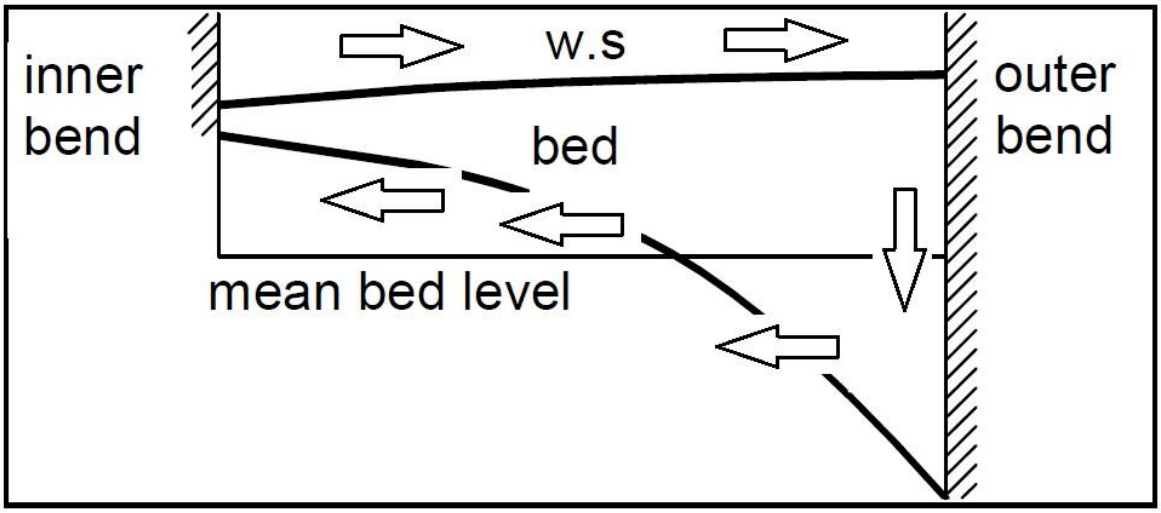

Fig. 9-7: Spiral flow, water level in river transect (Vriend, Havinga et al. 2011)

Transverse slope of the river bend

As mentioned previously a transverse slope can evolve in a river bend. A transverse slope can cause a preference for one of the two branches as explained earlier in this appendix. As said in the previous section about spiral flow in a river bend, the bifurcation is most likely to be in a river bend. This means that there will be a transverse slope. This will in most cases counteract the spiral flow. But with a more dynamic behaviour of sediment concentration and type the net result becomes less predictable.

In general the slope will form towards an equilibrium depth varying over the width of the channel. This means that velocities in the outer bend will reduce when the outer bend gets deeper. Hence there is an equilibrium state where it will move towards. The effect of a transverse slope at a bifurcation is further explained in appendix II, where the model by (Bolla Pittaluga, Repetto et al. 2003) is briefly elucidated.

II. 1D morphodynamic models

1D models that are used to predict the evolution of a bifurcation depend mainly on the determination of the distribution of sediment and water. In principle in most situations the stream prefers one branch for sediment and one for discharge. This means an unstable situation. How fast a bifurcation can destabilize is investigated with 1D models before (Wang, Fokkink et al. 1995) (Kleinhans, Jagers et al. 2008). The use of 1D models is mainly to save computational costs. The evolution of a bifurcation has a life time between several years to centuries. When this is done with a complete fine sediment transport model this would require endless computational time. Therefore a 1D description of the sediment division is more sensible. These relations however have been poorly investigated so far (Kleinhans, Jagers et al. 2008). The description however has been investigated in a mathematical en theoretical way by (Wang, Fokkink et al. 1995). The formulation that was derived in their research accounted for several input parameters. This is the formulation for a nodal point relation.

$$\frac{S_1}{S_2} = f\left(\frac{B_1}{B_2}, \frac{Q_1}{Q_2}, \frac{C_1}{C_2}, \frac{h_1}{h_2}, \dots\right) \tag{9.5}$$

With

- S_i = Sediment transport in branch one or two [kg/s]
- Q_i = Water discharge in branch one or two [m^3/s]
- h_i = Water depth in branch one or two [h]
- B_i = Channel width in branch one or two [m]
- C_i = Chézy coefficient in branch one or two [$m^{0.5}$ / s]

It is shown in the publication (Wang, Fokkink et al. 1995) that there is a formulation that can account for physically realistic situations. They showed that the following formulation did so.

$$\frac{S_1}{S_2} = \left[\frac{Q_1}{Q_2}\right]^k * \left[\frac{B_1}{B_2}\right]^{1-k} \tag{9.6}$$

k is a value that is constant for a given bifurcation. Since the ratio between channel widths is constant as well, the formulation describes a non-linear relation between discharge and sediment transport ratios. It needs to be noted that there is no method to predict the value of the k-value. It is an actual property of the system that contains all important properties of the system in one value. This means sediment properties, geometrical properties, resistance properties of the two branches and all other properties that have an influence on the sediment and discharge distribution.

The equations for sediment are as follows, (9.7) is the mass balance equation and (9.8) is a power-law for sediment transport

$$S_0 = S_1 + S_2 \tag{9.7}$$

$$S_i = B_i * m * \left(\frac{Q_i}{B_i * h_i}\right)^n \tag{9.8}$$

With:

- *m* = transport coefficient [-]
- *n* = transport exponent [n]

In combination with the nodal point relation from (9.5) the variables Q_i, S_i, h_i and i_i can be solved. When combining (9.2) and (9.3) one can state

$$\frac{Q_1}{Q_2} = \frac{B_1}{B_2} * \frac{C_1}{C_2} * \left(\frac{h_1}{h_2}\right)^{\frac{3}{2}} * \left(\frac{L_1}{L_2}\right)^{-\frac{1}{2}} \tag{9.9}$$

When (9.9) is combined with (9.8) one gets a relation between sediment transport and the depth ratio. This relation is important since the sediment transport dynamics are directly related to bottom changes due to sedimentation or erosion. The relation can be stated as follows

$$\frac{S_1}{S_2} = \frac{B_1}{B_2} * \left(\frac{C_1}{C_2}\right)^n * \left(\frac{h_1}{h_2}\right)^{\frac{n}{2}} * \left(\frac{L_1}{L_2}\right)^{-\frac{n}{2}} \tag{9.10}$$

When (9.9) is substituted in the nodal point relation (9.5) one gets the relation for the transport ratio and the depth ratio since other parameters are assumed constant over time.

$$\frac{S_1}{S_2} = f\left(\frac{h_1}{h_2}\right) \tag{9.11}$$

The width, roughness and length of the two branches are assumed to be known. Therefore (9.10) and (9.11) can be used to solve S_1/S_2 and h_1/h_2. With these ratio's the separate transport rates for sediment and water can be calculated from the mass-balances (9.1) for water and (9.7) for sediment). With the separate transport rates for sediment and water the two depths of the two branches can be calculated with (9.8).

It is important to understand that there are three realistic equilibrium states.

- Both branches are open
- Branch two is closed ($Q_2 = S_2 = a_2 = 0$), all transport through branch one
- Branch one is closed ($Q_1 = S_1 = a_1 = 0$), all transport through branch two

Which of these equilibrium states is reached depends on the stability of the system and on the initial state. The mathematical formulation for the stability of equilibrium states is given below.

Stability of the equilibrium states

The analysis of stability of a system is done by analysing the system out of balance. The behaviour next will be towards or away from the equilibrium, meaning stable or unstable respectively. In the analysis done in (Wang, Fokkink et al. 1995) this is shown as follows.

For ease of the analysis the bathymetry is assumed to be uniform and has single depth. This will yield a system of ordinary differential equations. The mass balance for sediment now gives

$$\frac{dh_i}{dt} = \frac{S_{i,e} - S_i}{B_i * L_i} \tag{9.12}$$

With:

- L_i = length of branch one or two [m]
- S_i = sediment transport supplied by the main channel [m^3/s]
- $S_{i,e}$ = sediment transport at the downstream boundary [m^3/s]
- t = time [s]

($S_{i,e}$ - S_i) is the surplus or deficit of sediment in the channel resulting in sedimentation or erosion respectively.

With (9.1), (9.2) and (9.3) the discharges in the two separate branches can be expressed now as a function of the water depth

$$Q_1 = \frac{\beta_1 * h_1^{\frac{3}{2}}}{\beta_1 * h_1^{\frac{3}{2}} + \beta_2 * h_2^{\frac{3}{2}}} * Q_0 \tag{9.13}$$

$$Q_2 = \frac{\beta_2 * h_2^{\frac{3}{2}}}{\beta_1 * h_1^{\frac{3}{2}} + \beta_2 * h_2^{\frac{3}{2}}} * Q_0 \tag{9.14}$$

With

$$\beta_i = B_i * C_i * L_i^{-\frac{1}{2}} \tag{9.15}$$

Since it's known that (9.11) holds for the nodal point relation (9.5), (9.7) can be rewritten by multiplying it with S_1/S_2 for al terms and rearranging. Now the sediment input S_i at the upstream end of each branch as a function of the ratio of depths is presented by.

$$S_1 = \frac{f\left(\frac{h_1}{h_2}\right)}{1 + f\left(\frac{h_1}{h_2}\right)} * S_0 = \frac{f\left(\frac{h_1}{h_2}\right)}{1 + f\left(\frac{h_1}{h_2}\right)} * \frac{m * Q_0^n}{B_0^{n-1} * h_0^n} \tag{9.16}$$

$$S_2 = \frac{1}{1 + f\left(\frac{h_1}{h_2}\right)} * S_0 = \frac{1}{1 + f\left(\frac{h_1}{h_2}\right)} * \frac{m * Q_0^n}{B_0^{n-1} * h_0^n} \tag{9.17}$$

Since we also need to know the transport capacity at the end of each branch we can use (9.8). This yields for the separate transport rates.

$$S_{i,e} = B_i * m * \frac{Q_i}{B_i * h} = B_i * m * C_i^n * h_i^{\frac{n}{2}} * L_i^{-\frac{n}{2}} \tag{9.18}$$

For the next step

$$S_{i,e} = B_i * m * \frac{Q_i}{B_i * h} = B_i * m * C_i^n * h_i^{\frac{n}{2}} * L_i^{-\frac{n}{2}} \tag{9.18}$$

is manipulated into

$$S_{i,e} = B_i * m * C_i^n * h_i^{\frac{n}{2}} * L_i^{-\frac{n}{2}} * \frac{Q_0^n}{\left(B_1 * C_1 * h_1^{\frac{3}{2}} * L_1^{-\frac{1}{2}} + B_2 * C_2 * h_2^{\frac{3}{2}} * L_2^{-\frac{1}{2}}\right)^n} \tag{9.19}$$

When for shorting the following is used

$$\gamma_i = m * B_i * C_i^n * L_i^{-\frac{n}{2}} \tag{9.20}$$

$$\beta_i = B_i * C_i * L_i^{-\frac{1}{2}} \tag{9.21}$$

A system of ordinary differential equations is derived when we substitute (9.16), (9.17) and (9.19) into (9.12).

$$\frac{dh_1}{dt} = \frac{Q_0^n}{B_1 * L_1}\left[\frac{\gamma_1 * h_1^{\frac{n}{2}}}{\left(\beta_1 * h_1^{\frac{3}{2}} + \beta_2 * h_2^{\frac{3}{2}}\right)} - \frac{f\left(\frac{h_1}{h_2}\right)}{1 + f\left(\frac{h_1}{h_2}\right)} * \frac{m}{B_0^{n-1} * h_0^n}\right] \tag{9.22}$$

$$\frac{dh_2}{dt} = \frac{Q_0^n}{B_2 * L_2}\left[\frac{\gamma_2 * h_2^{\frac{n}{2}}}{\left(\beta_1 * h_1^{\frac{3}{2}} + \beta_2 * h_2^{\frac{3}{2}}\right)} - \frac{1}{1 + f\left(\frac{h_1}{h_2}\right)} * \frac{m}{B_0^{n-1} * h_0^n}\right] \tag{9.23}$$

A system is in equilibrium when both differential equations are zero. This is possible with three situations as mentioned before. The stability can be assessed by looking at the eigenvalues of the Jacobian of this system of differential equations. If both eigenvalues have a negative real part the system is stable if it is set of its equilibrium state. When one of the eigenvalues has a positive real part the equilibrium is unstable. Any disturbance will grow faster and faster. In the publication it is

said that the eigenvalues cannot be determined when only general parameters are used. When symmetrical branches are used it gives the following Jacobian.

$$J(h_0, h_0) = \frac{S_0}{B_0 * h_0 * L_1} * \begin{bmatrix} -\frac{n}{4} - \frac{2 * h_0}{(1+f)^2} * \frac{\partial f}{\partial h_1} & -\frac{3 * n}{4} - \frac{2 * h_0}{(1+f)^2} * \frac{\partial f}{\partial h_2} \\ -\frac{3 * n}{4} - \frac{2 * h_0}{(1+f)^2} * \frac{\partial f}{\partial h_1} & -\frac{n}{4} - \frac{2 * h_0}{(1+f)^2} * \frac{\partial f}{\partial h_2} \end{bmatrix} \tag{9.24}$$

The eigenvalues are

$$-n \frac{S_0}{B_0 * h_0 * L_1} \tag{9.25}$$

$$\left(\frac{n}{2} + \frac{2 * h_0}{(1+f)^2} * \left(\frac{\partial f}{\partial h_2} - \frac{\partial f}{\partial h_1}\right)\right) * \frac{S_0}{B_0 * h_0 * L_1} \tag{9.26}$$

The first eigenvalue is negative in any realistic case. The second eigenvalue needs to be negative as well. This is true if the first part is negative when combined. This is when the following is satisfied

$$\frac{\partial f}{\partial h_1} - \frac{\partial f}{\partial h_2} > \frac{n * (1+f)^2}{4 * h_0} \tag{9.27}$$

It was found by (Wang, Fokkink et al. 1995) that for the nodal point relation as formulated in (9.6) there is a stable equilibrium if k>n/3 and unstable when k<n/3. This is the stability for a system with two open branches. There are two other equilibriums.

- Branch one is open and branch two is closed
- Branch one is closed and branch two is open

For these equilibriums the Jacobians are

$$J\left(2^{\frac{n-1}{n}} * h_0, 0\right) = \frac{S_0}{B_0 * h_0 * L_1} * \begin{bmatrix} -\frac{n}{2^{\frac{n-1}{n}}} & 0 \\ 0 & 0 \end{bmatrix} \tag{9.28}$$

$$J\left(0, 2^{\frac{n-1}{n}} * h_0\right) = \frac{S_0}{B_0 * h_0 * L_1} * \begin{bmatrix} 0 & 0 \\ 0 & -\frac{n}{2^{\frac{n-1}{n}}} \end{bmatrix} \tag{9.29}$$

These eigenvalues are independent of the nodal-point relation because there is only one channel. To find out whether or not these equilibriums are stable one needs to look at the equilibrium at

(h_0,h_0). If the system is stable at (h_0, h_0) than in $\left(2^{\frac{n-1}{n}} * h_0, 0\right)$ and $\left(0, 2^{\frac{n-1}{n}} * h_0\right)$ the system is unstable and vice versa. A phase diagrame shows this behaviour. On the axis one sees the water depth in either branch.

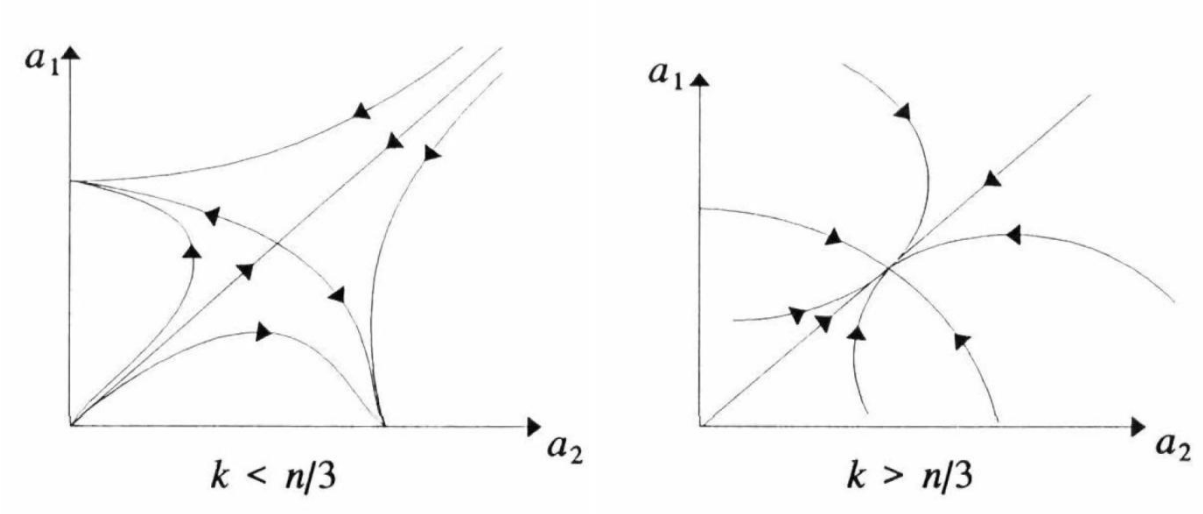

Fig. 9-8: Phase diagram (Wang, Fokkink et al. 1995)

Limitations to 1D models for bifurcations

The 1D model by (Wang, Fokkink et al. 1995) has several limitations. In the analytical approach, shown before with the nodal-point relation, there is a simplified theoretical basis. The 3D aspects mentioned before address the difficulty with which a nodal point relation needs to deal in 1D. A 1D model therefore needs to have the right input based on these 3D aspects. In practice this can reduce the predictive quality of such a model since these 3D models needs to be determined by measurement, 3D modelling or the maybe less reliable engineering assumptions. Either way the result strongly depends on the input. If the solution is not very sensitive than the errors will be small. However if there is no direct insight in the actual stability one will need to consider the use of other models.

As described in the previous paragraph, the mathematical approach has several simplifications.

- Simplified bathymetry to yield a system of ordinary differential equations
- Symmetrical branches to simplify the derivation of the eigenvalues of the Jacobian
- The value of k is kept constant. It doesn't change with an evolving bifurcation

These simplifications were done to make the mathematical approach more straightforward. In some way this is the purpose of 1D models in general. 3D models have much larger computational costs. If it is possible to build up a 1D model out of measurements or 3D computational results one can have a look at the future evolution of a bifurcation. The results of measurements or 3D computations or physical model tests can be matched with the 1D model with a least-squares-method.

In (Kleinhans, Jagers et al. 2008) 1D models were compared with optimised 3D models for long term simulations. It turns out that with the right calibration it is possible to find a calibrated 1D

model that can give accurate answers. Nevertheless they will lack input possibilities that are essential to describe the behaviour of the system.

The model by (Wang, Fokkink et al. 1995) did not account for changing properties of a bifurcation. Especially during floods the value of k is highly variable (Kleinhans, Jagers et al. 2008).

Some particular aspects that are neglected by 1D models and reduced into coefficients are listed below. These aspects can be highly dynamic and crucial for future development

- Bar forming and evolving
- Widening and narrowing of branches
- Transverse slope changes due to erosion/sedimentation
- Spiral flow due to river bends.
- Tidal influence propagating up the channels

3D models can account for this since they adapt the situation every morphological time step. In a 3D model such a nodal point relation is indirectly formulated in every cell in fact and these are updated every morphological time step. These formulations are a result of all the boundary conditions initial conditions and state of the system at that time step. All processes that play a role can enhance or dampen each other. This yields a large range of possible evolutions for every bifurcation. It is therefore there is no universal formulation yet.

Other nodal-point relations

Besides the nodal-point relation as mentioned before there are several others that deal with different aspects that were considered most important for the bifurcation dynamics.

For a transverse slope at the junction for example (Bolla Pittaluga, Repetto et al. 2003) have looked at the development of this slope during the 1D simulations. Basically they assumed that at a bifurcation with mainly bed load transport, there is initially a preferred branch for the sediment. This channel will start to silt up. Eventually the bottom will rise in that branch. Causing a slope towards that channel in a longitudinal directing. But since the other channel is not silting up or maybe even eroding there is a slope in the transverse direction. This process will deflect a part of the sediment load towards the deeper channel. Hence slowing down the sedimentation in the accreting channel. Three major conclusions can be drawn.

- This model can account for a stable two branch situation if the siltation stops before one channel silts up entirely. Otherwise one channel will remain. These are the same stable scenarios as with the first mentioned 1D model
- The model implements a 2D effect by converting two 1D aspects (the two different water depths in the two branches) into a slope. Note that this is in this research considered to be the strongest process in bifurcation stability.
- The situation at the bifurcation changes in time and is accounted for in the formulation of the slope that changes over time as well. This is in contrast with the model by (Wang, Fokkink et al. 1995) that uses a constant value of k that determines the division of sediment.

This model has shown good results. But nevertheless it is a simplification of a 3D situation. It needs to be noted that this model yields only good results in scenarios where bed load transport is dominant. Suspended sediment is not so much influenced by the bed slope when transported. In section 0 the gravitational pull is explained. This is the process that steers the sediment and creates a preference for the lower lying branch.

Another formulation for the nodal point relation is done by (Miori, Repetto et al. 2006). They suggested a more dynamic character of the channel width. In the two models described before the banks were fixed even if this was not in equilibrium with the hydraulic conditions. Normally in single channels the adaptation time for bank positions is much longer than for the bed level (Miori, Repetto et al. 2006). For bifurcations this is not necessarily true and could be of the same time scale. For this model the following conclusions can be drawn.

- When banks are able to erode as fast as the bed the models with fixed banks do to give a good view on the bed development. The bed level change has to account for all changes also the part that would have been accounted for by the banks. When bank evolution is included the entire evolution can be described more accurately
- The formulation by (Miori, Repetto et al. 2006) also reduces the time scale for system evolution. It doesn't use a downstream boundary condition. Hence the morphological equilibrium is determined by the nodal-point relation. It does mean that this formulation is not valid in coastal rivers.
- The freedom of banks gives an even larger possibility of asymmetrical evolution of the bifurcation. This is found to be true in reality where almost in every case there is an asymmetrical evolution.

As with the model by (Bolla Pittaluga, Repetto et al. 2003) the model of (Miori, Repetto et al. 2006) is still not regarding 3D effects, complex flow fields etc. These effects could result in a very different equilibrium state.

III. Bélanger and scour model

In this section the Bélanger and Scour model are explained. These are not included in the main report due to the fact that this was not a research target.

Bélanger method

As said before the first step was to come to a simple model that can determine a feasible bypass. For this two methods were looked at. Initially the formula of Bélanger was used to build a model for water levels in discharge distribution:

$$\frac{dh}{dx} = i_b * \left[\frac{h^3 - h_e^3}{h^3 - h_c^3}\right] \tag{9.30}$$

With

$$h_c = \left(\frac{q^2}{g}\right)^{1/3} \tag{9.31}$$

$$h_e = \left(\frac{q^2}{C^2 i_b}\right)^{1/3} \tag{9.32}$$

With:

- C = Chezy roughness [$m^{0.5}$ / s]
- g = gravity [m / s^{-2}]
- q = specific discharge [m^3 /m /s]
- i_b = bottom slope [-]

When integrated this formula gives a so called “back-water curve”. It describes the water level along the river axis.

The calibration of this model was done by data from a previous model by ARCADIS. Data about water levels from different discharges came from an observation point 3350 m upriver from the mouth. Validation was done with measurements from the APMT2 terminal which lies 2150 m upriver from the mouth. As a calibration parameter in this formulation the Manning value was used. That value was than validated with the measurement data. The results are shown below in Table 9-1

Discharge [m^3/s]	Manning value [-]	APMT2 (Delft3D observations) [m]	APMT (Calibrated values) [m]	Pilot station (Measured values) [m]	Pilot station (Validated values) [m]
1000	0.060985	0.02	0.02	0.02	0.0132
2500	0.026297	0.08	0.08	0.06	0.0532
5000	0.016325	0.3	0.30	0.21	0.2027
7250	0.0140215	0.61	0.61	0.45	0.4204
8000	0.013473	0.71	0.71	0.54	0.4923

Table 9-1: Calibration and validation data

What is clear about these results is that since the Pilot station is between the river mouth and the calibration station that in that part the model is optimistic in its predictions. But conservative beyond its calibration point. Another conclusion from these results is that the roughness seems to decline. There is no reason to believe that that is the case here since this phenomenon is not implied in the mentioned Delft3D model by ARCADIS. However, it is a known phenomenon that natural rivers can have a strongly decreasing roughness with higher discharges (Rijn 2007a).

After the calibration phase it was possible to apply this model for the situation of a two channel scenario. The input parameters were set by the current branch and the “to-be-designed” bypass. The distribution over the two channels had to be as such that the water levels at the junction were equal. Meaning that when integrating from the sea level towards the junction the total water level rise is the same.

Scour analysis method

During the floods of 2008 and 2011 large scour problems occurred. Since the basis of this project is not only about sedimentation but also about erosion it was obvious to look at how much reduction the discharge through the current channel would have to be to prevent erosive flow in the problem area. The biggest problems have been noticed in the harbour area where entire quay walls have collapsed and sunk into the river. This is caused by very high flow velocities. Below in Fig. 9-9 the consequences of the 2008 flood are shown. In Fig. 9-10 the peak velocities are shown as simulated in a previous research. (ARCADIS 2012c). Depth prior to the event is about 11-12 meters in this area. This is doubled due to scour up to 11 meters at some points.

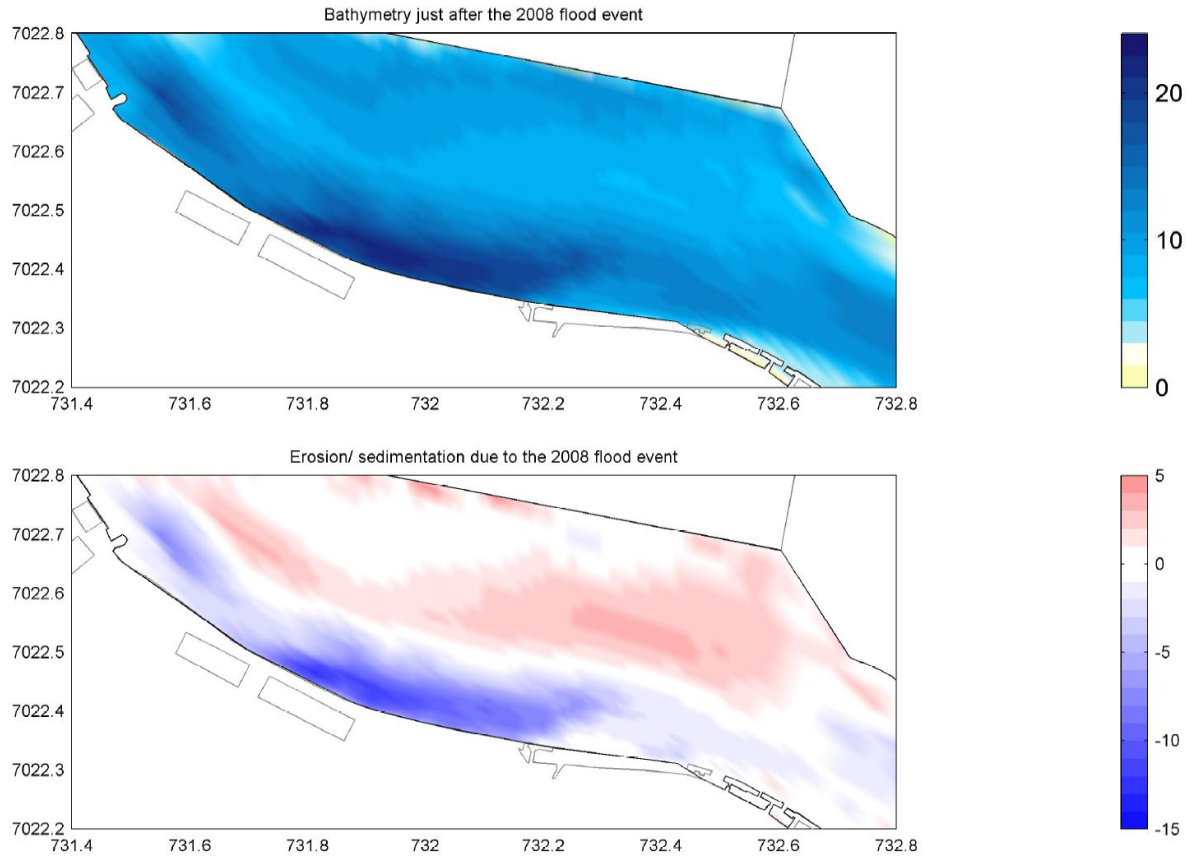

Fig. 9-9: Bathymetry measurements and differences after flood 2008

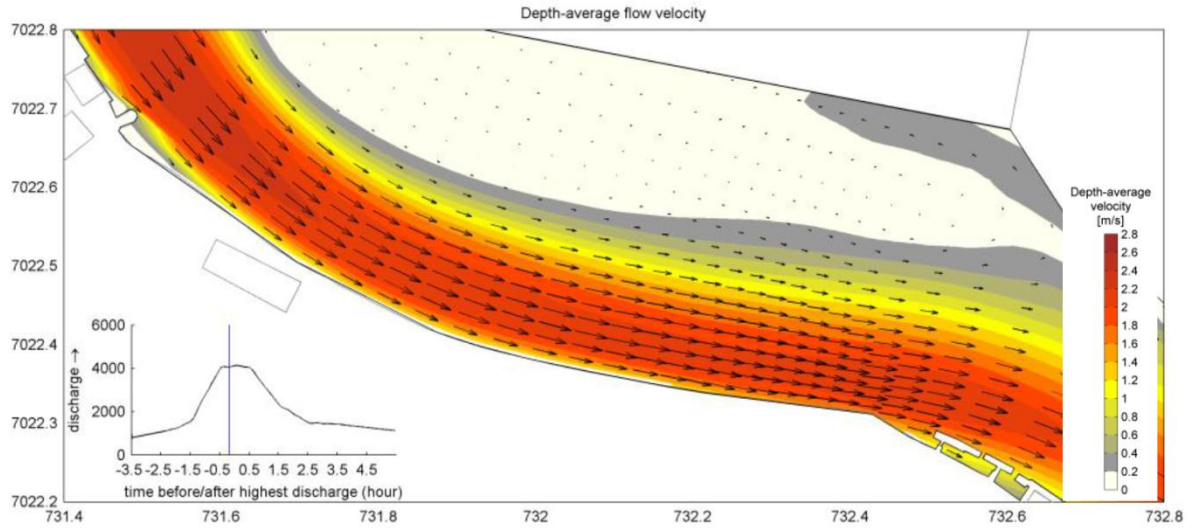

Fig. 9-10: Depth averaged flow velocities at peak of 2008 event

The method used here is to find the flow velocity that induces scour and link that to the discharge that causes it. For this the APMT terminals are chosen to calibrate the following scour formulation (Schiereck 2010).

$$h_{se} = \frac{h_0 * (0.5 * \alpha * u - u_c)}{u_c} \quad (9.33)$$

- h_o = water depth prior to event (11m) [m]
- α = turbulence factor (1.5-2.0) [-]
- u = upstream flow velocity [m/s]
- u_c = critical flow velocity [m/s]

$$u_c = 2.5\sqrt{\Psi_c * \Delta * g * D_{50}} * \ln\left(12 * \frac{h_0}{k_s}\right) \quad (9.34)$$

- Ψ_c = Shields stability parameter (0.03 iteratively determined by grain size calibration) [-]
- Δ = relative density under water of suspended material (=1.6) [-]
- g = gravitation [m/s2]
- D_{50} = median grain size [m]
- k_s = 2*D50 (estimation) [m]

When calibrated to the data from the simulated 2008 flood a grain size results of about 100µm. This is much larger than is measured in river itself. However under extreme flow conditions ripples and dunes can arise at the river bottom. This can cause a higher resistance.

The results from the scour formula are shown below in Table 9-2. Since the formulation hasn't been validated some research has been done about the validity. Since the harbour basin is almost everywhere 11-12 meters deep due to maintenance, it was clear that scour depths over the harbour basin differed according to the different flow velocities. As shown below, at a velocity of 1.6m/s there should be no erosion according to the scour formula. When comparing Fig. 9-9 and Fig. 9-10 it shows that indeed the turning point from erosion to accretion is in the area of 1.6 m/s.

Flow velocity [m/s]	Erosion depth [m]
1.6	11 + 0 = 11
1.67	11 + 1 = 12
1.74	11 + 2 = 13
1.82	11 + 3 = 14
1.89	11 + 4 = 15
1.96	11 + 5 = 16
2.04	11 + 6 = 17
2.11	11 + 7 = 18
2.18	11 + 8 = 19
2.25	11 + 9 = 20
2.33	11 + 10 = 21
2.4	11 + 11 = 22

Table 9-2: Flow velocities vs. depth + scour depth

Now the threshold flow velocity is known, the next step is finding the discharge that is fitting the flow velocities. This could be done with the Bélanger model. However, this model is configured with

the equilibrium depth at the bifurcation point. This is less deep than the harbour. The values below in Table 9-3 are found with the method of Bélanger.

Flow velocities [m/s]	Discharge [m^3/s]
1.6	2080
1.67	2230
1.74	2380
1.82	2530
1.89	2670
1.96	2790
2.04	2930
2.11	3050
2.18	3170
2.25	3280
2.33	3400
2.4	3500

Table 9-3: Flow velocities vs. Discharge

Since this gives very rough figures, some runs have been done with Delft3D to find the relation between flow velocity and total discharge. It was found that the figures above in Table 9-3 underestimate the discharge with 10-20%. The Delft3D output can be found in Appendix III. However, the discharges found in the Delft3D model are the maximum velocities over the cross-section, meaning that the velocities are over estimated. The choice was made to use the discharges from the scour formula method in combination with the Bélanger formula.

Conclusions

To determine the capacity it is important to state what is required. Since the safety levels and methods are unknown for Itajaí the following philosophy is formulated. The system should be able to meet expectations when a once in 50 year event occurs. Once every 50 years a discharge of 7250 m^3/s occurs. When reducing this to 2080 m^3/s this means a reduction of approximately 70%. The reduction with 70% and remaining discharge of 2080 m^3/s is based on the scour.

To achieve this the Bélanger model was used again. With this model it was possible to find a 70% distribution by adapting the width of the bypass. The depths were kept the same at the equilibrium depth of 7.6m and the total discharge was set to 7250 m^3/s. The result was a bypass that is 1.5-2 times as wide as the current river. That would make it 300 m wide. With the terrain height shown in Fig. 9-11 it is clear what areas should be avoided. Looking at the urbanized area it is possible to meet the two requirements of a short bypass and avoiding densely populated areas. Fig. 9-12 shows how and where the bypass is located. Together with the dimensioning with the scour and Bélanger method the bypass is ready to be used in the next phase to assess the consequences. The results of the Bélanger model in the form of backwater curves are shown in

Fig. 9-11: Terrain heights of the Itajaí area (Google 2013)

Fig. 9-12: Location and route of the bypass

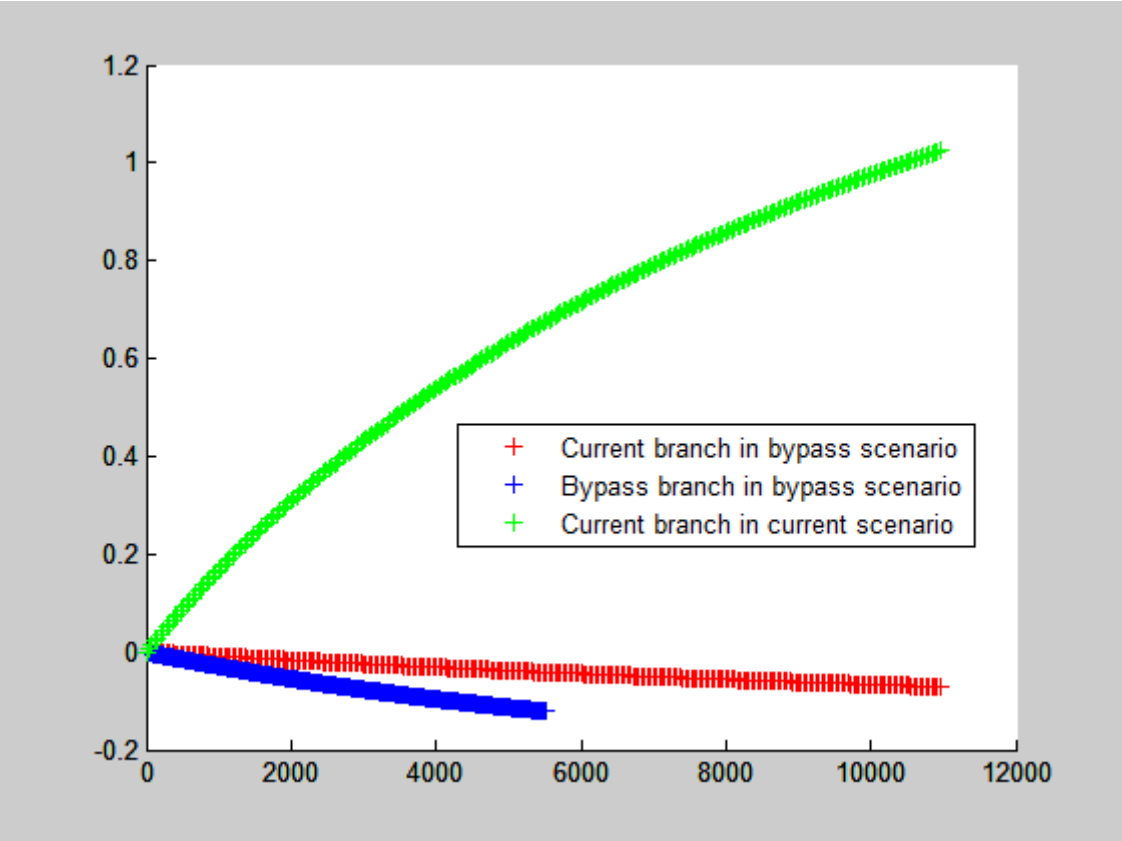

Fig. 9-13: Backwater curves for current and bypass scenario, discharge 7250 m^3/s, river axis (m) vs. water level relative to MSL (m)

IV. Flow velocities vs. discharges

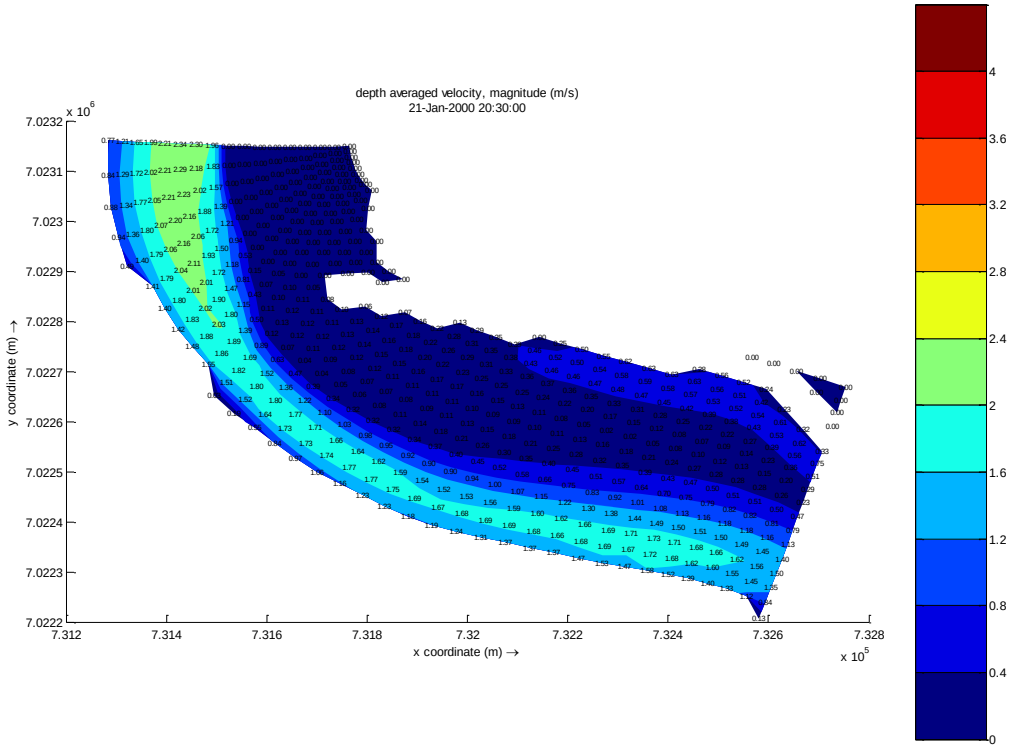

Fig. 9-14: 2250 m^3/s

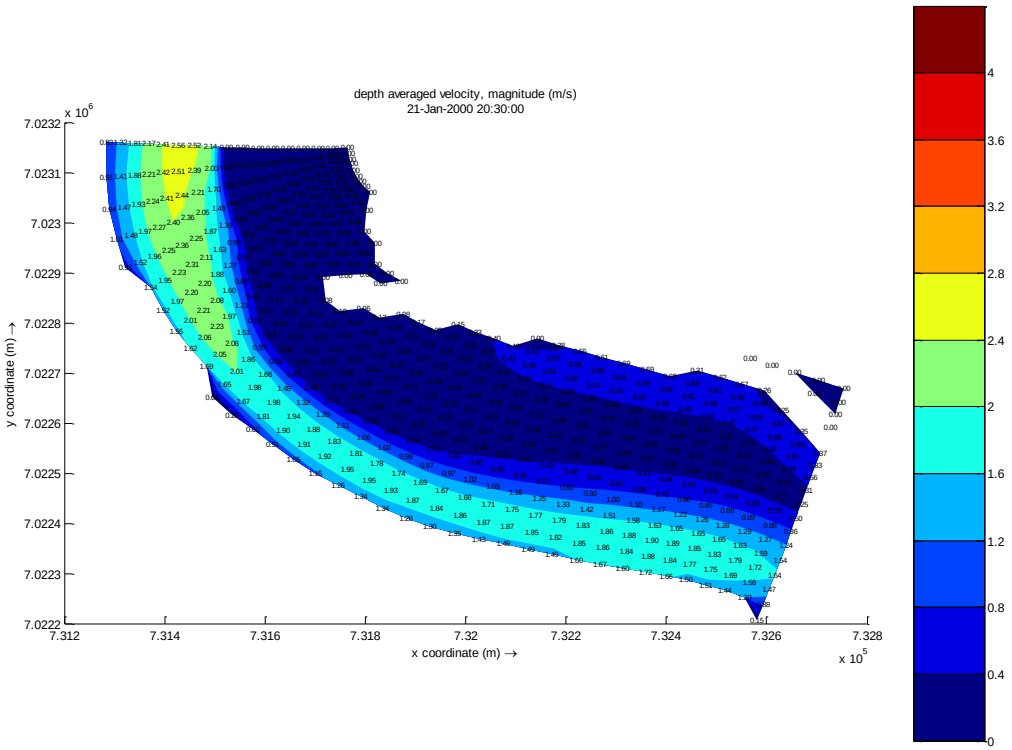

`

Fig. 9-15: 2500 m^3/s

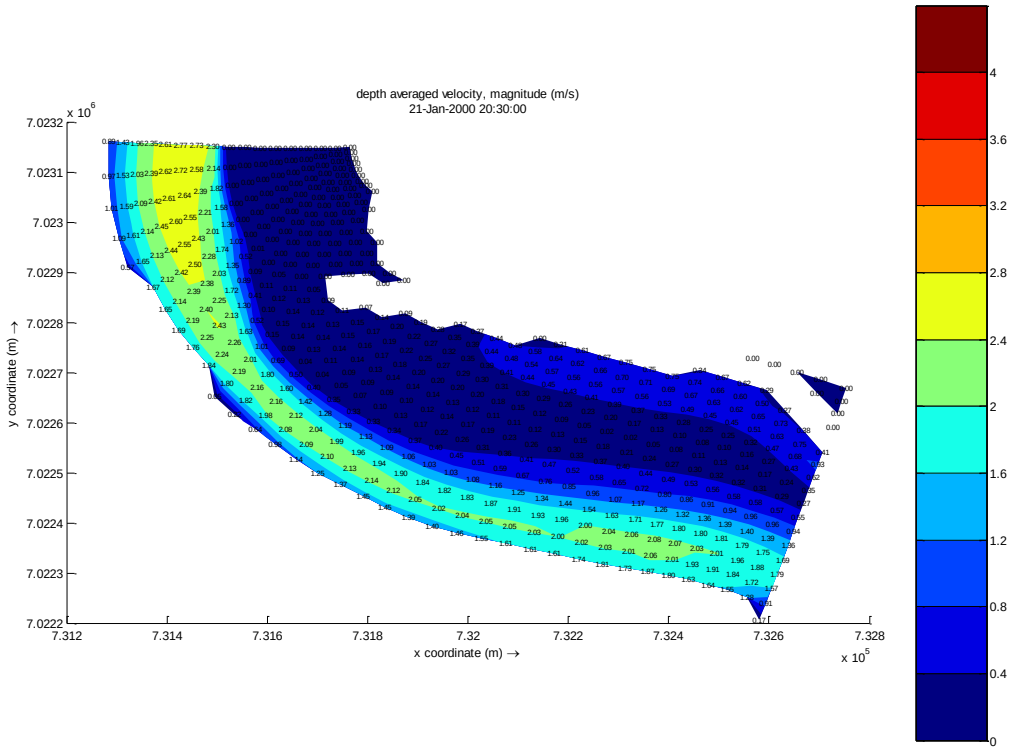

Fig. 9-16: 2750 m^3/s

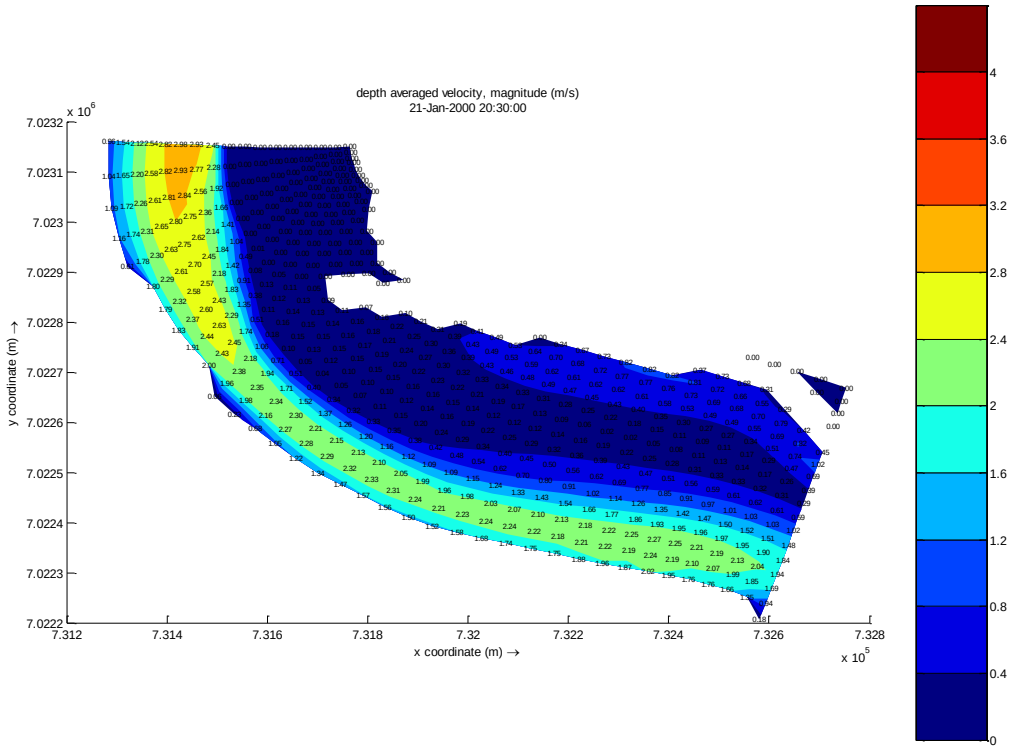

Fig. 9-17: 3000 m^3/s

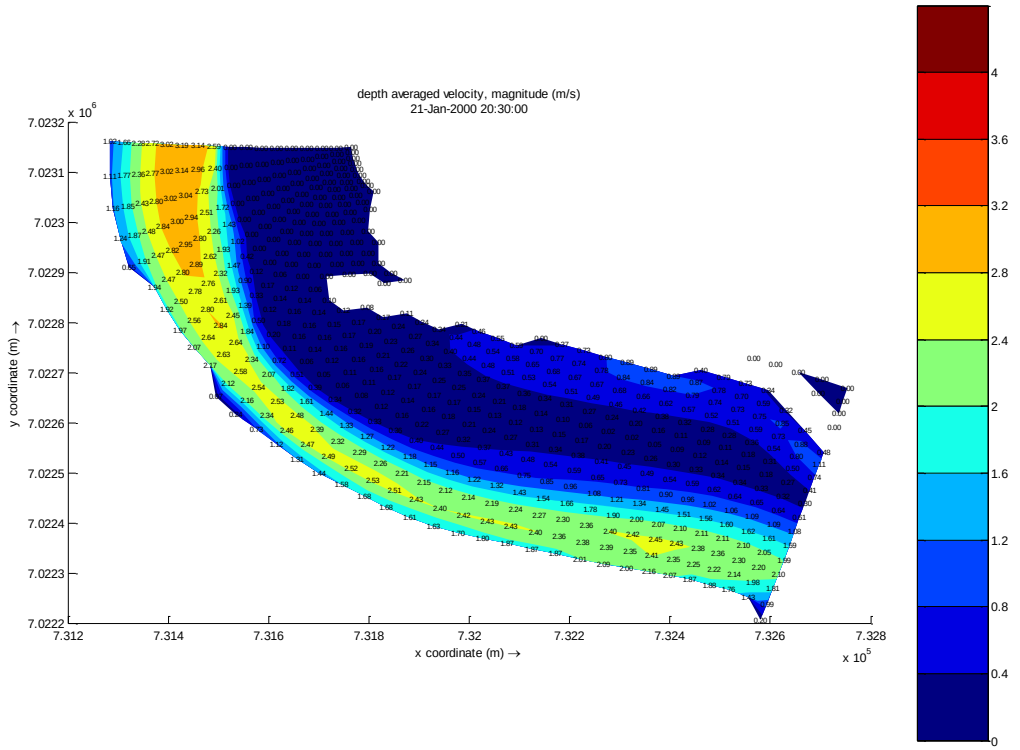

Fig. 9-18: 3250 m^3/s

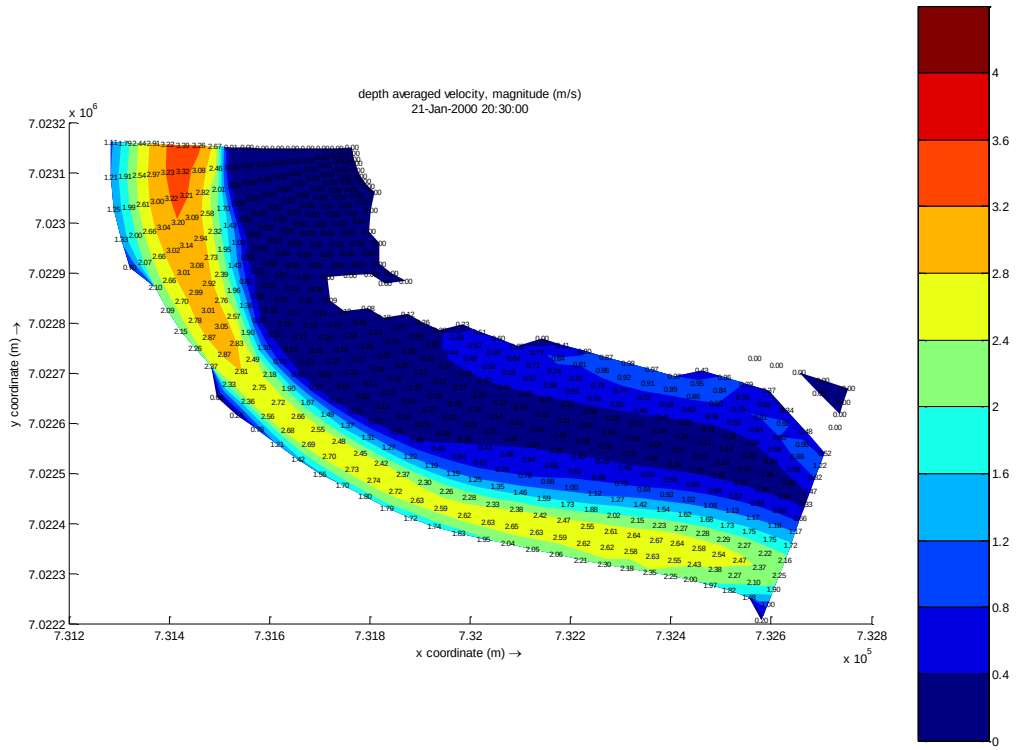

Fig. 9-19: 3500 m^3/s

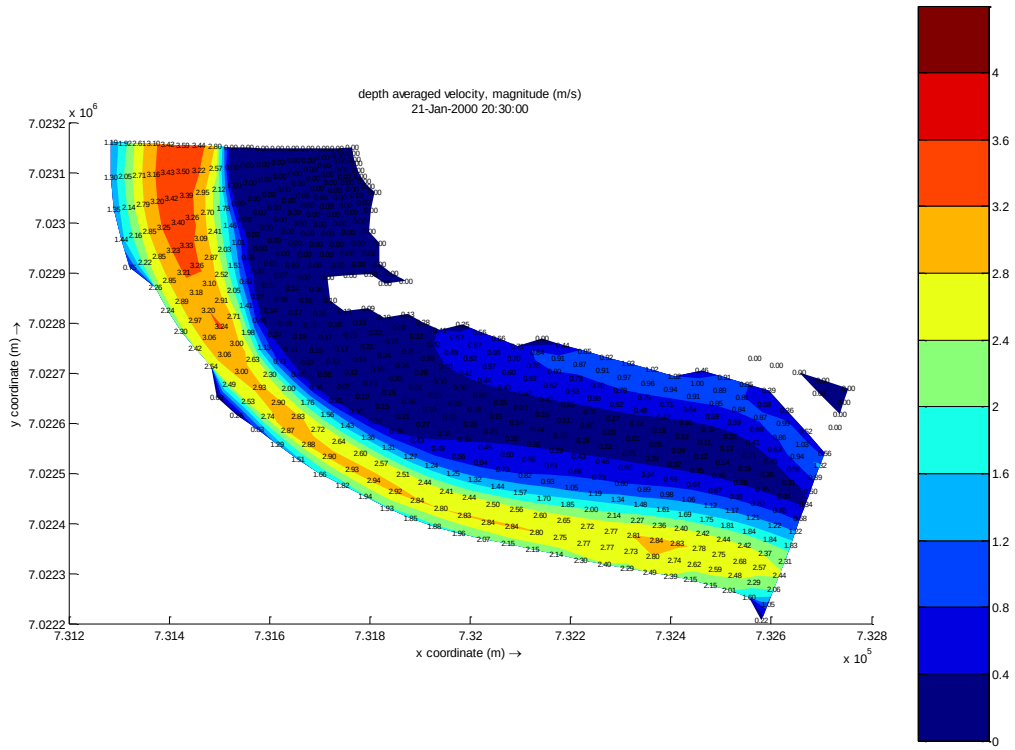

Fig. 9-20: 3750 m^3/s

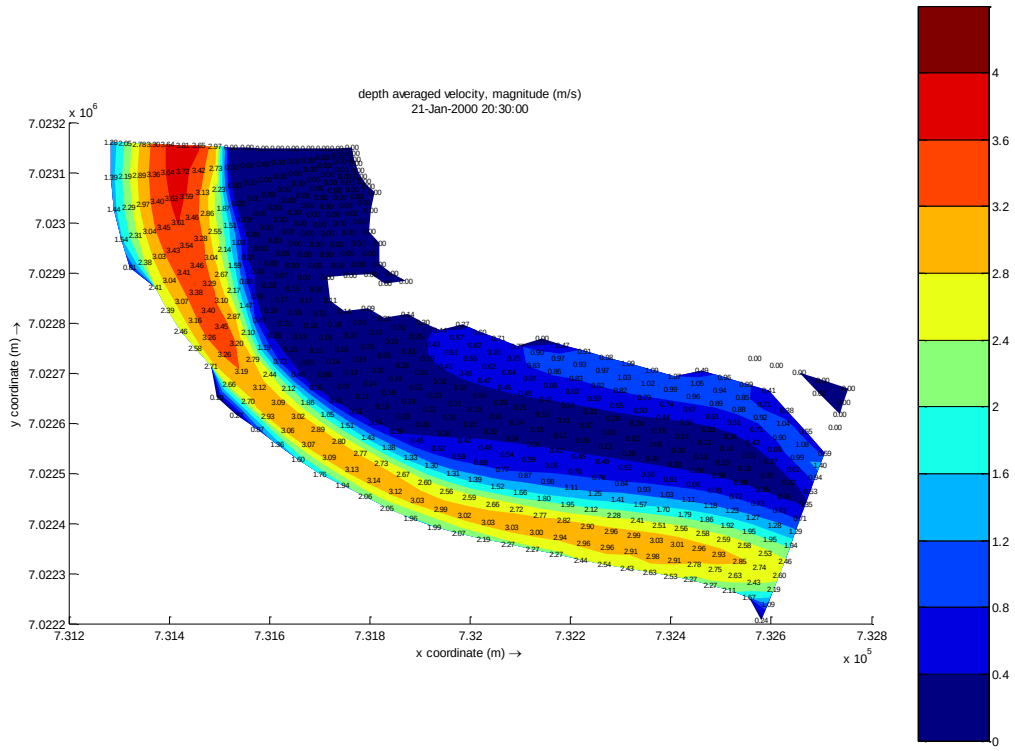

Fig. 9-21: 4000 m^3/s

V. Time step assessment

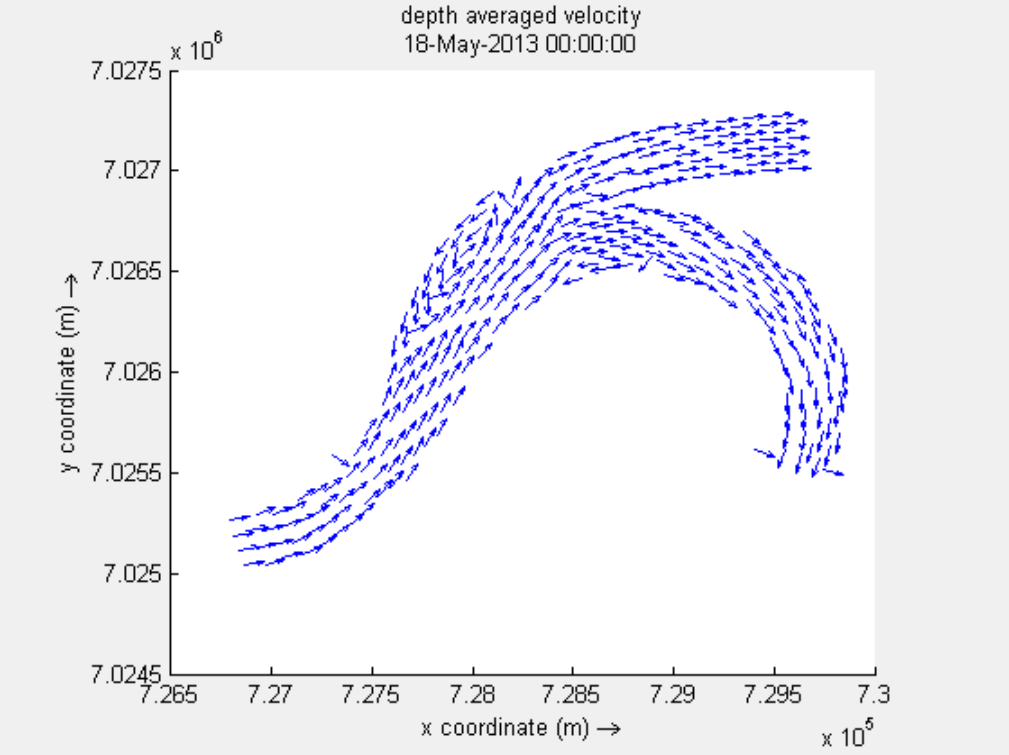

Fig. 9-22: Flow field at bifurcation, Δt=6s, 1000 m^3/s

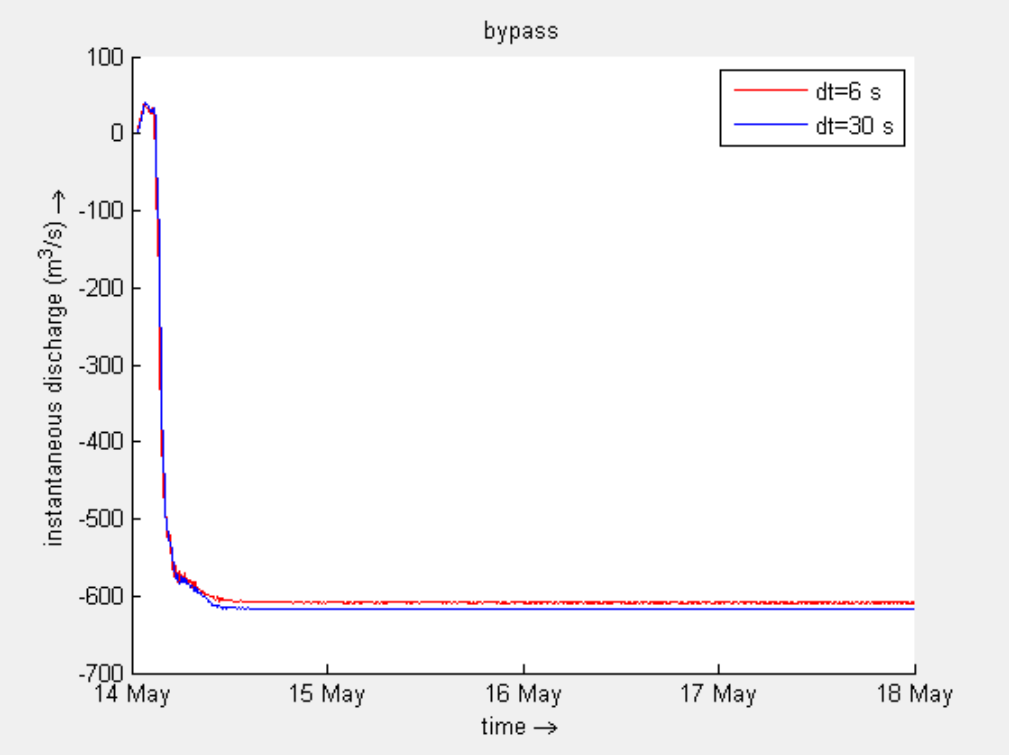

Fig. 9-23: Discharge comparison time step and depth of bypass 1000 m^3/s

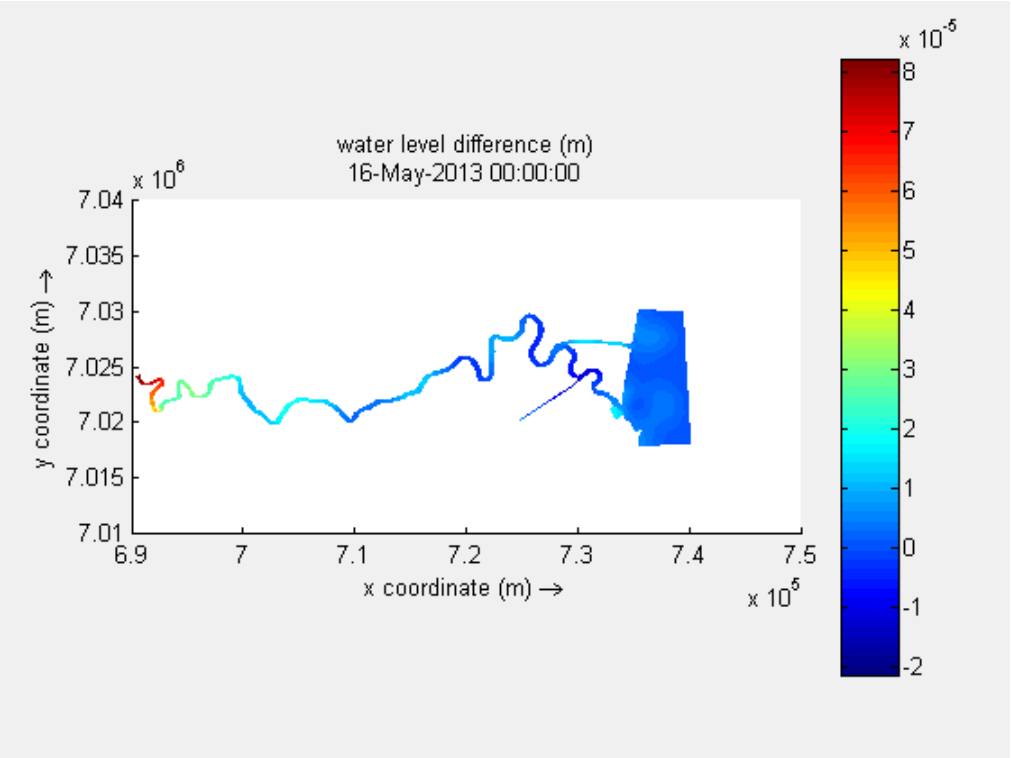

Fig. 9-24: Depth average velocity difference 150 m^3/s, Δt=6s and Δt=12s

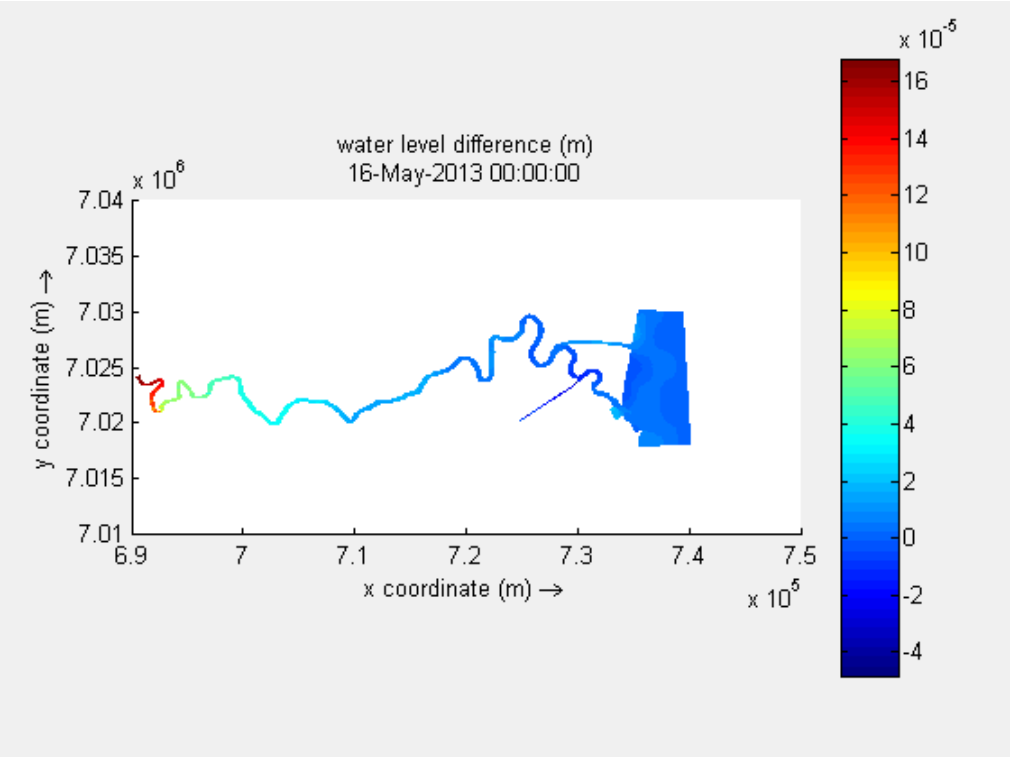

Fig. 9-25: Depth average velocity difference 230 m^3/s, Δt=6s and Δt=12s

VI. Relevant processes of "van Rijn" sediment transport module

In this module the vertical distribution of the suspended sediment is determined by the effective settling velocity, the bed shear velocity and the turbulence.

The effective settling velocity is determined by the product of the flocculation factor, the hinder settling factor and the sediment fall velocity of particles in clear water as determined by (Rijn 1993).

$$w_s = \varphi_{floc} * \varphi_{hs} * w_{s,0} \tag{9.35}$$

Where:

- w_s = effective sediment settling velocity [m/s]
- ϕ_{floc} = flocculation factor [-]
- ϕ_{ha} = hindered settling velocity factor [-]
- $w_{s,0}$ = sediment fall velocity in clear water (Rijn 1993) [m/s]

For flocculation of particles finer than 65 µm and salinities larger than 5 ppt, the flocculation factor is given by:

$$\varphi_{floc} = \left[4 + \log\left(\frac{2 * c}{c_{gel}}\right)\right]^{\alpha} \tag{9.36}$$

$$c_{gel} = \left(\frac{d_{50}}{d_{sand}}\right)^{\alpha} * \tag{9.37}$$

- c = mass concentration [kg/m^3]
- d_{50} = median particle of bed (range of 4-62 µm)
- d_{sand} = 62 µm = smallest particle size of non-cohesive bed (sand) [m]
- $c_{gel,s}$ = 1.722 kg/m^3 = dry bulk density by mass [kg/m^3]

$$\varphi_{hs} = \left[1 - 0.65 * \left(\frac{c_{vol}}{c_{vol,gel}}\right)\right]^{5} \tag{9.38}$$

- c_{vol} = volume concentration [kg/m^3]
- $c_{vol,gel}$ = gelling volume concentration for an immobile bed [kg/m^3]

VII. Bottom influence on salt intrusion

During the research on salinity it was found that the salt intrusion through the bypass is much stronger than through the current bypass. This intrusion is one of the reasons that the bypass is not suitable for permanent use since the salinity in the section between the bifurcation and the harbour mouth increases drastically. A way to find the reason for this is to run quick simulations with different settings that are derived from the difference between the current branch and the bypass as designed in the beginning.

There are four distinct differences between the current branch and the bypass.

- No breakwater in the bypass
- No sloping bottom in the bypass
- No bottom jump in the bypass as in the harbour basin in the Itajaí
- The cross-sectional shape of the bypass has a wide U shape the current branch has a more natural wide V shape.

Especially the last difference has shown to be very important. Below the results during ebb and flood are shown for the salt intrusion in the bottom layer.

Results

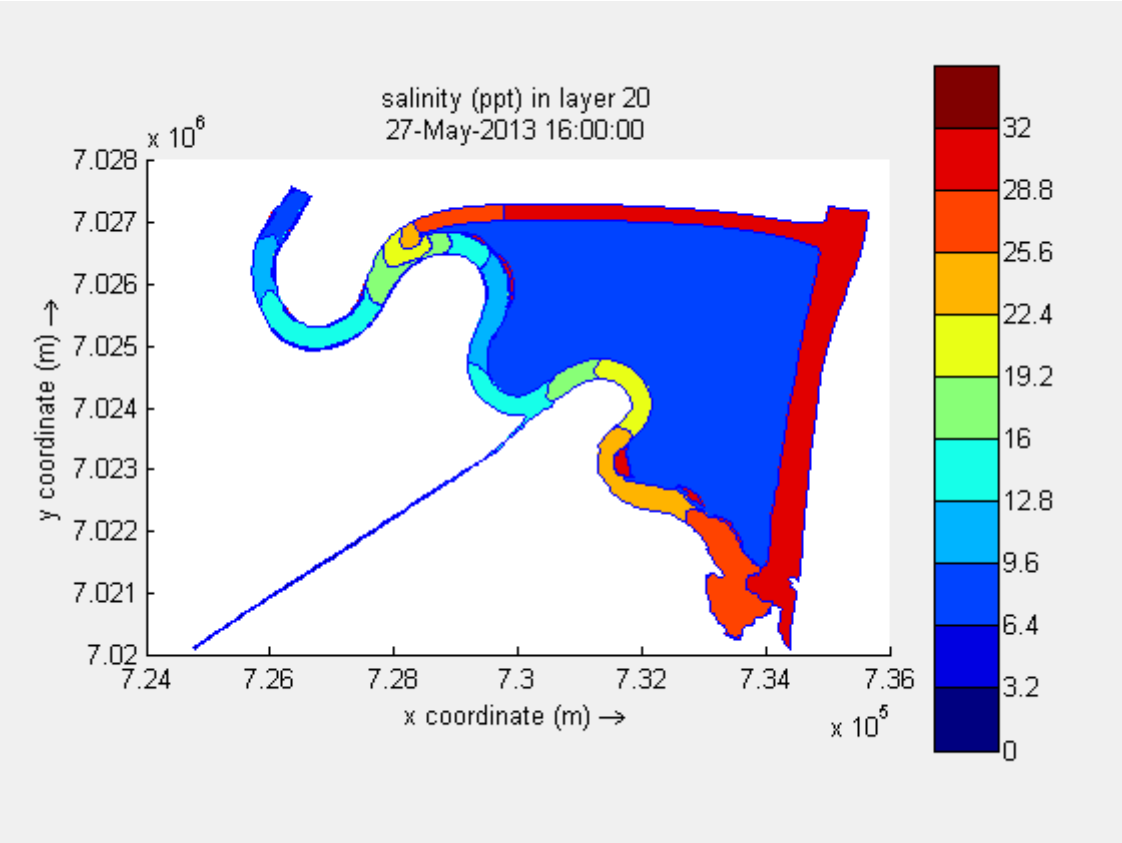

Fig. 9-26: Salt intrusion during flood in bottom layer. Breakwater scenario

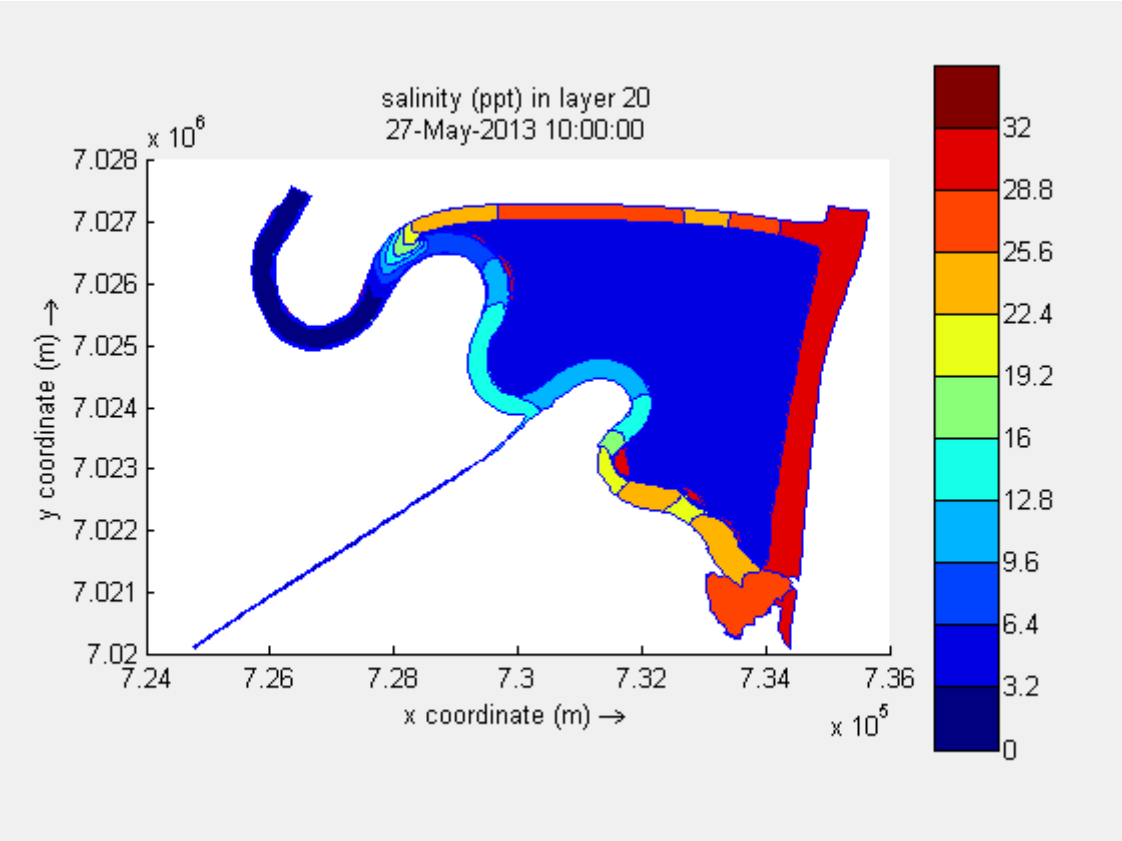

Fig. 9-27: Salt intrusion during ebb in bottom layer. Breakwater scenario

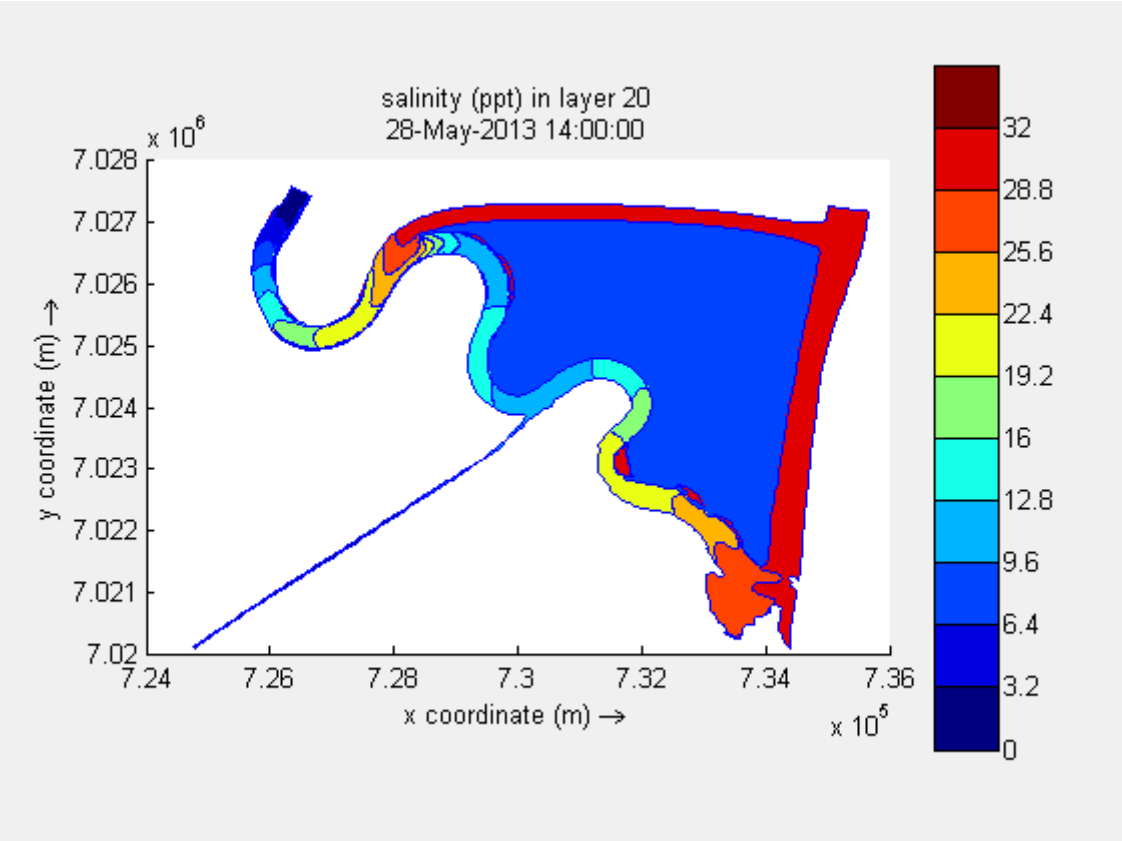

Fig. 9-28: Salt intrusion during flood in bottom layer. Steep slope bottom scenario

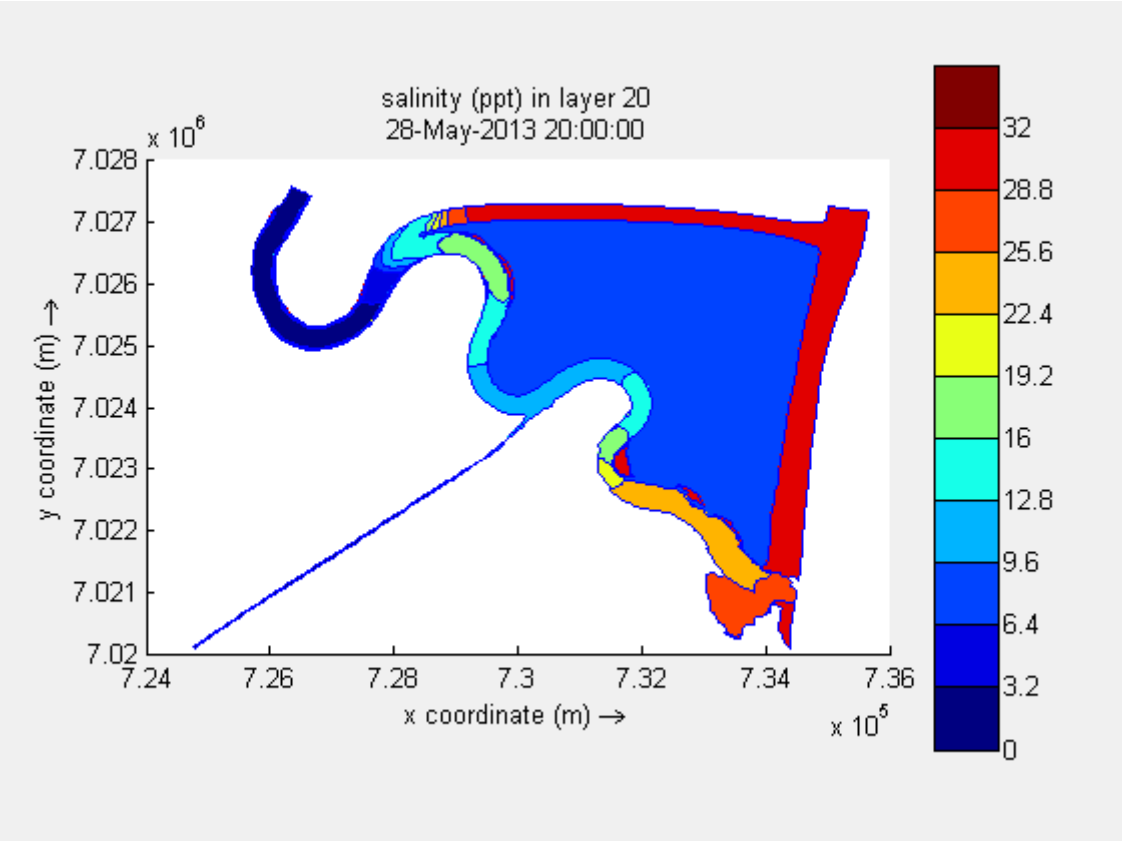

Fig. 9-29: Salt intrusion during ebb in bottom layer. Steep slope bottom scenario

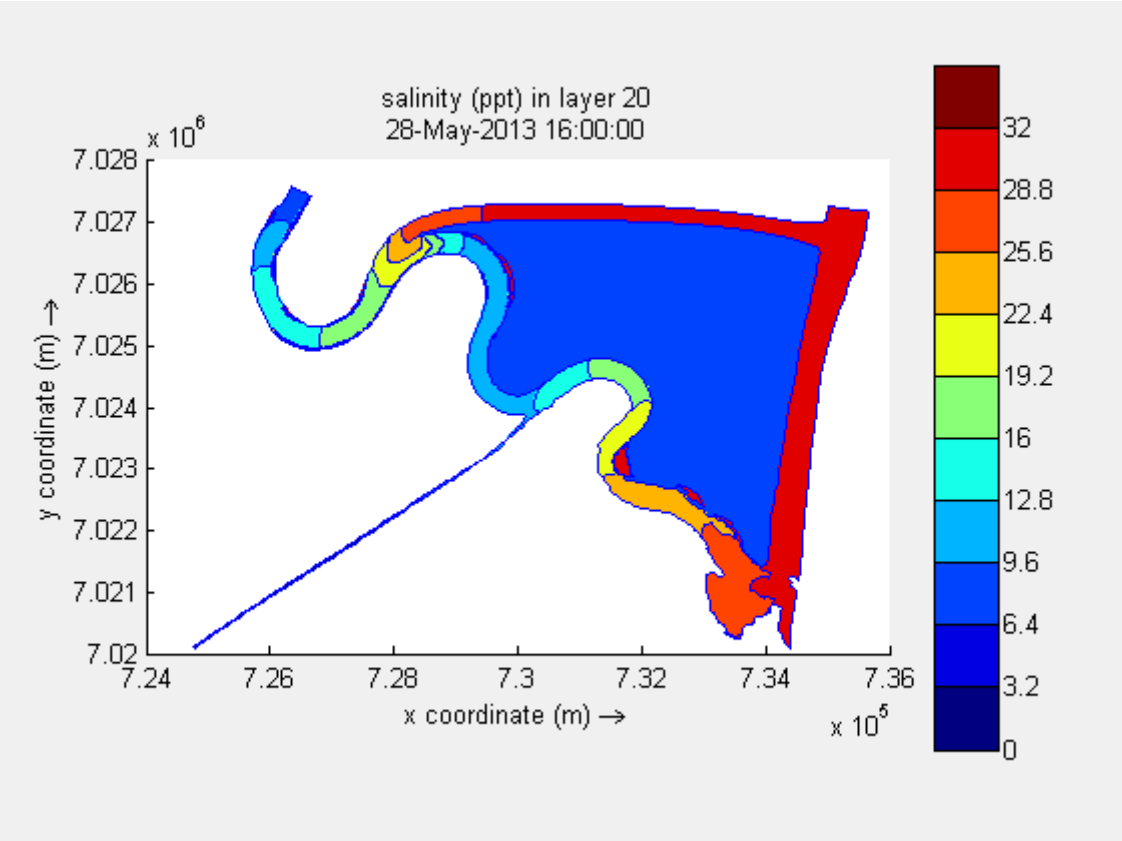

Fig. 9-30: Salt intrusion during flood in bottom layer. Step bottom scenario with breakwater

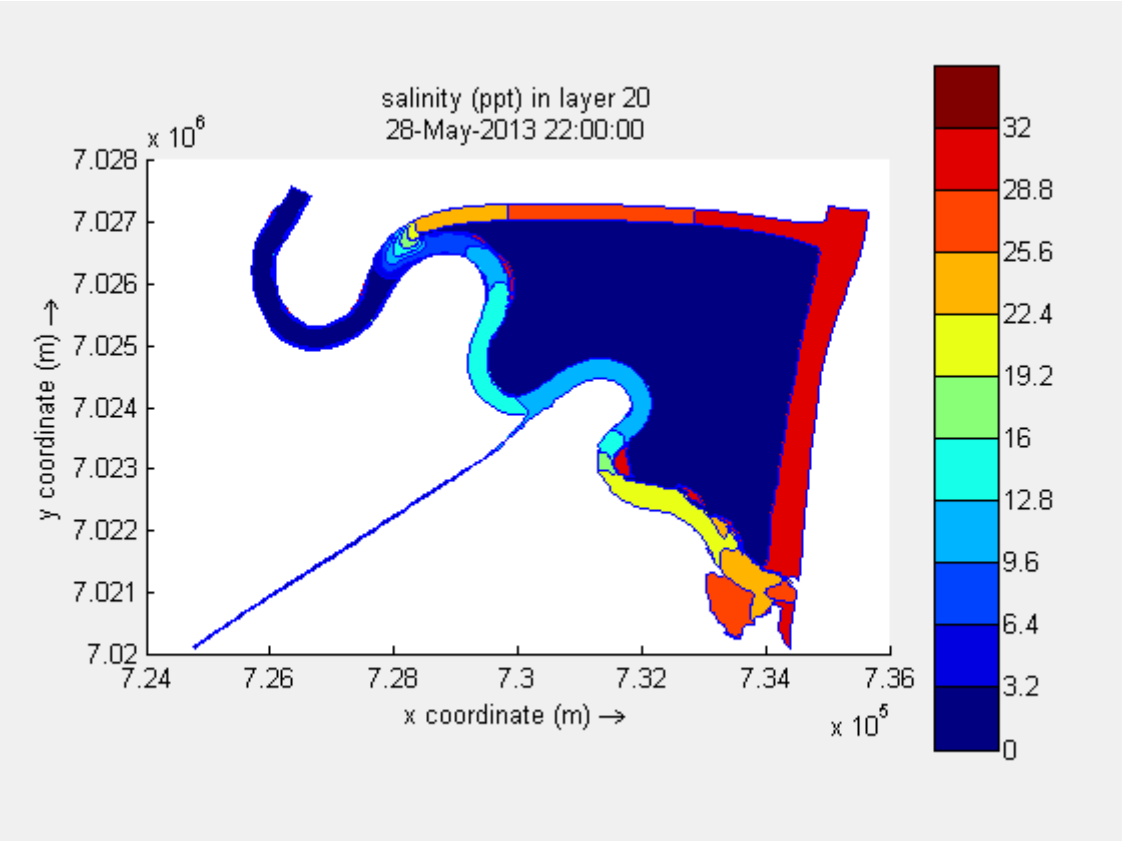

Fig. 9-31: Salt intrusion during ebb in bottom layer. Step bottom scenario with breakwater

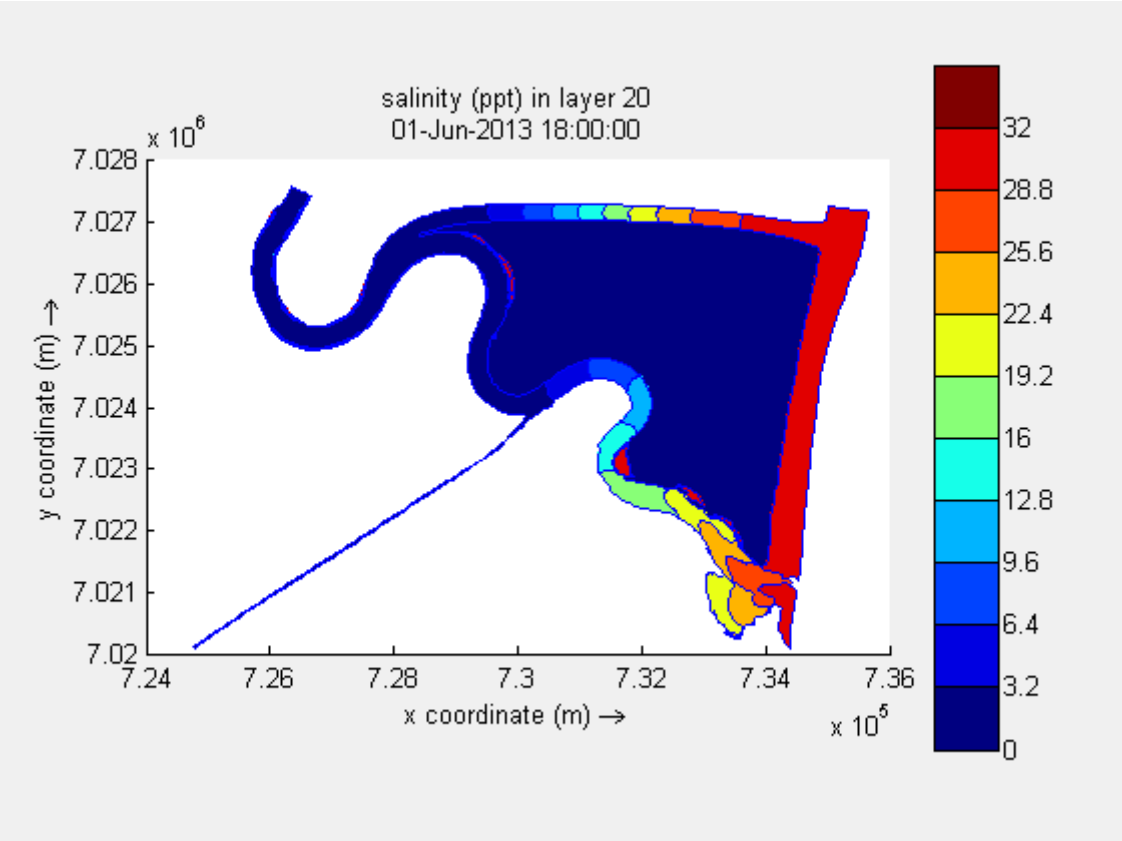

Fig. 9-32: Salt intrusion during flood in bottom layer. V-shape bottom scenario with breakwater

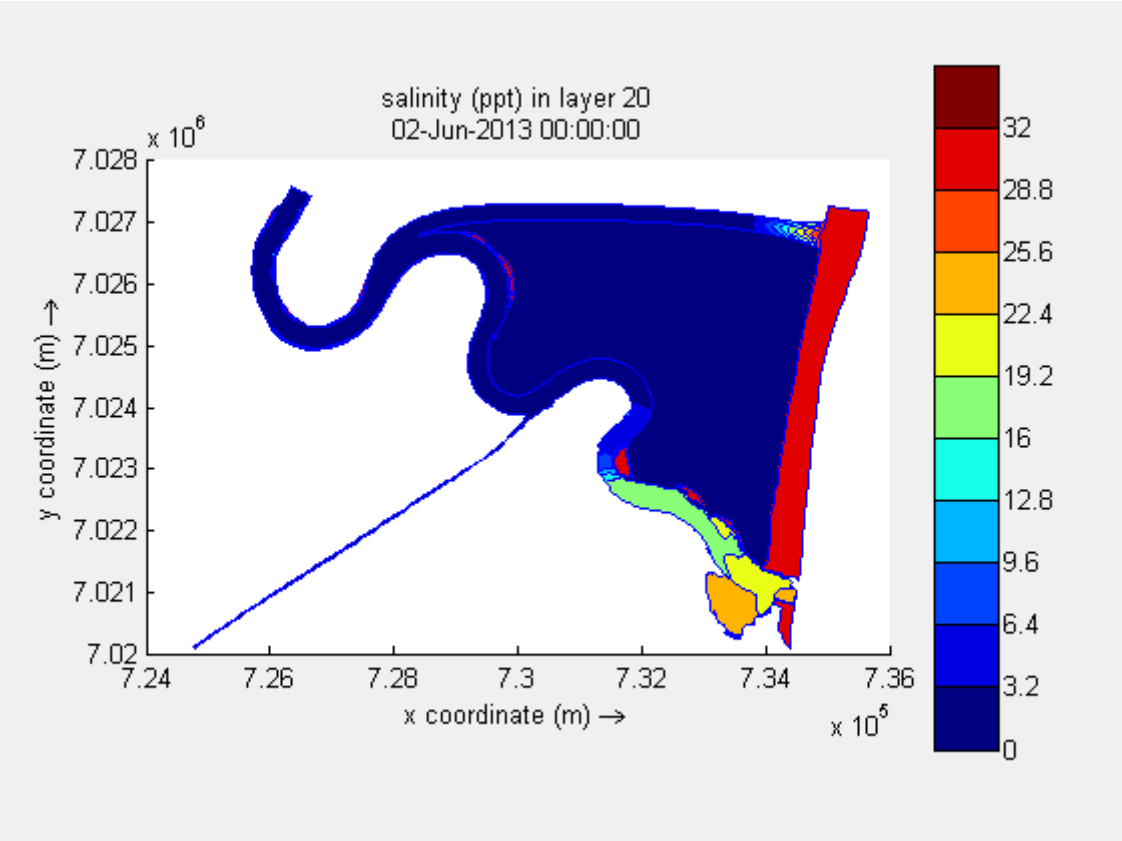

Fig. 9-33 Salt intrusion during ebb in bottom layer. V-shape bottom scenario with breakwater

Conclusion

The results from the last scenario are clear. The bottom profile is dominant for the salt intrusion. When minimizing the cross-sectional surface at larger depth compared to more at the surface the salt water body is less strong. This is however a disadvantage to the water transport capacity. When the average depth over width decreases the resistance increases. Also to keep the same cross-sectional surface this way a wider bypass is needed. All of this has to be considered when determining a more functional bypass.

VIII. Position of closure

For the positioning of the closure some advantages and disadvantages need to be addresses and when easily possible quantified. Below in Fig. 9-34 the two options are shown. The red closure is upstream at the bifurcation. This would mean that the bypass is separated from the river system during normal conditions. With the blue closure the bypass is always a part of the river system. During normal conditions when the closure is closed the bypass is a basin adding its tidal range to the current tidal prism.

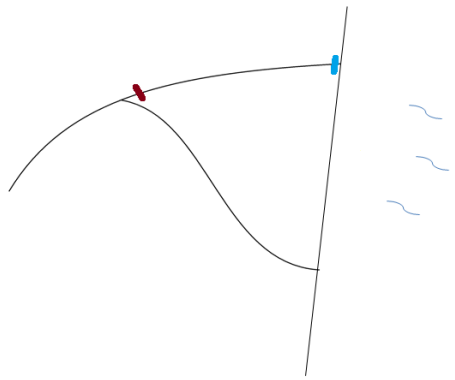

Fig. 9-34: Closure positions

Aspects

When determining where to place the closure some aspects that will arise can be addressed. Based on a first assessment of these aspects a valid conclusion can be drawn.

Salt intrusion

When the bypass is closed by the red closure it means that the bypass has turned into a basin with an opening at the sea side. The result will be a 100% salt intrusion for a its length of 5.5 km. This could become a problem for agriculture and other activities that require fresh ground water. On the other hand, in the area there is not much besides forestation.

Safety and protection

When the closure is place at the red location the sea gets another point of entry for waves. This might result in heavier protection needs for the walls. Also high water from the sea makes the dikes to be built an additional link in the safety chain that could fail. Nevertheless, the climate from the sea is not a governing safety issue. The issues at hand in Itajaí are coming from the extreme river discharges.

This would mean that when the blue closure is used and it fails that more area is prone to flooding than is nowadays. The length along the bypass that is now on the river side of the closure is now also at risk for flooding. Risk in hard to asses since partial failure can occur and it will depend on the kind of closing structure to be used. However knowing the sea climate the risk of a failing to open blue closure is carrying probably more risk than risk from the sea climate with a red closure scenario.

Internal basin

When the bypass is closed with the blue barrier, the bypass becomes an internal basin adding to the tidal prism of the system. It was found that indeed the tidal flow in the downstream section increases due to the increased tidal prism of filling and emptying the bypass during ebb and flood. This increased tidal flow is in the order of 8% to 11%. This is not a lot but will be noticeable for the maintenance dredging in the current branch since less accretion will take place in this section due to increased bottom friction over a tidal cycle by the increased flow.

Standing wave climate

Both closure positions will result in a standing wave at the closure. This means that flow velocities are 0 at the closure due to full reflection. In the end this means that sedimentation will occur at the closure. This will be the result for both the closures. The difference between the sedimentation results is that when the blue closure is used river sediment will settle in the basin. River born sediment is available in higher concentrations than sedimentation concentrations in water from the sea. Hence sea born sedimentation with the red closure is favourable above the river born sedimentation with the blue closure

Maintenance

Maintenance as it is done today in Itajaí is by injection dredging. This means that the bed sediment is fluidized by water injection and exits the basin as a density current. This is applicable in the closed bypass if the red closure is used since the blue closure would close of the opening to the sea. Maintenance of the bypass will be necessary in the bypass in any case. How much will depend on the regime of use. The current branch needs the extreme floods to flush out sediments to maintain is natural depth upstream of the harbour basin. The bypass will need to flush as well. The flush intensity will lower with the bypass. So both the current branch as the bypass will have a harder time to maintain themselves in a natural way. For the harbour basin this is not the case since it is very far under its natural depth by dredging. With hardly any flow through the bypass on a daily basis maintenance is inevitable. To comply with the dredging methods used nowadays the red closure is favourable.

Additional use

For additional functions of the bypass many options are available. As can be seen in the artistic representation on the cover of this thesis one of those functions could be an integrated harbour solution. This is most likely to happen with the red closure since with a blue closure the recreational ships would have to sail through the harbour of Itajaí which is unfavourable from any point of view.

Conclusions

Below in Table 9-4 the aspects of both alternatives are compared. Thus far it seems that a closure upstream is the safest, more efficient and more flexible. However these aspects cannot be compared in a straightforward manner. Therefore the best thing to look at is the motive to build the bypass. The key problems concerned siltation erosion and flood risk.

Because of that it is a good reason to place the closure at the bifurcation point. Since flood risk is a bigger issue than risk coming from the sea it is good to think in a worst case scenario. What if the closure doesn’t open when it should? At that moment the same situation as the current scenario is

happening. If the closure is located downstream the dikes along the bypass should hold during the flood. In other words, 11 km of dike is added to the system that could fail. Increasing the length of dikes that can fail make the system less reliable.

Besides mitigating flood risk also the maintenance issues are at play. As it was the intention to reduce maintenance of the constant siltation the way of maintaining the bypass is also important. When the closure is located at the downstream end the maintenance dredging would have to remove sediment from the channel and transport it by ship. The current method used in the harbour is by injection dredging. By injecting water into the mud a density current arises that leaves the harbour basin. To be able to do the same in the bypass the closure would need to be located at the upstream end of the bypass. In that way the bypass can be used to remove sediment from the bypass as maintenance.

	Red closure	Blue closure
Salt intrusion	-	+
Safety and protection	+	-
Internal basin	0	+
Standing wave climate	-	-
Maintenance	0	-
Additional use	+	-

Table 9-4: Criteria comparison red and blue closure

The conclusion is that the red closure would comply best with the requirements. Disadvantages are outweighed by the advantages especially on the key requirements.

IX. Maintenance dredging – numbers and figures

	Year	Volume	Minimum depth	Tolerance	Type	Channel width at turning circle
hopper volumes, hopper dredging	1958	200,000	6.50	0.5	maintenance	150 m
	1971	120,989	6.00	0.5	maintenance	
	1971	174,100	6.00	0.5	maintenance	
	1971	196,800	6.00	0.5	maintenance	
	1972	1,034	6.00	0.5	maintenance	
	1972	45,000	6.00	0.5	maintenance	
	1978	531,378	7.00	0.5	deepening	
	1978	396,165	7.00	0.5	maintenance	
	1978	358,133	7.00	0.5	maintenance	
	1980	43,147	8.00	0.5	deepening	
	1980	232,722	8.00	0.5	maintenance	
	1980	197,999	8.00	0.5	maintenance	
	1982	241,004	8.05	0.5	deepening	
	1982	237,058	8.05	0.5	maintenance	
	1982	106,573	8.05	0.5	maintenance	
	1989	172,000	8.05	0.5	maintenance	
	1990	1,596,694	8.10	0.5	deepening	
	1991	528,512	8.10	0.5	deepening	
	1992	842,611	8.10	0.5	maintenance	
	1993	841,180	8.10	0.5	maintenance	
volumes based on surveys, hopper dredging	1994	83,927	8.10	0.5	maintenance	230 m
	1995	796,870	8.10	0.5	maintenance	
	1996	2,250,000	8.15	0.5	maintenance	
	1997	898,787	8.15	0.5	maintenance	
	1998	1,500,000	9.15	0.5	maintenance + deepening	
volumes based on surveys, water injection dredging	1998	1,102,530	10.00	0.5	maintenance	330 m
	1999	1,234,345	10.00	0.5	maintenance	
	2000	2,000,000	10.00	0.5	maintenance	
	2001	1,870,000	10.00	0.5	maintenance	
	2002	1,800,000	10.00	0.5	maintenance + deepening	
	2003	1,893,750	10.00	0.5	maintenance	
	2004	1,850,430	10.00	0.5	maintenance	
	2006	2,100,000	11.00	0.5	maintenance	

Table 9-5: Dredging figures Van Oord

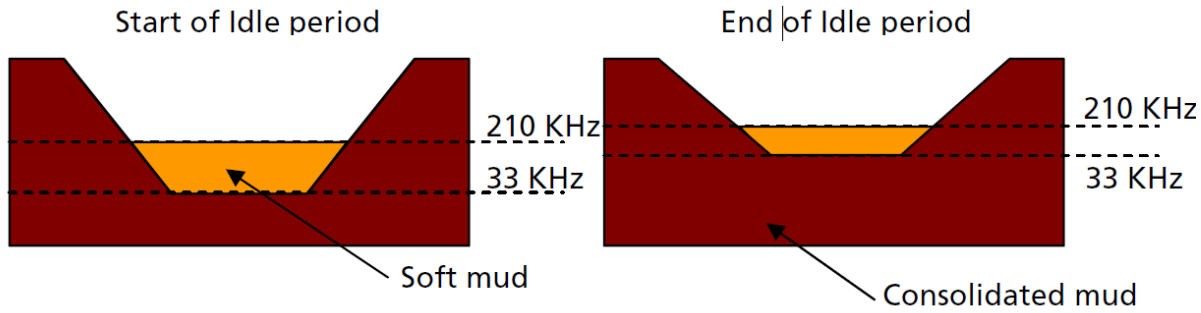

Fig. 9-35: Schematization of mud layers

Below the echo soundings from 4th of august and the 24th of September are subtracted from each other. Between these moments in time no dredging has taken place. This shows the accretion volumes in this area.

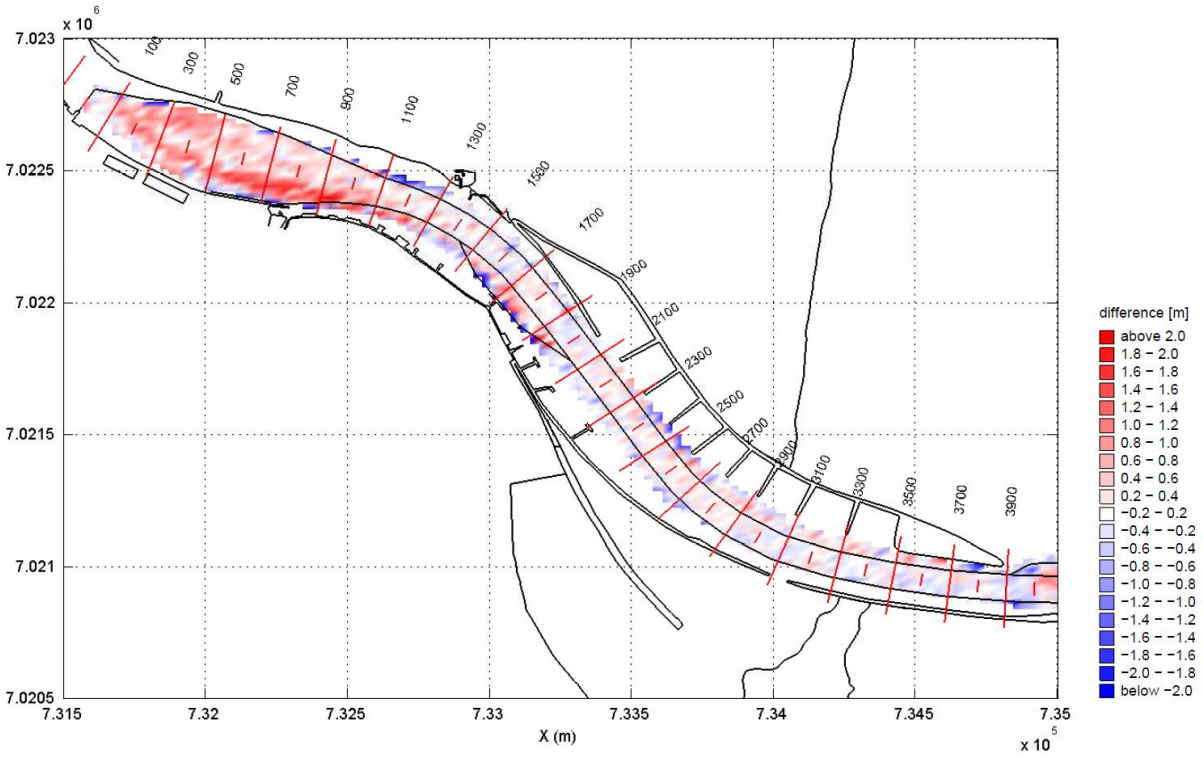

Fig. 9-36: Spatial differences in depth surveys (33 KHz consolidated mud) + is sedimentation

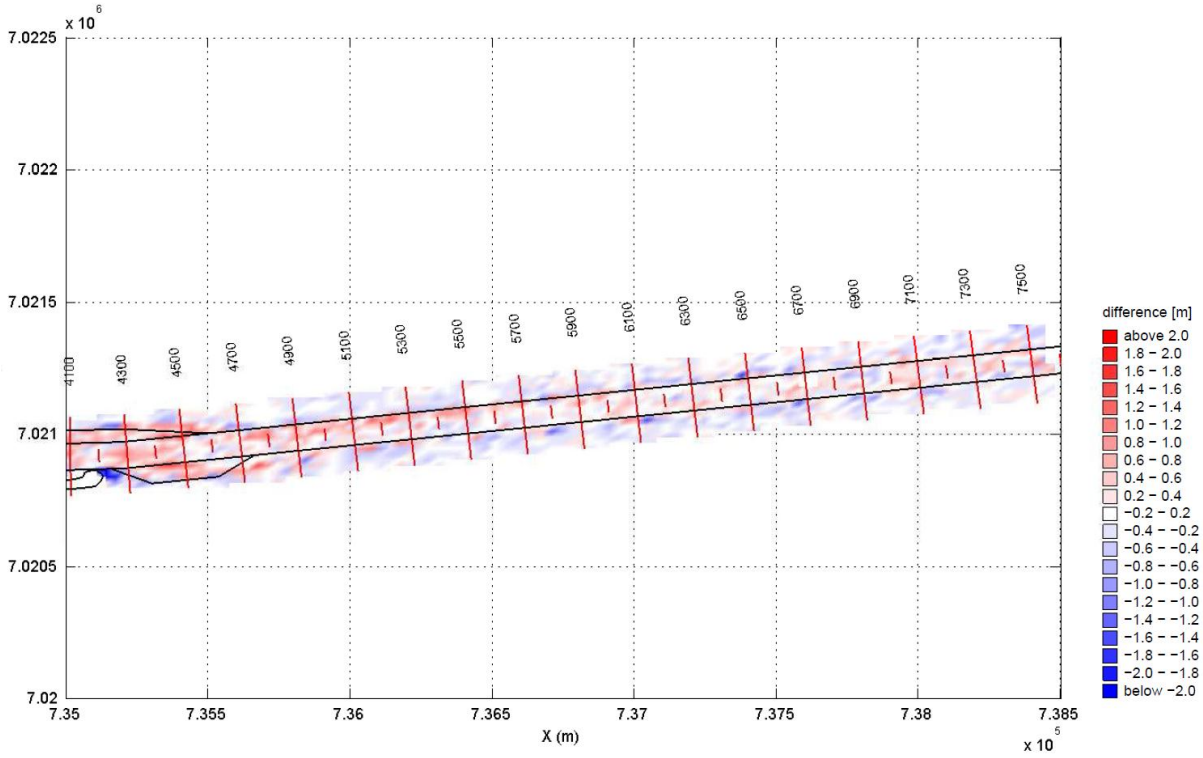

Fig. 9-37: Spatial differences in depth surveys (33 KHz consolidated mud) + is sedimentation

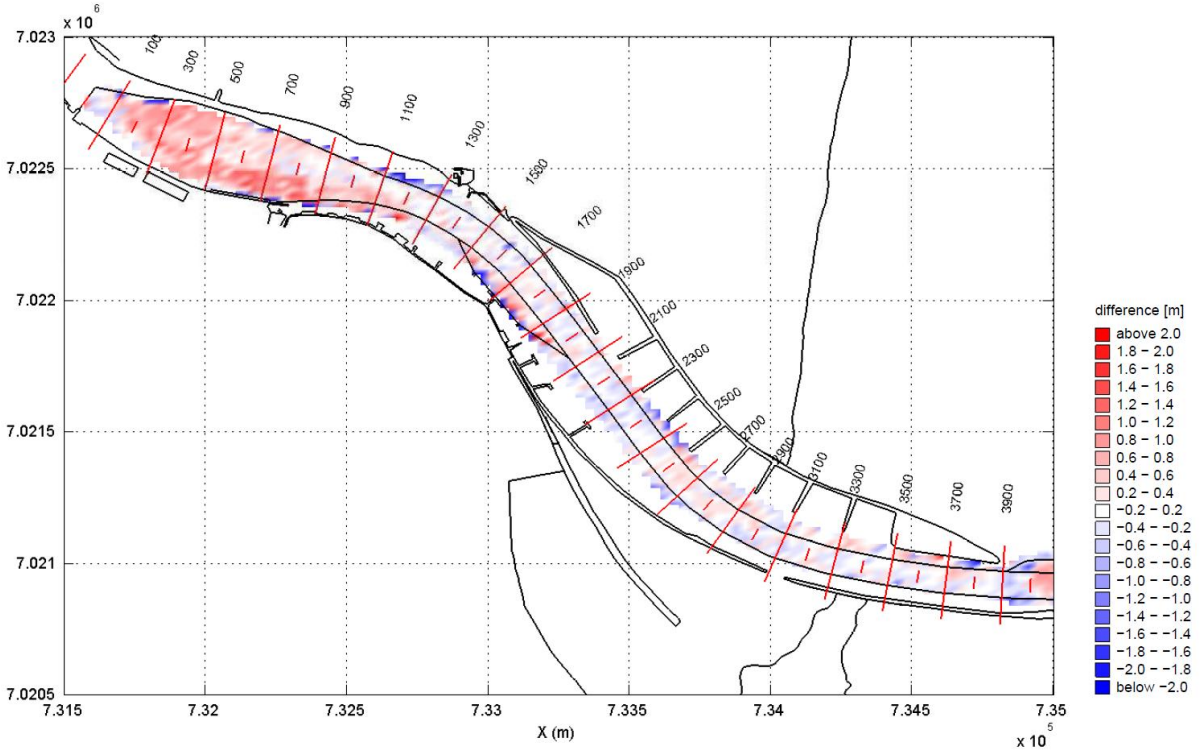

Fig. 9-38: Spatial differences in depth surveys (210 KHz top layer fluid mud) + is sedimentation

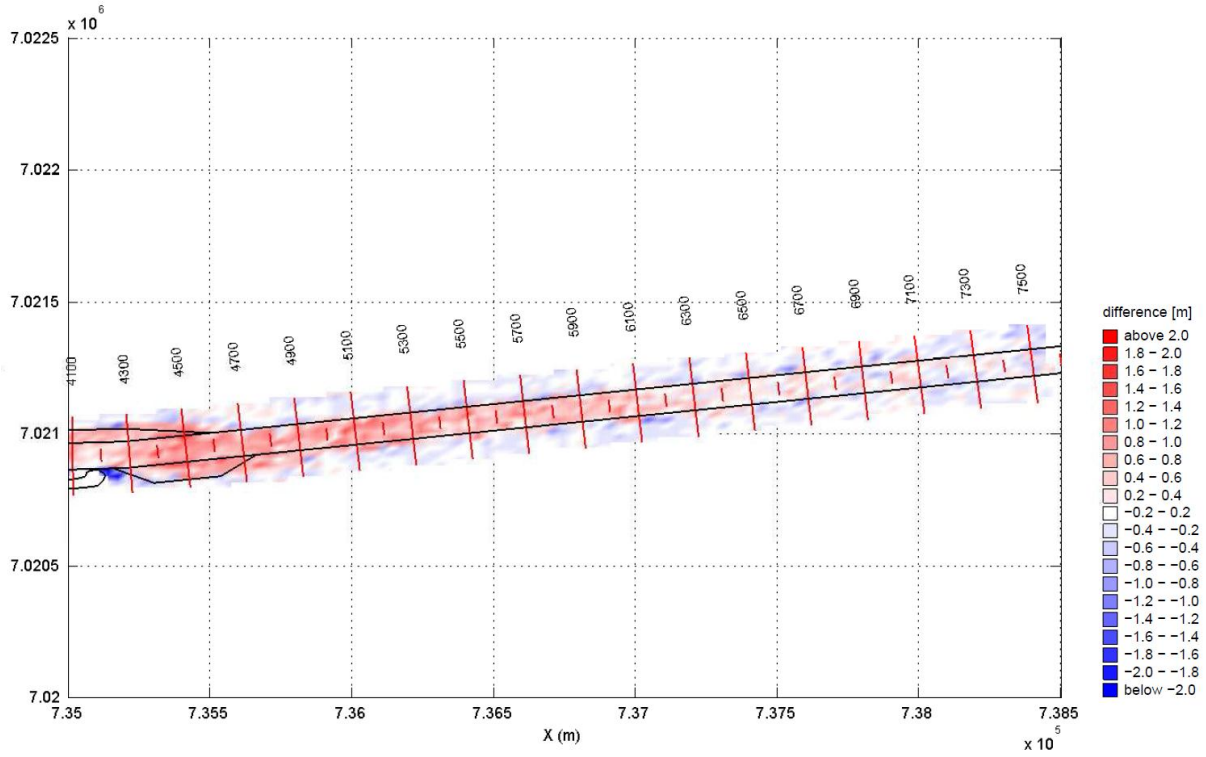

Fig. 9-39: Spatial differences in depth surveys (210 KHz top layer fluid mud) + is sedimentation

X. Bed shear stress – tidal scenario

This appendix shows the bed shear stress during ebb and flood for both the current scenario and the bypass scenario during a low discharge (150 m^3/s) and a high discharge (1000 m^3/s)

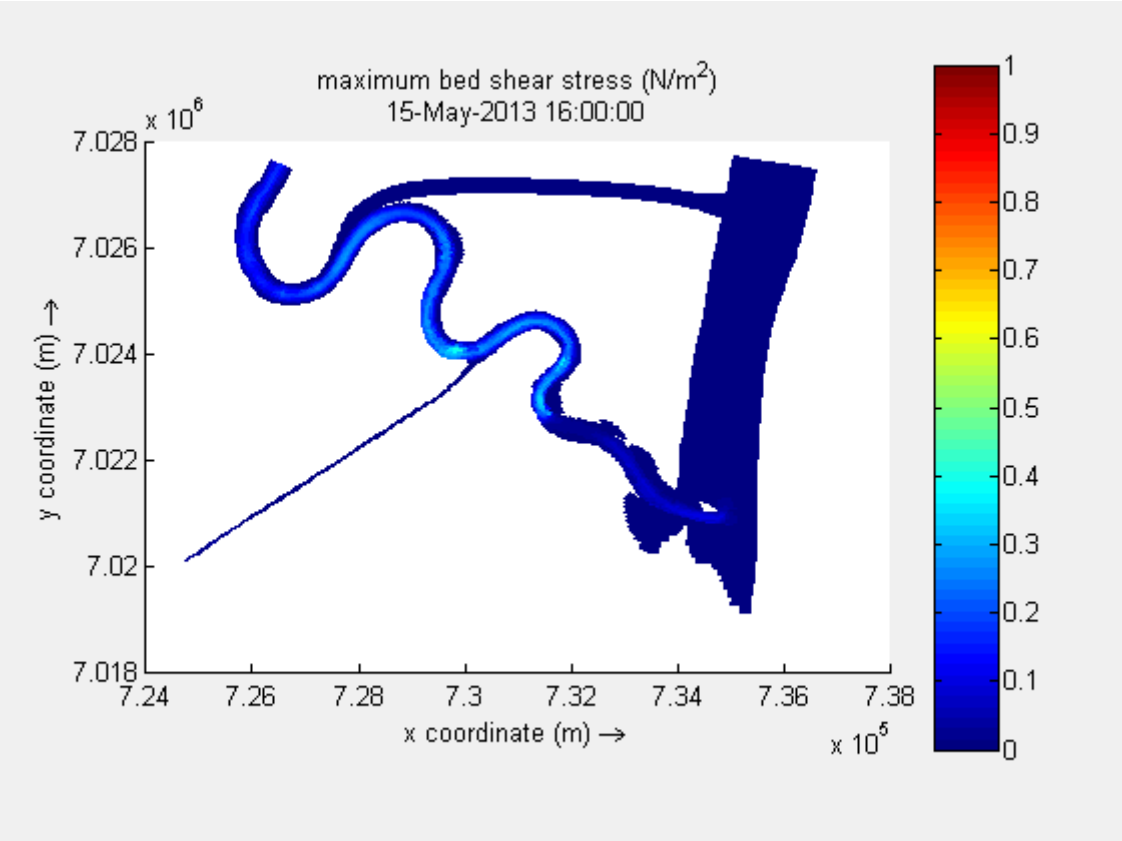

Fig. 9-40: Bed shear stress, 150 m^3/s, flood, current scenario, downstream section

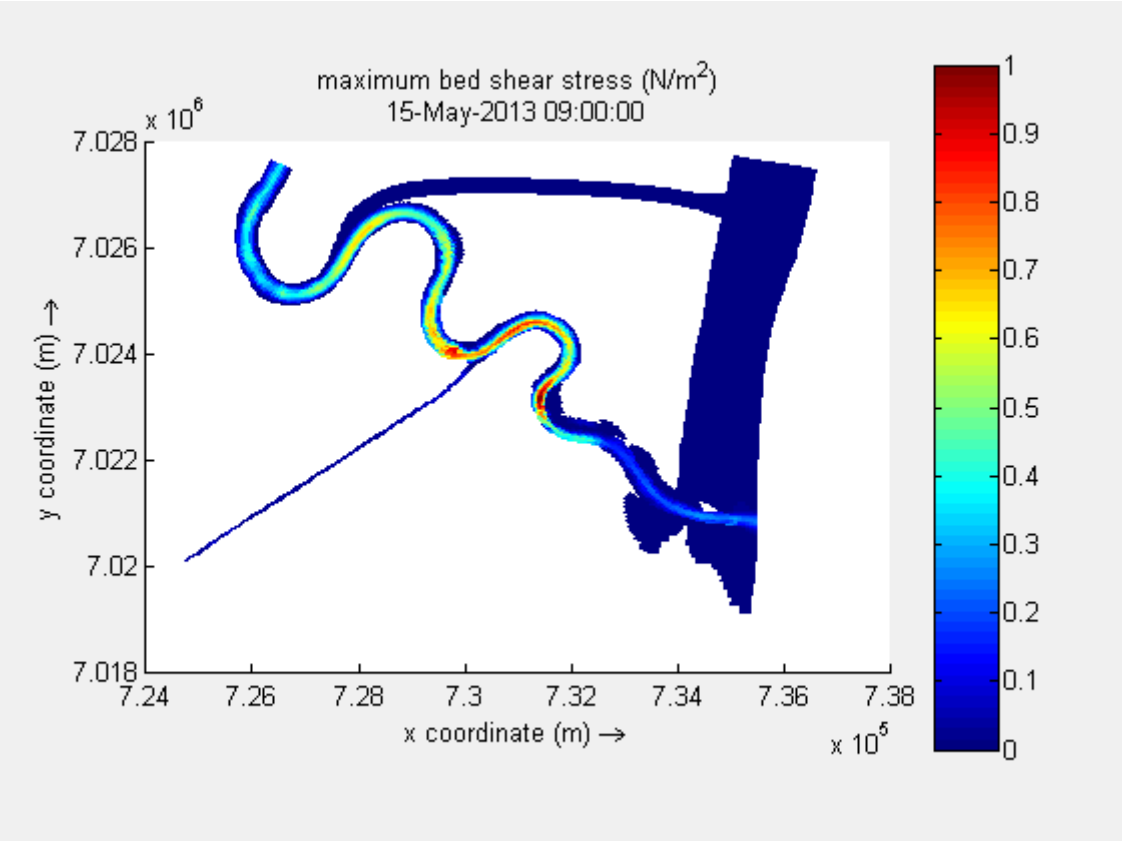

Fig. 9-41: Bed shear stress, 150 m^3/s, ebb, current scenario, downstream section

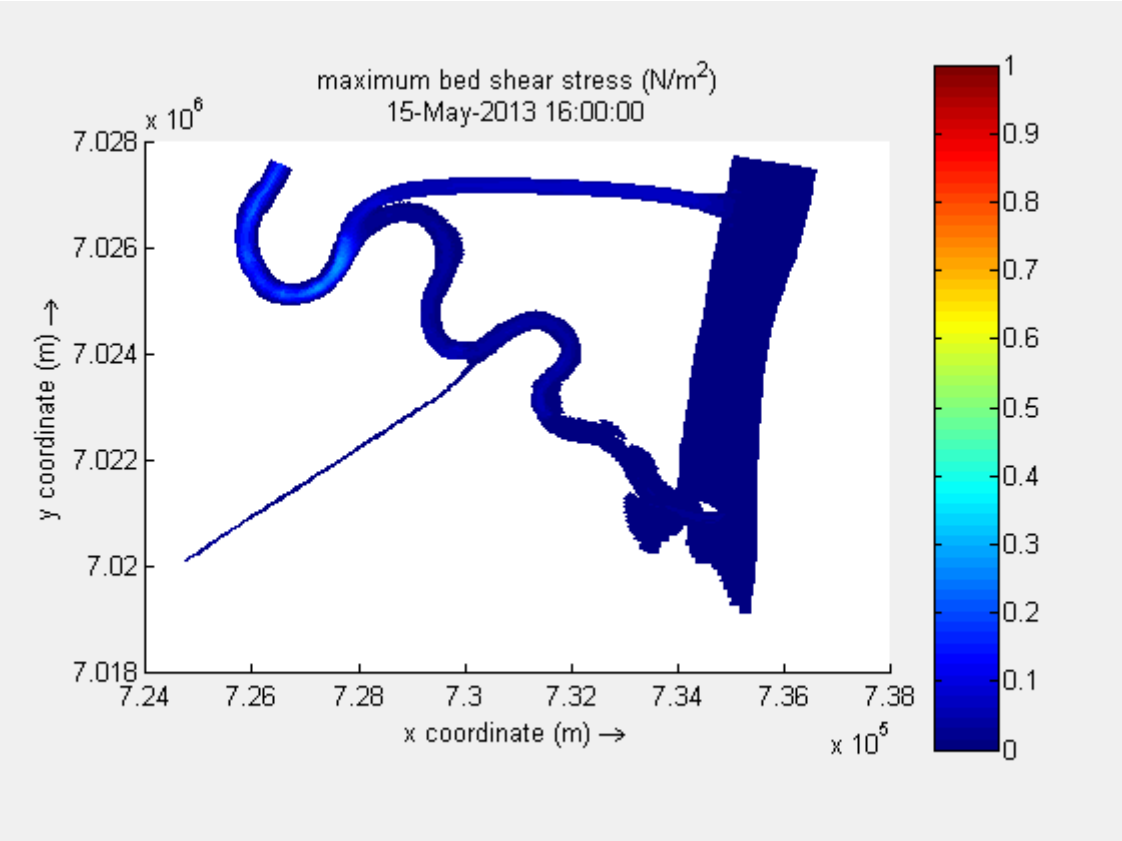

Fig. 9-42: Bed shear stress, 150 m^3/s, flood, bypass scenario, downstream section

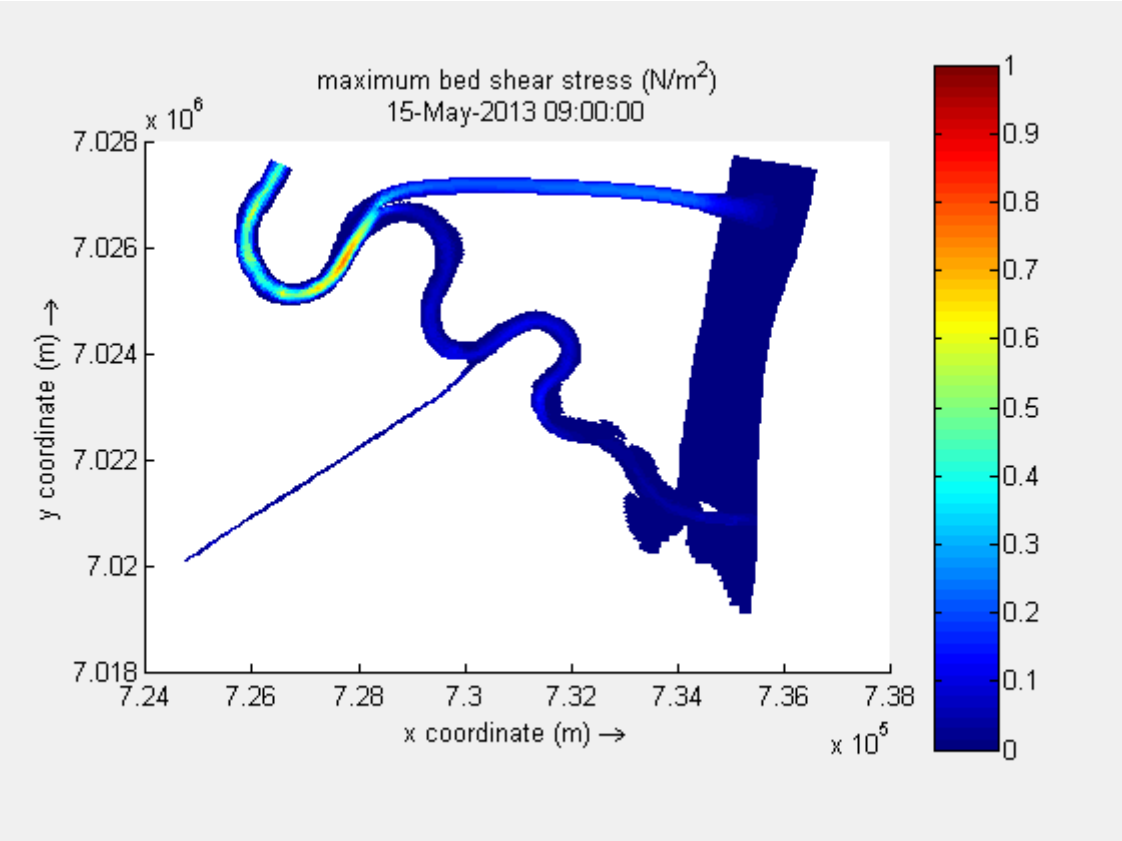

Fig. 9-43: Bed shear stress, 150 m^3/s, ebb, bypass scenario, downstream section

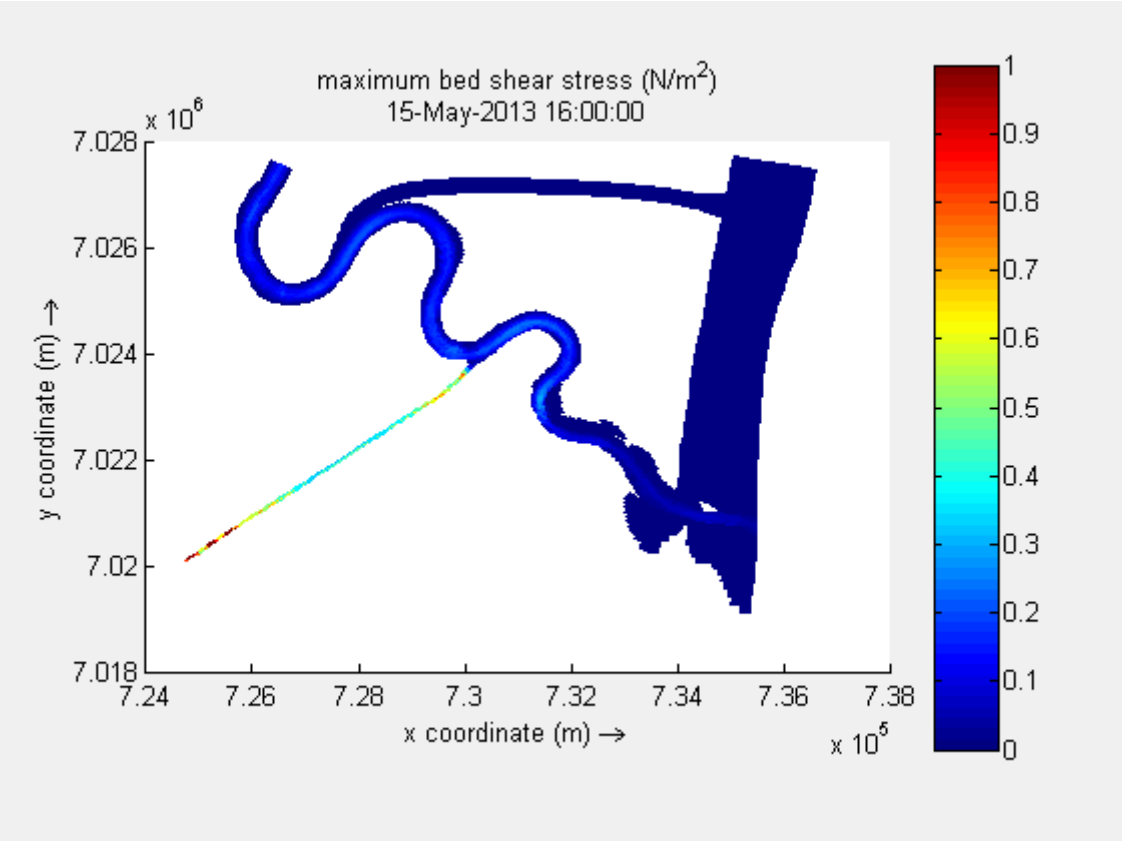

Fig. 9-44: Bed shear stress, 1000 m^3/s, flood, current scenario , downstream section

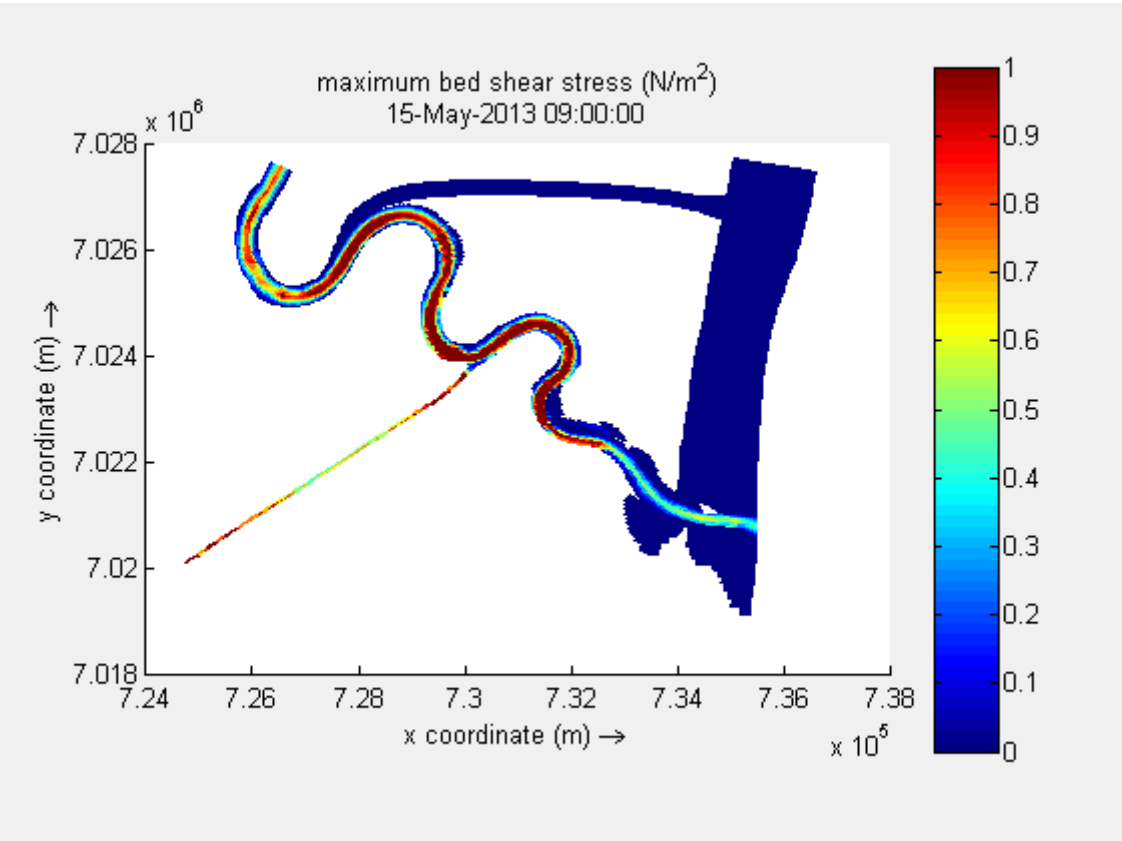

Fig. 9-45: Bed shear stress, 1000 m^3/s, ebb, current scenario, downstream section

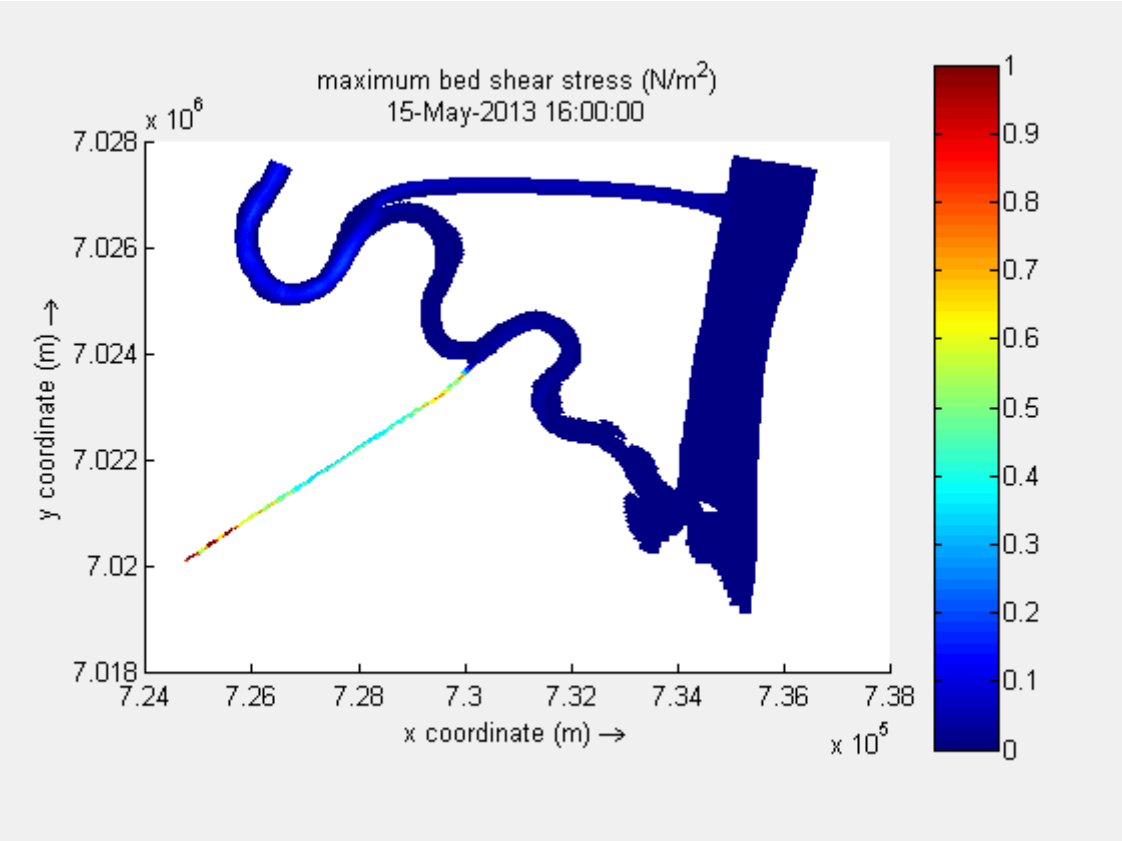

Fig. 9-46: Bed shear stress, 1000 m^3/s, flood, bypass scenario, downstream section

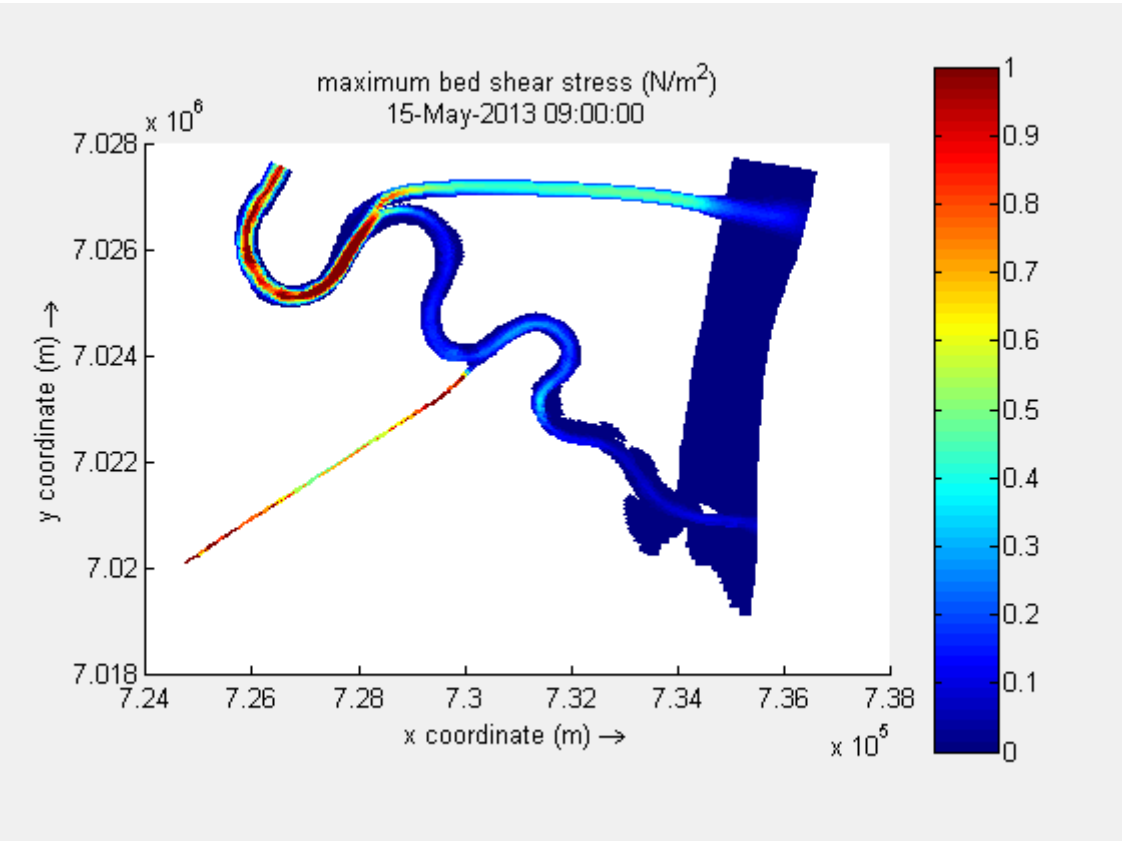

Fig. 9-47: Bed shear stress, 1000 m^3/s, flood, ebb scenario, downstream section

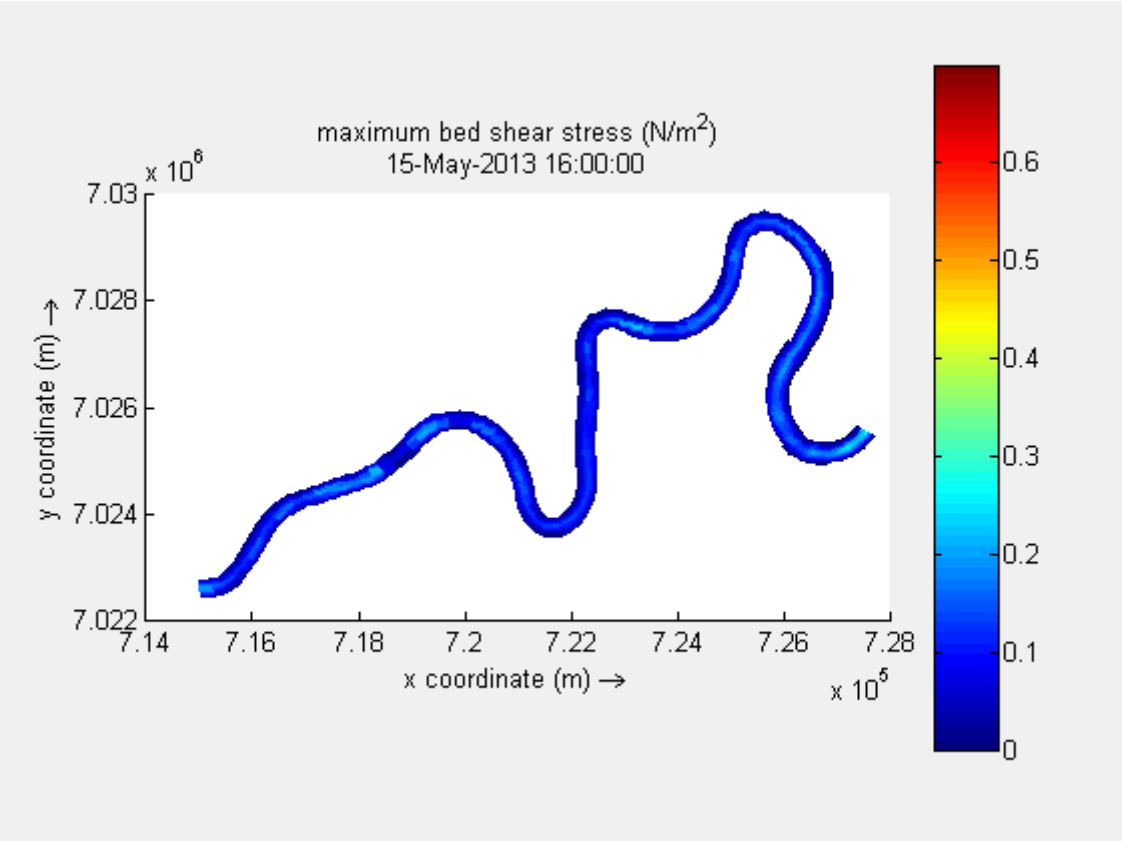

Fig. 9-48: Bed shear stress. 150 m^3/s, flood, current scenario, upstream section

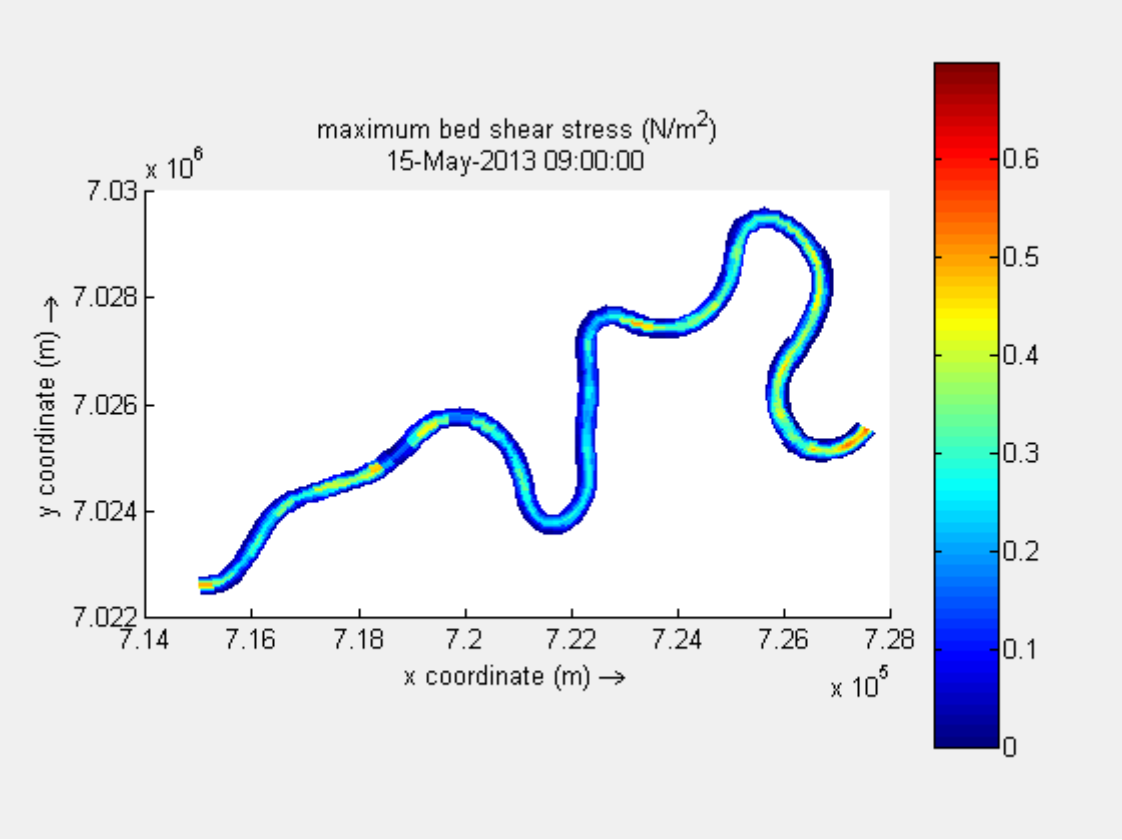

Fig. 9-49: Bed shear stress. 150 m^3/s, ebb, current scenario, upstream section

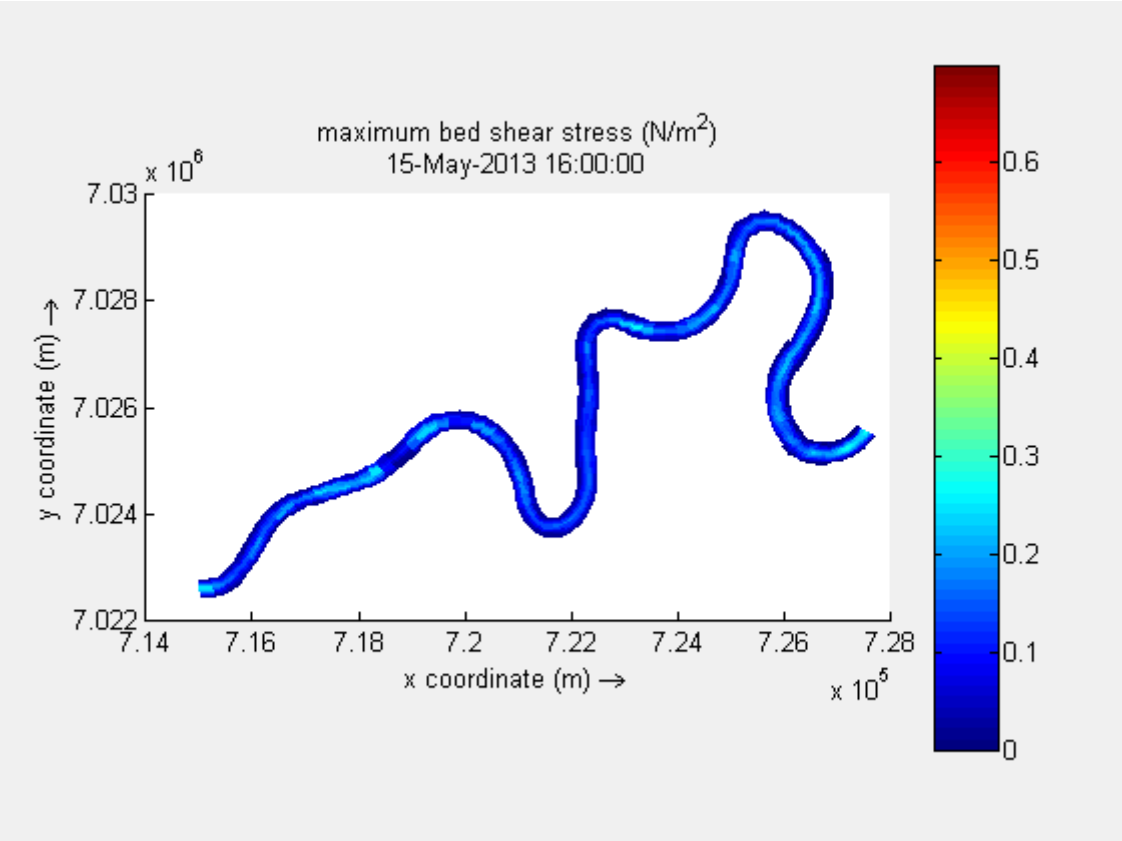

Fig. 9-50: Bed shear stress. 150 m^3/s, flood, bypass scenario, upstream section

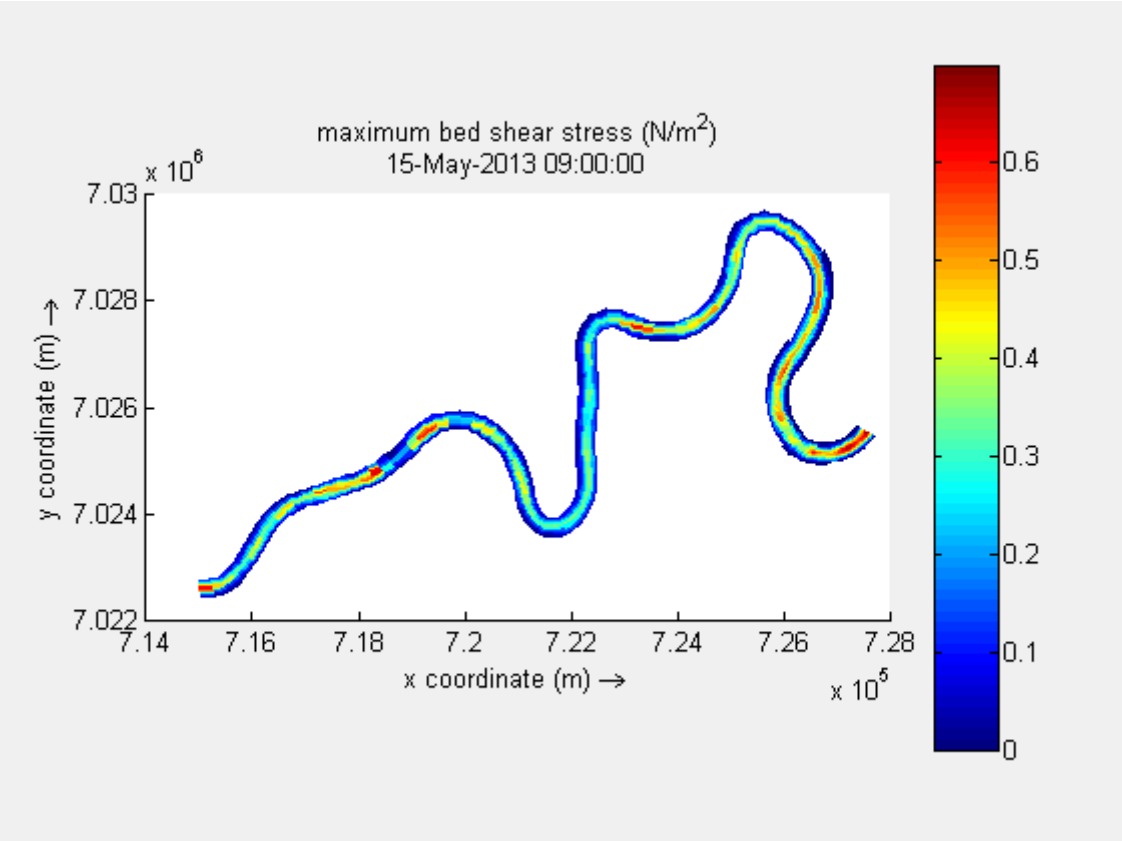

Fig. 9-51: Bed shear stress. 150 m^3/s, ebb, bypass scenario, upstream section

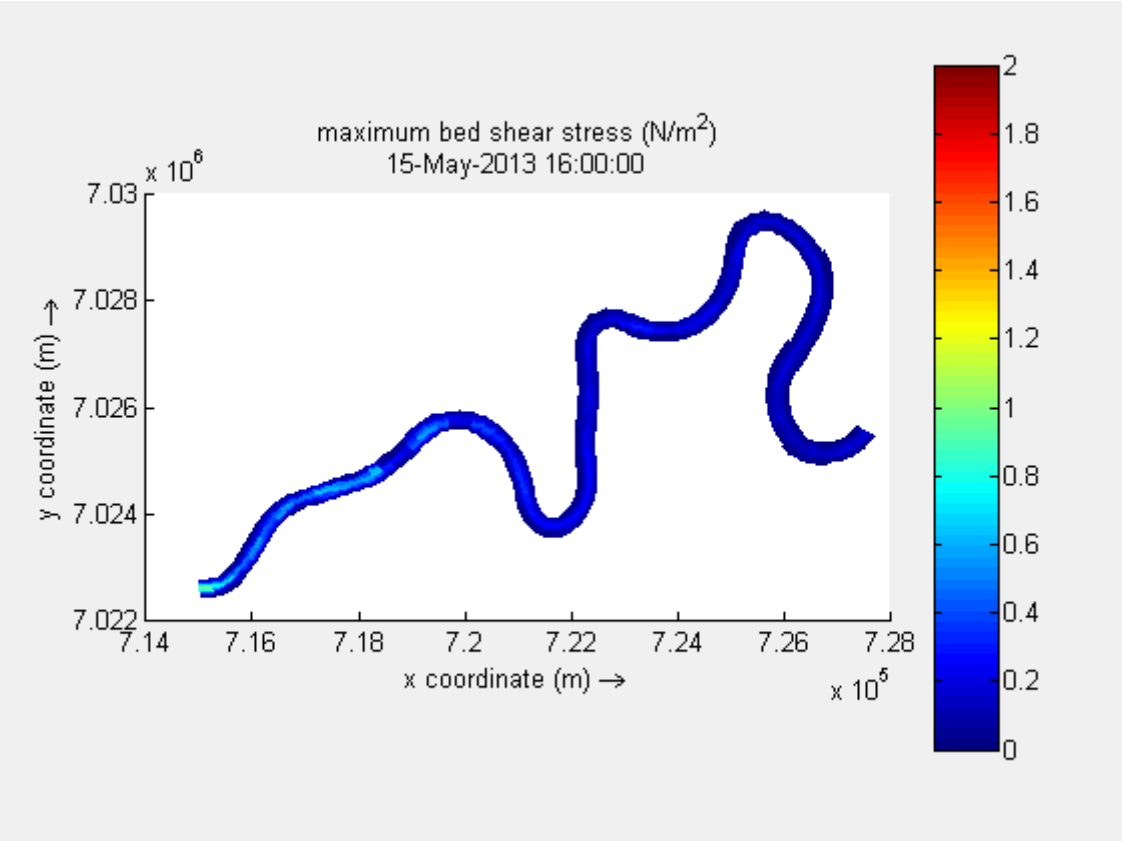

Fig. 9-52: Bed shear stress. 1000 m^3/s, flood, current scenario, upstream section

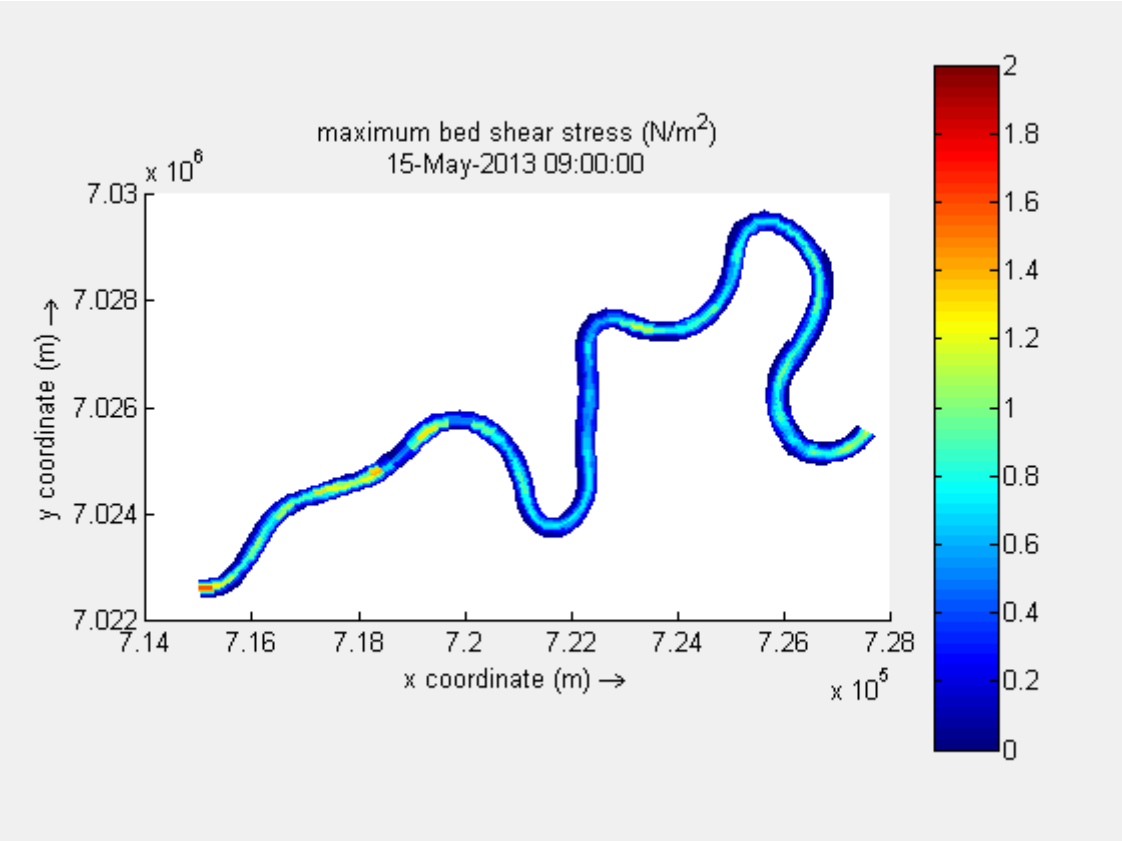

Fig. 9-53: Bed shear stress. 1000 m^3/s, ebb, current scenario, upstream section

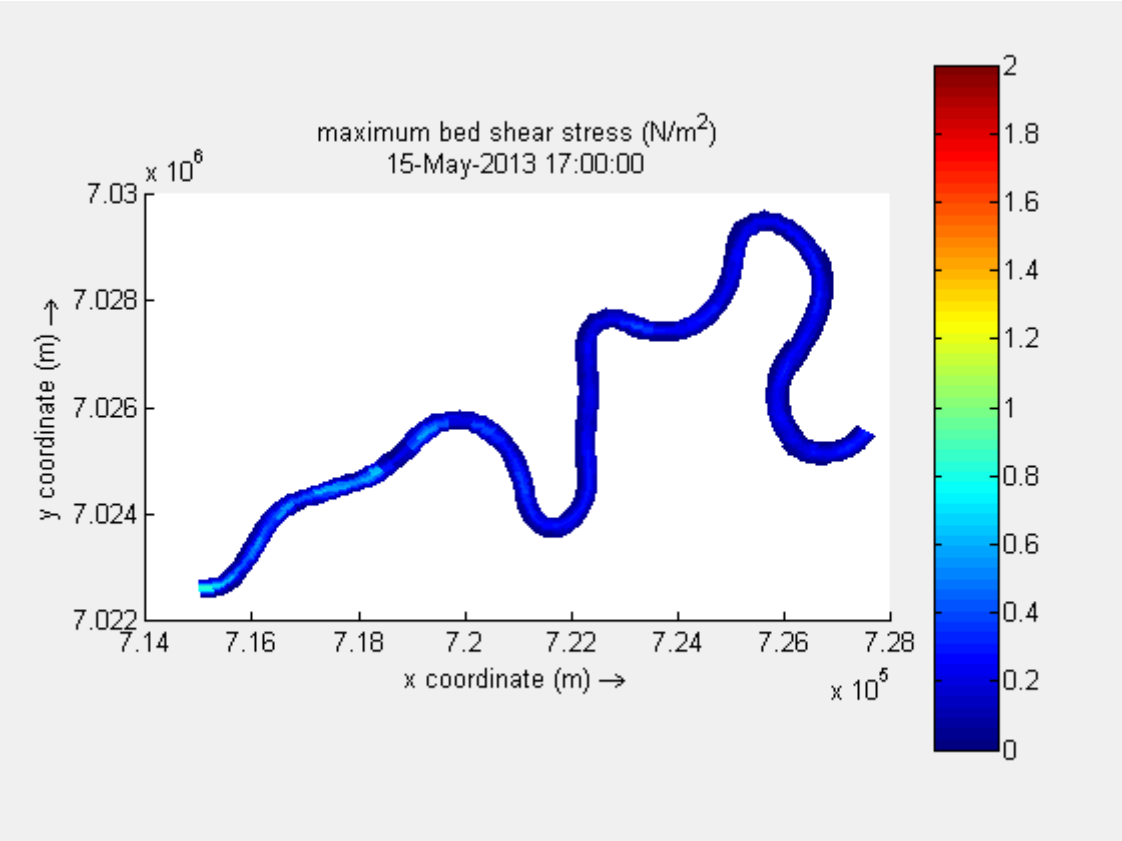

Fig. 9-54: Bed shear stress. 1000 m^3/s, flood, bypass scenario, upstream section

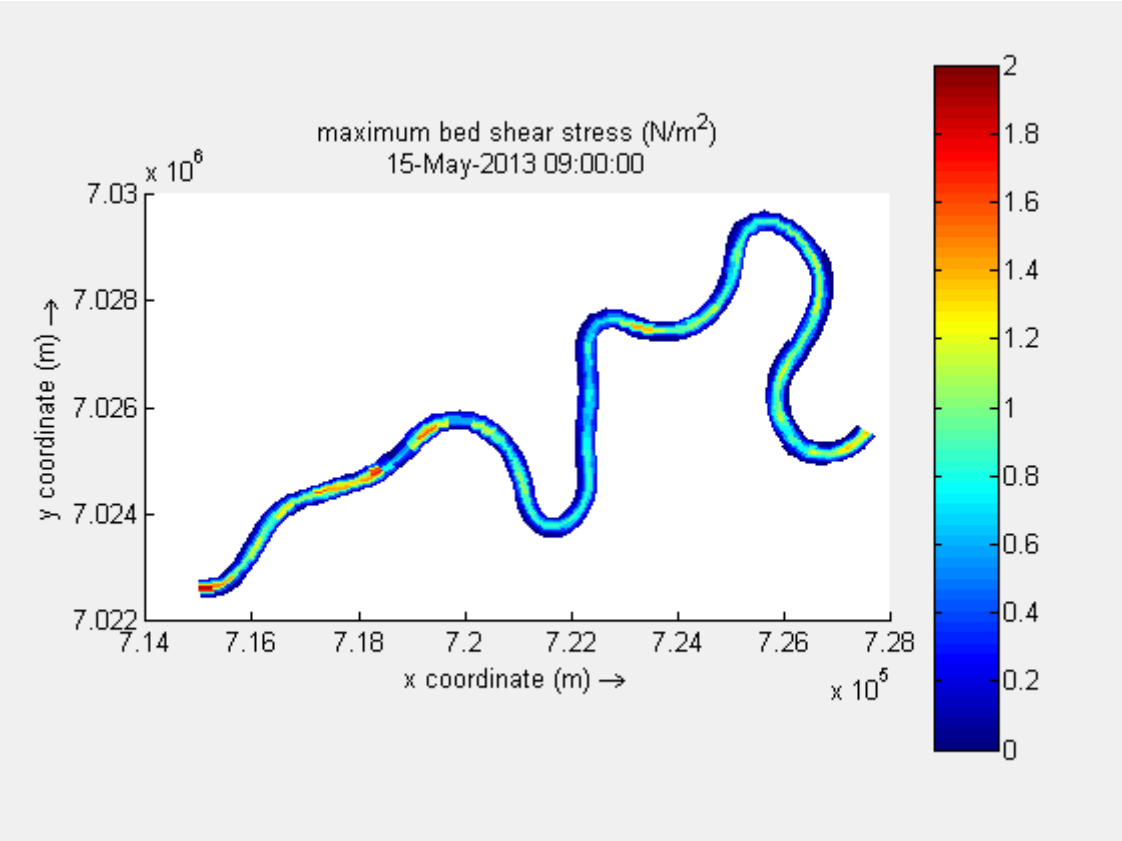

Fig. 9-55: Bed shear stress. 1000 m^3/s, ebb, bypass scenario, upstream section

XI. Salt intrusion

This appendix shows the salt intrusion for both the current scenario and the bypass scenario during a low discharge (150 m^3/s) and a high discharge (1000 m^3/s).

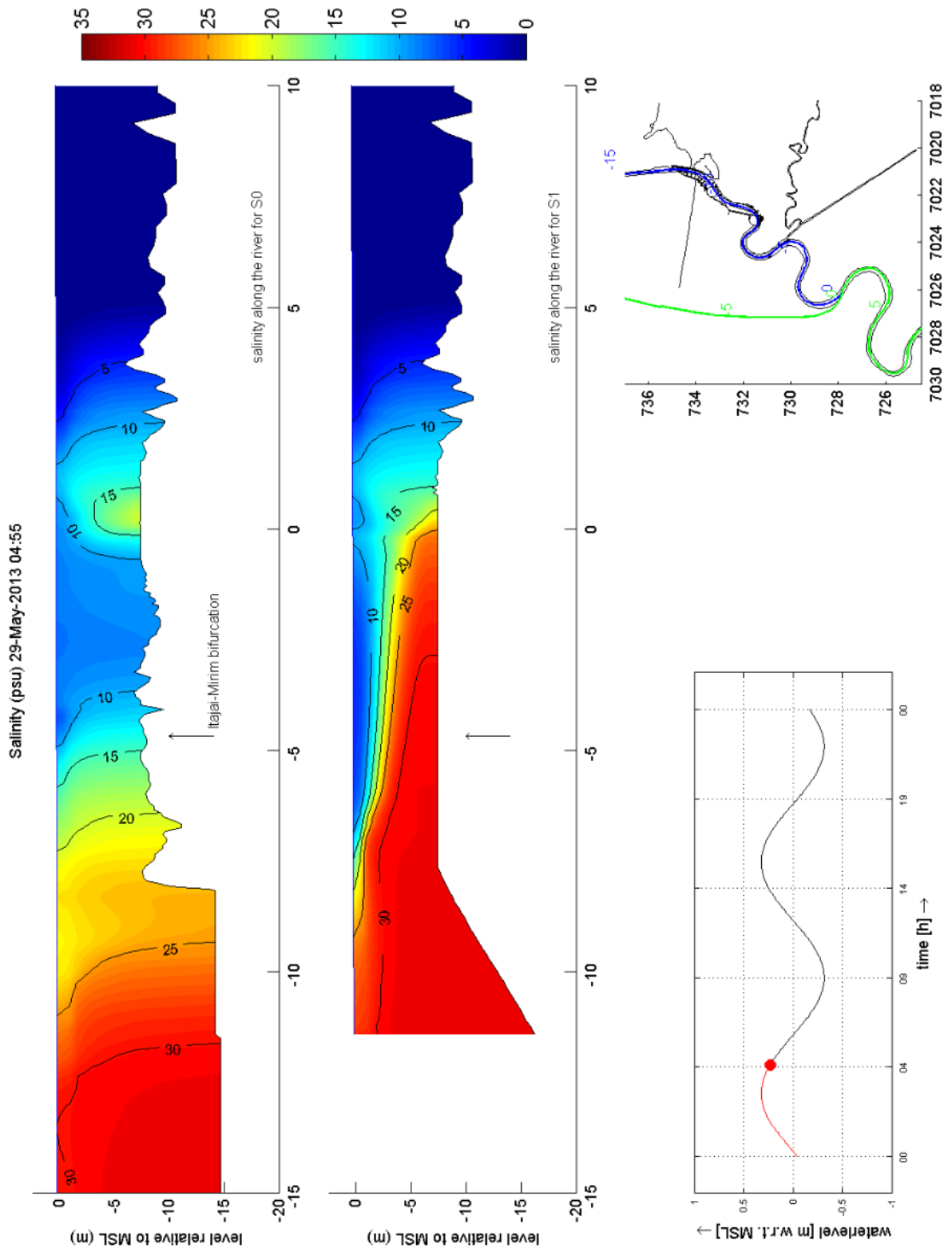

Fig. 9-56: Bypass scenario, salt intrusion during flood, 230 m^3/s

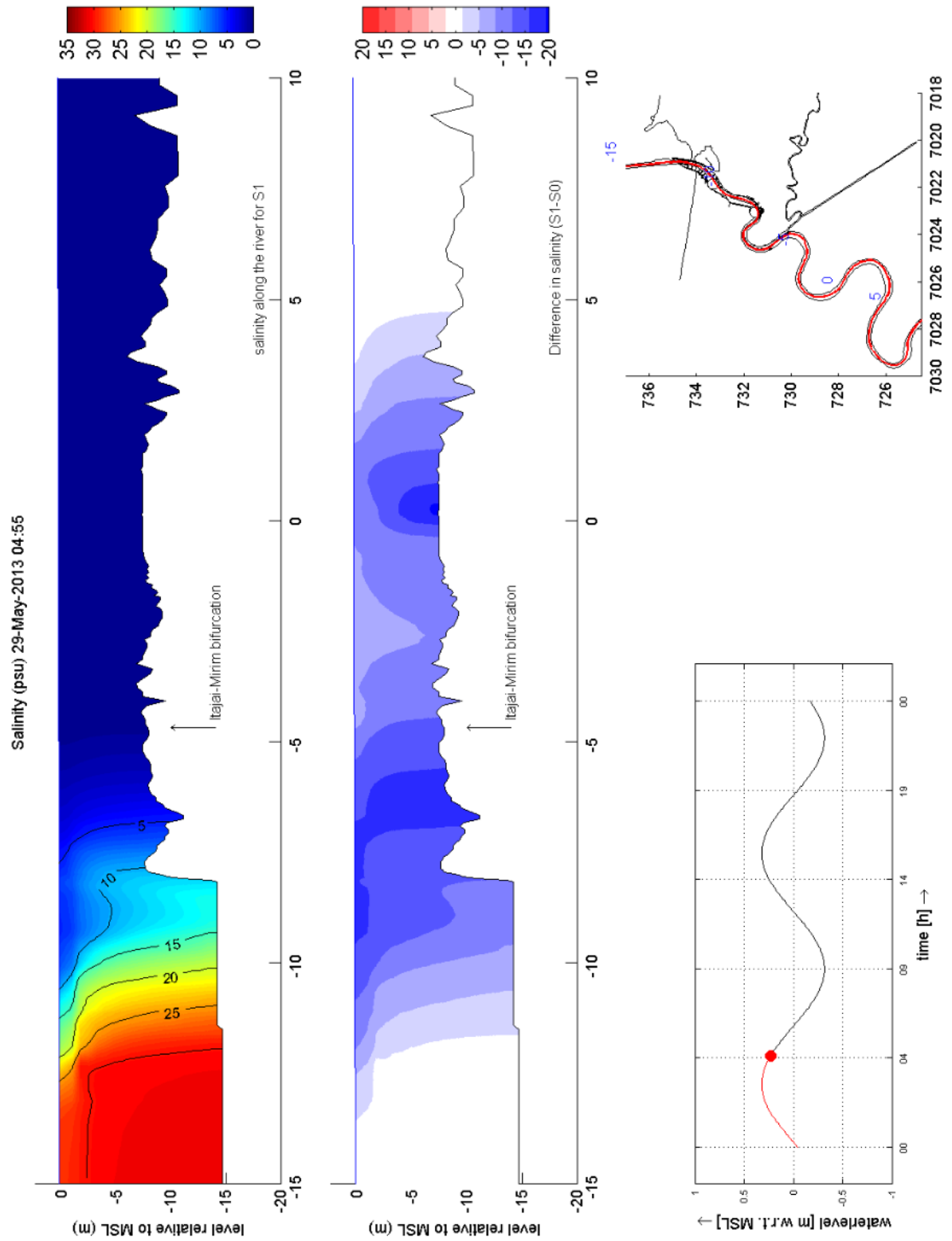

Fig. 9-57: Salt intrusion current situation and difference during flood, 230 m^3/s

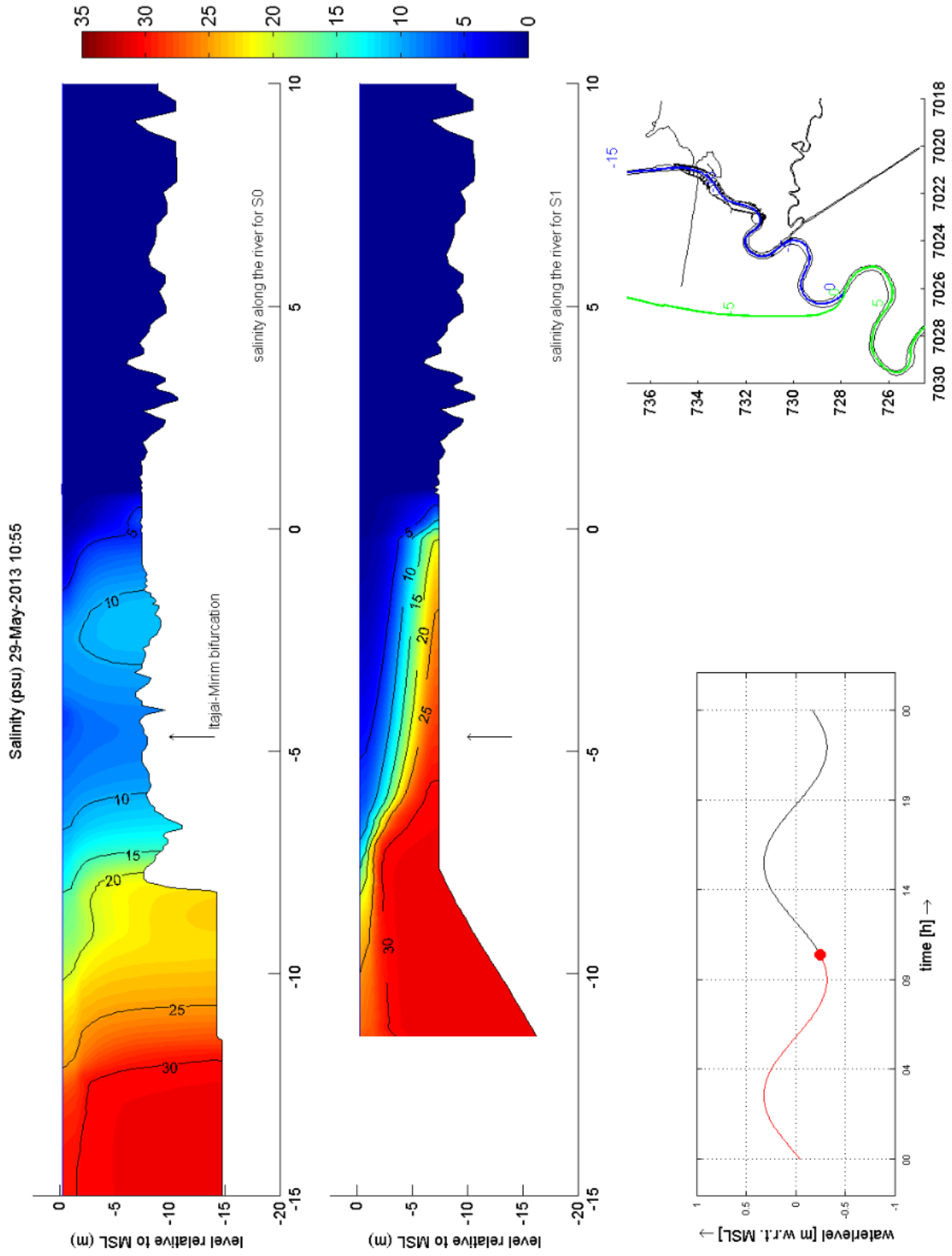

Fig. 9-58: Bypass scenario, salt intrusion during ebb, 230 m^3/s

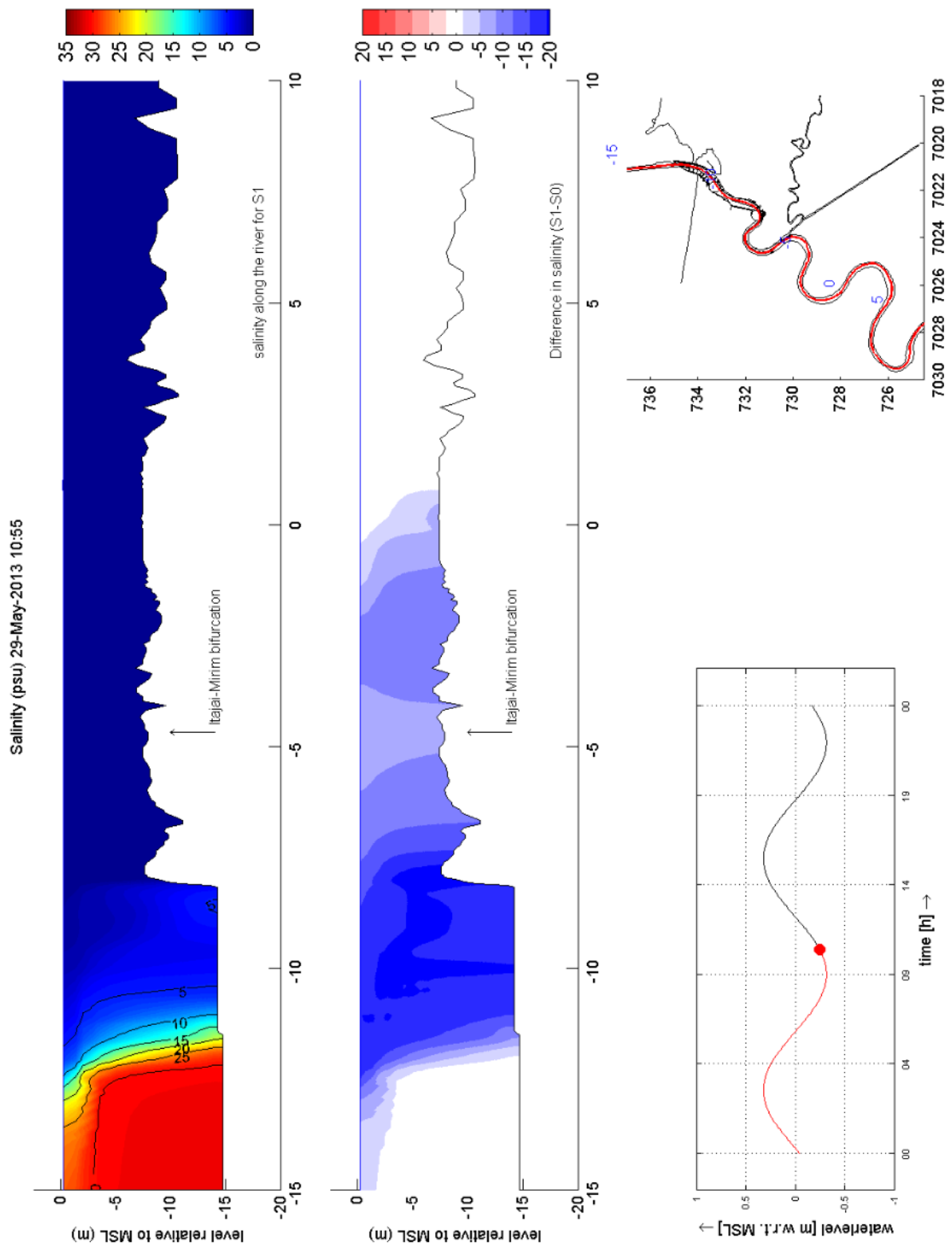

Fig. 9-59: Salt intrusion current situation and difference during ebb, 230 m^3/s

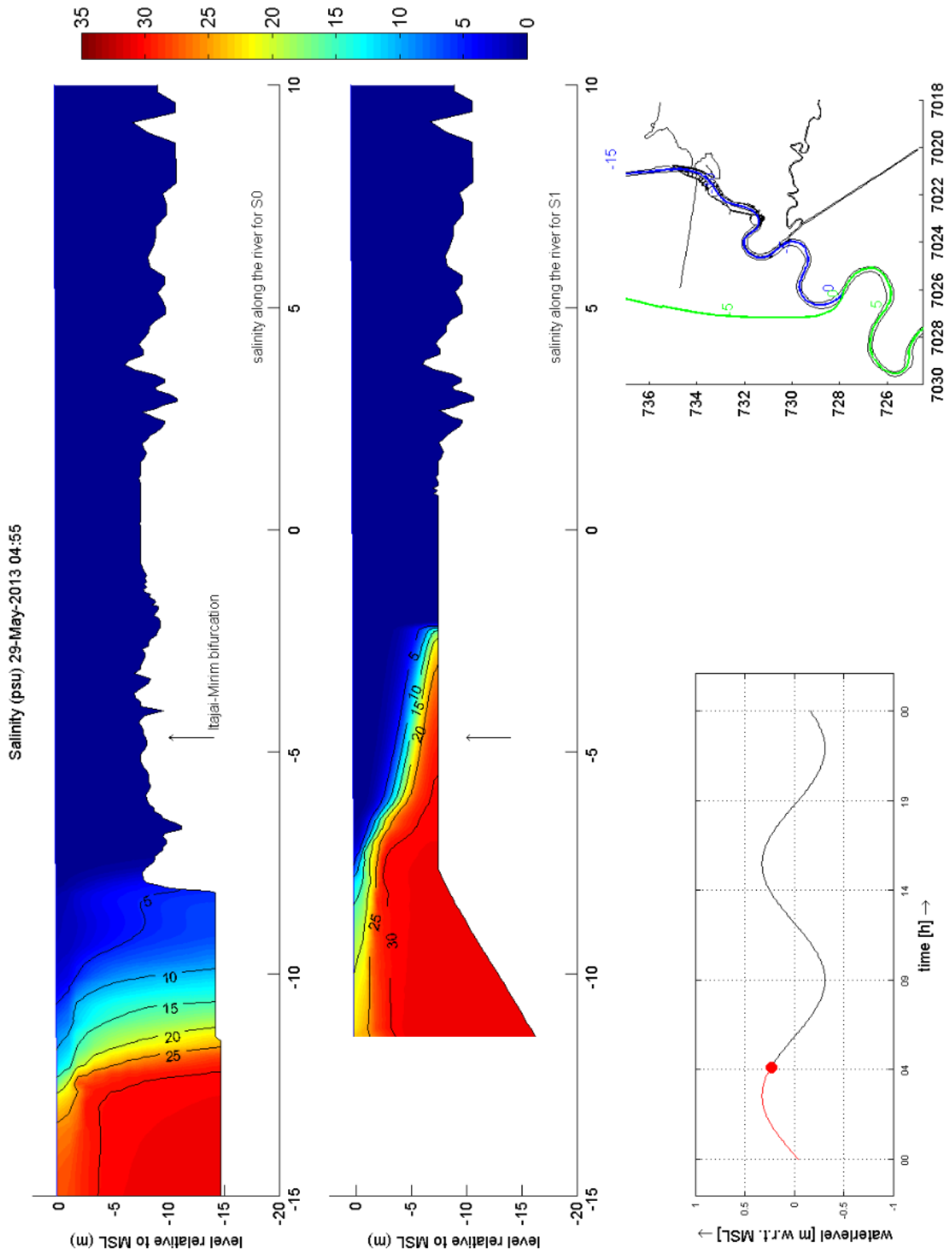

Fig. 9-60: Bypass scenario, salt intrusion during flood, 1000 m^3/s

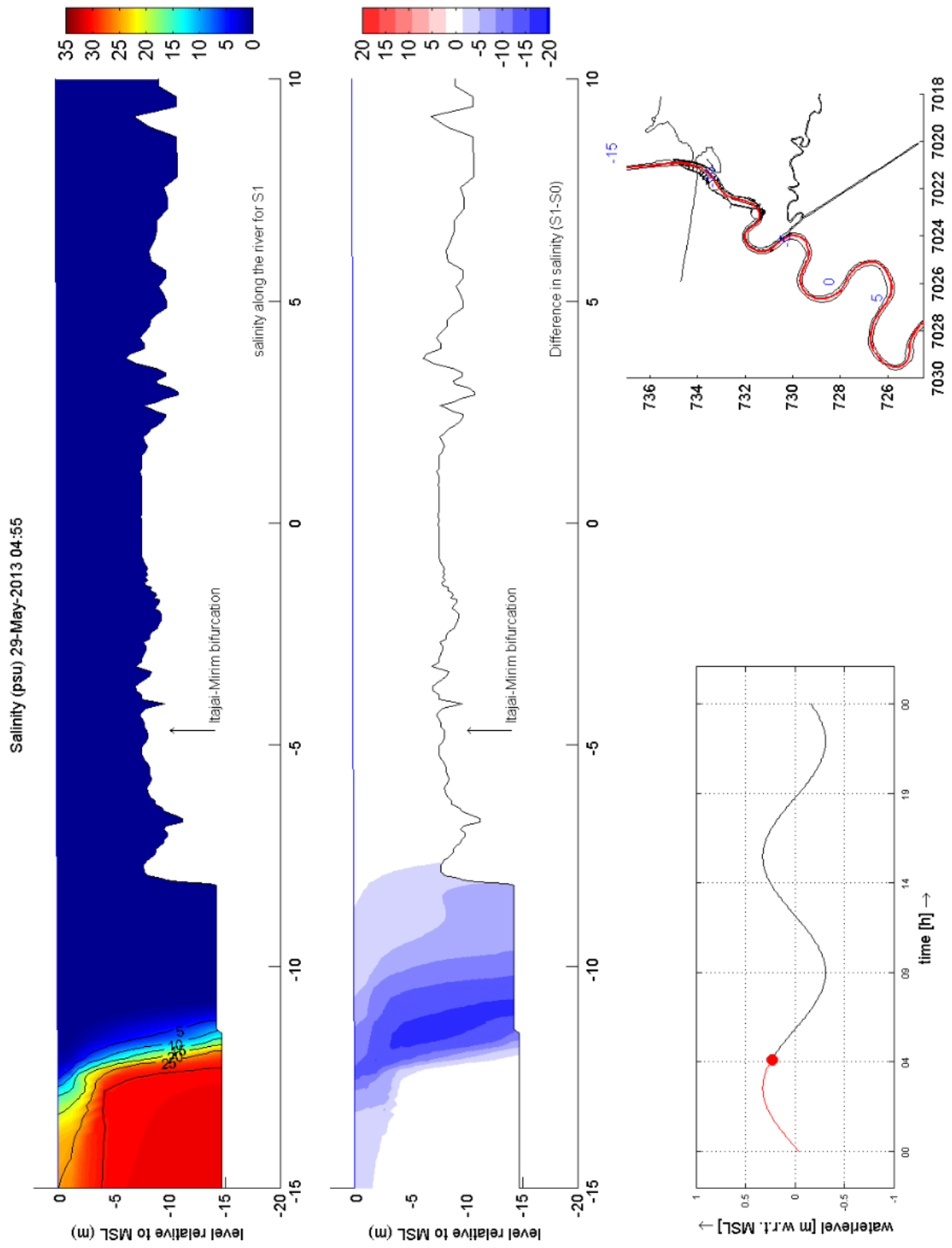

Fig. 9-61: Salt intrusion current situation and difference during flood, 1000 m^3/s

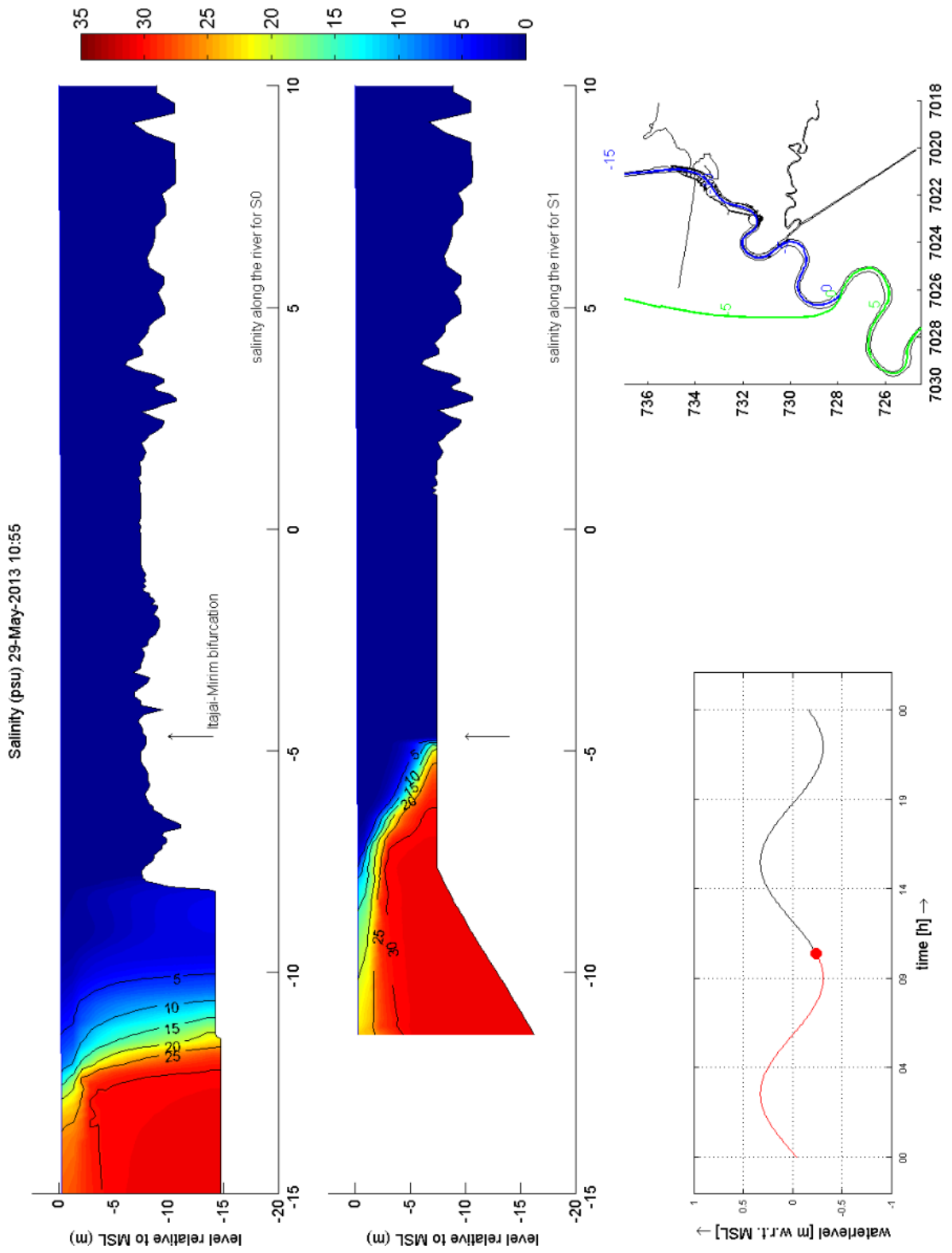

Fig. 9-62: Bypass scenario, salt intrusion during ebb, 1000 m^3/s

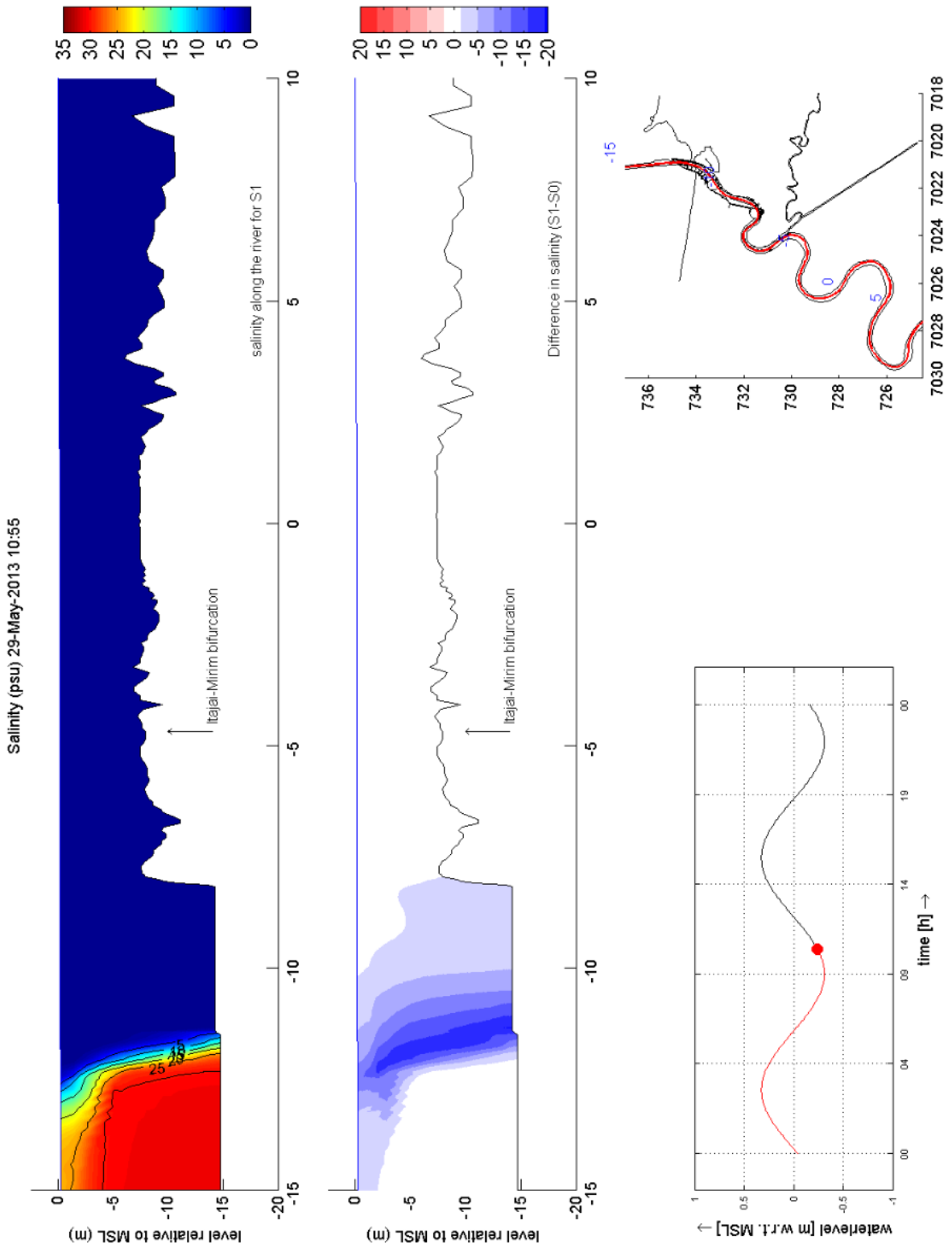

Fig. 9-63: Salt intrusion current situation and difference during ebb, 1000 m^3/s